2015

Holocene Palynology of the Gulf of Papua, Papua New Guinea: Using Modern Palynomorph Distribution to Better Constrain Paleoenvironmental Changes

Marie Louise Thomas
Louisiana State University and Agricultural and Mechanical College, mtho177@tigers.lsu.edu

HOLOCENE PALYNOLOGY OF THE GULF OF PAPUA, PAPUA NEW GUINEA: USING MODERN PALYNOMORPH DISTRIBUTION TO BETTER CONSTRAIN PALEOENVIRONMENTAL CHANGES

A Dissertation

Submitted to the Graduate Faculty of the
Louisiana State University and
Agricultural and Mechanical College
in partial fulfillment of the
requirements for the degree of
Doctor of Philosophy

in

The Department of Geology and Geophysics

by
Marie L. Thomas
B.S., Millsaps College, 2007
August 2015

For my parents, Catherine and Trey, and my grandmother, Lillian

ACKNOWLEDGEMENTS

The completion of this dissertation relied on the help of so many people who deserve acknowledgement. First and foremost, I must thank Dr. Sophie Warny and Dr. Samuel Bentley. Sophie and Sam have been the best mentors I could ask for while completing my Ph.D., and without them, there is no way I could have even known where to begin. Sophie's guidance in my dissertation has been the reason I am pursuing a career as an industry palynologist. She helped inspire in me such a fascination for the tiny world of microfossils. Sam's role in my Ph.D. was fundamental in leading me through the complex dynamic sedimentation processes in the Gulf of Papua and guiding my understanding of the physical factors influencing the assemblages we observed. The other members of my committee have played no small role. David Jarzen has been instrumental in guiding my identification of pollen and spores. Without his help, I would never have been sure of the species I was identifying under the microscope. Phil Bart has taught me so much about sequence and seismic stratigraphy. Before I took his classes, the concept of sea level and climate change was abstract and unquantifiable to me.

Numerous others have mentored me through the years. I must thank David Pocknall, Todd Boesiger, and Josh Miller, my mentors at Hess where I completed two internships, for their guidance and counseling. My professors at Millsaps, including Debora Mann, Zach Musselman, Jamie Harris, Stan Galicki, and Jim McKeown, inspired my love for biology and geology, and I would never have attended graduate school were it not for them.

Without the National Science Foundation (NSF) cruises and funding, this project would have been impossible. I must thank Sam, André, Chuck Nittrouer, and all the other

scientists that participated in the NSF Margins Source-to-Sink program in the Gulf of Papua, as well as NSF for its generous support. To Chuck Nittrouer, especially, I extend my thanks, because he allowed me to obtain additional samples.

I would like to thank the Marathon GeoDE Research Fellowship program and the Department of Geology and Geophysics at LSU for providing generous funding for all four years of my work. This allowed me to process samples for microscopy, attend conferences, and support myself while in graduate school. AASP – The Palynology Society, EnCana, and the Mary Jo Klosterman Professorship provided scholarships supporting my project, as well, so I offer many thanks to these organizations for their assistance.

So many others have supported me these past few years: my family, friends, and fellow graduate students. No matter how discouraged or excited I was about my work, these people were always there for me. I must especially thank the graduate students who have been there for me these past four years: Caroline Broderick, Shannon Ferguson, Madison Kymes, David Rau, Mitch Gregory, Kate Griener, Isil Akyuz, Jill Banks, Kevin Jensen, Carlos Santos, and Sandra Garzon.

TABLE OF CONTENTS

LIST OF TABLES

LIST OF FIGURES

ABSTRACT

Multiple NSF (National Science Foundation)-funded MARGINS Source-to-Sink cruises were conducted in the Gulf of Papua (GoP), Papua New Guinea (PNG), from 2003 through 2005 to better understand how sediment is created, transported, and deposited. Although much work has been done on the data collected during these cruises, palynological analysis has never been conducted on the hundreds of available cores. The first phase of this project (Chapters 2 and 3) examines the connection between modern depositional regimes in the GoP and species assemblages recovered. Statistical analysis of palynomaceral assemblages (Chapter 2) indicates a correlation between their distribution and bathymetry, sedimentation rate, and distance from shore. In particular, wood and cuticular material is found closer to shore and in areas with higher sedimentation rates, while SOM increases in abundance with increasing distance from shore and lower sedimentation rates. Characteristic palynomaceral assemblages appear in certain major depositional environments. Palynomorph assemblages (Chapter 3) also indicate a clear correlation with bathymetry, sedimentation rate, and distance from shore. Major groups found in palynological slides reflect the composition of vegetation on mainland PNG. Reworked palynomorphs also provide an indication of sediment source (e.g., from the Ok Tedi mine on the mainland), but this is complicated, because many ages of reworking (e.g., a mix of Cretaceous, Paleogene, Neogene, and Recent palynomorphs) are found in samples. The second phase of this project (Chapter 4) includes a paleoenvironmental reconstruction of the last ~14.5 kyr in the GoP. Three long cores (MD-50, MV-41, MV-46) were selected for this analysis. Changes in palynomorph assemblages allow delineation of four major climate intervals from 14.5 kyr to present,

including the Bølling-Allerød Interstadial (14.5 to 12.5 kyr BP), the Younger Dryas (12.5 to 11.5 kyr BP), Meltwater Pulse-1B (11.5 to 10.5 kyr BP), and the Holocene (10.5 kyr BP to present). Results indicate that mangrove pollen and marine indicators clearly delineate the end of the transgression between 5 to 6 kyr BP Palynomorph data and oxygen-18 isotopes from MD-50 also indicate an increase in El Niño Southern Oscillation (ENSO) activity at approximately 5 kyr BP.

CHAPTER 1. INTRODUCTION

Most of the world's population lives in coastal areas on continental margins, where the dynamics of sedimentary processes, including erosion, transportation, and deposition, are extremely complex. Understanding these processes is crucial to society, because the movement of sediment is an important part of the global carbon cycle, plays a role in effective resource management, and is key to deciphering changes in climate and sea level. The National Science Foundation (NSF)-funded MARGINS Source-to-Sink Initiative (S2S) examines the erosion, transport, and deposition of sediments from their source where they are created to their sink where they are deposited. The goals of this initiative include better understanding how tectonics, climate change, sea level change, and other forcing mechanisms, like solar insolation, impact sediment production, erosion, transportation, deposition, and how the stratigraphic record is built (NSF MARGINS Program Science Plans, 2004). As part of the S2S program, hundreds of cores were collected in the Gulf of Papua (GoP), Papua New Guinea (PNG), from 2003 through 2005. Numerous studies have already been published on the data obtained during this initiative (Dickens et al., 2006; Keen et al., 2006; Aalto et al., 2008; Alin et al., 2008; Aller et al., 2008a; 2008b; Carson et al., 2008; Crockett et al., 2008; Daniell, 2008; Day et al., 2008; Febo et al., 2008; Francis et al., 2008; Goni et al., 2008; Jorry et al., 2008; Lauer et al., 2008; Muhammad et al., 2008; Ogston et al., 2008; Slingerland et al., 2008a; 2008b; Swanson et al., 2008; Tcherepanov et al., 2008a; 2008b; 2010; Howell et al., 2014). Palynological analysis has never been performed on the sediment cores, and no work on palynology in the gulf, except along mangrove-dominated shorelines, has been published (Rowe et al., 2013). This study documents the modern distribution of

palynomorphs in the GoP using samples from the top four centimeters of sedimentary cover, as well as the distribution of palynomorphs in three long cores covering approximately the last 14.5 kyr BP (Figure 1.1).

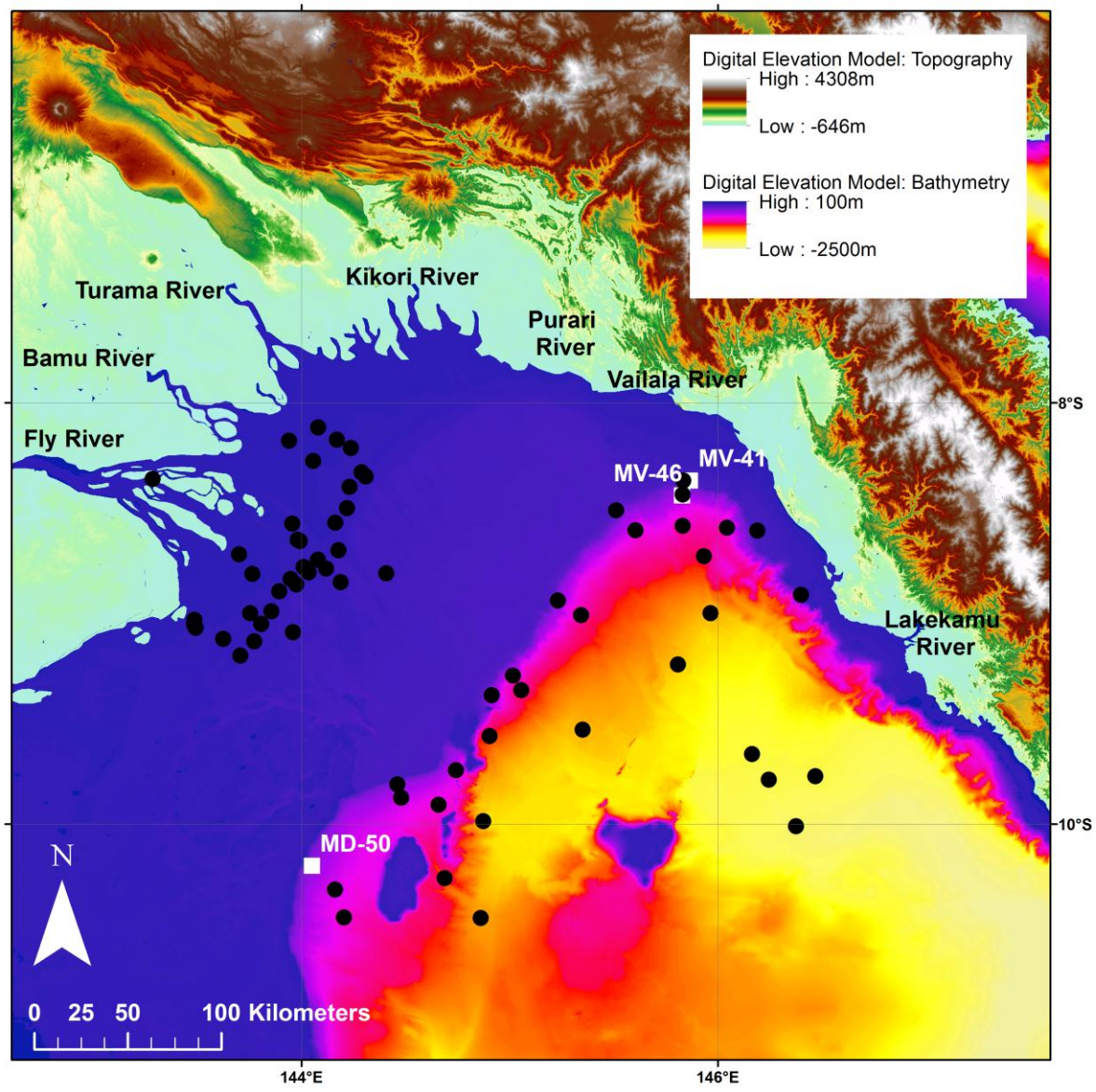

Figure 1.1. Sampling locations for all projects in the Gulf of Papua, Papua New Guinea. Circles are modern sampling locations. Squares are long core locations for paleoenvironmental analysis. Bathymetry and topography are from Daniell (2008).

Palynology, which is the study of organic microfossils (Jansonius and McGregor, 1996), has been shown by many authors to aid understanding of sedimentation dynamics and depostional settings, as well as climate and sea level changes (e.g., Batten, 1983; Gregory and Hart, 1990; Pocknall and Beggs, 1990; Batten, 1996; Oboh-Ikuenobe et al., 1997; Oboh-Ikuenobe et al., 1998; Jaramillo and Oboh-Ikuenobe, 1999; Courtinat et al., 2002; Ibrahim, 2002; Schiøler et al., 2002; Roncaglia, 2004; Roncaglia and Kuijpers, 2004; Carvalho et al., 2006; Pross et al., 2006; Skupien and Mohamed, 2008; Zobaa et al., 2008; Warny et al., 2009; Schiøler et al., 2010; Feakins et al., 2012). Vegetation is a very most sensitive indicator of climate, because it responds directly to changes in solar insolation, temperature, and rainfall. Quantifying changes in the distribution of plants is difficult over geologic timescales, so we must rely on pollen and spores produced from vegetation that are well-preserved in the geologic record (Traverse, 2007). Palynomorphs are transported and deposited as part of the sediment, so we can also use their distribution to help us understand shifts in sediment source, transport, and depositional processes (Stanley, 1966; Heusser, 1978; Kershaw, 1994; van der Kaars, 2001; Moss et al, 2005).

Physical Geography and Setting

The GoP occupies an area of 1.5×10^{11} m^2 to the southeast of PNG between 7.5°S to 11°S latitude and 142°E to 146°E longitude (Figure 1.1). Mainland PNG lies to the north of the GoP between 2°S to 10°S latitude and 140°E to 154°E longitude. The mainland and surrounding islands have a total area of 462,840 km^2 with a combined coastline of 5,152 km (CIA The World Factbook, 2014). The tropical climate results in temperatures that are warm year-round, and large amounts of precipitation that are ultimately delivered to the gulf (Wolanski et al., 1995). There are large topographic

variations across the mainland from sea level (0 meters) to the top of Mt. Wilhelm (4509 meters) (CIA The World Factbook, 2014). Multiple rivers (including the Fly, Bamu, Kikori, and Purari, as well as numerous smaller distributaries) bring large amounts of sediment to the gulf (3.84×10^8 tons per year (Milliman, 1995; Wolanski et al., 1995)), forming a predominantly clastic shelf. The shelf has an area of approximately 40,000 km^2 (Francis et al., 2008). The width of the continental shelf varies greatly across the gulf, from greater than 100 km offshore from the Fly River delta to less than ten km in the northeast.

Regional Geology

The geologic history of PNG is extremely complex and dominated by the collision of stable Australian continental crust with multiple terranes, including several volcanic arcs, small continents, and oceanic plateaus, during the Cenozoic (Pigram and Davies, 1987; Pigram et al., 1989). The landmass consists of four major tectonic provinces: the Fly Platform, the Papuan Fold Belt, the New Guinea Highlands/Papuan Peninsula, and a series of volcanic arc terranes (Abbot, 1995) (Figure 1.2). Continental crust rifted from the Australian craton makes up the relatively stable Fly Platform. The Papuan Fold Belt is an active fold-and-thrust belt. Collision of several terranes during the Oligocene and Miocene formed the New Guinea Highlands and Papuan Peninsula. Multiple volcanic arcs have been sutured to the continent during collision in the Neogene (Pigram et al., 1989; Abbot, 1995).

Understanding the geologic evolution of PNG and the GoP is important for understanding modern sedimentation dynamics. Beginning in the late Cretaceous to early Paleocene, Australia rifted from Antarctica and began its northward journey (Weissel and

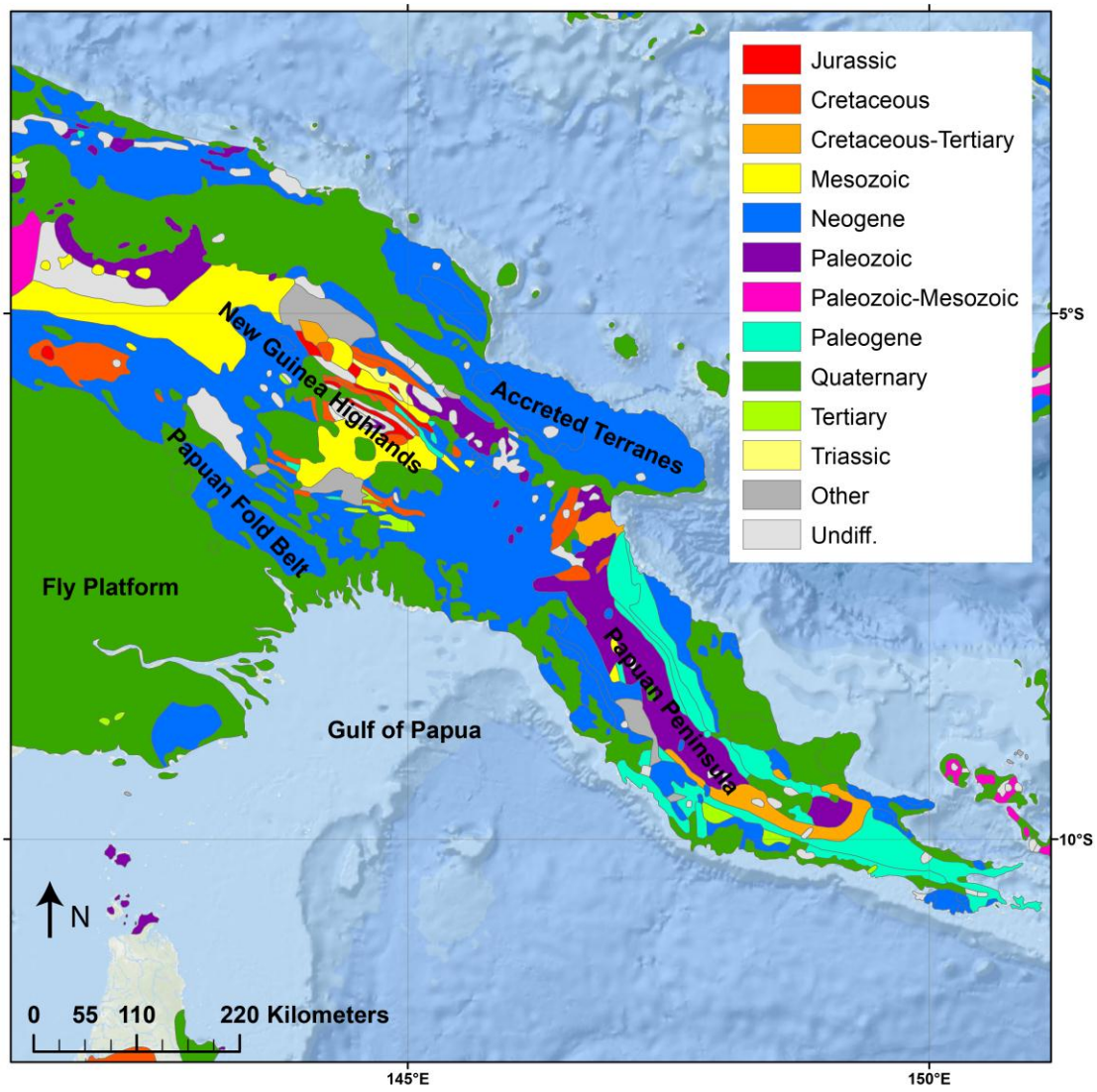

Figure 1.2. Geologic map of Papua New Guinea (PNG) (Steinshouer et al., 1999).

Hayes, 1972; Cande and Mutter, 1982). At this point, large volumes of siliciclastic sediment accumulated on the northern shelf (Brown et al., 1980). The Australian craton was a passive continental margin until the Oligocene (Pigram et al., 1989). Middle Oligocene collision of the Australian craton with the Pacific plate led to the creation of the Papuan Mountains and the GoP foreland basin, a large epeiric sea connecting the Coral Sea and Indian Ocean. This basin began to accumulate widespread carbonate sediments as early as the latest Oligocene forming a carbonate platform. Through the

Miocene, the GoP was starved of siliciclastic sedimentation, except for the narrow proximal foredeep in the northern part of the basin. As the basin accumulated more siliciclastic sediments through the Pliocene, the carbonate platform migrated south and was eventually buried by terrestrially derived material (Pigram et al., 1989). At present, carbonate sedimentation is restricted near the Great Barrier Reef and a series of isolated atolls (Boot Reef and Ashmore Fields Reef), and siliciclastic sediments sourced primarily from the major rivers and the Papuan Mountains dominate deposition in the gulf (Wolanski et al., 1995; Muhammad et al., 2008; Tcherepanov et al. 2008a). The GoP has numerous minibasins, including Ashmore, Pandora, and Moresby Troughs, formed during its evolution as a foreland basin, where these sediments ultimately accumulate (Figure 1.3) (Davies et al., 1989; Pigram et al., 1989; Symonds et al., 1991; Norvick et al., 2001; Howell et al., 2014). Petroleum exploration in the GoP and PNG has become increasingly economical in the past several years (Papua New Guinea Chamber of Mines and Petroleum, 2012), and studying modern depositional settings in the basin may increase our understanding of past depositional environments.

Oceanography

Many studies have examined the oceanography of the GoP (e.g., Thom and Wright, 1983; Wolanski et al., 1984; Brunskill et al., 1995; Wolanski and Alongi, 1995; Wolanski et al., 1995; Wolanski et al., 1999; Keen et al., 2006; Febo, 2007; Martin et al., 2008) (Figure 1.3). The dominant forcing for sediment transport in the Gulf of Papua are tidal variations and seasonal wind changes. Depositional settings with tropical climates, low seasonal differences in river discharge, and little influence from cyclonic storms (McAlpine and Keig, 1983) such as the GoP are particularly susceptible to the influence

of tidal currents (Martin et al., 2008). GoP river deltas, of which the Fly River delta is the largest, are mesotidal in nature, and tidal variations produce interlaminated mud and sand deposits that vary on monthly (i.e., spring-neap) timescales (Martin et al., 2008). The Fly River delta is characterized by funnel-shaped geometry and has three major distributaries, the southernmost of which carries the majority of material (Dalrymple et al., 2003).

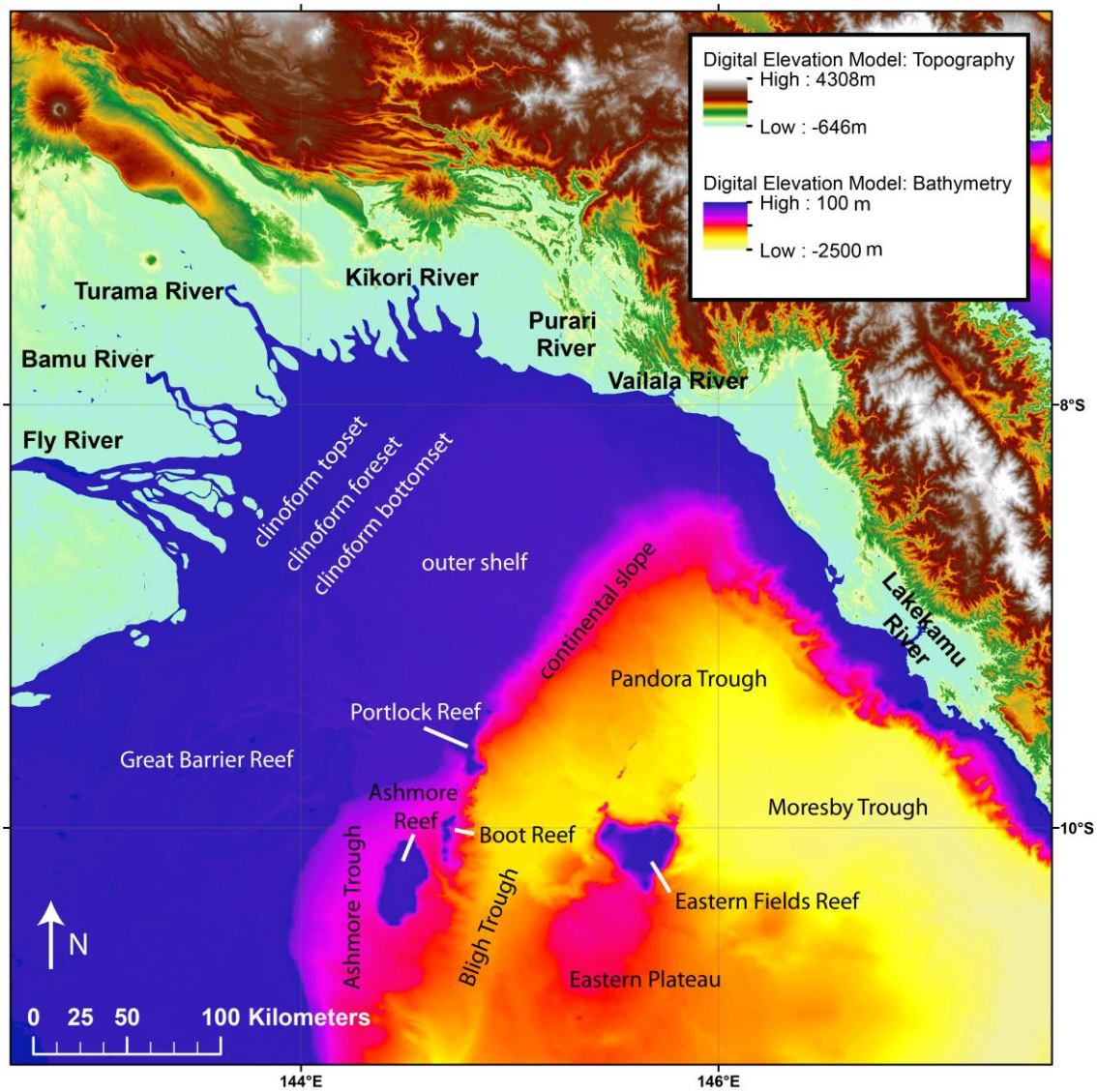

Figure 1.3. Bathymetric map of the Gulf of Papua (GoP) and topographic map of Papua New Guinea (PNG) (Daniell, 2008).

Seasonal wind changes also play an important role in influencing sediment transport. Summer monsoons occur from December to March when the winds blow from the northwest, and winter trade winds occur from May to October when winds blow from the southeast. Transitional periods of lower wind velocities occur in intervening months (e.g., Thom and Wright, 1983; McAlpine and Keig, 1983; Walsh et al., 2004). Changing wind directions result in changes in the GoP wave climate. The monsoon season is dominated by calm conditions and wave heights around 0.3 m. In contrast, the tradewind season results in much higher average wave heights near 1.3 m and rougher seas (Thom and Wright, 1983).

Transport of sediments and dissolved material on the shelf is mostly north-eastward due to the Coral Sea Coastal Current (Wolanski and Eagle, 1991; Brunskill et al., 1995; Wolanski and Alongi, 1995; Wolanski et al., 1995; Walsh et al., 2004), but researchers have noted transport is more complex in the northern and eastern parts of the GoP, especially between the Purari River and Port Moresby. Current measurements in this area indicate sediments are transported southward off the shelf onto the continental slope (MacFarlane, 1980; Wolanski et al., 1988; Wolanski and Eagle, 1991; Brunskill et al., 1995; Walsh et al., 2004; Martin et al., 2008). These sediments are preserved in several troughs and canyons as turbidites (Figure 1.3) (Ewing et al., 1970; Gardner, 1970; Winterer, 1970; Brunskill et al., 1995).

Due to large volumes of freshwater influx, there is strong salinity stratification in the GoP (Wolanski and Alongi, 1995; Ogston et al., 2008). During calm weather, the freshwater plume extends up to 70 km from shore, and the salinity maximum is at water depths of greater than 100 m. Under southeast trade wind conditions, winds transport

brackish water farther, and the freshwater plume can extend at least 100 km across the GoP (Wolanski and Alongi, 1995).

The El Niño Southern Oscillation (ENSO) also affects GoP oceanography by reducing precipitation and thus sedimentation during ENSO conditions (Rodbell et al., 1999; Kawahata and Gupta, 2004; Ogston et al., 2008). This disturbance limits the amount of sediments that accumulate in clinoform deposits during ENSO years (Ogston et al., 2008). ENSO conditions increase salinity in the GoP, by limiting the influx of freshwater. During La Niña years, precipitation and sedimentation are higher than average (Howell et al., 2014).

Modern Sedimentation Dynamics

Sedimentation in the GoP, which is classified as a mixed siliciclastic-carbonate system, has been extensively studied (e.g., Harris et al., 1993; Harris, 1994; Milliman, 1995; Wolanski and Alongi, 1995; Dalrymple et al., 2003; Walsh et al., 2004; Dickens et al., 2006; Keen et al., 2006; Francis et al., 2008; Martin et al., 2008; Muhammad et al., 2008; Ogston et al., 2008; Slingerland et al., 2008a; 2008b). Dynamics of sedimentation are highly variable across the GoP (Muhammad et al., 2008), due to seasonal wind changes, tidal variations (Wolanski and Alongi, 1995; Ogston et al., 2008; Slingerland et al., 2008a), land sourcing the sediments, and large volumes of sediment discharge (Wolanski et al., 1995). The inner shelf in the western GoP is characterized by a large Holocene clinoform with sediments sourced from multiple rivers, particularly the Fly River (Harris et al., 1993; Walsh et al., 2004) (Figure 1.3). Between the Holocene clinoform and the shelf-slope break, few sediments accumulate on a marine transgressive surface formed during the latest sea level rise (Harris et al., 1996; Crockett et al., 2008;

Francis et al., 2008). In the northern part of the gulf, clinoform deposits reach the shelf (Wolanski and Alongi, 1995), and siliciclastic material is delivered to the slope (Brunskill et al., 1995; Walsh and Nittrouer, 2004; Muhammad et al., 2008). Offshore from the continental margin, sediments accumulate mainly as a hemipelagic rain of muds (Muhammad et al., 2008) or as submarine fans in several minibasins (Febo, 2007). Carbonate influx mixes with siliciclastic sedimentation in the southwestern gulf near the Great Barrier Reef (Francis et al., 2008; Tcherepanov et al., 2008b). Widespread carbonate sediments were deposited on the shelf during the Oligocene through early Pliocene (Pigram et al., 1989).

Sedimentation on the continental shelf: GoP clinoform

Large volumes of siliciclastic sediment sourced primarily from the Fly, Kikori, and Purari Rivers, accumulate on the inner GoP shelf in clinoforms (Figure 1.3) (Wolanski and Alongi, 1995; Walsh et al., 2004). Clinoforms are often referred to as the "building blocks of continental margins" (e.g., Vail et al., 1977; Christie-Blick and Driscoll, 1995; Walsh et al., 2004). They are sigmoidal-shaped deposits built of primarily siliciclastic sediments sourced from river deltas. It is estimated that approximately 40% (0.85×10^8 tons per annum) of the sediment load from the major PNG rivers (Kikori, Fly, and Purari) accumulate in the clinoform (Harris et al., 1993). Walsh et al. (2004) examined the mechanics of the GoP clinoform, which is broken into three main components: topset, foreset, and bottomset beds. Topset beds extend down to approximately 20 meters below sea level (mbsl), are characterized by interbedded sands and muds, and have average sediment accumulation rates (SAR) of 0.7 cm/yr. Foreset beds are between 20 to 60 mbsl and are characterized by muds with high SAR between

1.5 to 4.0 cm/yr. Bottomset beds are deeper than 60 mbsl, are characterized by mix of mud and carbonate sand, and have SAR of less 0.4 cm/yr (Wolanski and Alongi, 1995; Walsh et al., 2004; Slingerland et al., 2008a; 2008b). Seasonal wind changes likely affect sedimentation patterns, with higher deposition rates during calmer NW-monsoon conditions. Event beds, approximately 5-10 cm thick, caused by increased winds during the SE-tradewind season, are generally located on the clinoform foreset and occur nearly annually (Walsh et al., 2004). Clinoform sediments are sourced predominately from the Fly Platform, the Papuan Fold Belt, and reworked marine Neogene sediments. Few sediments derived from igneous or metamorphic rocks (sourced from the Papuan Highlands) are present (Davies, 2012).

Sedimentation on the continental slope

The ultimate storage sites on geological timescales for sediments in the GoP are a series of minibasins on the continental slope, including Ashmore, Pandora, Bligh, and Moresby Troughs (Febo, 2007) (Figure 1.3). When sea level is low, sediments are delivered directly to these basins forming submarine fans (Posamentier and Vail, 1988; Harris et al., 1996; Flood and Piper, 1997; Maslin and Mikkelsen, 1997; Febo, 2007; Carson et al., 2008; Crockett et al., 2008; Muhammad et al., 2008). Sedimentation rates are lower on the GoP slope at present (approximately 0.2 cm/yr), and little sediment accumulates in the troughs due to sea level highstand (Muhammad et al., 2008). There are three other regions on the slope in addition to the troughs; these are Bligh Canyon, Moresby Canyon, and the Eastern Plateau. The two canyons often act as conduits for large mass transport flows, and the Eastern Plateau is characterized by a mix of hemipelagic and pelagic sediments (Francis et al., 2008).

Each of the major troughs on the GoP continental slope is characterized by different sedimentation regimes (Figure 1.3). Ashmore Trough (<1000 m water depth) recieves mainly carbonate sediments sourced from the Great Barrier Reef to the west and Ashmore, Boot, and Portlock Reefs to the east (Carson et al., 2008; Francis et al., 2008). Bligh Trough is connected to Ashmore Trough on its southern end, and also receives mostly carbonate sediments. Pandora Trough (between 1700 and 2000 m water depth) recieves a mixture of carbonate sediments from the south and siliciclastic sediments that have been transported past the shelf (Brunskill et al., 1995; Patterson, 2006; Febo et al., 2008; Francis et al., 2008; Jorry et al., 2008; Muhammad et al., 2008). Moresby Trough (approximately 3000 meters water depth) receives mainly siliciclastic sediments that are deposited as turbidites (Patterson, 2006; Francis et al., 2008). The siliciclastic sediments deposited in these troughs are predominantly sourced from the Papuan Highlands (Vailala and Lakekamu watersheds) and have much higher igneous and metamorphic components than shelf clinoform deposits (Davies, 2012).

The Last 14.5 kyr of Climate and Sea Level Change in the GoP

Multiple authors have focused their efforts on Quaternary sea level change in the GoP (e.g., Carson et al., 2008; Febo et al., 2008; Jorry et al., 2008; Tcherepanov et al., 2008a; 2008b; 2010; Howell et al., 2014). Sea level and climate play an important role in governing the nature and preservation of sedimentary deposits along continental margins (e.g., Gibbs, 1981; Bouma, 1982; Droxler and Schlager, 1985; Glaser and Droxler, 1993; Schlager et al., 1994; Andresen et al., 2003; Mallarino et al., 2006; Jorry et al., 2008). The time interval evaluated in this study ranges from the beginning of the latest marine transgression (14,500 yr BP) to present. Figure 1.4 shows the time scale of the study

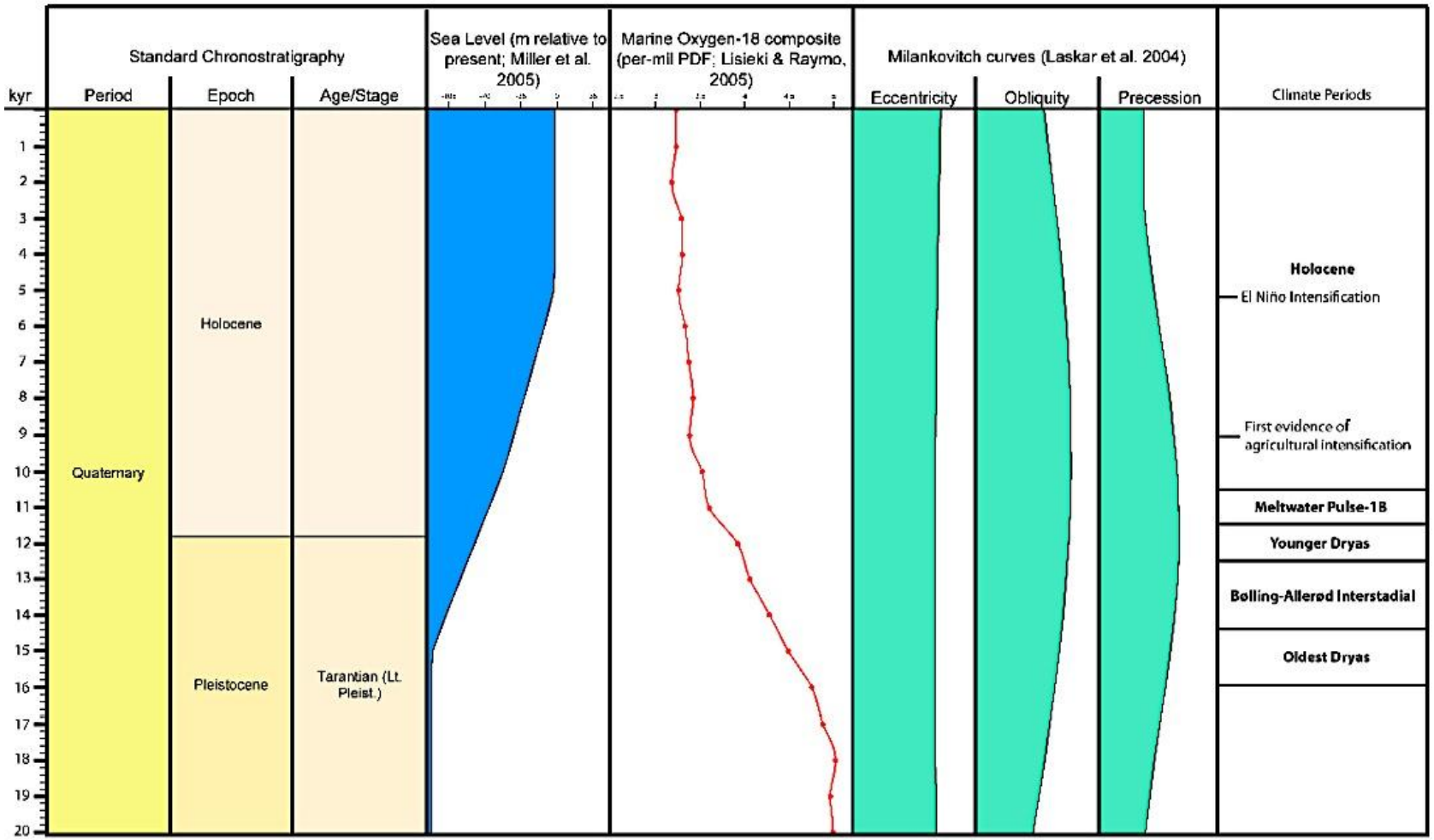

Figure 1.4. Timescale of important events during the last 20,000 years created with TimeScale Creator (TSCreator, 2015, accessed from http://www.tscreator.org). Sea level curve from Miller et al. (2005), $\delta^{18}O$ composite from Lisiecki and Raymo (2005), and Milankovitch cuves from Laskar et al. (2004). Climatic periods and events synthesized from Thom and Wright (1983), Hope et al. (1983), Denham et al. (2003) and Howell et al. (2014).

period with important events, including the Bølling-Allerød Interstadial (approximately 14.5 to 12.5 kyr BP), the Younger Dryas (approximately 12.5 to 11.5 kyr BP), Meltwater Pulse-1B (approximately 11.5 to 10.5 kyr BP), and the Holocene (approximately 10.5 kyr to present BP). At the Last Glacial Maximum (LGM) between 23 to 19 kyr BP, sea levels were ~120m lower (Fairbanks, 1989; Yokoyama et al., 2000; Clark et al., 2004; Jorry et al., 2008), and the majority of the continental shelf was exposed. This resulted in large volumes of siliciclastic material delivered directly to the continental slope (Febo et al., 2008). Meltwater Pulse-1A (MWP-1A) during the Bølling-Allerød Interstadial (RSL rise from -80 to -60 m, Jorry et al. (2008)) and MWP-1B (RSL rise from -60 to -40 m) caused by rapid warming and widespread ice melting at high latitudes resulted in transgressions on the GoP shelf and reductions in the volume of sediments delivered to the slope (Howell et al., 2014). The intervening Younger Dryas period (12.5-11.5 kyr BP) was characterized by cooler and drier conditions with little change in sea level and an increase in sediment delivery to the slope (Jorry et al., 2008). Temperatures increased and sea level continued to rise in the early Holocene until modern sea levels were reached by 6.5 kyr BP (Lambeck and Chappell, 2001; Liu et al., 2004; Kubo and Syvitski, 2006; Howell et al., 2014). Modern sea levels have restricted sediment influx to the slope (Harris et al., 1996), and Slingerland et al. (2008a) notes that the current GoP clinoform began aggrading as early as 9 kyr BP.

Quaternary Vegetation History and Anthropogenic Influence

Climate change results in rapid responses from vegetation, which is a very sensitive indicator of climatic conditions (Traverse, 2007). Many authors have examined the Quaternary vegetation record of Papua New Guinea and its surrounding islands using

a combination of botanical, palynological, archaeological, and phytolith analyses (Walker, 1966; Flenley, 1969; Flenley, 1972; Hope and Peterson, 1975; Smith, 1975; Walker and Guppy, 1976; Flenley, 1979; Walker and Flenley, 1979; Powell, 1982; Hope, 1983; Flenley, 1984; Wilson, 1985; Flenley, 1988; Hope et al., 1988; Johns, 1989; Conn, 1995; Gosden, 1995; Haberle, 1995; Henty, 1995; Womersley, 1995; Haberle, 1996; Flenley, 1997; Boyd et al., 1998; Flenley, 1998; Haberle, 1998; Haberle et al., 2001; Haberle and Ledru, 2001; McAlpine and Freyne, 2001; Denham et al., 2003; Haberle, 2003; Muke and Mandui, 2003; David et al., 2004; Jago and Boyd, 2005; Fairbairn et al., 2006; David et al., 2007; Haberle, 2007; Rowe, 2007a; 2007b, Denham and Mooney, 2008; Horrocks et al., 2008; Denham et al., 2009; Haberle et al., 2012; Torrence, 2012; Rowe et al., 2013). Several authors have also published on the palynology of pre-Quaternary strata in Papua New Guinea (Playford, 1982; Davey, 1987; Rigby, 1997; Rigby, 2001; Playford and Rigby, 2008).

Paijmans (1975) provides a synthesis of modern vegetation distribution on PNG (Figure 1.5). The highly variable topography of PNG leads to strong altitudinal distribution of vegetation (Paijmans, 1975; Walker and Flenley, 1979) (Figure 1.6). The major vegetation types include: mangrove forest, lowland rainforest, swamp forest, lower montane forest, upper montane forest, and scrub/savanna/grassland (Paijmans, 1975). Mangrove forest occupies brackish water at base level and includes genera such as *Rhizophora, Bruguiera, Avicennia,* and *Sonneratia*. Paijmans (1975) splits lowland rainforest vegetation (between sea level and approximately 1400 m) into many categories, but for this study, it is sufficient to group them together as these categories often grade into each other depending on soil type and amount of available water. Important lowland

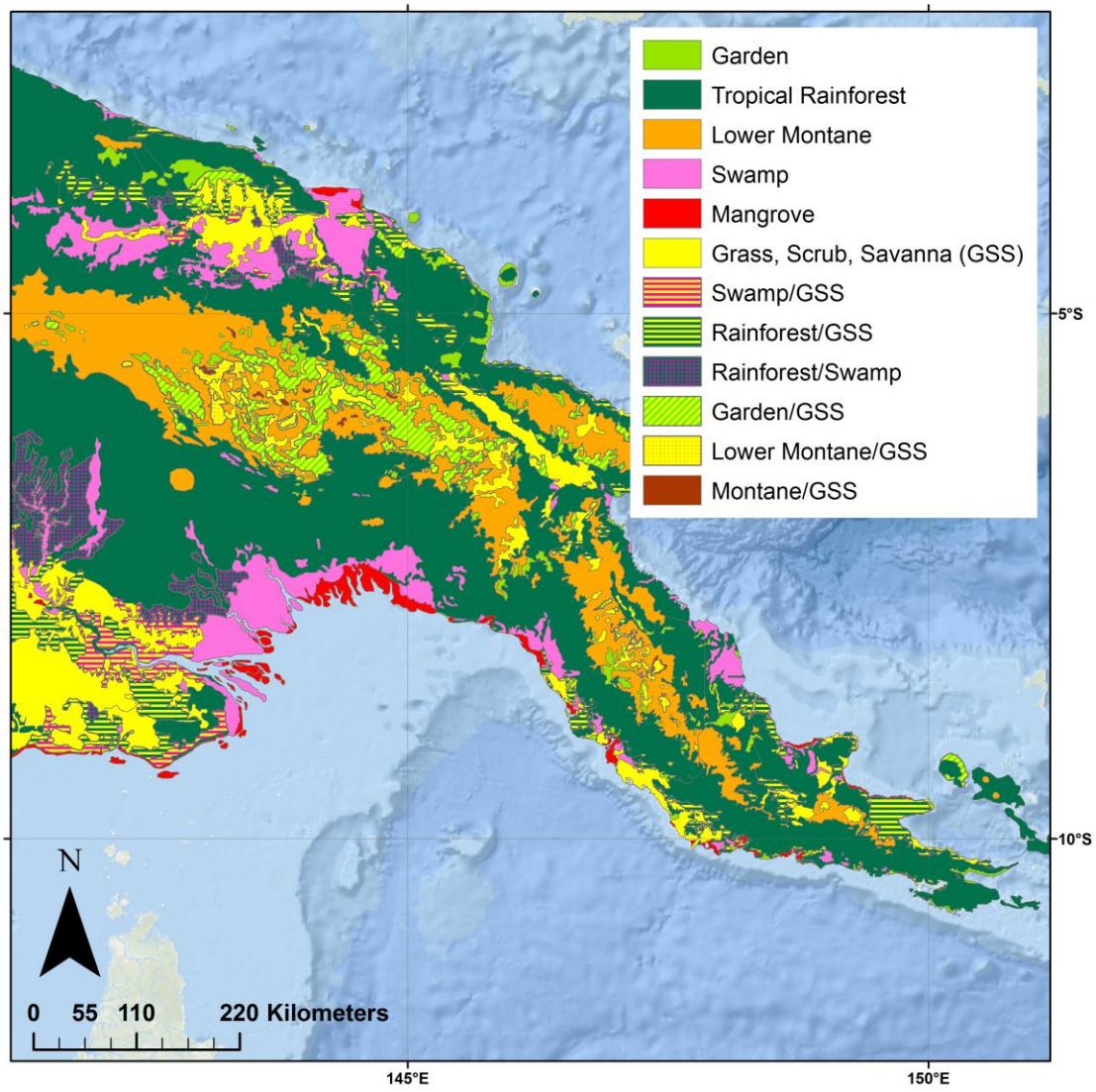

Figure 1.5. Map of modern vegetation distribution on Papua New Guinea (modified from Paijmans, 1975).

rainforest species include *Pometia*, *Canarium, Anisoptera, Cryptocarya, Terminalia Ficus, Celtis, Bombax,* and *Intsia.* Swamp vegetation occupies low to middle altitude, waterlogged areas and is characterized by *Casuarina, Campnosperma, Terminalia, Syzygium, Nauclea, Melaleuca, Myristica,* and a variety of palm species (Family Arecaceae). Lower montane forest (between approximately 1400 to 3400 m) includes *Nothofagus*, Lauraceae, Cunoniaceae, Elaeocarpaceae, *Lithocarpus, Castanopsis, Ilex,*

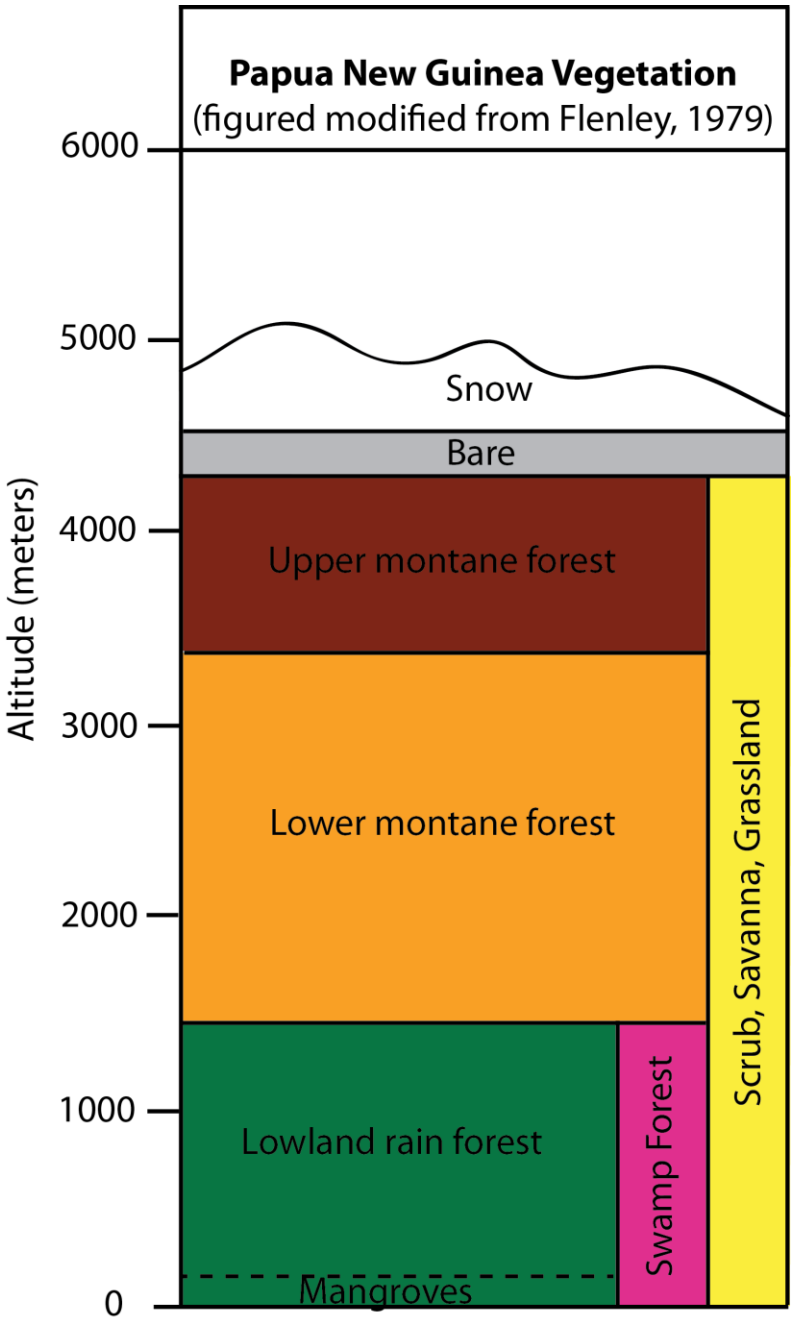

Figure 1.6. General altitudinal distribution of vegetation on Papua New Guinea (modified from van Steenis, 1934-1936; Brass, 1941; 1964; Paijmans, 1975; Walker and Flenley, 1979).

Araucaria, Dacrycarpus, Podocarpus, Phyllocladus, Papuacedrus, Myrtaceae, Myrsinaceae, and Ericaceae. Upper montane forest (above 3400 m) includes many of the same genera and families as lower montane forest but is also intermixed with high

latitude grassland vegetation, including Gramineae, *Festuca, Danthonia, Deyeuxia,* and *Deschampsia klossii.* Grassland vegetation on PNG is generally caused by anthropogenic influence and/or burning and exists at all latitudes. Lowland grass species include *Themeda australis, Imperata cylindrica, Saccharum spontaneum, Ophiuros tongcalingii, Pseudoraphis spinescens*, and sedges. Scrub and savanna vegetation exists in areas with low rainfall from low to high latitudes and includes genera such as *Eucalyptus, Melaleuca, Coprosma, Pittosporum, Xanthomyrtus, Tristania, Acacia, Xanthostemon, Cyathea,* Epacridaceae, and Ericaceae (Paijmans, 1975).

Understanding the distribution of modern vegetation on PNG is important, because vegetation distribution and thus the pollen record changes in response to climate. Pollen records from the highlands of Papua New Guinea indicate that the Last Glacial Maximum (LGM) was at least 5°C cooler (and upwards of 10°C at some sites) and significantly drier (Hope and Peterson, 1975; Walker and Flenley, 1979; Haberle, 1998). Oxygen isotope records from corals living at or near sea level indicate a similar value of 3-5°C temperature reduction during the LGM (Aharon and Chappell, 1986; Guilderson et al., 1994). This degree of cooling, even in lowland locations, has important consequences for vegetation biogeography. In cooler periods, such as the LGM, the lowland rainforest vegetation could only have lived approximately between 0 to 200 meters above sea level, with a concurrent expansion of lower and upper montane vegetation to lower altitudes (Flenley, 1972; Hope and Peterson, 1975; Walker and Flenley, 1979; Flenley, 1984; Flenley, 1997). Several authors have also noted increased abundances of grasslands and drought-tolerant species during cooler conditions (Flenley, 1984; Street-Perrott, 1994; Flenley, 1998).

Humans have occupied Papua New Guinea since at least 40 – 45 kyr BP (e.g., Machida et al., 1996; Torrence et al., 2004; Torrence, 2012), and a transition from hunter/gatherer to agricultural lifestyles occurred between approximately 7 to 9 kyr BP in PNG depending on the site (Robbins, 1963; Gillison, 1969; Powell et al., 1975; Flenley, 1988; Haberle, 2003; Haberle et al., 2012). It is difficult to separate the influence of agriculture and climate change in the palynological record, because both have similar signatures. Agricultural activities denude the landscape, generally resulting in the replacement of tropical or montane forests with grasslands or agricultural species (Denham et al., 2003; Haberle, 2003; Denham and Haberle, 2008; Sniderman et al., 2009; Haberle et al., 2012). Most authors find a concomittant increase in charcoal fragments associated with burning and land clearance due to human occupation (e.g., Flenley, 1969; Flenley, 1988; Whitlock and Larsen, 2001; Haberle, 2003; Haberle et al., 2012). Increased recovery of grassland pollen and charcoal fragments is also indicative of cooler, drier climate. The presence of pollen from cultivars, such as corn, bananas, sweet potato, sugar cane, and taro, can provide additional evidence for human occupation (Walker and Flenley, 1979; Lentfer and Torrence, 2007; Lentfer et al., 2010). As the beginning of agricultural activities on Papua New Guinea is relatively well constrained (7 to 9 kyr BP) (Robbins, 1963; Gillison, 1969; Powell et al., 1975; Flenley, 1988; Haberle, 2003; Haberle et al., 2012), we have at least a baseline for separating human from climatic influence in this study.

The Importance of Mangroves

Mangroves, and their associated pollen, are important indicators of sea level change because they occupy brackish water at base level. They are especially diverse in

Southeast Asia and Papua New Guinea (Ellison, 2008; Shearman, 2010; Rowe et al., 2013), and palynologists often use mangrove pollen distribution and changes in abundance to delineate sea level changes (e.g., Caratini, 1992; Tissot and Marius, 1992; Morley et al., 2003; Morley et al., 2004; Scourse et al., 2005; Hoorn, 2006; Morley and Morley, 2011; Morley et al., 2011). When sea levels are low, mangroves are restricted distally, and any shed mangrove pollen is incorporated proximally into lowstand deposits. Cooler climates during lowstands may also reduce the abundance of mangroves (Caratini, 1992). As sea level rises and the shoreline moves landward, mangroves expand across the continental shelf. Transgressions are generally recorded as an increase in mangrove pollen in the sedimentary record in both shelf and slope deposits. During sea level highstand when the shoreline is at its maximum landward extent, mangroves are restricted proximally, and most mangrove pollen is retained within the roots and sedimentary matrix of the mangrove forest. At highstands, little mangrove pollen escapes towards the shelf or basin (e.g., Tissot and Marius, 1992).

Several authors have examined the mangrove communities of Papua New Guinea, including Ellison (2005), Rowe (2006), Rowe (2007a), Ellison (2008), Shearman (2010), and Rowe et al. (2013). Mangrove communities are patterned based on features within river deltas, including point bars, levees, distributary channels, and floodplains, and certain species preferentially occupy specific areas depending on salinity and elevation (Figure 1.7). For example, *Rhizophora* spp./*Bruguiera* spp. generally live in outer-tidal areas subject to frequent inundation, while *Avicennia* spp. live in lower-inner tidal areas that are inundated less frequently (Rowe et al., 2013). Backmangrove species (*Sonneratia* spp.) and *Nypa fruticans*, a palm species, generally live further inland in less saline water

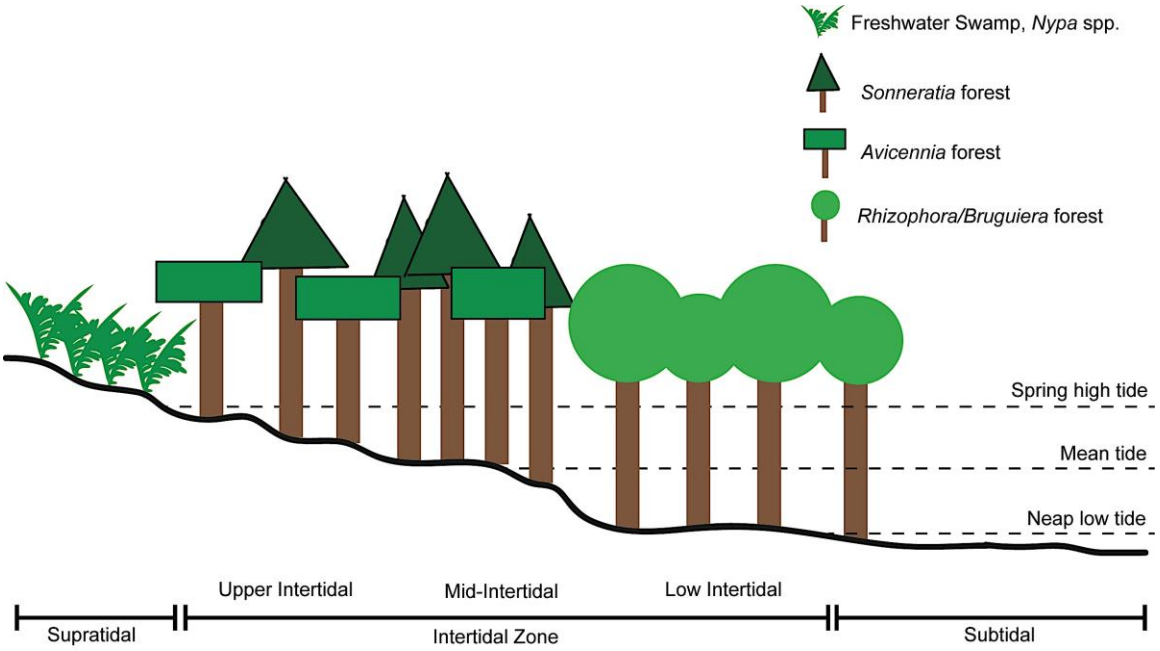

Figure 1.7. General patterning of mangrove communities (modified from Ellison, 2005; Rowe et al., 2013).

and higher elevations (Ellison, 2005). The dominant species listed here (*Rhizophora* spp. */Bruguiera* spp., *Avicennia* spp, *Sonneratia* spp., and *Nypa fruticans*) are the major representatives of mangrove pollen found in the samples for this study, so we plan to use their distribution to help reconstruct sea level changes (Rowe et al., 2013).

Objectives and Significance of Study

Palynology can provide insight into climatic and oceanographic changes (as well as dating these changes), sedimentation and depositional environment, and vegetation biodiversity. This project aims to accomplish four important objectives: 1) define and date past climatic and oceanographic changes from 14,500 years BP to present; 2) improve understanding of sedimentation dynamics using palynology as a tool to assess depositional settings; 3) apply palynology to assess biodiversity and vegetation distribution at present and in the past; and 4) determine human impact on the dominant components of Papua New Guinea flora spatially and temporally. We believe palynology

will provide a better understanding of climatology and oceanography over the time period studied, as well as improve our understanding of sedimentation and biodiversity.

Objective 1: Define and date past climatic and oceanographic changes from the Bølling-Allerød Interstadial (14,500 yr BP) to present.

Determining past variation in climate and defining what caused these changes can allow scientists to better predict future variations by providing climate modelers with key information regarding past conditions. Better predicting climatic changes is increasingly important in our modern world, especially in regions where most of the population lives in coastal regions, such as Papua New Guinea. Near-surface temperatures in Papua New Guinea have risen 0.50°C ± 0.15°C since the mid-1970s, while sea-surface-temperatures have risen approximately 0.6 to 1.0°C in the past 100 years (United Nations Development Programme, 2010). Rising temperatures ultimately mean higher sea levels, more variable weather conditions, and changes in precipitation patterns. Better documentation of climate changes over the last 14,500 years can allow the country of Papua New Guinea to further develop its strategy in the face of today's rapidly warming climate. Previous researchers have utilized sedimentary cover obtained from the Gulf of Papua to document climatic changes and fluctuating sea levels. They have focused particularly on understanding changes in sedimentation dynamics due to fluctuating sea levels over the late Pleistocene and Holocene (Febo et al., 2008; Francis et al., 2008; Carson et al., 2008; Jorry et al., 2008; Jorry et al., 2010; Howell et al., 2014). Some attention has been paid to the biologically produced components of the sedimentary record. Carson et al. (2008) examined the response of benthic foraminifers to sea level change in Ashmore Trough, and Febo et al. (2008) determined the $\delta^{13}C$ and C/N ratio for sediment samples from Pandora Trough to constrain whether the source of organic-carbon was derived from

marine organic matter, C3 plants, or C4 plants. However, the palynological record has not yet been studied. Performing palynology, including analysis of pollen and spores from the terrestrial realm and dinoflagellate cysts from the marine realm, on material obtained from cores covering the latest marine transgression and sea level highstand should allow us to better reconstruct climate and sea level changes for the last 14.5 kyr.

Objective 2: Improve understanding of sedimentation dynamics using palynology as a tool to assess depositional environments.

In addition to its widely accepted use in biostratigraphic zonation (Warny and Wrenn, 2002; Garzon et al., 2012) and understanding climatic changes (Warny et al., 2009; Feakins et al., 2012), palynology and palynofacies analysis can also be utilized to better understand sedimentation dynamics and energy of the environment (Batten, 1983; Gregory and Hart, 1990; Pocknall and Beggs, 1990; Batten, 1996; Oboh-Ikuenobe et al., 1997; Oboh-Ikuenobe et al., 1998; Jaramillo and Oboh-Ikuenobe, 1999; Courtinat et al., 2002; Ibrahim, 2002; Schiøler et al., 2002; Roncaglia, 2004; Roncaglia and Kuijpers, 2004; Carvalho et al., 2006; Pross et al., 2006; Zobaa et al., 2008; Skupien and Mohamed, 2008; Schiøler et al., 2010). Studying modern palynomorphs in the Gulf of Papua could greatly improve understanding of the sedimentation regime, which could provide assistance in paleoenvironmental interpretation. Palynofacies analysis has been shown by multiple authors to assist in paleoenvironment interpretation and further understanding of sedimentation and energy of the environment (e.g., Lorente, 1990; van der Zwan, 1990; Batten, 1996; Jaramillo and Oboh-Ikuenobe, 1999; Ibrahim, 2002; Schiøler et al., 2002; Carvalho et al., 2006). Because the modern coring sites for this dissertation span from river mouth to continental shelf to the deep ocean basin, we believe they will effectively illustrate variations in common marine environments of deposition, including tidal deltas,

clinoforms (topset, foreset, and bottomset deposits), turbidites, and hemipelagic/pelagic ocean basin deposits.

Objective 3: Apply palynology as a tool to assess biodiversity and vegetation distribution at present and in the past.

Although it occupies less than 1% of the world's landmass, Papua New Guinea is host to up to 7% of the world's biodiversity. Over 6,700 endemic species reside on the island, but those are only the ones that have been identified. Countless more endemic species could call the island home, but the difficulty of obtaining access to the remote reaches of Papua New Guinea has limited researchers in finding them. Additionally, lack of qualified scientists has created problems in sorting and taxonomically cataloging organisms that have already been found (Kaluwin et al., 2000). Without knowing more about Papua New Guinea's rich biodiversity, it is difficult to protect threatened and potentially threatened species. Palynology has been shown to be an effective tool in determining vegetation composition on Papua New Guinea, but this research thus far has only focused restricted regions of the island and is generally associated with archaeological sites (Flenley, 1979; Walker and Flenley, 1979; Hope et al., 1983; Flenley, 1988; Hope et al., 1988; Flenley, 1998; Haberle et al., 2001; Haberle and Ledru, 2001; Denham et al., 2003; Hope et al., 2004; Jago and Boyd, 2005; Kershaw et al., 2007; Haberle, 2007; Hope, 2008; Hope, 2009). Although assaying vegetation composition using the marine samples from the Gulf of Papua is not optimal, as only a fraction of the pollen produced will make it to the sediment, this is the only way to have a snapshot of a wide range of locations (including those little-influenced by man). Because of the high fluvial discharge (365 million tons/yr; Wolanski et al., 1995), the Gulf of Papua receives a large concentration of pollen and spores produced by terrestrial vegetation. This should

give us some trends in changes in species diversity through time. A long lake or swamp core covering the last 14,500 years would be more optimal (as used by Haberle and Ledru (2001) and Hope (2009), for example) for such a study, but the approach proposed should provide a more regional picture of vegetation change, as well as allow us to reconstruct oceanographic changes with marine dinoflagellate cysts which cannot be done with terrestrial studies.

Objective 4: Determine the widespread human impact on Papua New Guinea vegetation spatially and temporally.

The interplay between humans, vegetation, and climate is complex. Numerous authors (Flenley, 1979; Walker and Flenley, 1979; Hope et al., 1983; Flenley, 1988; Hope et al., 1988; Flenley, 1998; Haberle et al., 2001; Haberle and Ledru, 2001; Denham et al., 2003; Hope et al., 2004; Jago and Boyd, 2005; Kershaw et al., 2007; Haberle, 2007; Hope, 2008; Hope, 2009) have already examined the influence of human occupation and changing climate on vegetation structure in the latest Quaternary using the terrestrial vegetation record, including pollen, spores, phytoliths, and plant macrofossils. We plan to analyze pollen and spore distribution in the Gulf of Papua to determine the degree to which it has been affected by humans and the extent to which it is controlled by climate. Both human impact and climate change alter biodiversity, but it can be difficult to separate out what effects are due to humans and what are due to climate. In general, man has acted to lessen biodiversity since his occupation on the island, and he has introduced numerous agricultural species that can be observed in the palynological record. Climate change, on the other hand, results in fluctuations in biodiversity, lessening it in glacial periods and increasing it in interglacial periods. Detailed analysis that will be performed in this project will further elucidate how climate and humanity interact to produce the

observed vegetation distribution. At present, Papua New Guinea's biodiversity is more severely threatened by human development than climate change, but this influence play can change as climate continues warming. Man lived in relative harmony for approximately 30,000 years with the island's flora and fauna from his initial occupation 40,000 B.P (Denham et al., 2009). Hunting and gathering during that period was his primary subsistence strategy, and comparatively little land was cleared. Beginning approximately 9,000 years ago, the development of agricultural practices such as burning and clearing land for crop growth became widespread (Hope et al., 1983; Denham et al., 2003). Planting crops and destroying natural forests for agricultural purposes has used approximately 6,000,000 hectares of land on Papua New Guinea. Logging for economic gain in more recent periods has used an additional 1,000,000 hectares of forestland (Kaluwin et al. 2000). The loss of natural forest vegetation and replacement with agricultural crops such as corn (*Zea mays*), bananas (*Musa* spp.), sweet potato *(Ipomoea batatas*), sugar cane (*Saccharum officianum*), and taro (*Colocasia esculenta*) appear in Papua New Guinea's terrestrial palynological record (e.g., Walker and Flenley, 1979; Lentfer and Torrence, 2007; Lentfer et al. 2010). Loss of tropical rainforest species and the appearance of human cultivars, such as the species mentioned above, are expected in palynological material in this project from 9,000 years BP. After determining regional vegetation diversity in Objective 3, we plan to determine the regional extent to which that biodiversity has been affected by human influence by analyzing samples from cores MD-50, MV-41, and MV-46 which contain a record of the last 14,500 years (Figure 1.1).

References

Aalto, R., Lauer, J.W., Dietrich, W.E., 2008. Spatial and temporal dynamics of sediment accumulation and exchange along Strickfland River floodplains (Papua New

Guinea) over decadal-to-centennial timescales. Journal of Geophysical Research 113, F01S04, doi:10.1029/2006JF000627.

Abbott, L.D., 1995. Neogene tectonic reconstruction of the Adelbert-Finisterre-New Britain collision, northern Papua New Guinea. Journal of Southeast Asian Earth Sciences 11, 33-51.

Aharon, P., Chappell, J., 1986. Oxygen isotopes, sea level changes and the temperature history of a coral reef environemnt in New Guinea over the last 105 years. Palaeogeography, Palaeoclimatology, Palaeoecology 56, 337-379.

Alin, S.R., Aalto, R., Goni, M.A., Richey, J.E., Dietrich, W.E., 2008. Biogeochemical characterization of carbon sources in the Strickland and Fly rivers, Papua New Guinea. Journal of Geophysical Research 113, F01S05, doi:10.1029/2006JF000625.

Aller, J.Y., Alongi, D.M., Aller, R.C., 2008a. Biological indicators of sedimentary dynamics in the central Gulf of Papua: seasonal and decadal perspectives. Journal of Geophysical Research 113, F01S08, doi:10.1029/2007JF000823.

Aller, R.C., Blair, N.E., Brunskill, G.J., 2008b. Early diagenetic cycling, incineration, and burial of sedimentary organic carbon in the central Gulf of Papua (Papua New Guinea). Journal of Geophysical Research 113, F01S09, doi:10.1029/2006JF000689.

Andresen, N., Reijmer, J.J.G., Droxler, A.W., 2003. Timing and distribution of calciturbidites around a deeply submerged carbonate platform in a seismically active setting (Pedro Bank, Northern Nicaragua Rise Caribbean Sea). International Journal of Earth Science 92, 573-592.

Batten, D.J., 1983. Identification of amorphous sedimentary organic matter by transmitted light microscopy. Geological Society of London Special Publications 12, 275-287.

Batten, D.J., 1996. Chapter 26A. Palynofacies and palaeoenvironmental interpretation, In: Jansonius, J., McGregor, D.C. (Eds.), Palynology: Principles and Applications. American Association of Stratigraphic Palynologists Foundation, Salt Lake City, pp. 1011-1064.

Bouma, A.H., 1982. Intraslope basins in the northwest Gulf of Mexico: a key to ancient submarine canyons and fans, In: Watkins, J.S., Drake, C.L. (Eds.), Studies in Continental Margin Geology. American Association of Petroleum Geologists Memoires Series, Houston, pp. 567-581.

Boyd, W.E., Lentfer, C.J., Torrence, R., 1998. Phytolith analysis for a wet tropics environment: methodological issues and implications for the archaeology of Garua Island, West New Britain, Papua New Guinea. Palynology 22, 213-228.

Brass, L., 1941. The 1938-39 expedition to the Snow Mountains, Netherlands New Guinea. Journal of Arnold Arbor 22, 271-342.

Brass, L., 1964. Results of the Archibold Expeditions No. 86, summary of the sixth Archibold Expedition to New Guinea (1959), Bulletin of the American Museum of Natural History 127, 145-216.

Brown, C.M., Pigram, C.J., Skwarko, S.K., 1980. Mesozoic stratigraphy and geological history of Papua New Guinea. Palaeogeography, Palaeoclimatology, Palaeoecology 29, 301-322.

Brunskill, G.J., Woolfe, K.J., Zagorskis, I., 1995. Distribution of riverine sediment chemistry on the shelf, slope and rise of the Gulf of Papua. Geo-Marine Letters 15, 160-165.

Cande, S.C., Mutter, J.C., 1982. A revised identification of the oldest sea-floor anomalies between Australia and Antarctica. Earth and Planetary Science Letters 58, 151-160.

Caratini, C., 1992. Mangrove pollen in marine Quaternary sediments: marker of regional climatic evolution and global eustatic changes, In: Singh, K.P., Singh, J.S. (Eds.), Tropical Ecosystems: Ecology and Management. Wiley Eastern Limited, New Delhi, pp. 349-357.

Carson, B.E., Francis, J.M., Leckie, R.M., Droxler, A.W., Dickens, G.R., Jorry, S.J., Bentley, S.J. Sr., Peterson, L.C., Opdyke, B.N., 2008. Benthic foraminiferal response to sea level change in the mixed siliciclastic-carbonate system of southern Ashmore Trough (Gulf of Papua). Journal of Geophysical Research 113, F01S20, doi:10.1029/2006JF000629.

Carvalho, M.A., Filho, J.G.M., Menezes, T.R., 2006. Paleoenvironmental reconstruction based on palynofacies analysis of the Aptian-Albian succession of the Sergipe Basin, Northeastern Brazil. Marine Micropaleontology 59, 56-81.

Christie-Blick, N., Driscoll, N.W., 1995. Sequence Stratigraphy. Annual Review of Earth and Planetary Sciences 23, 451-478.

CIA The World Factbook, 2014. Papua New Guinea. Central Intelligence Agency, Washington, D.C. 22 February 2015. Available from: https://www.cia.gov/library/publications/the-world-factbook/geos/pp.html.

Clark, P.U., Marshall, A., McCabe, A., Mix, A.C., Weaver, A.J., 2004. Rapid rise of sea level 19000 years ago and its global implications. Science 304, 1141-1144.

Conn, B.J., editor, 1995. Handbooks of the Flora of New Guinea, Volume III. Melbourne University Press, Victoria.

Courtinat, B., Rio, M., Malartre, F., 2002. Palynofacies of marginal marine deposits: the Rhaetian of the east margin of the Massif Central (France). Revue de Micropaléontologie 45, 47-55.

Crockett, J.S., Nittrouer, C.A., Ogston, A.S., Naar, D.F., Donahue, B.T., 2008. Morphology and filling of incised submarine valleys on the continental shelf near the mouth of the Fly River, Gulf of Papua. Journal of Geophysical Research 113, F01S12, doi:10/1029/2006JF000674.

Dalrymple, R.W., Baker, E.K., Harris, P.T., Hughes, M.G., 2003. Sedimentology and stratigraphy of a tide-dominated foreland-basin delta (Fly River, Papua New Guinea), Tropical Deltas of Southeast Asia – Sedimentology, Stratigraphy, and Petroleum Geology. SEPM Special Publication No. 76, pp. 147-173.

Daniell, J.J., 2008. Development of a bathymetric grid for the Gulf of Papua and adjacent areas: a note describing its development. Journal of Geophysical Research 113, F01S15, doi:10.1029/2006JF000673.

Davey, R.J., 1987. Palynological zonation of the Lower Cretaceous, Upper and upper most Middle Jurassic in the northwestern Papuan Basin of Papua New Guinea. Geological Survey of Papua New Guinea Memoir 13, 33.

David, B., Fairbairn, A., Aplin, K., Murepe, L., Green, M., Stanisic, J., Weisler, M., Simala, D., Kokents, T., Dop, J., Muke, J., 2007. OJP, a Terminal Pleistocene archaeological site from the Gulf Province lowlands, Papua New Guinea. Archaeology in Oceania 42, 31-33.

David, B., Mcniven, I., Mitchell, R., Orr, M., Haberle, S., Brady, L., Crouch, J., 2004. Badu 15 and the Papuan-Austronesian settlement of Torres Strait. Archaeology in Oceania 39, 65-78.

Davies, H.L., 2012. The geology of New Guinea – The cordilleran margin of the Australian continent. Episodes 35, 87-102.

Davies, P.J., Symonds, P.A., Feary, D.A., Pigram, C.J., 1989. The evolution of the carbonate platforms of Northeast Australia, In: Crevello, P.D. (Ed.), Controls on Carbonate Platform and Basin Development, SEPM Special Publication vol. 44, Tulsa, pp. 233-258.

Day, G., Dietrich, W.E., Rowland, J.C., Marshall, A., 2008. The depositional web on the floodplain of the Fly River, Papua New Guinea. Journal of Geophysical Research 113, F01S02, doi:10.1029/2006JF000622.

Denham, T., Fullagar, R., Head, L., 2009. Plant exploitation on Sahul: from colonisation to the emergence of regional specialisation during the Holocene. Quaternary International 202, 29-40.

Denham, T., Haberle, S.G., 2008. Agricultural emergence and transformation in the Upper Wahgi Valley, Papua New Guinea during the Holocene: theory, method and practice. The Holocene 18, 499-514.

Denham, T., Mooney, S., 2008. Human-environment interactions in Australia and New Guinea during the Holocene. The Holocene 18, 365-371.

Denham, T.P., Haberle, S.G., Lentfer, C.J., Fullagar, R., Field, J., Therin, M., Porch, N., Winsborough, B., 2003. Origins of agriculture at Kuk Swamp in the highlands of New Guinea. Science 301, 189-193.

Dickens, G.R., Droxler, A.W., Bentley, S.J. Sr., Peterson, L.C., Opdyke, B.N., Beaufort, L., Daniell, J.J., Febo, L.A., Francis, J.M., Harris, P.T., Jorry, S., Mallarino, G., McFadden, M., Muhammad, Z., Carson, B., Patterson, L., Tcherepanov, E., Zarikian, C.A., 2006. Sediment accumulation on the shelf edges, adjacent slopes, and basin floors of the Gulf of Papua. NSF-MARGINS Newsletter 16, 1-4.

Droxler, A.W., Schlager, W., 1985. Glacial versus interglacial sedimentation rates and turbidite frequency in the Bahamas. Geology 13, 799-802.

Ellison, J., 2005. Holocene palynology and sea-level change in two estuaries in Southern Irian Jaya. Palaeogeography, Palaeoclimatology, Palaeoecology 220, 291-309.

Ellison, J., 2008. Long-term retrospection on mangrove development using sediment cores and pollen analysis: a review. Aquatic Botany 89, 93-104.

Ewing, J.J., Houtz, R.E., Ludwig, W.J., 1970. Sediment distribution in the Coral Sea. Journal of Geophysical Research 75, 1963-1972.

Fairbairn, A.S., Hope, G.S., Summerhayes, G.R., 2006. Pleistocene Occupation of New Guinea's highland and subalpine environments. World Archaeology 38, 371-386.

Fairbanks, R.G., 1989. A 17,000 year glacio-eustatic sea level record; influence of glacial melting rates on the Younger Dryas event and deep ocean circulation. Nature 342, 637-642.

Feakins, S.J., Warny, S., Lee, J.-E., 2012. Hydrologic cycling over Antarctica during the Middle Miocene warming. Nature Geoscience 5, 557-560.

Febo, L.A., 2007. Paleoceanography of the Gulf of Papua using multiple geophysical and micropaleontological proxies, Ph.D. thesis, Department of Geology & Geophysics. Louisiana State University, p. 163.

Febo, L.A., Bentley, S.J. Sr., Wrenn, J.H., Droxler, A.W., Dickens, G.R., Peterson, L.C., Opdyke, B.N., 2008. Late Pleistocene and Holocene sedimentation, organic-carbon delivery and paleoclimatic inferences on the continental slope of the northern Pandora Trough. Journal of Geophysical Research 113, F01S18, doi:10/1029/2006JF000677.

Flenley, J.R., 1969. The Vegetation of the Wabag Region, New Guinea Highlands: A Numerical Study. Journal of Ecology 57, 465-490.

Flenley, J.R., 1972. Evidence of Quaternary Vegetational Change in New Guinea, In: Ashton, P., Ashton, M. (Eds.), The Quaternary Era in Malesia. Transactions of the Second Aberdeen Hull Symposium on Malesian Ecology. Institute for South-East Asian Biology, University of Hull, pp. 99-109.

Flenley, J.R., 1979. The Late Quaternary vegetational history of the equatorial mountains. Progress in Physical Geography 3, 488-509.

Flenley, J.R., 1984. Late Quaternary changes of vegetation and climate in the Malesian Mountains. Erdwissenschaftliche Forschung 18, 261-267.

Flenley, J.R., 1988. Palynological Evidence for Land Uses Changes in South-East Asia. Journal of Biogeography 15, 185-197.

Flenley, J.R., 1997. The Quaternary in the tropics: an introduction. Journal of Quaternary Science 12, 345-346.

Flenley, J.R., 1998. Tropical forests under the climates of the last 30,000 years. Climatic Change 39, 177-197.

Flood, R., Piper, D., 1997. Amazon fan sedimentation: the relationship to equatorial climate change, continental denudation, and sea-level fluctuations, In: Flood, R.D., Piper, D.J.W., Klaus, A., Peterson, L.C. (Eds.), Proceedings of the Ocean Drilling Program Scientific Results no. 155, pp. 653-675.

Francis, J.M., Daniell, J.J., Droxler, A.W., Dickens, G.R., Bentley, S.J. Sr., Peterson, L.C., Opdyke, B.N., Beaufort, L., 2008. Deep water geomorphology of the mixed siliciclastic-carbonate system, Gulf of Papua. Journal of Geophysical Research 113. F01S16, doi:10.1029/2007JF000851.

Gardner, J.V., 1970. Submarine geology of the Western Coral Sea. Geological Society of America Bulletin 81, 2599-2614.

Garzon, S., Warny, S., Bart, P.J., 2012. Sequence stratigraphic interpretation of Santonian-Maastrichtian strata from the Upper Magdalena oil-producing basin, central Colombia: a palynological approach. Palynology 36, 112-133.

Gibbs, R.J., 1981. Sites of river-derived sedimentation in the ocean. Geology 9, 77-80.

Gillison, A.N., 1969. Plant succession in an irregularly fired grassland area – Doma Peaks Region, Papua. Journal of Ecology 57, 415-428.

Glaser, K.S., Droxler, A.W., 1993. Controls and development of late Quaternary periplatform carbonate stratigraphy in Walton Basin (Northern Nicarauga Rise Caribbean Sea). Paleoceanography 8, 243-274.

Goni, M.A., Monacci, N., Gisewhite, R., Crockett, J., Nittrouer, C., Ogston, A., Alin, S.R., Aalto, R., 2008. Terrigenous organic matter in sediments from the Fly River delta-clinoform system (Papua New Guinea). Journal of Geophysical Research 113, F01S10, doi:10.1029/2006JF000653.

Gosden, C., 1995. Aboriculture and agriculture in coastal Papua New Guinea. Antiquity 69, 807-817.

Gregory, W.A., Hart, G.F., 1990. Subdivision of Wilcox Group (Sabinian) argillaceous sediments using particulate organic matter. Palynology 14, 105-121.

Guilderson, T.P., Fairbanks, R.G., Rubenstone, J.L., 1994. Tropical temperature variations since 20,000 years ago: modulating interhemispheric climate change. Science 263, 663-665.

Haberle, S.G., 1995. Identification of cultivated *Pandanus* and *Colocasia* in pollen records and the implications for the study of early agriculture in New Guinea. Vegetation History and Archaeobotany 4, 195-210.

Haberle, S.G., 1996. Palaeoenvironmental changes in the eastern highlands of Papua New Guinea. Archaeology in Oceania 31, 1-11.

Haberle, S.G., 1998. Dating the evidence for agricultural change in the highlands of New Guinea: the last 2000 years. Australian Archaeology 47, 1-19.

Haberle, S.G., 2003. The emergence of an agricultural landscape in the highlands of New Guinea. Archaeology in Oceania 38, 149-158.

Haberle, S.G., 2007. Prehistoric human impact on rainforest biodiversity in highland Papua New Guinea. Philosophical Transactions of the Royal Society London Series B 362, 219-228.

Haberle, S.G., Hope, G.S., van der kaars, S., 2001. Biomass burning in Indonesia and Papua New Guinea: natural and human-induced fire events in the fossil record. Palaeogeography, Palaeoclimatology, Palaeoecology 171, 259-268.

Haberle, S.G., Ledru, M.-P., 2001. Correlations among charcoal records of fires from the past 16,000 years in Indonesia, Papua New Guinea, and Central and South America. Quaternary Research 55, 97-104.

Haberle, S.G., Lentfer, C., O'Donnell, S., Denham, T., 2012. The palaeoenvironments of Kuk Swamp from the beginnings of agriculture in the highlands of Papua New Guinea. Quaternary International 249, 129-139.

Harris, P.T., 1994. Incised valleys and backstepping deltaic deposits in a foreland-basin setting, Torres Strait and Gulf of Papua, Australia, In: Dalrymple, R.W., Boyd, R., Zaitlin, B.A. (Eds.), Incised Valley Systems: Origin and Sedimentary Sequences, SEPM Special Publication No. 51., Society for Sedimentary Geology, pp. 97-108.

Harris, P.T., Baker, E.K., Cole, A.R., Short, S.A., 1993. Preliminary study of sedimentation in the tidally dominated Fly River Delta, Gulf of Papua. Continental Shelf Research 13, 441-472.

Harris, P.T., Pattiaratchi, C.B., Keene, J.B., Dalrymple, R.W., Gardner, J.V., Baker, E.K., Cole, A.R., Mitchell, D., Gibbs, P., Schroeder, W.W., 1996. Late Quaternary deltaic and carbonate sedimentation in the Gulf of Papua foreland basin: response to sea level change. Journal of Sedimentary Research 66, 801-819.

Henty, E.E., 1995. Handbooks of the Flora of New Guinea, Volume II. Melbourne University Press, Victoria, p. 286.

Heusser, L.E., 1978. Spores and pollen in the marine realm, In: Haq, B., Boersma, A. (Eds.), Introduction to Marine Micropaleontology. Elsevier, New York, pp. 327-340.

Hoorn, C., 2006. Mangrove forests and marine incursions in Neogene Amazonia (lower Apaporis River, Colombia). Palaios 21, 197-209.

Hope, G., 1983. The vegetational changes of the last 20,000 years at Telefomin, Papua New Guinea. Singapore Journal of Tropical Geography 4, 25-33.

Hope, G., Gillieson, D., Head, J., 1988. A comparison of sedimentation and environmental change in New Guinea shallow lakes. Journal of Biogeography 15, 603-618.

Hope, G., Kershaw, A.P., van der kaars, S., Xiangjun, S., Liew, P.-M., Heusser, L.E., Takahara, H., McGlone, M., Miyoshi, N., Moss, P.T., 2004. History of vegetation and habitat change in the Austral-Asia region. Quaternary International 118-119, 103-126.

Hope, G.S., 2008. Palaeoecology and Resilience in Melanesia: How can palaeoecology contribute to climate change response planning? In: Leisz, S.J., Burnett, J.B. (Eds.), Climate Change and Biodiversty in Melanesia. Bishop Museum Technical Report, Honolulu, p. 14.

Hope, G.S., 2009. Environmental change and fire in the Owen Stanley Ranges, Papua New Guinea. Quaternary Science Reviews 28, 2261-2276.

Hope, G.S., Golson, J., Allen, J., 1983. Palaeoecology and prehistory in New Guinea. Journal of Human Evolution 12, 37-60.

Hope, G.S., Peterson, J.A., 1975. Glaciation and vegetation in the high New Guinea mountains. Bulletin of the Royal Society of New Zealand 13, 153-162.

Horrocks, M., Bulmer, S., Gardner, R.O., 2008. Plant microfossils in prehistoric archaeological deposits from Yuku rock shelter, Western Highlands, Papua New Guinea. Journal of Archaeological Science 35, 290-301.

Howell, A.L., Bentley, S.J. Sr., Xu, K., Ferrell, R.E.J., Muhammad, Z., Septama, E., 2014. Fine sediment mineralogy as a tracer of latest Quaternary sediment delivery to a dynamic continental margin: Pandora Trough, Gulf of Papua, Papua New Guinea. Marine Geology 357, 108-122.

Ibrahim, M.I.A., 2002. Late Albian-Middle Cenomanian palynofacies and palynostratigraphy, Abu Gharadig-5 well, Western Desert, Egypt. Cretaceous Research 23, 775-788.

Jago, L., Boyd, W.E., 2005. How a wet tropical rainforest copes with repeated volcanic destruction. Quaternary International 64, 399-406.

Jansonius, J., McGregor, D.C., 1996. Chapter 1. Introduction, In: Jansonius, J., McGregor, D.C. (Eds.), Palynology: Principles and Applications. American Association of Stratigraphic Palynologists Foundation, Salt Lake City, pp. 1-10.

Jaramillo, C.A., Oboh-Ikuenobe, F.E., 1999. Sequence stratigraphic interpretations from palynofacies, dinocyst and lithological data of Upper Eocene-Lower Oligocene strata in southern Mississippi and Alabama, U.S. Gulf Coast. Palaeogeography, Palaeoclimatology, Palaeoecology 145, 259-302.

Johns, R.J., 1989. The influence of drought on tropical rainforest vegetation in Papua New Guinea. Mountain Research and Development 9, 248-251.

Jorry, S.J., Droxler, A.W., Francis, J.M., 2010. Deepwater carbonate deposition in response to re-flooding of carbonate bank and atoll-tops at glacial terminations. Quaternary Science Reviews 29, 2010-2026.

Jorry, S.J., Droxler, A.W., Mallarino, G., Dickens, G.R., Bentley, S.J. Sr., Beaufort, L., Peterson, L.C., Opdyke, B.N., 2008. Bundled turbidite deposition in the central Pandora Trough (Gulf of Papua) since Last Glacial Maximum: linking sediment nature and accumulation to sea level fluctuations at millennial timescale. Journal of Geophysical Research 113, F01S19, doi:10.1029/2006JF000649.

Kaluwin, C., Ashton, J., Saulei, S., 2000. Papua New Guinea Initial National Communication Under the United Nations Framework Convention on Climate Change. Government of Papua New Guinea Port Moresby, p. 83.

Kawahata, H., Gupta, L.P., 2004. Settling Particles Flux in Response to El Niño/Southern Oscillation (ENSO) in the Equatorial Pacific, In: Shiyomi, M., Kawahata, H., Koizumi, H., Tsuda, A., Awaya, Y. (Eds.), Global Environmental Change in the Ocean and on Land. TERRAPUB, Tokyo, pp. 95-108.

Keen, T.R., Ko, D.S., Slingerland, R.L., Riedlinger, S., Flynn, P., 2006. Potential transport pathways of terrigenous material in the Gulf of Papua. Geophysical Research Letters 33, L04608, doi:10.1029/2005GL025416.

Kershaw, A.P., 1994. Pleistocene vegetation of the humid tropics of northeastern Queensland, Australia. Palaeogeography, Palaeoclimatology, Palaeoecology 109, 399-412.

Kershaw, A.P., van der kaars, S., Flenley, J.R., 2007. Chapter 4: The Quaternary history of far eastern rainforests, In: Bush, M.B., Flenley, J.R., Gosling, W.D. (Eds.), Tropical Rainforest Responses to Climatic Change. Springer, Berlin, p. 454.

Kubo, Y., Syvitski, J.P.M., 2006. Inverse modeling of post Last Glacial Maximum transgressive sedimentation using 2D-SedFlux: application to the Northern Adriatic Sea. Marine Geology 234, 233-243.

Lambeck, K., Chappell, J., 2001. Sea level change through the last glacial cycle. Science 292, 679-686.

Laskar, J., Robutel, P., Joutel, F., Gastineau, M., Correia, A.C.M., Levrard, B., 2004. A long-term numerical solution for the insolation quantities of the Earth. Astronomy and Astrophysics 428, 261-285.

Lauer, J.W., Parker, G., Dietrich, W.E., 2008. Response of the Strickland and Fly River confluence to postglacial sea level rise. Journal of Geophysical Research 113, F01S06, doi:10.1029/2006JF000626.

Lentfer, C., Pavlides, C., Specht, J., 2010. Natural and human impacts in a 35,000-year history in central New Britain, Papua New Guinea. Quaternary Science Reviews 29, 3750-3767.

Lentfer, C., Torrence, R., 2007. Holocene volcanic activity, vegetation succession, and ancient human land use: unraveling the interactions on Garua Island, Papua New Guinea. Review of Palaeobotany and Palynology 143, 83-105.

Lisiecki, L.E., Raymo, M.E., 2005. A Pliocene-Pleistocene stack of 57 globally distributed benthic $\delta^{18}O$ records. Paleoceanography 20.

Liu, J.P., Milliman, J.D., Gao, S., Cheng, P., 2004. Holocene development of the Yellow River's subaqueous delta, North Yellow Sea. Marine Geology 209, 45-67.

Lorente, M.A., 1990. Textural characteristics of organic matter in several subenvironments of the Orinoco Upper Delta. Geologie en Mijnbouw 69, 263-278.

MacFarlane, J.W., 1980. Surface and bottom sea currents in the Gulf of Papua and Western Coral Sea, Department of Primary Industries Research Bulletin No. 27, Port Moresby, p. 132.

Machida, H., Blong, R., Specht, J., Torrence, R., Moriwaki, H., Hayakawa, Y., Talai, B., Lolock, D., Pain, C., 1996. Holocene explosive eruptions of Witori and Dakataua caldera volcanoes in West New Britain, Papua New Guinea. Quaternary International 34-36, 65-78.

Mallarino, G., Beaubouef, R.T., Droxler, A.W., Abreu, V., Labeyrie, L., 2006. Sea-level influence on the nature and timing of a minibasin sedimentary fill (northwestern Gulf of Mexico). AAPG Bulletin 90, 1089-1119.

Martin, D.P., Nittrouer, C.A., Ogston, A.S., Crockett, J.S., 2008. Tidal and seasonal dynamics of a muddy inner shelf environment, Gulf of Papua. Journal of Geophysical Research 113, F01S07, doi:10.1029/2006JF000681.

Maslin, M., Mikkelsen, N., 1997. Amazon fan mass transport deposits and underlying intergalcial deposits: age estimates and fan dynamics, In: Flood, R.D., Piper, D.J.W., Klaus, A., Peterson, L.C. (Eds.), Proceedings of the Ocean Drilling Program Scientific Results 155, pp. 353-365.

McAlpine, J.R., Freyne, D.F., 2001. Land use change and intensification in Papua New Guinea 1975-1996. Asia Pacific Viewpoint 42, 209-218.

McAlpine, J.R., Keig, G., 1983. Climate of Papua New Guinea. Australian National University Press, Canberra.

Miller, K.G., Kominz, M.A., Browning, J.V., Wright, J.D., Mountain, G.S., Katz, M.E., Sugarman, P.J., Cramer, B.S., Christie-Blick, N., Pekar, S.F., 2005. The Phanerozoic record of global sea-level change. Science 310, 1293-1298.

Milliman, J.D., 1995. Sediment discharge to the ocean from small mountainous rivers: the New Guinea example. Geo-Marine Letters 15, 127-133.

Morley, R.J., Morley, H.P., 2011. Neogene climate history of the Makassar Straits, Indonesia. Geological Society of London Special Publications 355, 319-322.

Morley, R.J., Morley, H.P., Restrepo-Pace, P., 2003. Unravelling the tectonically-controlled stratigraphy of the West Natuna Basin by means of palaeo-derived Mid Tertiary climate changes, Proceedings of the Twenty-ninth Annual Convention and Exhibition of the Indonesian Petroleum Association, p. 24.

Morley, R.J., Morley, H.P., Wonders, A.A.H., Sukarno, van der kaars, S., 2004. Biostratigraphy of modern (Holocene and Late Pleistocene) sediment cores from the Makassar Straits, Proceedings of the Deepwater and Frontier Exploration in Asia and Australasia Symposium, Indonesian Petroleum Association, p. 11.

Morley, R.J., Swiecicki, T., Pham, D.T.T., 2011. A sequence stratigraphic framework for the Sunda region, based on integration of biostratigraphic, lithological and seismic data from Nam Con Son Basin, Vietnam, Proceedings of the Thirty-fifth Annual Convention and Exhibition of the Indonesian Petroleum Association, p. 22.

Moss, P.T., Kershaw, A.P., Grindrod, J., 2005. Pollen transport and deposition in riverine and marine environments within the humid tropics of northeastern Australia. Review of Palaeobotany and Palynology 134, 55-69.

Muhammad, Z., Bentley, S.J. Sr., Febo, L.A., Droxler, A.W., Dickens, G.R., Peterson, L.C., Opdyke, B.N., 2008. Excess ^{210}Pb inventories and fluxes along the continental slope and basins of the Gulf of Papua. Journal of Geophysical Research 113, F01S17, doi:10.1029/JF000676.

Muke, J., Mandui, H., 2003. In the shadows of Kuk: evidence for prehistoric agriculture at Kana, Wahgi Valley, Papua New Guinea. Archaeology in Oceania 38, 177-185.

Norvick, M.S., Smith, M.S., Power, M.R., 2001. The plate tectonic evolution of Eastern Australasia guided by the stratigraphy of the Gippsland Basin, In: Hill, K.C., Bernecker, T. (Eds.), Eastern Australasian Basins Symposium 2001: A Refocused Energy Perspective for the Future. Petroleum Exploration Society of Australia, Melbourne, pp. 15-23.

NSF MARGINS Program Science Plans 2004. MARGINS Office, Columbia University, New York.

Oboh-Ikuenobe, F.E., Yepes, O., Gregg, J.M., 1998. 25. Palynostratigraphy, palynofacies, and thermal maturation of Cretaceous-Paleogene sediments from the Côte D'Ivoire-Ghana transform margin. Proceedings of the Ocean Drilling Program Scientific Results 159, 277-318.

Oboh-Ikuenobe, F.E., Yepes, O., Mascle, J., Clift, P., Akamaluk, T., Ask, M., Barton, E., Bellier, J.-P., Benkhelil, J., Brantuoh, E., et al., 1997. Palynofacies analysis of sediments from the Côte d'Ivoire-Ghana transform margin: preliminary correlation with some regional events in the Equatorial Atlantic. Palaeogeography, Palaeoclimatology, Palaeoecology 129, 291-314.

Ogston, A.S., Sternberg, R.W., Nittrouer, C.A., Martin, D.P., Goni, M.A., Crockett, J.S., 2008. Sediment delivery from the Fly River tidally dominated delta to the nearshore marine environment and the impact of El Niño. Journal of Geophysical Research 113, F01S11, doi:10.1029/2006JF000669.

Paijmans, K., 1975. Explanatory notes to the vegetation map of Papua New Guinea. Commonwealth Scientific and Industrial Research Organization, Melbourne.

Papua New Guinea Chamber of Mines and Petroleum, 2012. Petroleum in PNG. Papua New Guinea Chamber of Mines and Petroleum, Port Moresby. 22 February 2015. Available from: http://pngchamberminpet.com.pg/petroleum-in-png/.

Patterson, L., 2006. Petrological and geochemical investigations of deep sea turbidite sands in the Pandora and Moresby Troughs: Source to Sink Papua New Guinea Focus Area, M.Sc. Thesis, Department of Geology and Geophysics. Louisiana State University.

Pigram, C.J., Davies, H.L., 1987. Terranes and accretion history of the New Guinea orogen. Bureau of Mineral Resources Journal of Australian Geology and Geophysics 107, 331-353.

Pigram, C.J., Davies, P.J., Feary, D.A., Symonds, P.A., 1989. Tectonic controls on carbonate platform evolution in southern Papua New Guinea: Passive margin to foreland basin. Geology 17, 199-202.

Playford, G., 1982. Neogene palynomorphs from the Huon Peninsula, Papua New Guinea. Palynology 6, 29-54.

Playford, G., Rigby, J.F., 2008. Permian palynoflora of the Ainim and Aiduna formations, West Papua. Revista Española de Micropaleontología 40, 1-57.

Pocknall, D.T., Beggs, J.M., 1990. Palynofacies as a tool for the interpretation of depositional environments in the Waikato and Taranaki Basins, New Zealand, 1989 New Zealand Oil Exploration Conference. Petroleum and Geothermal Unit, Ministry of Commerce, Wellington.

Posamentier, H.W., Vail, P.R., 1988. Eustatic controls on clastic deposition II – sequence and systems tract models, In: Wilgus, C.K., Hastings, B.S., Kendall, C.G.S.C., Posamentier, H.W., Ross, C.A., van Wagoner, J.C. (Eds.), Sea-level Changes: An Integrated Approach, SEPM Special Publications No. 42, Tulsa.

Powell, J.M., 1982. Plant resources and palaeobotanical evidence for plant use in the Papua New Guinea Highlands. Archaeology in Oceania 17, 28-37.

Powell, J.M., Kulunga, A., Moge, R., Pono, C., Zimike, F., Golson, J., 1975. Agricultural traditions on the Mount Hagen area, In: Occasional Paper No. 12, Department of Geography, University of Papua New Guinea, Port Moresby.

Pross, J., Link, E., Rug, M., Aigner, T., 2006. Delineating sequence stratigraphic patterns in deeper ramp carbonates: quantitative palynofacies data from the Upper Jurassic (Kimmeridgian) of southwest Germany. Journal of Sedimentary Research 76, 524-538.

Rigby, J.F., 1997. The significance of a Permian flora from Irian Jaya (west New Guinea) containing elements related to coeval floras of Gondwanaland and Cathaysialand. The Palaeobotanist 45, 295-302.

Rigby, J.F., 2001. A review of early Permian flora from Papua (west New Guinea), In: Metcalfe, I., Smith, J.M.B., Morwood, M., Davidson, I. (Eds.), Faunal and Floral Migrations and Evolution in SE Asia-Australasia. Balkema, Lisse, pp. 85-95.

Robbins, R.G., 1963. Correlation of plant patterns and population migration into the Australian New Guinea Highlands, In: Barrau, J. (Ed.), Plants and Migration of the Pacific Peoples, Symposium of the 10th Pacific Science Conference. Bishop Museum, Honolulu.

Rodbell, D.T., Seltzer, G.O., Anderson, D.M., Abbott, M.B., Enfield, D.B., Newman, J.H., 1999. An ~15,000-year record of El Niño-driven alluviation in Southwestern Ecuador. Science 283, 516-520.

Roncaglia, L., 2004. Palynofacies analysis and organic-walled dinoflagellate cysts as indicators of palaeo-hydrographic changes: An example from Holocene sediments in Skálafjord, Faroe Islands. Marine Micropaleontology 50, 21-42.

Roncaglia, L., Kuijpers, A., 2004. Palynofacies analysis and organic-walled dinoflagellate cysts in late-Holocene sediments from Igaliku Fjord, South Greenland. The Holocene 14, 172-184.

Rowe, C., 2006. A Holocene history of vegetation change in the western Torres Strait region, Queensland, Australia, Ph.D. thesis, School of Geography and Environmental Science. Monash University.

Rowe, C., 2007a. A palynological investigation of Holocene vegetation change in Torres Strait, seasonal tropics of northern Australia. Palaeogeography, Palaeoclimatology, Palaeoecology 251, 83-103.

Rowe, C., 2007b. Vegetation change following mid-Holocene marine transgression of the Torres Strait shelf: a record from the island of Mua, northern Australia. The Holocene 17, 927-937.

Rowe, C., McNiven, I.J., David, B., Richards, T., Leavesley, M., 2013. Holocene pollen records from Caution Bay, southern mainland Papua New Guinea. The Holocene 23, 1130-1142.

Schiøler, P., Crampton, J.S., Laird, M.G., 2002. Palynofacies and sea-level changes in the Middle Coniacian-Late Campanian (Late Cretaceous) of the East Coast Basin, New Zealand. Palaeogeography, Palaeoclimatology, Palaeoecology 188, 101-125.

Schiøler, P., Rogers, K., Sykes, R., Hollis, C.J., Ilg, B., Meadows, D., Roncaglia, L., Uruski, C., 2010. Palynofacies, organic geochemistry and depositional environments of the Tartan Formation (Late Paleocene), a potential source rock in the Great South Basin, New Zealand. Marine and Petroleum Geology 27, 351-369.

Schlager, W., Reijmer, J.J.G., Droxler, A.W., 1994. Highstand shedding of carbonate platforms. Journal of Sedimentary Research 64, 270-281.

Scourse, J., Marret, F., Versteegh, G.J.M., Jansen, J.H.F., Schefuβ, E., van der Plicht, J., 2005. High-resolution last deglaciation record from the Congo fan reveals significance of mangrove pollen and biomarkers as indicators of shelf transgression. Quaternary Research 64, 57-69.

Shearman, P., 2010. Recent change in the extent of mangroves in the northern Gulf of Papua, Papua New Guinea. AMBIO 39, 181-189.

Skupien, P., Mohamed, O., 2008. Campanian to Maastrichtian palynofacies and dinoflagellate cysts of the Silesian unit, outer western Carpathians. Czech Republic Bulletin of Geoscience 83, 207-224.

Slingerland, R., Driscoll, N.W., Milliman, J.D., Miller, J.R., Johnstone, E.A., 2008a. Anatomy and growth of a Holocene clinothem in the Gulf of Papua. Journal of Geophysical Research 113, F01S13, doi:10.1029/2006JF000628.

Slingerland, R., Selover, R.W., Ogston, A.S., Keen, T.R., Driscoll, N.W., Milliman, J.D., 2008b. Building the Holocene clinothem in the Gulf of Papua: an ocean circulation study. Journal of Geophysical Research 113, F01S14, doi:10.1029/2006JF000680.

Smith, J.M.B., 1975. Mountain grasslands of New Guinea. Journal of Biogeography 2, 27-44.

Sniderman, J.M.K., Finn, J., Denham, T.P., 2009. A late Holocene palaeoecological record from Ambra Crater in the highlands of Papua New Guinea and implications for agricultural history. The Holocene 19, 449-458.

Stanley, E.A., 1966. The problem of reworked pollen and spores in marine sediments. Marine Geology 4, 397-408.

Street-Perrot, A., 1994. Palaeo-perspectives: changes in terrestrial ecosystems. AMBIO 23, 37-43.

Swanson, K.M., Watson, E., Aalto, R., Lauer, J.W., Bera, M.T., Marshall, A., Taylor, M.P., Apte, S.C., Dietrich, W.E., 2008. Sediment load and floodplain deposition rates: Comparison of the Fly and Strickland rivers, Papua New Guinea. Journal of Geophysical Research 113, F01S03, doi:10.1029/2006JF000623.

Symonds, P.A., Davies, P.J., Pigram, C.J., Feary, D.A., Chaproniere, G.C.H., 1991. Northeast Australia, Torres Shelf–Pandora Trough. Continental Margins Program Folio 4, 27.

Tcherepanov, E.N., Droxler, A.W., Lapointe, P., Dickens, G.R., Bentley, S.J. Sr., Beaufort, L., Peterson, L.C., Daniell, J., Opdyke, B.N., 2008a. Neogene evolution of the mixed carbonate-siliciclastic system in the Gulf of Papua, Papua New Guinea. Journal of Geophysical Research 113, F01S21, doi:10.1029/2006JF000684.

Tcherepanov, E.N., Droxler, A.W., Lapointe, P., Mohn, K., 2008b. Carbonate seismic stratigraphy of the Gulf of Papua mixed depositional system: Neogene stratigraphic signature and eustatic control. Basin Research 20, 185-209.

Tcherepanov, E.N., Droxler, A.W., Lapointe, P., Mohn, K., Larsen, O.A., 2010. Siliciclastic influx and burial of the Cenozoic carbonate system in the Gulf of Papua. Marine and Petroleum Geology 27, 533-554.

Thom, B.G., Wright, L.D., 1983. Geomorphology of the Purari Delta, In: Petr, T. (Ed.), The Purari: Tropical Environment of a High Rainfall River Basin. Dr. W. Junk, The Hague, pp. 64-84.

Tissot, C., Marius, C., 1992. Holocene evolution of the mangrove ecosystem in French Guiana: a palynologial study, In: Singh, K.P., Singh, J.S. (Eds.), Tropical Ecosystems: Ecology and Management. Wiley Eastern Limited, New Delhi, pp. 333-347.

Torrence, R., 2012. Volcanic disasters and agricultural intensification: a case study from Willaumez Peninsula, Papua New Guinea. Quaternary International 249, 151-161.

Torrence, R., Neall, V., Doelman, T., Rhodes, E., Mckee, C., Davies, H., Bonetti, R., Guglielmetii, A., Manzoni, A., Oddone, M., Parr, J., Wallace, C., 2004. Pleistocene colonisation of the Bismarck Archipelago: new evidence from West New Britain. Archaeology in Oceania 39, 101-130.

Traverse, A., 2007. Paleopalynology. Springer, Dordrecht, p. 813.

TSCreator, 2015. TimeScale Creator version 6.4, In: Gradstein, F.M., Ogg, J.G., Schmitz, M.D., Ogg, G.M. (Eds.). Geologic TimeScale Foundation.

United Nations Development Programme, 2010. Pacific adaptation to climate change, Papua New Guinea: report of in-country consultations, In: Global Environment Facility, Secretariat of the Pacific Environment Programme.

Vail, P.R., Mitchum, R.M.J., Todd, R.G., Widmier, J.M., Thompson, S.I., Sangree, J.B., Bubb, J.N., Hatlelid, W.G., 1977. Seismic stratigraphy and global changes of sea level, In: Payton, C.E. (Ed.), Seismic Stratigraphy Applications to Hydrocarbon Exploration. AAPG Memoir 29, Tulsa, pp. 49-211.

van der kaars, S., 2001. Pollen distribution in marine sediments from the south-eastern Indonesian waters. Palaeogeography, Palaeoclimatology, Palaeoecology 171, 341-361.

van der Zwan, C.J., 1990. Palynostratigraphy and palynofacies reconstruction of the Upper Jurassic to Lowermost Cretaceous of the Draugen Field, offshore mid Norway. Review of Palaeobotany and Palynology 62, 157-186.

van Steenis, C. G. G. J., 1934-1936. On the origin of the Malaysian mountain flora, Bulletin du Jardin Botanique de Buitenzorg Series III, 135-262, 289-417, 156-172.

Walker, D., 1966. Vegetation of the Lake Ipea region, New Guinea Highlands: I. forest, grassland and ‘garden'. Journal of Ecology 54, 503-533.

Walker, D., Flenley, J.R., 1979. Late quaternary vegetational history of the Enga Province of upland Papua New Guinea. Philosophical Transactions of the Royal Society London Series B 286, 265-344.

Walker, D., Guppy, J.C., 1976. Generic plant assemblages in the highland forests of Papua New Guinea. Australian Journal of Ecology 1, 203-212.

Walsh, J.P., Nittrouer, C.A., 2004. Mangrove-bank sedimentation in a mesotidal environment with large sediment supply, Gulf of Papua. Marine Geology 208, 225-248.

Walsh, J.P., Nittrouer, C.A., Palinkas, C.M., Ogston, A.S., Sternberg, R.W., Brunskill, G.J., 2004. Clinoform mechanics in the Gulf of Papua, New Guinea. Continental Shelf Research 24, 2487-2510.

Warny, S., Askin, R.A., Hannah, M.J., Mohr, B.A.R., Raine, J.I., Harwood, D.M., Florindo, F., SMS Science Team, 2009. Palynomorphs from a sediment core reveal a sudden remarkably warm Antarctica during the middle Miocene. Geology 37, 955-958.

Warny, S., Wrenn, J.H., 2002. Upper Neogene dinoflagellate cyst ecostratigraphy of the Atlantic coast of Morocco. Micropaleontology 48, 257-272.

Weissell, J.K., Hayes, D.E., 1972. Magnetic anomalies in the southeast Indian Ocean, In: Hayes, D.E. (Ed.), Antarctic Oceanology II, the Australian New Zealand sector, American Geophysical Union Antarctic Research Series. 19, pp. 165-196.

Whitlock, C., Larsen, C., 2001. Charcoal as a fire proxy, In: Smol, J.P., Birks, H.J.B., Last, W.M. (Eds.), Tracking Environmental Change Using Lake Sediments. Terrestrial, Algal and Siliceous indicators, vol. 3. Kluwer Academic Publishers, Dordrecht, pp. 75-98.

Wilson, S.M., 1985. Phytolith analysis at Kuk, an early agricultural site in Papua New Guinea. Archaeology in Oceania 20, 90-97.

Winterer, E.L., 1970. Submarine valley systems around the Coral Sea basin (Australia). Marine Geology 8, 229-244.

Wolanski, E., Alongi, D.M., 1995. A hypothesis for the formation of a mud bank in the Gulf of Papua. Geo-Marine Letters 15, 166-171.

Wolanski, E., Eagle, M., 1991. Oceanography and fine sediment transport, Fly River Estuary and Gulf of Papua, In: Bell, R.G., Hume, T.M., Healy, T.R. (Eds.), Coastal Engineering, Climate for Change; Proceedings of 10th Australasian conference on Coastal and Ocean Engineering 21. Water Quality Centre, pp. 453-457.

Wolanski, E., Norro, A., King, B., 1995. Water circulation in the Gulf of Papua. Continental Shelf Research 15, 185-212.

Wolanski, E., Pickard, G.L., Jupp, D.L.B., 1984. River plumes, coral reefs and mixing in the Gulf of Papua and the Northern Great Barrier Reef. Estuarine, Coastal, and Shelf Science 18, 291-314.

Wolanski, E., Ridd, P., Inoue, M., 1988. Currents through Torres Strait. Journal of Physical Oceanography 18, 1535-1545.

Wolanski, E., Spagnol, S., King, B., Ayukai, T., 1999. Patchiness in the Fly River plume in Torres Strait. Journal of Marine Systems 18, 369-381.

Womersley, J.S., 1995. Handbooks of the Flora of New Guinea, volume I. Melbourne University Press, Victoria, p. 296.

Yokoyama, Y., Lambeck, K., De Deckker, P., Johnston, P., Fifield, K., 2000. Timing of the Last Glacial Maximum from observed sea-level minima. Nature 406, 713-716.

Zobaa, M., Botero, C.S., Browne, C., Oboh-Ikuenobe, F.E., Ibrahim, M., 2008. Kerogen and palynomorph analyses of the Mid-Cretaceous Bahariya Formation and Abu Roash "G" Member, North Western Desert, Egypt. Gulf Coast Association Geological Society Transactions 58, 933-943.

CHAPTER 2. ASSESSING PALEOBATHYMETRY AND SEDIMENTATION RATES USING PALYNOMACERAL ANALYSIS: A STUDY OF MODERN SEDIMENTS FROM THE GULF OF PAPUA, PAPUA NEW GUINEA*

Introduction

Palynofacies and palynomaceral analysis has been shown to provide an indirect method of assessing sedimentation dynamics and energy of the environment and assist in paleoenvironment interpretation (e.g., Lorente, 1990; van der Zwan, 1990; Batten, 1996; Jaramillo and Oboh-Ikuenobe, 1999; Ibrahim, 2002; Schiøler et al., 2002; Carvalho et al., 2006). This project is part of the Source-to-Sink (S2S) initiative of the NSF-funded MARGINS program (NSF Grant No. OCE20-25294) focused on improving understanding of sedimentation and the stratigraphic architecture at continental margins, specifically examining factors that control sedimentation rate, transport, and accumulation (Dickens et al., 2006). The primary impetus behind performing palynomaceral analysis in this study is to better understand the distribution of the non-palynomorph fraction of palynological residues and the relationship between these fragments and environmental variables, including bathymetry, sedimentation rate, and distance from the shore and shelf-slope break. If modern palynomaceral recovery is governed by these factors, then these fragments in pre-modern samples could inform researchers of paleoenvironmental conditions, including paleobathymetry and sedimentation dynamics in ancient environments. Cores for this project taken from 64 sites during multiple oceanographic cruises conducted from 2003 to 2005 were selected

*This chapter previously appeared in Thomas, M.L., Pocknall, D.T., Warny, S., Bentley, S.J. Sr., Droxler, A.W., Nittrouer, C.A., 2015. Assessing palaeobathymetry and sedimentation rates using palynomaceral analysis: a study of modern sediments from the Gulf of Papua, offshore Papua New Guinea. Palynology, doi:10.1080/01916122.2015.1014526. It is reprinted by permission of AASP – The Palynology Society.

from the Gulf of Papua (GoP), Papua New Guinea. Because these sites span river deltas on the continental shelf to the abyssal plain, we believe they effectively illustrate variations in most common marine environments of deposition.

Palynomacerals

Palynomacerals and palynofacies analyses have been used by biostratigraphers for decades to interpret sedimentation dynamics and depositional environments in both ancient and modern sediments (e.g., Batten, 1983; Whitaker, 1984; Boulter and Riddick, 1986; Gregory and Hart, 1990; Pocknall and Beggs, 1990; van der Zwan, 1990; Batten, 1996; Oboh-Ikuenobe et al., 1997; Oboh-Ikuenobe et al., 1998; Jaramillo and Oboh-Ikuenobe, 1999; Courtinat et al., 2002; Ibrahim, 2002; Schiøler et al., 2002; Roncaglia, 2004; Roncaglia and Kuijpers, 2004; Carvalho et al., 2006; Pross et al., 2006; Zobaa et al., 2008; Skupien and Mohamed, 2008; Schiøler et al., 2010). As mentioned above, our study strictly focuses on the modern component of the palynomaceral record, in order to better our understanding of present palynomacerals in the modern Gulf of Papua. Despite the widespread use of palynomacerals, explaining this component of the sedimentary record can be complicated and counter-intuitive due to multiple classification schemes and various processing techniques (Tyson, 1995). A precise modern characterization is fundamental if we want to use palynomacerals from ancient depositional settings as paleoenvironmental proxies.

Terminology

The term ‘maceral,’ first proposed by Stopes (1935), originates from the field of organic petrology where it is used to classify the organic particles comprising coals (Crelling and Dutcher, 1980). Within organic petrology, macerals are broken down into

three broad categories: vitrinite/huminite (derived from plant tissues and still possessing some evidence of cellular structuring), liptinite/exinite (includes the exines of pollen and spores, as well as other palynomorphs), and inertinite (plant tissues that have been highly degraded) (Tyson, 1995). Whitaker (1984) used the term 'palynomaceral' to refer to these coal maceral categories of organic particles that can be identified in palynological preparations. The terms vitrinite, inertinite, and cutinite, while generally equivalent to the palynomacerals found in palynological preparations cannot be used here (although they have been used before as such, e.g., Jäger (2002)), because they are defined for reflected light microscopy (Crelling and Dutcher, 1980). In this paper, the term palynomaceral is used to refer to all organic material, including both structured and unstructured fragments, that can be found in palynological preparations, excluding what are traditionally thought of as palynomorphs (organic-walled microfossils, such as pollen, spores, dinoflagellate cysts, and acritarchs) (Tschudy, 1961).

Multiple authors have proposed varying terminology for what we define as palynomacerals, such as 'phytoclasts' (Bostick, 1974), 'palynodebris' (Manum, 1976; Habib, 1979; Tyson, 1984; Boulter and Riddick, 1986; Pocock et al., 1988; Mudie, 1989; van Bergren et al., 1990), 'organic debris' (Piasecki, 1980), 'dispersed organic matter' (Cope, 1981), and 'kerogen' (Brooks, 1981). The definitions of these terms vary depending on the author, specifically whether they choose to include or exclude palynomorphs and structureless/amorphous organic matter. This factor makes it difficult to compare and contrast between results achieved. Definition of organic matter subgroups is even more variable among authors. For example, Boulter and Riddick (1986) initially included 21 categories of amorphous matter, including specks, unstructured debris,

cuticle, wood, and black debris, that they subsequently grouped into two overarching categories upon statistical analysis (amorphous matter and palynowafers). In another example, Hart et al. (1986) and Darby and Hart (1994) proposed a classification scheme of 12 categories of macerals depending on preservational state and biologic origin. It is difficult to know which of many schemes to use and ultimately which categories will be most useful in paleoenvironmental interpretation. We have chosen to follow the scheme of Whitaker (1984) and van der Zwan (1990) because of its simplicity and approximation with coal petrological terms, which are still widely used in the petroleum industry to classify palynomacerals in palynological preparations.

van der Zwan (1990) provides a synthesis of coal maceral terminology and palynomaceral terminology from Whitaker (1984) and Boulter and Riddick (1986) (Table 2.1). Vitrinite includes clearly observable wood with cellular structures, cutinite includes leaf cuticle, and inertinite includes black debris that can be bladed or equidimensional and is probably highly degraded wood. Sporinite and liptinite include pollen and spore exines, fungal spores, and marine palynomorphs. Structureless organic matter (SOM) can be derived *in situ* from organic production in the water column or from terrestrial material. Marine SOM is roughly equivalent to liptinite in coal maceral terms (Whitaker, 1984; Boulter and Riddick, 1986; van der Zwan, 1990). Other researchers have also applied modified versions of this scheme to their analyses of palynomaceral fragments (Bryant et al., 1988; Whitaker et al., 1992; Courtinat et al., 2002). In this study, a modified scheme from these authors is used to classify palynomaceral fragments (Table 2.1, Figure 2.1).

Table 2.1. Comparison of palynomaceral terminology used in this paper with coal maceral equivalents and palynodebris categories of Whitaker (1984), Boulter and Riddick (1986), and van der Zwan (1990). Table modified from van der Zwan (1990).

<table>
<tr><td rowspan="2">Coal Macerals (approximate equivalents)</td><td colspan="2">Palynodebris Categories</td><td rowspan="2">This Study (Palynomacerals)</td></tr>
<tr><td>Modified after Whitaker (1984) and van der Zwan (1990)</td><td>Modified after Boulter and Riddick (1986)</td></tr>
<tr><td></td><td>Dark Structureless Organic Matter (SOM)</td><td>Comminuted and Degraded Debris</td><td>Structureless Organic Matter (SOM)</td></tr>
<tr><td rowspan="2">VITRINITE</td><td>Palynomaceral 1</td><td rowspan="2">Brown Wood, Well-preserved Wood, Parenchyma</td><td rowspan="2">Palynomaceral 1-2</td></tr>
<tr><td>Palynomaceral 2</td></tr>
<tr><td>CUTINITE</td><td>Palynomaceral 3</td><td>Leaf cuticle, Unstructured Plant Debris</td><td>Palynomaceral 3</td></tr>
<tr><td>INERTINITE</td><td>Palynomaceral 4 (equidimensional and bladed)</td><td>Black Debris</td><td>Palynomaceral 4</td></tr>
<tr><td rowspan="3">SPORINITE/ LIPTINITE</td><td>Pollen and spores (bisaccate pollen, fungal spores, and plant spores)</td><td>Pollen and Spores</td><td rowspan="2">Not Included in this Study</td></tr>
<tr><td>Marine palynomorphs (dinoflagellate cysts, acritarchs, and marine algae)</td><td>Marine Palynomorphs</td></tr>
<tr><td>Structureless Organic Matter (SOM)</td><td>Amorphous Matter, Specks</td><td>Structureless Organic Matter (SOM)</td></tr>
</table>

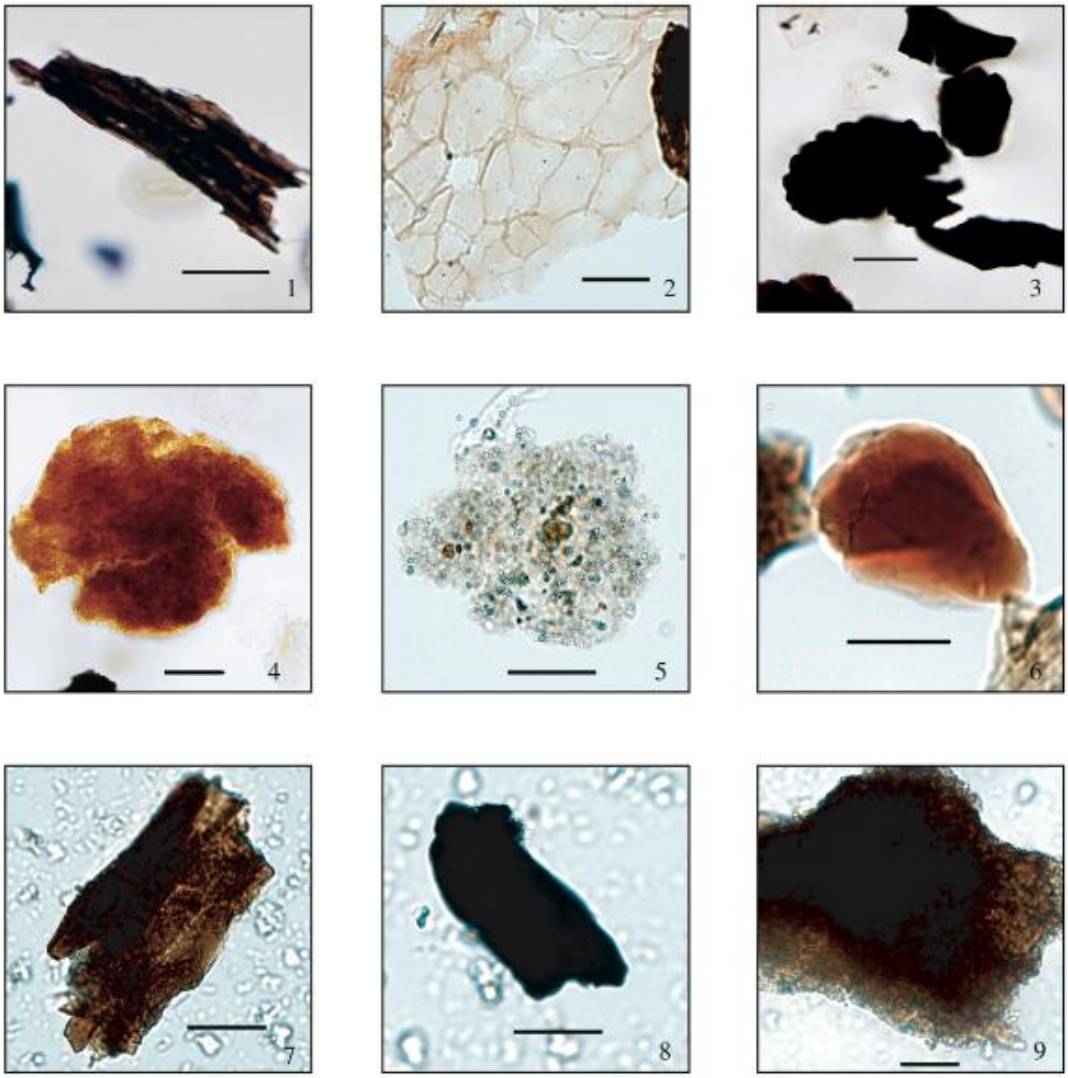

Figure 2.1. Light photomicrographs of palynomaceral categories at 600x magnification. 1) PM1-2 (palynomaceral 1-2), brown wood, from consultant's processing. 2) PM3 (palynomaceral 3), leaf cuticle, from consultant's processing. 3) PM4 (palynomaceral 4), black debris, from consultant's processing. 4) SOM (structureless organic matter of terrestrial origin probably derived from land plant material, from consultant's processing. 5) SOM of marine origin with pyrite nodules, derived *in situ*, from consultant's processing. 6) Resin, from consultant's processing. 7) PM1-2, brown wood, authors' processing. 8) PM4, black debris, from authors' processing. 9) SOM of terrestrial origin, from authors' processing.

In our study, palynomaceral 1-2 (PM1-2) is brown wood (vitrinite) derived from land plant material that may or may not have cellular structuring. It can also include gel-like substances formed by the decay of plant material *in situ* (van der Zwan, 1990). Resin is often included in the PM1-2 category (e.g. Whitaker, 1984; Boulter and Riddick, 1986; van der Zwan, 1990), but we have chosen to record it separately in order to determine if it occurs preferentially in any one of the environments. PM3 is leaf cuticle (cutinite) that shows cellular structuring and often stomata. PM4 is black debris (inertinite) that is highly degraded plant material and charcoal (Whitaker, 1984; Boulter and Riddick, 1986; van der Zwan, 1990).

SOM is used to define all amorphous material (amorphous organic material/AOM) with no structuring or evidence of tissue. Most SOM recovered in this study contains pyrite nodules, so it is likely derived from bacterial production *in situ* (Brooks, 1981). Some SOM recovered in near shore samples lacks pyrite nodules and could be terrestrially derived (Figure 2.1). Environmental factors are generally related to the appearance of SOM/AOM in palynological preparations (Traverse, 2007). Oboh (1992) notes AOM derived terrestrially appears yellow and gel-like, whereas AOM derived in the marine realm is grey. We have chosen to combine both terrestrially and *in situ*-derived SOM as one category, because it varies greatly in its appearance. Processing methodology can bias pyrite recovery, and SOM particles recovered in this study can vary in color from nearly clear to brown to grey.

The need for an in-depth palynomaceral analysis

This study departs from traditional palynofacies analyses in that it does not include palynomorphs (pollen, spores, dinoflagellate cysts, acritarchs, foraminifera

linings, etcetera) (e.g., Batten, 1983; Gregory and Hart, 1990; Pocknall and Beggs, 1990; van der Zwan, 1990; Batten, 1996; Oboh-Ikuenobe et al., 1997; Oboh-Ikuenobe et al., 1998; Jaramillo and Oboh-Ikuenobe, 1999; Courtinat et al., 2002; Ibrahim, 2002; Schiøler et al., 2002; Roncaglia, 2004; Roncaglia and Kuijpers, 2004; Carvalho et al., 2006; Pross et al., 2006; Zobaa et al., 2008; Skupien and Mohamed, 2008; Schiøler et al., 2010). There are two primary reasons behind excluding palynomorphs. First, this study's primary goal is to provide a fully quantitative analysis of the palynomacerals so that future comparison with palynomorph counts is better constrained. Most palynological consultants to the petroleum industry only provide an estimate of the recovery of palynomaceral fragments instead of an actual count, and many authors only use semi-quantitative estimates for these categories (Tyson, 1995). In the tropical environment studied here, this approach would make it difficult to compare with palynomorph counts, so a focused palynomaceral study is essential. Second, the palynological assemblage recovered is extremely complex and will be dealt with in a future study.

Factors impacting modern palynomaceral recovery

A variety of factors can impact the recovery of palynomacerals and fragile palynomorphs in preparations (e.g., Dale, 1976; Reid, 1974; Schrank, 1988; Batten, 1996). The terrestrial source from which they were derived, transportation processes, organic production in the marine realm, and diagenesis after deposition play a role in governing assemblages present. Additionally, palynomaceral size, shape, density, buoyancy, and type influence how they are transported and deposited. Processing methodology is particularly important for ensuring consistency within samples (Batten, 1996; Batten and Stead, 2005).

Sediment source impacts the type of palynomaceral present (Traverse, 2007). A densely vegetated area will be expected to source sediments having higher percentages of palynomacerals 1-2 and 3 (PM1-2, PM3), while a sparsely vegetated area will not. Distance from shore and time in transport or residence also impacts palynomaceral recovery. For example, PM4 is more buoyant than PM1-2 and PM3 and can be transported over longer distances (van der Zwan and van Veen, 1978; Richelot and Streel, 1985; van der Zwan, 1990). PM1-2, PM3, and PM4 are primarily terrestrially derived, and their abundance is predicted to decrease with increasing distance from shore and water depth. Abundances of these three categories are expected to increase with increasing sedimentation rate, as sedimentation rates are usually higher near shore.

SOM in this study appears to be mostly of marine origin (grey and possesses pyrite nodules) and is predicted to increase with increasing water depth and distance from shore and shelf/slope break where burial of marine organic matter outweighs delivery and deposition of terrestrial organic matter. SOM can also be derived from terrestrial material (Batten, 1983), although transport of this type of SOM to far offshore locations is unlikely. Bacterial production in the water column creates *in situ* SOM/amorphous organic matter (AOM), which can be associated with partially anaerobic and stagnant water bottom conditions (Demaison and Moore, 1980; van der Zwan, 1990), although some degree of oxygenation is needed for bacterial activity (e.g., Staplin, 1969; Philp et al., 1978; Batten, 1983; Batten, 1996). In general, amorphous material is best recovered in settings where the preservation potential is high (Tyson, 1993; Carvalho et al., 2006).

Many authors, including van der Zwan (1990), Tyson (1995), Batten (1996), Oboh-Ikuenobe et al. (1998), Jaramillo and Oboh-Ikuenobe (1999), and Batten and Stead

(2005), have noted the importance of processing methodology when analyzing palynomaceral assemblages. Oxidation in particular can reduce the amount of SOM found in palynological preparations, so palynomaceral analysis is best performed on unoxidized kerogen slides (Batten, 1996). Processing techniques must be carefully controlled in order to ensure uniform representation among samples (Batten, 1996; Batten and Stead, 2005). Slight oxidation can improve the identification of palynomacerals, especially PM1-2 and PM3 (van der Zwan, 1990), but this approach is not standard for analyses of this sort. Some authors have performed palynofacies analysis on oxidized slides (Batten, 1983; Schiøler et al., 2002; Schiøler et al. 2010).

The composition of the palynomaceral assemblage can inform us about sediment source, transport, and depositional processes (Batten, 1996; Tyson and Follows, 2000). Other factors, such as climate, could influence palynomaceral production but because we are focusing our analysis on modern sediments and climate is considered to be consistent across the study area, we predict that climate will not play a large role in palynomaceral content. Likewise, as the sediments are all modern (deposited within approximately the last 100 years), we do not believe tectonic events will cause variation among palynomaceral assemblages. Four factors should have the predominant impact on palynomaceral distribution for the modern study area; these are water depth, distance from shore, distance from shelf-slope break, and sediment accumulation rate. The goal of the study is to understand how palynomaceral distribution is influenced by these four factors in a modern setting, and therefore better understand how to utilize palynomaceral assemblages to reconstruct paleoenvironmental conditions.

Study Area

The Gulf of Papua (GoP) is located to the southeast of Papua New Guinea between approximately 8-10°S latitude and 143-147°E longitude (Figure 2.2). Two climatic seasons occur every year: a northwest monsoon from December to March and a southeast monsoon from May to October. Semidiurnal tides reach a peak spring tide of five meters (Wolanski et al., 1995; Harris et al., 2004; Ogston et al., 2008). Mainland

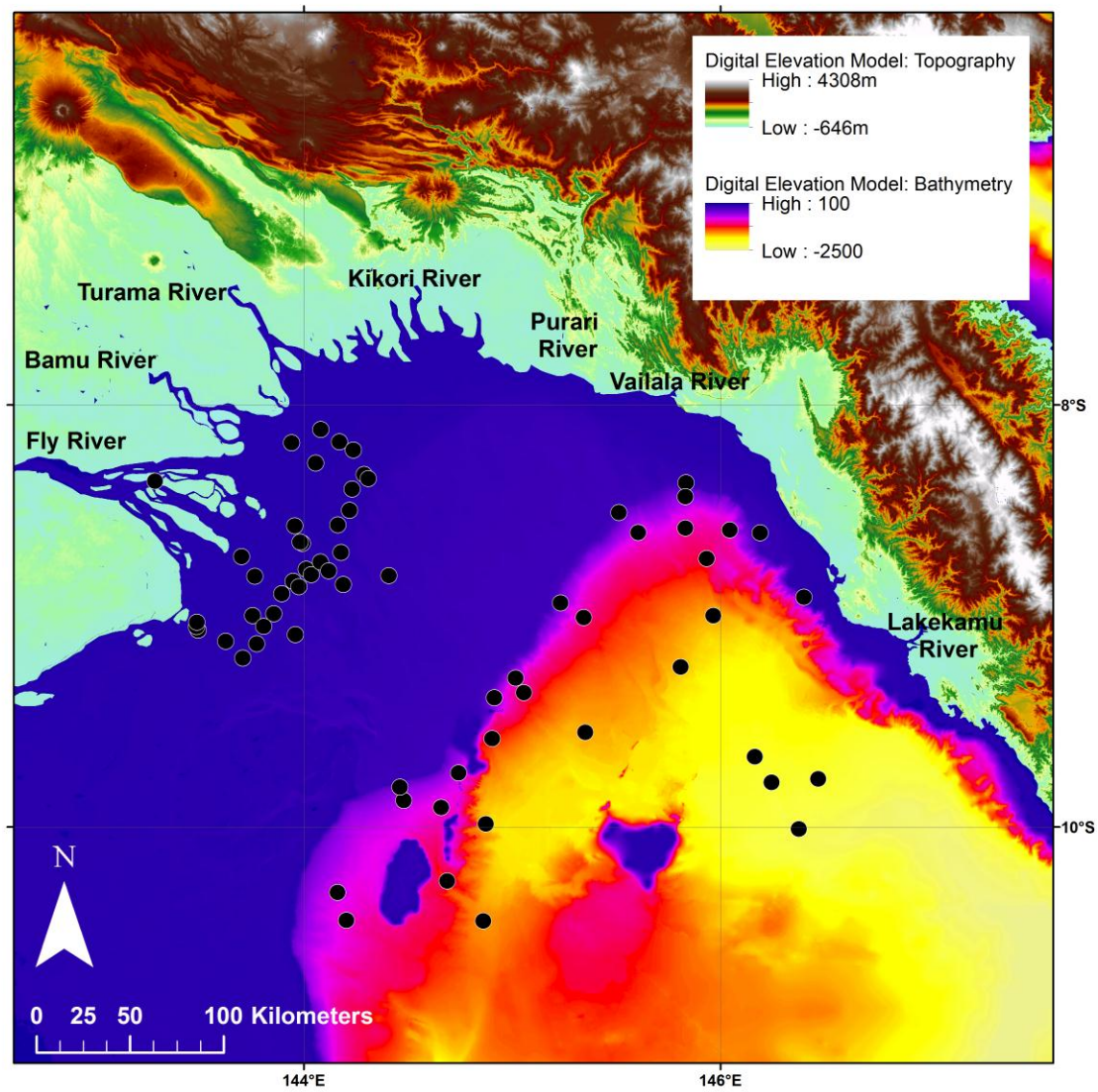

Figure 2.2. Sampling locations for palynomaceral analysis in the Gulf of Papua, Papua New Guinea. Bathymetry from Daniell (2008).

Papua New Guinea and its surrounding islands, which number greater than 1400, have a combined 5,152 km of coastline. The combined factors of high rainfall and tall mountains mean that sediment discharge into the Gulf of Papua reaches approximately 3.84 x 10^8 tons per year, one of the highest discharges known globally (Milliman, 1995; Wolanski et al., 1995). The distance from the shoreline to the shelf-slope break is less than ten km in the northeastern gulf, while in the northwestern and western gulf, the distance is greater than 100 km.

Sedimentation dynamics vary greatly throughout the Gulf of Papua (Muhammad et al., 2008) due to factors such as seasonal changes in wind direction, tidal variations on daily/monthly timescales (Wolanski and Alongi, 1995; Ogston et al., 2008; Slingerland et al., 2008), the area of land draining into the gulf, and high sediment discharge (Wolanski et al., 1995). Deposition of coarser sands and silts dominates near-shore locations, while offshore, finer-grained muds are deposited mainly as a hemipelagic rain (Muhammad et al., 2008). Carbonate deposition occurs in the southwest portion of the gulf at the northernmost extension of the Great Barrier Reef (Tcherepanov et al., 2008). A synthesis of the major depositional environments in the Gulf of Papua (Walsh et al., 2004; Carson et al., 2008; Crockett et al., 2008; Francis et al., 2008; Martin et al., 2008; Howell et al., 2014), as well as ages of exposed geologic formations in Papua New Guinea and northern Australia (Steinshouer et al., 1999) is shown in Figure 2.3. The sampling locations for this project span many depositional settings, which are described below.

Nearshore sedimentation: Western Gulf of Papua clinoform

Sedimentation from numerous rivers, of which the Fly, Bamu, Turama, Kikori, Purari, Vailala, and Lakekamu Rivers are the largest (Figure 2.2), has resulted in the

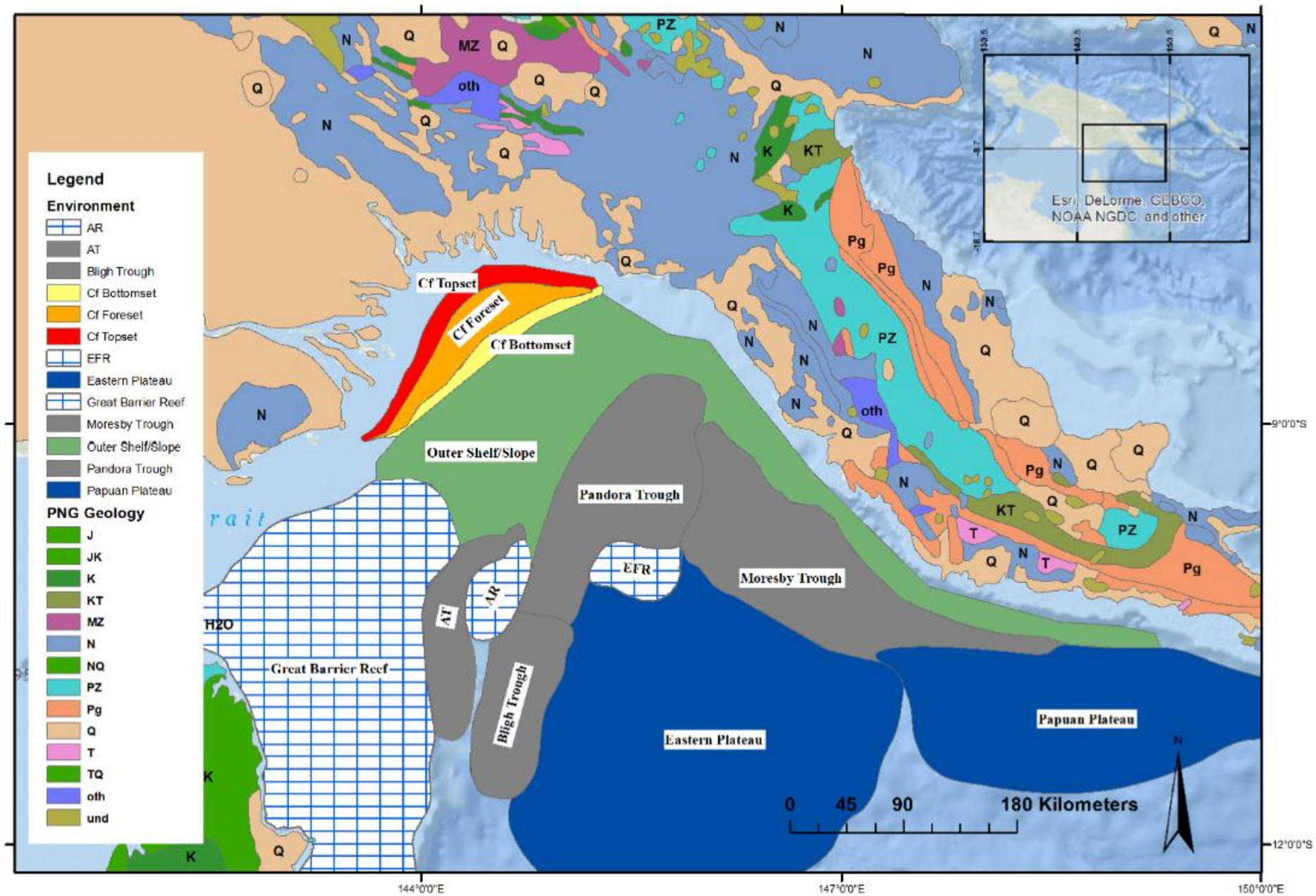

Figure 2.3. Synthesis of major Gulf of Papua depositional environments (Walsh et al., 2004; Carson et al., 2008; Crockett et al., 2008; Francis et al., 2008; Martin et al., 2008; Howell et al., 2014). AT = Ashmore Trough, AR = Ashmore Reef, EFR = Eastern Fields Reef. Terrestrial geologic data is synthesized from Steinshouer et al. (1999). Papua New Guinea geology abbreviations are for formation ages (J = Jurassic, JK = Jurassic-Cretaceous, K = Cretaceous, KT = Cretaceous-Tertiary, MZ = Mesozoic, N = Neogene, NQ = Neogene-Quaternary, PZ = Paleozoic, Pg = Paleogene, Q = Quaternary, T = Tertiary, TQ = Tertiary-Quaternary, oth = other, und = undifferentiated).

formation of a late Holocene clinoform that extends offshore from these rivers in the western Gulf of Papua (GoP) (Walsh et al., 2004) (Figure 2.3). Understanding clinoform deposition is important, because it has been estimated by Walsh et al. (2004) that up to 95% of the sediment budget delivered to the GoP accumulates in the clinoform, predominantly in less than 60 meters of water depth in clinoform topset beds, mangrove belts, and river deltas. Topset beds are characterized by sedimentation rates of approximately 0.7 cm/yr with depths to topset beds at approximately 20 mbsl (meters below sea-level). Foreset bed sedimentation rates are much higher, between 1.5 to 4.0 cm/yr and extend to approximately 60 mbsl. Bottomset beds have much lower sedimentation rates of less than 0.7 cm/yr and are deeper than 60 mbsl (Wolanski and Alongi, 1995; Walsh et al., 2004; Slingerland et al., 2008). Sediments in the northeastern GoP shelf accumulate in a mud belt due to advection and current transport (Harris et al., 1993; Harris et al., 1996; Walsh et al., 2004). Clinoform sediments are dominated by terrestrial reworked sediments predominately sourced by the large rivers mentioned above. The bedrock geology of western Papua New Guinea consists of uplifted terrestrial and marine sedimentary deposits of Neogene age (Davies, 2012), with lesser quantities of Neogene volcanics and low-grade metamorphic rocks (Milliman, 1995; Brunskill, 2004).

Offshore sedimentation: Deep ocean basin

In the northeastern GoP where the shelf is narrower, sedimentation rates are much lower (approximately 0.2 cm/yr) (Muhammad et al., 2008). Sediments accumulate in the deep ocean basin past the shelf-slope break in basins including Ashmore, Pandora and Moresby Troughs (Figure 2.3). In the southwestern GoP, accumulation rates of siliciclastic sediments are very low due to the current highstand of sea level and the

clockwise current that transports sediment towards the northeast. Sediments sourced from the Vailala and Lakekamu Rivers (Figure 2.2) of northern and northeastern Papua New Guinea include high proportions of igneous and metamorphic components derived from the Papuan Mountains (Davies et al., 1989; Pigram et al., 1989; Symonds et al., 1991; Norvick et al., 2001; Davies, 2012).

Materials and Methods

Sampling and environmental variables

Samples from 64 core locations were sub-sampled from the top 0-4 cm of the core. The samples are archived at Louisiana State University, Baton Rouge, LA, U.S.A., and the University of Washington, Seattle, WA, U.S.A. Multi-core methodology was used to collect the 27 offshore samples. Kasten core and box core methodology was used to collect 36 of the 37 near shore samples. One sample (C2-A11) was collected using a grab sampler. Although it is possible that the different coring methods used to obtain the samples could have affected the results of this study, we are confident the impact is minimal. Core types were included in initial statistical analyses and did not change the results. Sample names (which are also the core and site name for this study), core type, sample interval obtained (cm), geographic coordinates (decimal degrees), water depth (m, more negative values indicate deeper water), distance from shore (km), distance from shelf-slope break (km, negative values indicate samples are on the shelf, positive values indicate samples are on the slope, rise, or abyssal plain), and sedimentation rates are provided (Table 2.2, Table 2.3).

Water depths were measured when the sediment cores were taken. Distance from shore and shelf-slope break was measured as the shortest straight-line distance between

Table 2.2. Sample data. Includes sample name, core type (MC = multi-core, KC = Kasten core, BC = box core, GC = grab sample), sample interval (centimeters), weight (grams), latitude and longitude (decimal degrees), depth (meters), distance from shore (kilometers), distance from shelf-slope break (kilometers), and sedimentation rate (cm/yr). Sedimentation rates synthesized from Walsh et al. (2004) and Muhammad et al. (2008).

Sample	Core Type	Int. (cm)	Weight (g)	Latitude	Longitude	Depth (m)	Dist. from Shore (km)	Dist. from Shelf Break (km)	Sed. Rate (cm/yr)
10MC	MC	0-4	28.9	-9.8742	144.4812	-584	148	10	0.05
12MC	MC	0-4	35.4	-9.8120	144.4620	-372	142	2.4	0.09
14MC	MC	0-4	34.6	-9.9073	144.6608	-760	166	18.5	0.23
16MC	MC	0-4	39.9	-9.7443	144.7443	-686	164	2.4	0.05
18MC	MC	0-4	13.9	-8.5109	145.5134	-262	61	2.9	0.26
19MC	MC	0-4	40.2	-8.5234	145.5066	-229	64	0.4	0.18
20MC	MC	0-4	34.3	-9.2948	145.0185	-661	162.5	5.6	0.12
21MC	MC	0-4	26.3	-9.3648	145.0570	-1009	165	15	0.05
24MC	MC	0-4	16.6	-9.7890	146.2478	-2102	92	75	0.14
26MC	MC	0-4	17.7	-10.0090	146.3785	-2232	97	80	0.07
28MC	MC	0-4	22.3	-10.1668	147.1333	-2426	52.5	38	0.10
30MC	MC	0-4	17.9	-9.6667	146.1667	-2023	87	69	0.10
32MC	MC	0-4	27.6	-9.5520	145.3532	-1620	150	52	0.05
38MC	MC	0-4	22.2	-9.0083	145.3450	-977	120	17	0.10
39MC	MC	0-4	12.2	-8.6053	145.6060	-690	68	13.5	0.13
42MC	MC	0-4	12.8	-8.3698	145.8367	-91	35.5	-3.2	0.35
43MC	MC	0-4	21.7	-8.9120	146.4023	-62	15.5	-1.9	0.34
44MC	MC	0-4	10.8	-8.6072	146.1918	-99	17.5	-2.5	0.28
47MC	MC	0-4	5.8	-8.4347	145.8337	-399	40	9	0.28
50MC	MC	0-4	11.9	-8.5933	146.0457	-795	30	10	0.13

(Table 2.2 continued)

Sample	Core Type	Int. (cm)	Weight (g)	Latitude	Longitude	Depth (m)	Dist. from Shore (km)	Dist. from Shelf Break (km)	Sed. Rate (cm/yr)
53MC	MC	0-4	15	-8.7288	145.9358	-1111	48	25	0.21
56MC	MC	0-4	22.6	-8.9392	145.2343	-450	112	2.5	0.08
60MC	MC	0-4	21.7	-9.2423	145.8103	-1674	88	70	0.07
69MC	MC	0-4	17.6	-9.9845	144.8745	-1638	195	22.5	0.05
70MC	MC	0-4	17.5	-8.2160	145.1500	-1758	39.5	-47	0.12
72MC	MC	0-4	31.5	-10.2543	144.6890	-1320	195	57	0.07
76MC	MC	0-4	21.4	-10.4432	144.8629	-1551	225	72	0.07
C2-8	KC	0-4	20	-8.5743	143.9577	-18	15.5	-130	0.70
C2-A11	GC	0-4	19.7	-8.6559	143.9938	-25	23.5	-121	1.50
CC5	KC	0-4	19.8	-8.1796	143.9417	-7	16.5	-160	0.70
CC7	KC	0-4	19.6	-8.2753	144.0579	-5	33	-136	0.70
CT	KC	0-1, 2-3	19.5	-8.5764	143.9633	-18	16	-130	0.70
D2	KC	0-4	19.6	-8.8133	143.7658	-15.9	19	-126	0.70
D6	KC	0-4	19.5	-8.7200	143.7019	-26	7.6	-145	1.50
E4	KC	0-4	20.7	-8.9078	143.5953	-10.4	19.5	-120	0.70
EE5	KC	0-4	19.8	-8.1166	144.0822	-4	21.5	-150	0.70
EE7	KC	0-4	20.4	-8.1752	144.1726	-8	34	-145	0.70
EE9	KC	0-4	19.7	-8.2145	144.2385	-12	42	-128	0.70
G2	KC	0-4	20.6	-9.0685	143.4930	-6	6.6	-120	0.70
G3	KC	0-2	19.6	-9.0521	143.4851	-5	5.3	-121	0.70
G5	KC	0-4	20.5	-9.0315	143.4870	-6	4.9	-123	0.70
T10-20	BC	0-4	19.4	-9.1208	143.6250	-15	22.5	-105	0.70
T10-60	BC	0-4	20.4	-9.2000	143.7080	-26.1	35	-94	1.50

(Table 2.2 continued)

Sample	Core Type	Int. (cm)	Weight (g)	Latitude	Longitude	Depth (m)	Dist. from Shore (km)	Dist. from Shelf Break (km)	Sed. Rate (cm/yr)
T11-20	KC	0-4	19.1	-8.5700	144.1650	-20.8	37	-112	1.50
T1-20	KC	0-4	21.4	-8.8100	144.4100	-62.1	72	-75	0.40
T12-20	BC	0-4	20.1	-8.5000	144.2200	-20.7	43	-115	1.50
T1-25	BC	0-4	21.2	-8.4000	144.2333	-19.1	45	-119	0.70
T13-20C	KC	0-4	20.2	-8.3300	144.2900	-29	55	-117	1.50
T13-30C	BC	0-4	20.5	-8.3500	144.3100	-37	56	-114	2.50
T2-30	BC	0-2	19	-9.1333	143.7750	-23.9	38.5	-94	1.50
T3-20KC	BC	4-6	18	-9.0000	143.7550	-20.2	33.5	-109	1.50
T3-30	BC	0-4	21.5	-9.0500	143.8083	-28.2	39.5	-100	1.50
T4-30	BC	0-4	20	-8.9900	143.8575	-28.8	44.5	-105	1.50
T4-50	BC	0-4	19.2	-9.0900	143.9600	-47.4	56.5	-90	0.70
T5-20	BC	0-4	19.4	-8.8950	143.8950	-23.2	36	-116	1.50
T6-20	KC	0-4	19.4	-8.8375	143.9500	-19.3	36	-117	0.70
T6-30	KC	0-4	19.5	-8.8620	143.9770	-30.8	39.5	-102	2.50
T7-20	KC	0-4	19.7	-8.7800	144.0125	-21.8	34.5	-105	1.50
T7-30	KC	0-4	19.5	-8.8050	144.0363	-33.2	38	-100	2.50
T8-20B	KC	0-4	22	-8.6500	143.9833	-21.3	21.5	-118	1.50
T8-30	KC	0-2	20.5	-8.7450	144.0800	-34.9	36.5	-108	2.50
T8-50	KC	4-5	11.7	-8.7875	144.1200	-67.5	43.5	-95	0.40
T8-60	KC	0-4	19.7	-8.8525	144.1900	-80	54	-86	0.40
T9-30	KC	0-4	19.8	-8.7000	144.1800	-34.8	43.5	-95	2.50

Table 2.3. Counts for palynomaceral categories. PM1-2 = palynomaceral 1-2, PM3 = palynomaceral 3, PM4 = palynomaceral 4, SOM = structureless organic matter.

Sample	Lycopo-dium	Lyco./ Tablet	# Tablets	PM1-2	PM3	PM4	SOM	Resin
10MC	196	12542	2	41	0	136	125	1
12MC	52	12542	2	91	2	86	139	1
14MC	52	12542	2	72	0	143	107	5
16MC	34	12542	2	71	0	193	47	9
18MC	1	12542	2	60	0	198	50	5
19MC	1	12542	2	60	1	216	44	8
20MC	2	12542	2	50	0	225	47	6
21MC	1	12542	2	94	0	214	46	4
24MC	6	12542	2	67	0	153	99	12
26MC	1	12542	2	67	0	109	156	20
28MC	3	12542	2	99	1	126	78	19
30MC	2	12542	2	64	0	219	134	27
32MC	1	12542	2	70	0	192	53	6
38MC	1	12542	2	86	0	198	39	11
39MC	1	12542	2	54	1	136	114	18
42MC	35	12542	2	85	2	172	74	17
43MC	117	12542	2	107	4	105	79	28
44MC	155	12542	2	64	0	105	168	4
47MC	180	12542	2	94	2	163	176	11
50MC	160	12542	2	82	0	114	117	9
53MC	25	12542	2	112	1	137	120	4
56MC	1	12542	2	97	9	204	43	4
60MC	3	12542	2	132	2	173	59	6
69MC	4	12542	2	99	0	228	40	1
70MC	3	12542	2	117	0	166	86	7
72MC	1	12542	2	94	0	219	42	5
76MC	2	12542	2	97	1	137	84	4
C2-8	7	20848	1	135	5	166	44	0
C2-A11	2	20848	1	172	2	99	44	3
CC5	4	20848	1	141	2	118	43	4
CC7	5	20848	1	134	5	127	44	7
CT	6	20848	1	136	2	129	34	7
D2	6	20848	1	144	4	137	31	4
D6	7	20848	1	120	10	145	35	3
E4	5	20848	1	97	0	188	26	2
EE5	5	20848	1	166	15	87	35	3
EE7	13	20848	1	142	7	116	49	3

(Table 2.3 continued)

Sample	Lycopo-dium	Lyco./ Tablet	# Tablets	PM1-2	PM3	PM4	SOM	Resin
EE9	8	20848	1	122	4	150	39	0
G2	2	20848	1	117	2	116	87	0
G3	5	20848	1	128	3	149	41	3
G5	6	20848	1	115	2	163	35	0
T10-20	8	20848	1	86	3	165	62	4
T10-60	11	20848	1	111	1	145	48	7
T11-20	9	20848	1	113	2	161	30	1
T1-20	21	20848	1	94	0	191	41	4
T12-20	11	20848	1	113	3	165	36	3
T1-25	75	20848	1	111	0	140	74	8
T13-20C	7	20848	1	132	5	143	61	7
T13-30C	5	20848	1	133	1	140	37	3
T2-30	8	20848	1	128	0	191	13	5
T3-20KC	7	20848	1	137	0	158	32	2
T3-30	3	20848	1	103	1	131	75	3
T4-30	6	20848	1	160	5	100	51	11
T4-50	9	20848	1	150	4	139	44	7
T5-20	7	20848	1	104	3	177	56	6
T6-20	9	20848	1	102	0	163	40	5
T6-30	8	20848	1	87	1	188	25	1
T7-20	10	20848	1	77	0	190	29	0
T7-30	7	20848	1	99	1	182	27	3
T8-20B	6	20848	1	141	2	137	32	8
T8-30	1	20848	1	143	3	133	34	4
T8-50	13	20848	1	137	2	124	46	8
T8-60	19	20848	1	102	0	126	77	3
T9-30	4	20848	1	137	0	103	85	6

the sampling location and shore or shelf-slope break. Sedimentation rates (in cm/yr) from ^{210}Pb-dating are available for offshore samples from Muhammad et al. (2008). Sedimentation rates for near shore sites are based on averages of ^{210}Pb-dating results obtained from several studies of clinoform sedimentation in the GoP including Walsh et al. (2004), Crockett et al. (2008), and Martin et al. (2008). Because clinoform topset, foreset, and bottomset beds are deposited at characteristic ranges of water depths (Walsh

et al., 2004), we chose to assign average sedimentation rates to the samples based on the following parameters:

- Clinoform topset:
    - Water depth between 0 – 20 m, sedimentation rate = 0.7 cm/yr.
- Clinoform foreset:
    - Water depth between 21 – 30 m, sedimentation rate = 1.5 cm/yr.
    - Water depth between 30 – 45 m, sedimentation rate = 2.5 cm/yr.
- Clinoform bottomset:
    - Water depth between 46 – 60 m, sedimentation rate = 0.7 cm/yr.
    - Water depth between 61 – 80 m, sedimetnation rate = 0.4 cm/yr.

Sediments deposited on the clinoform foreset have the highest sediment accumulation rates, while topset and bottomset deposition rates are lower. Past 80 m water depth, clinoform bottomset deposition grades into outer shelf deposition with sedimentation rates lower than 0.4 cm/yr. There are no available samples for study on the outer shelf. Oceanographic currents, particularly tidal variations and seasonal wind changes, also play a role in influencing the deposition of sediments and organic matter (Wolanski et al., 1995; Ogston et al., 2008), although this data is only available from a limited number of locations (Martin et al., 2008; Ogston et al., 2008; Slingerland et al., 2008). Because of the limited data availability, and because water depth and distance from shore/shelf break are often used as proxies for wave and current energy, current observations are not incorporated in this study.

Processing

Samples were processed by an external consultant using standard techniques and spiked with *Lycopodium* tablets (one or two per sample) to provide for absolute abundance calculations (Traverse, 2007). Carbonates and silicates were dissolved using 10% HCL and 70% HF solutions. Heavy liquid separation was performed using $ZnBr_2$. Slight oxidation for thirty seconds was performed with Schulze's reagent (potassium chlorate and nitric acid) . Samples were sieved at 10 microns, and slides were mounted in clear resin. Unoxidized kerogen slides were not provided, although palynomaceral/palynofacies analysis is traditionally conducted on unoxidized material (e.g., van der Zwan, 1990; Oboh-Ikuenobe et al., 1998; Jaramillo and Oboh-Ikuenobe, 1999). Slightly oxidized samples (like the ones used in this study) can allow for easier identification of palynomacerals (van der Zwan, 1990), and can be used for palynomaceral analayis although oxidation does result in lower recovery of SOM. Because these samples were collected on cruises conducted over a decade ago, and the GoP is difficult to access, all samples could not be reprocessed for an unoxidized analysis.

Twenty-nine nearshore samples were still available, and the authors re-processed them without HF and oxidants to determine the impact of the oxidative processing technique used by the consultant on palynomaceral recovery. Although most researchers perform palynofacies and palynomaceral analysis on unoxidized kerogen slides, some authors such as Batten (1983), Schiøler et al. (2002), and Schiøler et al. (2010) have run their analyses on oxidized slides. We have chosen to compare both methodologies to demonstrate how processing techniques could affect palynomaceral interpretation.

A modification of O'Keefe and Eble's (2012) methodology was utilized for reprocessing available samples. *Lycopodium* spp. tablets were not used. Carbonates were dissolved using 10% HCl. Samples were disaggregated overnight in a 1% Liquinox solution to disperse clays. In a departure from O'Keefe and Eble's (2012) method, potassium hydroxide was not used because it is known to swell and degrade more fragile palynomorphs such as modern dinocysts (e.g., Dale, 1976; Harland, 1981; Harland, 1983; Hughes and Harding, 1985; Schrank, 1988). Heavy liquid separation was performed using sodium polytungstate (specific gravity of 2.0). Samples were not stained, and slides were mounted in glycerol using volumetric methodology (Jörgensen, 1967).

Microscopy

Slides were examined under transmitted light on an Olympus BX43 microscope. The palynomaceral component of the slides was counted to at least 300 particles at 1000x magnification (Tables 2.3, 2.4), similar to standard techniques used for counting palynomorphs (Traverse, 2007). No particles smaller than 5 microns were counted. Counts of *Lycopodium* markers were tabulated for slides produced by the consultant in order to calculate absolute abundances; however this data could not be used for statistical calculations. *Lycopodium* recovery for offshore samples is highly variable, and we believe many of the markers were lost during processing for most of the samples (Table 2.3). The calculation of absolute abundances of palynomacerals, therefore, is skewed and seriously affects statistical analysis. On the other hand, raw results from both processing sets are somewhat comparable, and these raw counts were used instead of attempting to use the absolute abundances calculated from the various techniques to avoid further bias. Indeed, multiple factors during processing can impact the distribution, size, and thus

Table 2.4. Counts of samples reprocessed by the authors.

Sample	PM1-2	PM3	PM4	SOM	Resin
C2-8	166	3	149	7	0
C2-A11	196	0	157	10	4
CC5	166	0	114	34	0
CC7	203	5	90	30	3
CT	92	0	197	17	3
D6	209	8	83	46	4
E4	226	2	108	24	2
EE5	204	2	103	26	0
EE7	196	1	56	55	0
EE9	231	3	87	29	2
G2	198	1	107	13	1
G3	186	0	126	7	0
G5	169	1	107	36	5
T1-20	143	0	183	8	4
T10-20	114	0	171	35	1
T10-60	120	0	132	54	8
T11-20	137	0	170	5	4
T12-20	124	0	167	17	2
T13-20C	196	0	117	7	2
T13-30C	160	1	128	34	1
T2-30	141	3	143	51	2
T4-30	139	1	162	12	4
T6-20	125	0	170	12	0
T6-30	118	0	190	13	2
T7-30	154	1	147	14	0
T8-20B	219	4	88	11	6
T8-30	181	0	124	39	0
T8-60	122	0	85	117	0
T9-30	116	0	139	56	2

counts of palynomaceral fragments, including water pressure used during sieving, the sieve sized used, cover slip mounting (Boulter and Riddick, 1986), and oxidation (e.g., Tyson, 1995). For this reason, many researchers choose semi-quantitative or estimation methods to determine the number of palynomaceral fragments (Boulter and Riddick, 1986). These estimations are subjective, so individual particles were counted, similar to

Carvalho et al. (2006), instead of making an estimate of their percentages, while keeping in mind that processing methodology can influence the size and distribution of palynomacerals on the slides. Spatial bubble plots of counted palynomacerals for the consultant's slides were created using ArcGIS 10.2 (ArcGIS Desktop, 2014) (Figures 2.4, 2.5). Categories were plotted as a percent of the total palynomaceral count.

Statistical analysis

Principal component analysis (PCA) was performed using Canoco5 (Šmilauer, 2012**)** to determine if environmental factors, including water depth, distance from shore, distance from the shelf-slope break, and sedimentation rates influenced palynomaceral distribution. PCA was chosen, because the environmental factors selected in this study might not be the only factors impacting palynomaceral distribution. For example, current speed, time in transport, amount of bacterial activity, and source could impact recovery, and these variables are difficult to account for in statistical analysis. Palynomaceral data were analysed unconstrained, and environmental variables (water depth (m), distance from shore (km), distance from shelf-slope break (km), and sediment accumulation rate (cm/yr)) were used to help interpret the results. Four PCA axes were computed, and response data were log-transformed.

PCA results for the consultant's samples are presented as a triplot with the first PCA axis plotted on the x axis and the second PCA axis plotted on the y axis (Figure 2.6, Table 2.5). Palynomaceral arrows (filled black) and environmental variables (empty black) point in the direction of steepest increase. Their length indicates degree of fit for that category. Acute angles between arrows indicate positive correlation, and obtuse angles indicate negative correlation. Samples are plotted by their Euclidean distance.

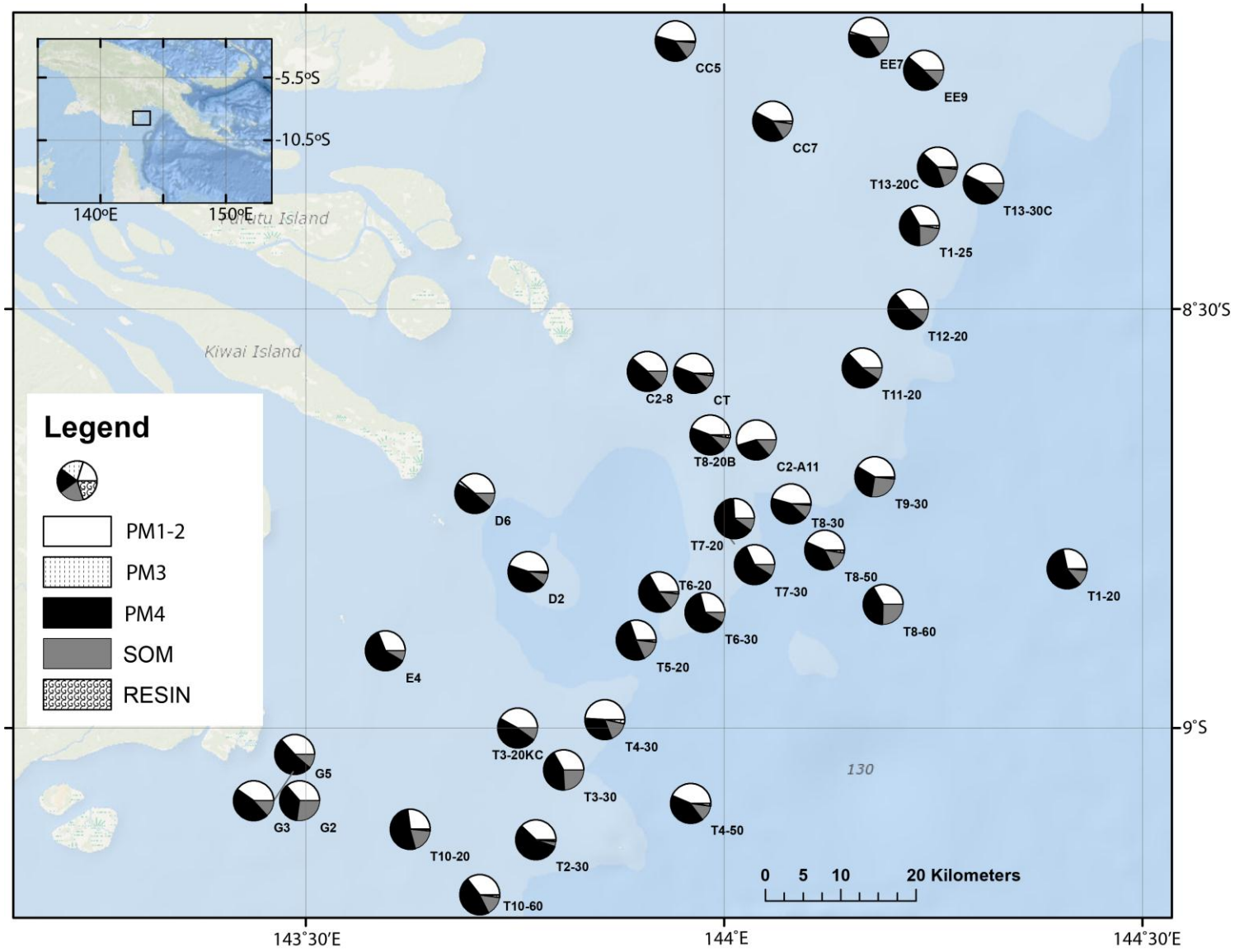

Figure 2.4. Spatial bubble plots for nearshore palynomacerals. Each category is plotted as a percentage of the total count. Palynomaceral 1-2 (PM1-2), palynomaceral 2 (PM3), palynomaceral 4 (PM4), structureless organic matter (SOM). Basemap from ESRI (2014).

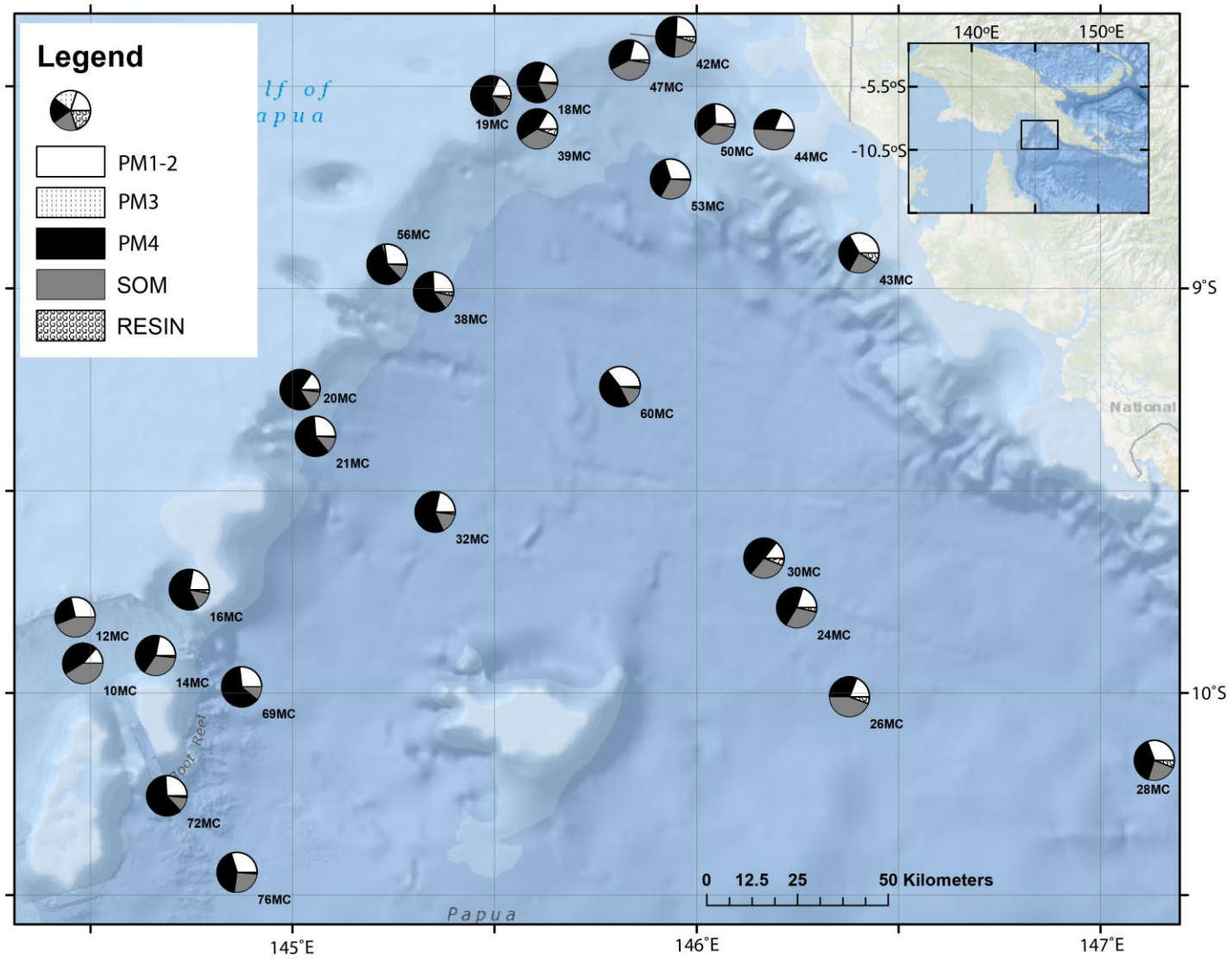

Figure 2.5. Spatial bubble plots for offshore palynomacerals. Each category is plotted as a percentage of the total count. Palynomaceral 1-2 (PM1-2), palynomaceral 2 (PM3), palynomaceral 4 (PM4), structureless organic matter (SOM). Basemap from ESRI (2014).

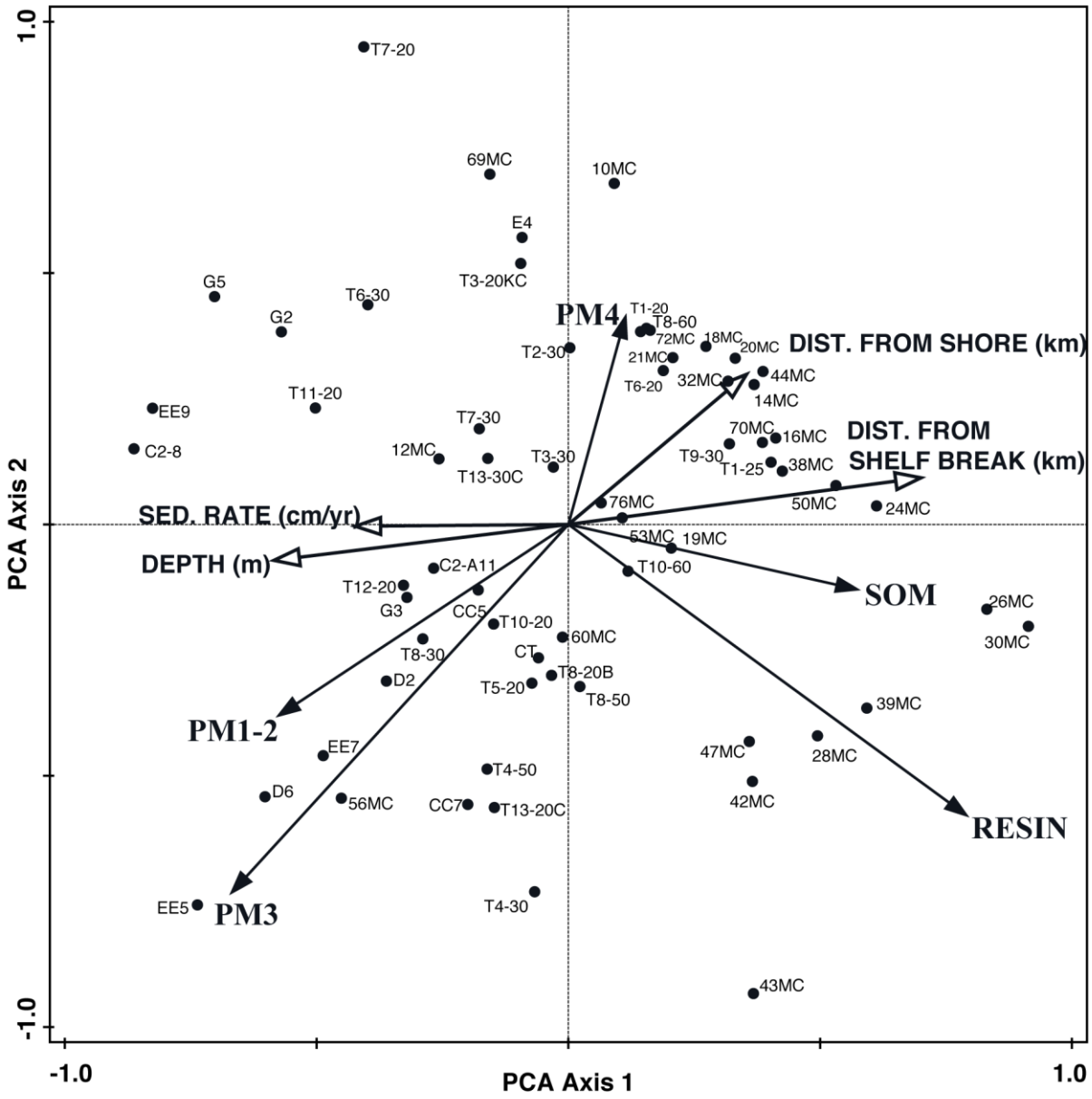

Figure 2.6. Principal component analysis (PCA) results with environmental variables for samples. Samples are plotted by their Euclidean distance scores. Arrows indicate the direction of steepest increase for the corresponding palynomaceral category or environmental variable. Acute angles between arrows indicate positive correlation, obtuse angles indicate negative correlation. Palynomaceral 1-2 (PM1-2), palynomaceral 2 (PM3), palynomaceral 4 (PM4), structureless organic matter (SOM).

Table 2.5. Results from unconstrained principal component analysis (PCA) with supplementary environmental variables for samples processed by the consultant.

Unconstrained PCA with Environmental Variables				
Total Variation			101.49	
Supplementary variables account for			32.00%	
Statistic	Axis 1	Axis 2	Axis 3	Axis 4
Eigenvalues	0.4715	0.3336	0.1423	0.0411
Explained variation (cumulative)	47.15	80.51	94.74	98.85
Pseudo-canonical correlation (suppl.)	0.7302	0.3519	0.3536	0.4444

Those plotting farther apart are more dissimilar, while those plotting nearer to each other are less dissimilar. An acute angle between an environmental variable and palynomaceral category indicates a positive correlation, while an obtuse angle indicates a negative correlation.

Consultant samples were then plotted by their Euclidean distance scores without palynomaceral or environmental variable arrows and labelled according to their corresponding sedimentary environment (Figure 2.3) to determine if samples from the same environment were less dissimilar to samples from other environments (Figure 2.7). The following sedimentary environments were included: clinoform topset, clinoform foreset, clinoform bottomset, and offshore samples (slope, rise, or abyssal plain). Dissimilarity between the palynomaceral counts for the two processing methods was analysed using PCA without supplementary variables (Figure 2.8, Table 2.6). Samples are plotted by their Euclidean distance scores. Samples processed by the authors have an R appended to their name. If the samples processed by the authors and the consultants have the same recovery of palynomacerals, then the symbols should plot on top of or very

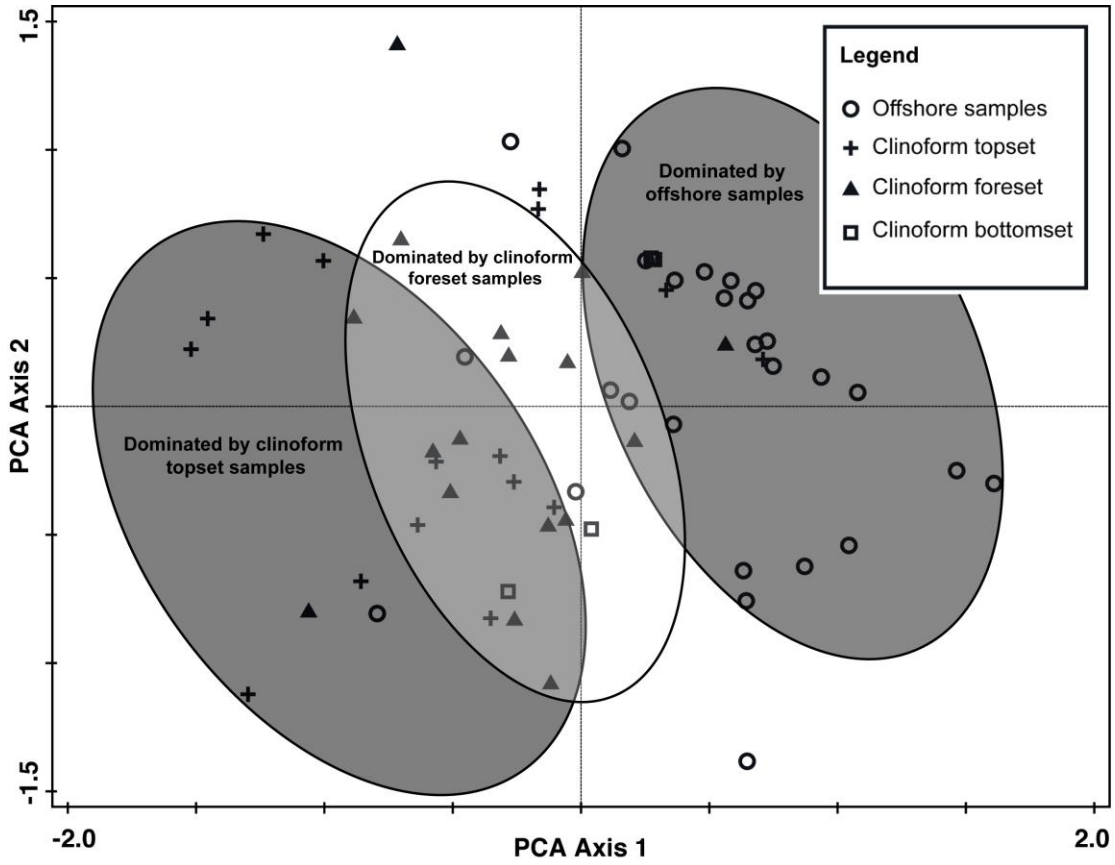

Figure 2.7. Principal component analysis (PCA) with environmental variables results for samples. Samples are plotted by their Euclidean distance score, and symbol corresponds to the depositional environment. Crosses are clinoform topset samples, triangles are clinoform foreset samples, squares are clinoform bottomset samples, and open circles are offshore basin samples. Ovals indicate where the majority of samples for each environment plot. There are not enough bottomset samples (four) to conclusively determine how they relate to each other.

near to each other. The amount of dissimilarity between the two processing methods is indicated by the distance between the points for a particular sample.

To help quantify the variability between the consultant's and the authors' processing methodologies, t-tests were performed for each palynomaceral category to compare the means of each group (Tables 2.7, 2.8, 2.9, 2.10, 2.11). The mean of each palynomaceral category was calculated with its standard deviation for both the authors'

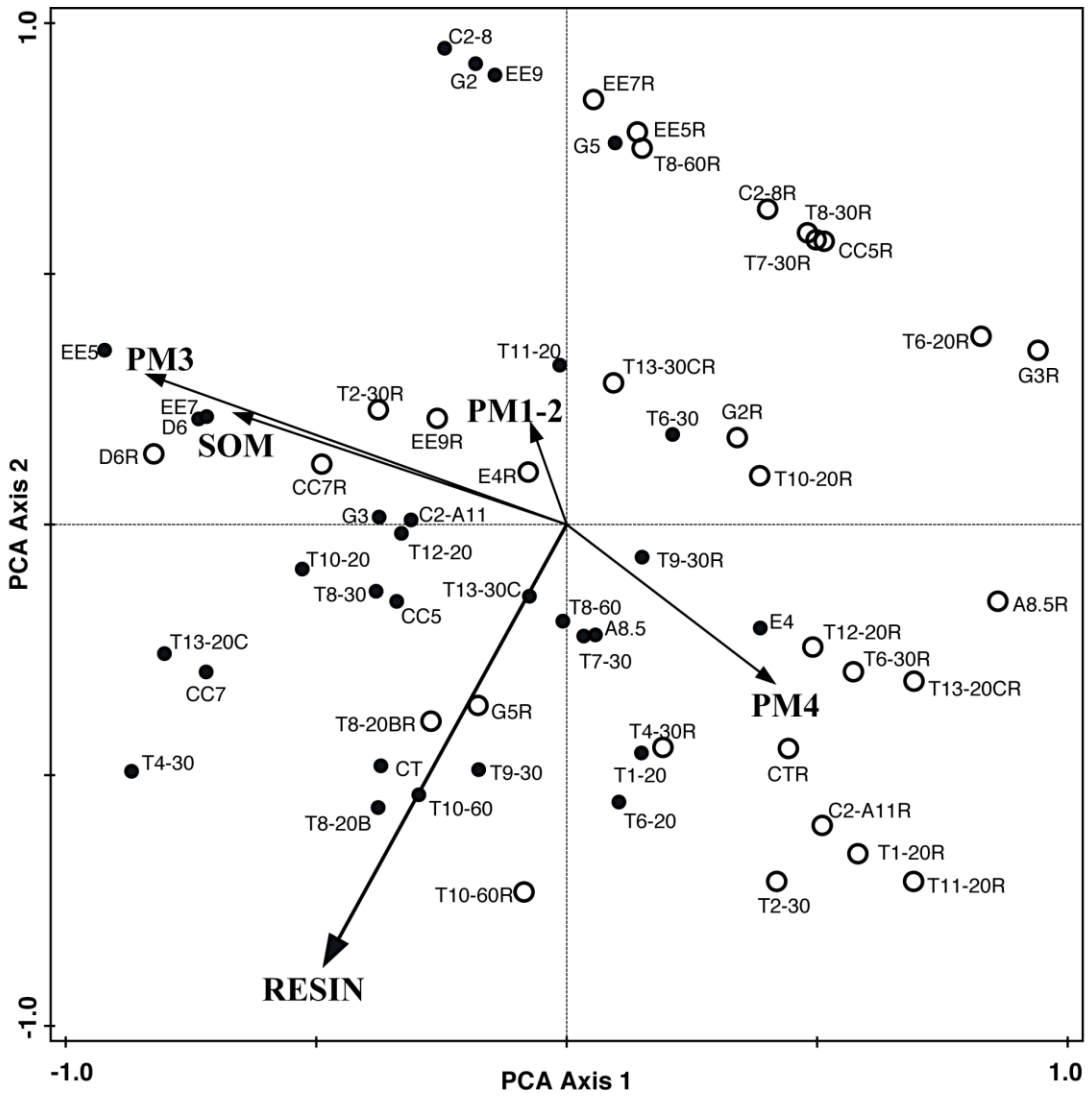

Figure 2.8. Principal component analysis (PCA) results comparing the dissimilarity between processing methodology. Samples are plotted by their Euclidean distance scores. Consultant-processed samples are filled dots, and author-processed samples are open circles (reprocessed samples are labeled with an "R" following the sample name). Supplementary variables are not included.

and consultant's samples. The number of occurrences for each group is 29, and the degrees of freedom are 56. The null hypothesis for these t-tests predicts that processing methodology does not affect palynomaceral recovery. P values of less than 0.05 indicate that the differences between the two processing techniques are not due solely due to chance, meaning the results are statistically significant.

Table 2.6. Results from unconstrained PCA without supplementary variables comparing consultant's and authors' processing techniques.

Unconstrained PCA comparing consultant and CENEX samples				
Total Variation			100.05	
Statistic	Axis 1	Axis 2	Axis 3	Axis 4
Eigenvalues	0.4358	0.2863	0.2177	0.0557
Explained variation (cumulative)	43.58	72.21	93.99	99.56

Table 2.7. Unpaired t-test for Palynomaceral 1-2. SEM = standard error of the mean, N = number of samples, df = degrees of freedom. P values < 0.05 indicate statistical significance.

Unpaired t-test for Palynomaceral 1-2		
Data		
	Consultant	Authors
Mean	124.34 ± 22.31	163.83 ± 39.14
SEM	4.14	7.27
N	29	29
Calculation		
t-statistic		4.7194
df		56
Standard error of difference		8.366
P value (two-tailed)		<0.0001

Table 2.8. Unpaired t-test for Palynomaceral 3. SEM = standard error of the mean, N = number of samples, df = degrees of freedom.

Unpaired t-test for Palynomaceral 3		
Data		
	Consultant	Authors
Mean	2.97 ± 3.29	1.24 ± 1.90
SEM	0.61	0.35
N	29	29
Calculation		
t-statistic		2.4435
df		56
Standard error of difference		0.706
P value (two-tailed)		0.0177

Table 2.9. Unpaired t-test for Palynomaceral 4. SEM = standard error of the mean, N = number of samples, df = degrees of freedom.

Unpaired t-test for Palynomaceral 4		
Data		
	Consultant	Authors
Mean	144.34 ± 29.48	131.03 ± 36.57
SEM	5.47	6.79
N	29	29
Calculation		
t-statistic		1.526
df		56
Standard error of difference		8.723
P value (two-tailed)		0.1326

Table 2.10. Unpaired t-test for SOM (structureless organic matter). SEM = standard error of the mean, N = number of samples, df = degrees of freedom.

Unpaired t-test for SOM		
Data		
	Consultant	Authors
Mean	43.28 ± 17.11	28.24 ± 23.57
SEM	3.18	4.38
N	29	29
Calculation		
t-statistic		2.7796
df		56
Standard error of difference		5.409
P value (two-tailed)		0.0074

Results

The results for counted palynomacerals for near shore and offshore sample sites from the consultant's processing procedure are mapped (Figures 2.4, 2.5, Table 2.4). Nearshore sample sites show much higher abundances of PM1-2, while offshore sites show much higher abundances of PM4 and SOM. Samples with particularly high SOM

Table 2.11. Unpaired t-test for Resin. SEM = standard error of the mean, N = number of samples, df = degrees of freedom.

Unpaired t-test for Resin		
Data		
	Consultant	Authors
Mean	3.79 ± 2.68	2.14 ± 2.08
SEM	0.5	0.39
N	29	29
Calculation		
t-statistic		2.6276
df		56
Standard error of difference		0.63
P value (two-tailed)		0.0111

recoveries also have the highest marine palynomorph recovery (dinoflagellate cysts and acritarchs). Other authors, including Brooks (1981) and Carvalho et al. (2006), have noted an increase in amorphous organic matter (AOM) recovery in samples with high organic production in the water column. PM3 and resin recoveries are low throughout the study area. Principal component analysis (PCA) with supplementary (environmental) variables indicates strong positive correlation between PM1-2 and PM3 (Figure 2.6). SOM and resin are also positively correlated. PM4 has a strong negative correlation with all palynomaceral categories, except SOM, with which its positive correlation is weak. PM1-2 and PM3 counts are positively correlated (their counts increase) with increasing sedimentation rates and shallower water depths (bathymetry values are negative in the statistical analysis, so less negative values indicate shallower depths), and they are negatively correlated with increasing distance from shore and shelf-slope break. PM4, SOM, and resin are positively correlated (counts increase) with increasing distance from shore and shelf-slope break, and they are negatively correlated with sedimentation rate and shallower water depths. The total variation among samples is 101.49 (Table 2.5), and

supplementary variables account for 32.00% of the variation. The remaining 64% of the variation among samples must be explained by factors unaccounted for in this study. The first four PCA axes account for 98.85% of the cumulative explained variation.

Plotting Euclidean distance scores of samples and labelling them by their sedimentary environment allows us to determine if samples from the same environment are more similar to each other than those from other environments (Figure 2.7). The ovals around the plotted samples indicate where the majority of samples from each depositional environment plot. Results from this plot are less clear, which is why sample names and arrows have been removed. Three populations have been identified and are labelled. One subset is dominated by offshore samples, one by clinoform topset samples, and one by clinoform foreset samples, although it has more variable representation of other environments. Offshore samples (labelled by empty circles) appear to be less dissimilar to each other than to nearshore samples (triangles, crosses, and empty squares). Clinoform topset samples (crosses) generally plot closer to each other than to clinoform foreset (triangles) and bottomset (empty square samples). There are not enough bottomset samples to conclusively determine if these samples are more or less dissimilar from the other environmental groups.

The dissimilarity between the samples processed by the consultant and the authors is also compared using PCA (Figure 2.8). Environmental variables are not included in this analysis, because the aim is to determine the differences between processing techniques. Samples plotting more closely together are less dissimilar, and those plotting farther apart are more dissimilar. Because only 29 nearshore samples are included in analysis and processing affects recovery, correlation among the palynomaceral categories

is different. PM1-2, PM3, and SOM are positively correlated with each other, and negatively correlated with PM4 and resin. Resin and PM4 are only weakly positively correlated. Results demonstrate processing clearly affects recovery, because reprocessed samples rarely plot near the same sample processed by the consultant. Reprocessed samples in general have higher counts of PM1-2 and PM4 with lower recovery of PM3, SOM, and resin. The total variation among the samples in this analysis is 100.05, and the first four PCA axes explain 99.56% of the cumulative variation (Table 2.6).

T-tests indicate significant deviations from the null hypothesis for all palynomaceral categories except PM4 ($p = 0.1326$) (Tables 2.7, 2.8, 2.9, 2.10, 2.11). In particular, the P value for PM1-2 is less than 0.0001 (0.01%), which is extremely significant. PM1-2 counts for reprocessed samples are much higher; the mean of PM1-2 for reprocessed samples is 163.83 ± 22.31 compared to 124.34 ± 22.31 for the consultant's samples. P values for PM3 ($p = 0.0177$), SOM ($p = 0.0074$), and resin ($p = 0.011$) are also significant. It is unlikely that the difference between means for PM4 could be caused by chance alone, because all other palynomaceral categories show significant P values. These results demonstrate that the processing methodology influences palynomaceral recovery.

Discussion

Despite the bias introduced by the use of the two processing techniques, both sets of results show that the distribution of palynomacerals in sediments is indeed governed by key factors, but not as strongly as we expected. Water depth, distance from shore and shelf break, and sediment accumulation rate were predicted to account for the variation in palynomaceral assemblages among samples. Our results show that these variables explain

32% of the variation in assemblages (Table 2.5, Figure 2.6). Counts of PM1-2 and PM3 increase with increasing sedimentation rate and shallower water depths. PM1-2 and PM3 counts decrease with increasing distance from shore and shelf break. Because PM1-2 and PM3 are derived from vegetation, this results fits with the prediction that these categories will decrease with increasing distance from shore/shelf break and water depth. Sedimentation rates are much higher in near shore sites (Figures 2.2, 2.3) (Walsh et al., 2004; Muhammad et al., 2008), which helps to explain why increases in PM1-2 and PM3 are positively correlated with increasing sedimentation rates. These results fit with the observations of van der Zwan (1990), who also found increased PM1-2 and PM3 recovery sites nearer to shore.

Principal component analysis (PCA) results for resin are not as clear (Figure 2.6). Counts for this category are low (Table 2.4). Other authors have included resinous substances in PM1-2 and PM3 groups (Whitaker, 1984; Boulter and Riddick, 1986; van der Zwan, 1990). Resin was predicted to be higher in nearshore and shallow water settings, but PCA indicates it increases with increasing distance from shore and in deeper water. This would indicate resin is more robust or more buoyant and can be transported longer distances. The low recovery of resin could have skewed these results, so in future analyses, resin should be included within PM1-2, as it is terrestrially derived.

Palynomaceral 4 (PM4) increases in abundance with increasing distance from shore/shelf break and water depth. Recovery of PM4 is higher in sites with lower sedimentation rates (Figure 2.6). Boulter and Riddick (1986), van der Zwan (1990), and Carvalho et al. (2006) note that this black debris is probably highly degraded plant tissue. The observation that PM4 increases in abundance with increasing distance from shore

and in deeper water depths indicates these fragments are more buoyant and can be transported longer distances, similar to findings by van der Zwan and van Veen (1978), Richelot and Streel (1985), and van der Zwan (1990).

Structureless organic matter (SOM) is positively correlated with distance from shore and shelf break and negatively correlated with depth and sedimentation rate (Figure 6). SOM is particularly abundant in offshore samples, especially where marine productivity is high as indicated by increased abundances of dinoflagellate cysts. The recovery of SOM is highest in depositional environments where energy of the environment is low and productivity is high (Tyson, 1993; Carvalho et al., 2006). Results from PCA (Figure 2.6) support the conclusion that most of the SOM identified in this study is derived in the marine realm from *in situ* production.

The remainder of the variation (64%) in palynomaceral assemblages must be explained by other factors, which can include the proximity of vegetation to water, sediment source (Traverse, 2007), transportation processes and currents, productivity, bioturbation, and reworking (Tyson, 1995; Batten, 1996). It is difficult to quantify these factors for statistical analysis. Palynomacerals can also be sorted based on their size, shape, and buoyancy (van der Zwan and van Veen, 1978; Richelot and Streel, 1985; van der Zwan, 1990), which cannot adequately be accounted for in the simple classification scheme proposed here. Processing techniques also impacts the recovery of palynomacerals and must be carefully controlled (van der Zwan, 1990; Tyson, 1995; Batten, 1996; Oboh-Ikuenobe et al., 1998; Jaramillo and Oboh-Ikuenobe, 1999; Batten and Stead, 2005).

Samples from each sedimentary environment are more similar to each other than those from other sedimentary environments (Figure 2.7). Cluster analysis would more definitely reveal if certain palynomaceral assemblages are characteristic of each sedimentary environment. In general, clinoform samples possess higher counts of PM1-2 and PM3, while offshore samples have higher abundances of PM4 and SOM. Future work would elucidate if a particular range of palynomaceral counts is indicative of each environment.

Comparing the consultant's processing methodology with the authors' processing methodology yields statistically significant differences between the techniques (Figure 2.8, Tables 2.7, 2.8, 2.9, 2.10, 2.11). All categories except PM4 show a statistically significant deviation from the null hypothesis. The means of PM1-2 and PM4 recovery is higher in reprocessed samples, while the means of PM3, SOM, and resin recovery is lower. It is odd that SOM recovery in the consultant's slightly oxidized samples is higher, because SOM recovery is generally higher in un-oxidized, kerogen slides (van der Zwan, 1990; Tyson, 1995; Batten, 1996; Oboh-Ikuenobe et al., 1998; Jaramillo and Oboh-Ikuenobe, 1999). The authors' use of Liquinox during processing (modified from O'Keefe and Eble, 2012) could have disaggregated SOM particles to sizes smaller than five microns, making them too small to count. Processing without a dispersant would likely increase recovery of SOM

Results from comparing the two processing techniques illustrate differences in the palynomaceral content. van der Zwan (1990) also notes that slight oxidation provides for easier identification of palynomaceral particles, and we have found this to be true in our sample suite. Our reprocessed samples (without oxidation) were much harder to count,

especially with the presence of small amorphous material. Despite this, we agree with previous authors (e.g., Oboh-Ikuenobe et al., 1998; Jaramillo and Oboh-Ikuenobe, 1999) that analysing unoxidized kerogen slides provides the most unbiased approach to gathering the appropriate data to interpret palynomaceral fragments in the palynological record. In future studies, analyses of this type should be reserved for kerogen slides, although as demonstrated here, the palynomaceral assemblage of oxidized slides partially reflect the influence of bathymetry, distance from shore and shelf break, and sediment accumulation rates.

Conclusions

Palynomaceral analysis can provide important insights into the modern sedimentary record. Understanding how these fragments behave in modern sediments is important in helping palynologists make interpretations about ancient depositional environments. When interpreting ancient sedimentary deposits, researchers must keep in mind that preservation and diagenesis can also impact palynomaceral recovery. Results from using the simple classification scheme of five categories (PM1-2, PM3, PM4, SOM, and resin) show relative abundances of these particles can aid in predicting bathymetry, distance from shore, and sediment accumulation rate. Although these seem to be the key factors governing distribution, they only account for 32% of the overall variability of palynomaceral assemblages. A multitude of other factors, such as productivity, source, reworking, and bacterial alteration, outside the scope of the analysis presented here, can also impact palynomaceral assemblages. Despite the inability of the environmental factors selected to adequately explain the total variation in palynomaceral assemblages, some important results have emerged from the analysis. PM1-2 and PM3 are more

common in sites nearer shore, in shallower water depths, and with higher sedimentation rates (Figure 2.6). PM4 is more buoyant and perhaps more resistant than PM1-2 and PM3, so it is more common in deeper offshore sites. SOM is higher in offshore sites that could have higher organic production. Future application of this simple five category classification scheme to fossil palynomaceral assemblages could give biostratigraphers an important tool for understanding changes in paleobathymetry and sediment accumulation rates in ancient sedimentary environments.

References

ArcGIS Desktop, 2014. ArcGIS Version 10.2. Esri, Redlands.

Batten, D.J., 1983. Identification of amorphous sedimentary organic matter by transmitted light microscopy. Geological Society of London Special Publications 12, 275-287.

Batten, D.J., 1996. Chapter 26A. Palynofacies and palaeoenvironmental interpretation, In: Jansonius, J., McGregor, D.C. (Eds.), Palynology: principles and applications. American Association of Stratigraphic Palynologists Foundation, Salt Lake City, pp. 1011-1064.

Batten, D.J., Stead, D.T., 2005. Palynofacies analysis and its stratigraphic application, In: Koutsoukos, E.A.M. (Ed.), Applied Stratigraphy. Springer, Dordrecht, pp. 203-226.

Bostick, N.H., 1974. Phytoclasts as indicators of thermal metamorphism, Franciscan assemblage and Great Valley Sequence (Upper Mesozoic), California. Geological Society of America Special Papers 153, 1-17.

Boulter, M.C., Riddick, A., 1986. Classification and analysis of palynodebris from the Palaeocene sediments of the Forties Field. Sedimentology 33, 871-876.

Brooks, J., 1981. Organic maturation of sedimentary organic matter and petroleum exploration - A review, In: Brooks, J. (Ed.), Organic Maturation Studies and Fossil Fuel Exploration. Academic Press, London, pp. 1-38.

Brunskill, G.J., 2004. New Guinea and its coastal seas, a testable model of wet tropical coastal processes: an introduction to Project TROPICS. Continental Shelf Research 24, 2273-2295.

Bryant, I.D., Kantorowicz, J.D., Love, C.F., 1988. The origin and recognition of laterally continuous carbonate-cemented horizons in the Upper Lias Sands of Southern England. Marine and Petroleum Geology 5, 108-133.

Carson, B.E., Francis, J.M., Leckie, R.M., Droxler, A.W., Dickens, G.R., Jorry, S.J., Bentley, S.J. Sr., Peterson, L.C., Opdyke, B.N., 2008. Benthic foraminiferal response to sea level change in the mixed siliciclastic-carbonate system of southern Ashmore Trough (Gulf of Papua). Journal of Geophysical Research 113, F01S20, doi:10.1029/2006JF000629.

Carvalho, M.A., Filho, J.G.M., Menezes, T.R., 2006. Paleoenvironmental reconstruction based on palynofacies analysis of the Aptian-Albian succession of the Sergipe Basin, Northeastern Brazil. Marine Micropaleontology 59, 56-81.

Cope, M.J., 1981. Products of natural burning as a component of the dispersed organic matter in sedimentary rocks, In: Brooks, J. (Ed.), Organic Maturation Studies and Fossil Fuel Exploration. Academic Press, London, pp. 89-110.

Courtinat, B., Rio, M., Malartre, F., 2002. Palynofacies of marginal marine deposits: the Rhaetian of the east margin of the Massif Central (France). Revue de Micropaléontologie 45, 47-55.

Crelling, J.C., Dutcher, R.R., 1980. Principles and applications of coal petrology, S.E.P.M.-Geological Society of America Meeting. Indiana University, Bloomington, p. 32.

Crockett, J.S., Nittrouer, C.A., Ogston, A.S., Naar, D.F., Donahue, B.T., 2008. Morphology and filling of incised submarine valleys on the continental shelf near the mouth of the Fly River, Gulf of Papua. Journal of Geophysical Research 113, F01S12, doi:10/1029/2006JF000674.

Dale, B., 1976. Cyst formation, sedimentation, and preservation: Factors affecting dinoflagellate assemblages in Recent sediments from Trondheimsfjord, Norway. Review of Palaeobotany and Palynology 22, 39-60.

Darby, J.D., Hart, G.F., 1994. Chapter 10, Organic sedimentation in a carbonate region, In: Traverse, A. (Ed.), Sedimentation of Organic Particles. Cambridge University Press, Cambridge, pp. 177-197.

Davies, H.L., 2012. The geology of New Guinea – the cordilleran margin of the Australian continent. Episodes 35, 87-102.

Davies, P.J., Symonds, P.A., Feary, D.A., Pigram, C.J., 1989. The evolution of the carbonate platforms of Northeast Australia, In: Crevello, P.D. (Ed.), Controls on Carbonate Platform and Basin Development, SEPM Special Publication vol. 44, Tulsa, pp. 233-258.

Demaison, G.J., Moore, G.T., 1980. Anoxic environments and oil source bed genesis. Bulletin of the American Association of Petroleum Geologists 64, 1179-1209.

Dickens, G.R., Droxler, A.W., Bentley, S.J. Sr., Peterson, L.C., Opdyke, B.N., Beaufort, L., Daniell, J.J., Febo, L.A., Francis, J.M., Harris, P.T., et al, 2006. Sediment

accumulation on the shelf edges, adjacent slopes, and basin floors of the Gulf of Papua. NSF-MARGINS Newsletter 16, 1-4.

Francis, J.M., Daniell, J.J., Droxler, A.W., Dickens, G.R., Bentley, S.J. Sr., Peterson, L.C., Opdyke, B.N., Beaufort, L., 2008. Deep water geomorphology of the mixed siliciclastic-carbonate system, Gulf of Papua. Journal of Geophysical Research 113. F01S16, doi:10.1029/2007JF000851.

Graphpad Software, Inc., 2015. T-test Calculator. Graphpad Software, Inc., La Jolla. 23 January 2015. Available from: http://www.graphpad.com/quickcalcs/ttest1/.

Gregory, W.A., Hart, G.F., 1990. Subdivision of Wilcox Group (Sabinian) argillaceous sediments using particulate organic matter. Palynology 14, 105-121.

Habib, D., 1979. Sedimentology of palynomorphs and palynodebris in Cretaceous carbonaceous facies south of Vigo Seamount. Initial Reports of the Deep Sea Drilling Program 47, 451-467.

Harland, R., 1981. Cysts of the colonial dinoflagellate *Polykrikos schwartzii* Biitschli 1873 (Gymnodiniales) from Recent sediments, Firth of Forth, Scotland. Palynology 5, 65-79.

Harland, R., 1983. Distribution maps of recent dinoflagellate cysts in bottom sediments from the North Atlantic Ocean and adjacent seas. Palaeontology 26, 321-387.

Harris, P.T., Baker, E.K., Cole, A.R., Short, S.A., 1993. Preliminary study of sedimentation in the tidally dominated Fly River Delta, Gulf of Papua. Continental Shelf Research 13, 441-472.

Harris, P.T., Hughes, M.G., Baker, E.K., Dalrymple, R.W., Keene, J.B., 2004. Sediment transport in distributary channels and its export to the pro-deltaic environment in a tidally dominated delta: Fly River, Papua New Guinea. Continental Shelf Research 24, 2431-2454.

Harris, P.T., Pattiaratchi, C.B., Keene, J.B., Dalrymple, R.W., Gardner, J.V., Baker, E.K., Cole, A.R., Mitchell, D., Gibbs, P., Schroeder, W.W., 1996. Late Quaternary deltaic and carbonate sedimentation in the Gulf of Papua foreland basin: response to sea level change. Journal of Sedimentary Research 66, 801-819.

Hart, G.F., Pasley, M.A., Gregory, W.A., 1986. Classification and origin of organic matter in clastic systems. Palynology 10, 1-23.

Howell, A.L., Bentley, S.J. Sr., Xu, K., Ferrell, R.E.J., Muhammad, Z., Septama, E., 2014. Fine sediment mineralogy as a tracer of latest Quaternary sediment delivery to a dynamic continental margin: Pandora Trough, Gulf of Papua, Papua New Guinea. Marine Geology 357, 108-122.

Hughes, N.F., Harding, I.C., 1985. Wealden occurrence of an isolated Barremian dinocyst facies. Palaeontology 28, 555-565.

Ibrahim, M.I.A., 2002. Late Albian-Middle Cenomanian palynofacies and palynostratigraphy, Abu Gharadig-5 well, Western Desert, Egypt. Cretaceous Research 23, 775-788.

Jäger, H., 2002. Palynology of the Lower Carboniferous (Mississippian) Kammquartzite Formation in the Rhenohercynian Zone, Germany. Senckenberiana Lethaea 82, 609-637.

Jaramillo, C.A., Oboh-Ikuenobe, F.E., 1999. Sequence stratigraphic interpretations from palynofacies, dinocyst and lithological data of Upper Eocene-Lower Oligocene strata in southern Mississippi and Alabama, U.S. Gulf Coast. Palaeogeography, Palaeoclimatology, Palaeoecology 145, 259-302.

Jörgensen, S., 1967. A method of absolute pollen counting. New Phytologist 66, 489-493.

Lorente, M.A., 1990. Textural characteristics of organic matter in several subenvironments of the Orinoco Upper Delta. Geologie en Mijnbouw 69, 263-278.

Lowry, R., 2015. Chapter 11. T-test for the significance of the difference between the means of two independent samples Concepts and Applications of Inferential Statistics, New York. 23 January 2015. Available from: http://vassarstats.net/textbook/ch11pt1.html.

Manum, S.B., 1976. Dinocysts in Tertiary Norwegian-Greenland Sea sediments (Deep Sea Drilling Project Leg 38), with observations on palynomorphs and palynodebris in relation to environment. Initial Reports of the Deep Sea Drilling Program 38, 897-919.

Martin, D.P., Nittrouer, C.A., Ogston, A.S., Crockett, J.S., 2008. Tidal and seasonal dynamics of a muddy inner shelf environment, Gulf of Papua. Journal of Geophysical Research 113, F01S07, doi:10.1029/2006JF000681.

Milliman, J.D., 1995. Sediment discharge to the ocean from small mountainous rivers: the New Guinea example. Geo-Marine Letters 15, 127-133.

Mudie, P.J., 1989. Palynology and dinocyst biostratigraphy of the Late Miocene to Pleistocene, Norwegian Sea: ODP Leg 104, Sites 642 to 644. Proceedings of the Ocean Drilling Program, Scientific Results 104, 587-610.

Muhammad, Z., Bentley, S.J. Sr., Febo, L.A., Droxler, A.W., Dickens, G.R., Peterson, L.C., Opdyke, B.N., 2008. Excess ^{210}Pb inventories and fluxes along the continental slope and basins of the Gulf of Papua. Journal of Geophysical Research 113, F01S17, doi:10.1029/JF000676.

Norvick, M.S., Smith, M.S., Power, M.R., 2001. The plate tectonic evolution of Eastern Australasia guided by the stratigraphy of the Gippsland Basin, In: Hill, K.C., Bernecker, T. (Eds.), Eastern Australasian Basins Symposium 2001: A Refocused Energy Perspective for the Future. Petroleum Exploration Society of Australia, Melbourne, pp. 15-23.

O'Keefe, J.M.K., Eble, C.F., 2012. A comparison of HF-based and non-HF-based palynology processing techniques in clay-rich lignites from the Claiborne Group, upper Mississippi Embayment. Palynology 36, 116-130.

Oboh, F.E., 1992. Multivariate statistical analysis of palynodebris from the middle Miocene of the Niger Delta and their environmental significance. Palaios 7, 559-573.

Oboh-Ikuenobe, F.E., Yepes, O., Gregg, J.M., 1998. 25. Palynostratigraphy, palynofacies, and thermal maturation of Cretaceous-Paleogene sediments from the Côte D'Ivoire-Ghana transform margin. Proceedings of the Ocean Drilling Program Scientific Results 159, 277-318.

Oboh-Ikuenobe, F.E., Yepes, O., Mascle, J., Clift, P., Akamaluk, T., Ask, M., Barton, E., Bellier, J.-P., Benkhelil, J., Brantuoh, E., et al., 1997. Palynofacies analysis of sediments from the Côte d'Ivoire-Ghana transform margin: preliminary correlation with some regional events in the Equatorial Atlantic. Palaeogeography, Palaeoclimatology, Palaeoecology 129, 291-314.

Ogston, A.S., Sternberg, R.W., Nittrouer, C.A., Martin, D.P., Goni, M.A., Crockett, J.S., 2008. Sediment delivery from the Fly River tidally dominated delta to the nearshore marine environment and the impact of El Niño. Journal of Geophysical Research 113, F01S11, doi:10.1029/2006JF000669.

Philp, R.P., Calvin, M., Brown, S., Yano, E., 1978. Organic geochemical studies on kerogen precursors in recently deposited algal mats and oozes. Chemical Geology 22, 207-231.

Piasecki, S., 1980. Dinoflagellate cyst stratigraphy of the Miocene Hodde and Gram Formations. Bulletin of the Geological Society of Denmark 29, 53-76.

Pigram, C.J., Davies, P.J., Feary, D.A., Symonds, P.A., 1989. Tectonic controls on carbonate platform evolution in southern Papua New Guinea: passive margin to foreland basin. Geology 17, 199-202.

Pocknall, D.T., Beggs, J.M., 1990. Palynofacies as a tool for the interpretation of depositional environments in the Waikato and Taranaki Basins, New Zealand, 1989 New Zealand Oil Exploration Conference. Petroleum and Geothermal Unit, Ministry of Commerce, Wellington.

Pocock, S.A.J., Vasanthy, G., Venkatachala, B.S., 1988. Introduction to the study of particulate organic materials and ecological perspectives. Journal of Palynology 23-24, 167-188.

Pross, J., Link, E., Rug, M., Aigner, T., 2006. Delineating sequence stratigraphic patterns in deeper ramp carbonates: quantitative palynofacies data from the Upper Jurassic (Kimmeridgian) of southwest Germany. Journal of Sedimentary Research 76, 524-538.

Reid, P.C., 1974. Gonyaulacean dinoflagellate cysts from the British Isles. Nova Hedwigia 25, 579-637.

Richelot, C., Streel, M., 1985. Transport et sédimentation du pollen par les courants aériens, fluviatiles et marins á Calvi (Corse). Pollen et Spores 3-4, 349-364.

Roncaglia, L., 2004. Palynofacies analysis and organic-walled dinoflagellate cysts as indicators of palaeo-hydrographic changes: an example from Holocene sediments in Skálafjord, Faroe Islands. Marine Micropaleontology 50, 21-42.

Roncaglia, L., Kuijpers, A., 2004. Palynofacies analysis and organic-walled dinoflagellate cysts in late-Holocene sediments from Igaliku Fjord, South Greenland. The Holocene 14, 172-184.

Schiøler, P., Crampton, J.S., Laird, M.G., 2002. Palynofacies and sea-level changes in the Middle Coniacian-Late Campanian (Late Cretaceous) of the East Coast Basin, New Zealand. Palaeogeography, Palaeoclimatology, Palaeoecology 188, 101-125.

Schiøler, P., Rogers, K., Sykes, R., Hollis, C.J., Ilg, B., Meadows, D., Roncaglia, L., Uruski, C., 2010. Palynofacies, organic geochemistry and depositional environments of the Tartan Formation (Late Paleocene), a potential source rock in the Great South Basin, New Zealand. Marine and Petroleum Geology 27, 351-369.

Schrank, E., 1988. Effects of chemical processing on the preservation of peridinioid dinoflagellates: a case study from the Late Cretaceous of NE Africa. Review of Palaeobotany and Palynology 56, 123-140.

Skupien, P., Mohamed, O., 2008. Campanian to Maastrichtian palynofacies and dinoflagellate cysts of the Silesian unit, outer western Carpathians. Czech Republic Bulletin of Geoscience 83, 207-224.

Slingerland, R., Selover, R.W., Ogston, A.S., Keen, T.R., Driscoll, N.W., Milliman, J.D., 2008. Building the Holocene clinothem in the Gulf of Papua: an ocean circulation study. Journal of Geophysical Research 113, F01S14, doi:10.1029/2006JF000680.

Šmilauer, P., 2012. Canoco5 Version 5.0. Plant Research International, Wageningen.

Staplin, F.L., 1969. Sedimentary organic matter, organic metamorphism and oil and gas occurrence. Bulletin of the Canadian Journal of Petroleum Geology 17, 47-66.

Steinshouer, D.W., Qiang, J., McCabe, P.J., Ryder, R.T., 1999. Maps showing geology, oil and gas fields, and geologic provinces of the Asia Pacific Region U.S. Geological Survey Open File Report 97-470F. U.S.G.S., Reston.

Stopes, M.C., 1935. On the petrology of banded bituminous coals. Fuel 14, 4-13.

Symonds, P.A., Davies, P.J., Pigram, C.J., Feary, D.A., Chaproniere, G.C.H., 1991. Northeast Australia, Torres Shelf–Pandora Trough. Continental Margins Program Folio 4, 27.

Tcherepanov, E.N., Droxler, A.W., Lapointe, P., Mohn, K., 2008. Carbonate seismic stratigraphy of the Gulf of Papua mixed depositional system: Neogene stratigraphic signature and eustatic control. Basin Research 20, 185-209.

Traverse, A., 2007. Paleopalynology. Springer, Dordrecht, p. 813.

Tschudy, R.H., 1961. Palynomorphs as indicators of facies environments in Upper Cretaceous and Lower Tertiary strata, Colorado and Wyoming, In: Wiloth, G., Hale, L.A., Randall, A.G., Garrison, L. (Eds.), 16th Annual Field Conference Guidebook, Symposium on Late Cretaceous Rocks, Wyoming and Adjacent Areas. Wyoming Geological Association, Wyoming, pp. 53-59.

Tyson, R.V., 1984. Palynofacies investigation of Callovian (Middle Jurassic) sediments from DSDP Site 534, Blake-Bahama Basin, western Central Atlantic. Marine and Petroleum Geology 1, 3-13.

Tyson, R.V., 1993. Palynofacies analysis, In: Jenkins, D.J. (Ed.), Applied Micropaleontology. Kluwer Academic Publishers, Dordrecht, pp. 153-191.

Tyson, R.V., 1995. Sedimentary Organic Matter: Organic Facies and Palynofacies. Chapman & Hall, London.

Tyson, R.V., Follows, B., 2000. Palynofacies prediction of distance from sediment source: a case study from the Upper Cretaceous of the Pyrenees. Geology 28, 569-571.

van Bergren, P.F., Janssen, N.M.M., Alferink, M., Kerp, J.H.F., 1990. Recognition of organic matter types in standard palynological slides, In: Fermont, W.J.J., Weegink, J.W. (Eds.), Proceedings of the International Symposium on Organic Petrology. Mededelingen Rijks Geologische Dienst, Zeist, pp. 9-21.

van der Zwan, C.J., 1990. Palynostratigraphy and palynofacies reconstruction of the Upper Jurassic to Lowermost Cretaceous of the Draugen Field, offshore mid Norway. Review of Palaeobotany and Palynology 62, 157-186.

van der Zwan, C.J., van veen, P.M., 1978. The Devonian-Carboniferous transition sequence in southern Ireland: integration of paleogeography and palynology. Palinologia 1, 469-479.

Walsh, J.P., Nittrouer, C.A., Palinkas, C.M., Ogston, A.S., Sternberg, R.W., Brunskill, G.J., 2004. Clinoform mechanics in the Gulf of Papua, New Guinea. Continental Shelf Research 24.

Whitaker, M.F., 1984. The usage of palynology in definition of Troll Field geology, 6th Meeting of the Offshore Northern Seas Conference and Exhibition. Norks Petroleumsforening, Stavanger, p. 44.

Whitaker, M.F., Giles, M.R., Cannon, J.C., 1992. Palynological review of the Brent Group, UK sector, North Sea, In: Morton, A.C., Haszeldine, R.S., Giles, M.R., Brown, S. (Eds.), Geology of the Brent Group. Geological Society of America Special Publications 61, pp. 169-202.

Wolanski, E., Alongi, D.M., 1995. A hypothesis for the formation of a mud bank in the Gulf of Papua. Geo-Marine Letters 15, 166-171.

Wolanski, E., Norro, A., King, B., 1995. Water circulation in the Gulf of Papua. Continental Shelf Research 15, 185-212.

Zobaa, M., Botero, C.S., Browne, C., Oboh-Ikuenobe, F.E., Ibrahim, M., 2008. Kerogen and palynomorph analyses of the Mid-Cretaceous Bahariya Formation and Abu Roash "G" Member, North Western Desert, Egypt. Gulf Coast Association Geological Society Transactions 58, 933-943.

CHAPTER 3. DISTRIBUTION OF MODERN PALYNOMORPHS IN THE GULF OF PAPUA, PAPUA NEW GUINEA, AND THEIR RELATIONSHIP TO SEDIMENT SOURCE, TRANSPORT, AND DEPOSITION*

Introduction

The Gulf of Papua (GoP), southeast of Papua New Guinea (PNG), is a foreland basin with one of the highest sediment discharge volumes in the world (Figure 3.1) (Milliman, 1995). Seven research campaigns in the GoP were conducted from 2003 to 2005 in order to fully quantify how the GoP's sedimentary system works, from the sediment's creation at its "source" to its final deposition at its "sink" (NSF MARGINS Program, 2004). Hundreds of sediment cores were taken throughout the GoP, from the mouth of the Fly River (PNG's largest river) to the continental slope and ocean basin during this initiative. While numerous studies have been published on the cores and data gathered during the cruises (e.g., Keen et al., 2006; Carson et al., 2008; Crockett et al., 2008; Daniell, 2008; Francis et al., 2008; Muhammad et al., 2008; Ogston et al., 2008; Slingerland et al., 2008a; 2008b; Tcherepanov et al., 2008a; 2008b; Howell et al., 2014), a palynological study has yet to be done. Thomas et al. (2015) provided data on the non-palynomorph component of the palynological record (organic particles, including black/brown wood, leaf cuticle, resin, and structureless organic matter). They showed that the distribution of these particles is, in part, governed by the same processes controlling sediment distribution, including bathymetry, sedimentation rate, and distance from shore. Rowe et al. (2013) published a study on a mangrove-dominated shoreline in Caution Bay near Port Moresby, PNG. However, neither of these studies documents the extant palynomorph composition of sediments in the GoP. The present study has two

*This paper is in preparation for submission to the journal Marine Geology with the following coauthors: Sophie Warny, David M. Jarzen, Samuel J. Bentley, Sr., André W. Droxler, Charles A. Nittrouer, and Kehui Xu. It will be submitted by August 1, 2015.

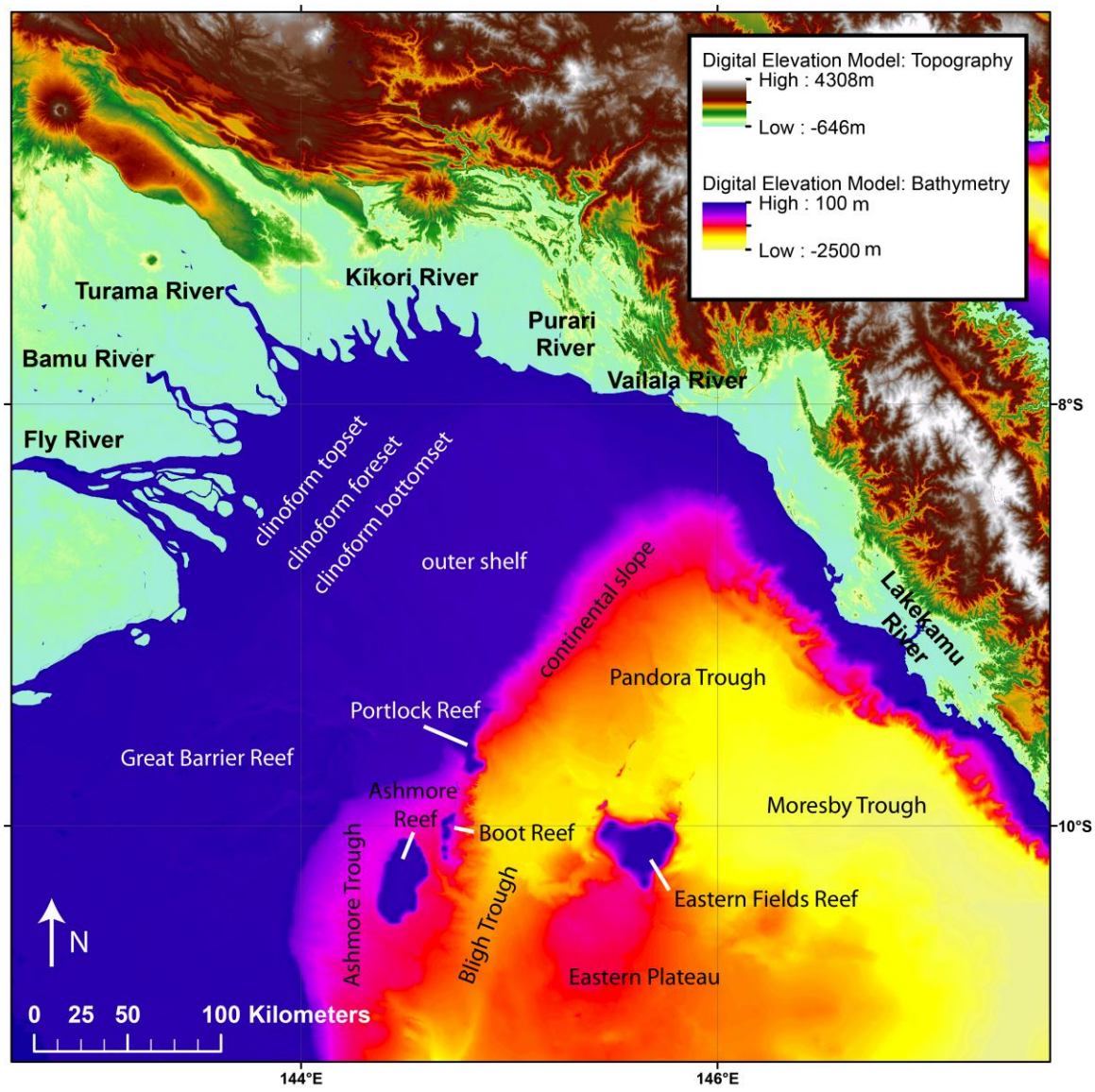

Figure 3.1. Bathymetric map of the Gulf of Papua and topographic map of Papua New Guinea (digital elevation model (DEM) from Daniell, 2008).

major goals: 1) use the palynological record to enhance understanding of modern sedimentary dynamics in the GoP; and 2) relate the distribution of palynomorphs (particularly pollen, spore, and dinoflagellate cysts) to the distribution of the living vegetation or organism that produced them.

Many researchers have shown how useful palynomorphs can be when interpreting sediment source, transport, and depositional environment (Muller, 1959; Stanley, 1965;

Traverse and Ginsburg, 1966; Heusser and Balsam, 1977; Heusser, 1983; Melia, 1984; Moss et al., 2005). Pollen and spores are useful because they are transported as part of the silt to very fine sand size load of the sediment, so their distribution is controlled, to a large degree, by the same factors that control sediment distribution, including erosion rates, current speed and direction, and particle density and morphology (Hoffmeister, 1954).

Pollen and spores, which are produced by vegetation, are an excellent representation of the dominant vegetation components living on land (Traverse, 2007). Numerous studies of the Quaternary flora of PNG have been published (e.g., Flenley, 1969; Flenley, 1972; Paijmans, 1975; Flenley, 1979; Walker and Flenley, 1979; Conn, 1995; Henty, 1995; Womersley, 1995). Here, we analyzed the recovered pollen and spores found in GoP sediments to compare this record with modern vegetation distribution (including mangroves, tropical rainforest, montane forests, swamps, and scrub/savanna/grassland) on the mainland to better understand the relationship between them.

Dinoflagellate cysts and other marine indicators, including foraminifer linings, copepod eggs, tintinnids, and acritarchs, will be analyzed to allow a better understanding of oceanographic conditions, including temperature, salinity, and primary productivity. Numerous researchers have demonstrated that dinoflagellate cyst distribution is related to oceanographic conditions (e.g., Traverse and Ginsburg, 1966; Melia, 1984; de Vernal et al., 1993; Hodgkiss and Ho, 1997; Marret and de Vernal, 1997; Warny and Wrenn, 1997; Warny and Wrenn, 2002; Marret and Zonneveld, 2003; Warny et al., 2003; Azanza et al.,

2004; de Vernal et al., 2005; Esper and Zonneveld, 2007; Bouimetarhan et al., 2009; Limoges et al., 2010).

Area of study

The GoP is southeast of PNG just south of the equator (7-11°S, 142-146°E, area of 1.5 x 10^{11} m^2) (Figure 3.1). The majority of material entering the GoP is sourced from mainland PNG and its surrounding islands (2-10°S, 140-154°E, area of 4.6 x 10^{11} m^2). The GoP has a depth range of zero to 3000 meters below sea level (mbsl). Mainland PNG has large topographic variations, from the coast at zero meters above sea level (masl) to 4509 masl (Daniell, 2008). The wet tropical setting results in near-constant warm temperatures and large rainfall volumes (Wolanski et al., 1995). The annual load of sediment delivered to the GoP from PNG (3.84 x 10^8 tons/yr, Milliman, 1995; Wolanski et al., 1995) is roughly equivalent to that delivered by all the rivers of North America, so the GoP is a particularly interesting area for studying how sediments are delivered to the ocean (Milliman, 1995). The sources of these sediments are several large rivers (Figure 3.1) including the Fly, Bamu, Kikori, Purari, Vailala, and Lakekamu Rivers that drain the mainland (Milliman, 1995; Wolanski et al., 1995). Sediments are delivered to a large, predominantly clastic shelf with an area of approximately 40,000 km^2 in the western gulf, while in the northeastern gulf where the continental shelf is very narrow (less than 10 km), sediments are delivered to the continental slope via channels (Milliman, 1995; Francis et al., 2008).

Climate and oceanography

Oceanographic conditions in the GoP have been extensively studied in recent years (e.g., Thom and Wright, 1983; Wolanski et al., 1984; Brunskill et al., 1995;

Wolanski and Alongi, 1995; Wolanski et al., 1995; Wolanski et al., 1999; Keen et al., 2006; Martin et al., 2008). Tidal influences are particularly important in the GoP because of its tropical setting, low seasonality, and small influence from cyclonic storms (McAlpine and Keig, 1983; Martin et al., 2008). In addition to tides, seasonal wind changes (austral summer monsoons and winter trade winds) play an important role in the GoP's oceanography (Thom and Wright, 1983; McAlpine and Keig, 1983; Walsh et al. 2004). Other factors include the Coral Sea Current (CSC) (Wolanski and Eagle, 1991; Brunskill et al., 1995, Wolanski and Alongi, 1995; Wolanski et al., 1995; Walsh et al., 2004) and the El Niño Southern Oscillation (ENSO) (Rodbell et al., 1999; Kawahata and Gupta, 2004; Ogston et al., 2008).

The largest river entering the GoP is the Fly River, and its impacts to GoP oceanography apply to the other smaller rivers (Bamu, Kikori, Purari, Vailala, and Lakekamu Rivers). The Fly River delta is mesotidal in nature, with an average range of two to four meters. Tidal variations produce interlaminated mud and sand deposits that vary on spring-neap timescales (Martin et al., 2008). The river's delta is funnel-shaped (as is characteristic of most tide-dominated deltas), and it has three major distributaries, the southernmost of which carries the most sediment (Dalrymple et al., 2003).

Two major wind regimes exist in the GoP. A summer monsoon occurs from December to March, and during this time, winds blow from the northwest. This season is relatively calm with average wave heights of approximately 0.3 meters. A winter trade winds period occurs from May to October, and during this time, winds blow from the southeast. This season is less calm with rougher seas and an average wave height of 1.3

meters. There are transitional periods with lower wind velocities during the intervening months (Thom and Wright, 1983; McAlpine and Keig, 1983; Walsh et al. 2004).

The CSC transports most sediments and dissolved material to the northeast on the western GoP shelf (Wolanski and Eagle, 1991; Brunskill et al., 1995; Wolanski and Alongi, 1995; Wolanski et al., 1995; Walsh et al., 2004). Sediments here are retained on the continental shelf and rarely escape to the slope. This transport is more complex in the northern and eastern GoP where the CSC breaks down, especially between the Purari River and Port Moresby (Keen et al., 2006). In this area, current measurements indicate that instead of being transported to the northeast, sediments are transported to the south from the shelf to the adjacent continental slope (MacFarlane, 1980; Wolanski et al., 1988; Wolanski and Eagle, 1991; Brunskill et al., 1995; Walsh et al., 2004; Keen et al., 2006; Martin et al., 2008). Sediments are preserved on the slope in several troughs and canyons (Ewing et al., 1970; Gardner, 1970; Winterer, 1970; Brunskill et al. 1995; Muhammad et al., 2008).

The El Niño Southern Oscillation (ENSO) plays an important role in GoP oceanography on yearly timescales (Rodbell et al., 1999; Kawahata and Gupta, 2004; Ogston et al., 2008). During ENSO conditions, less rainfall than average occurs, reducing the amount of discharge and sediment to the GoP. This results in less sediment accumulation on the GoP shelf during ENSO years (Ogston et al., 2008). It also increases salinity, by limiting the influx of freshwater. During La Niña years, more rainfall than average occurs, increasing discharge and sediment input to the GoP, as well as decreasing salinity (Ogston et al., 2008; Howell et al., 2014).

Regional geology

An overview of the regional geology of PNG and the GoP is key to understanding the sedimentary dynamics of the GoP and provide information needed to evaluate the source of pre-Quaternary species that could be found in palynological preparations. Both the geology of PNG and the sedimentary processes operating in the GoP are exceedingly complex due to the modern day tectonic processes operating in the area, including collision of rifted Australian crust with multiple terranes in the Cenozoic and the subsequent development of the GoP foreland basin (Pigram and Davies, 1987; Pigram et al., 1989; Abbott, 1995; Davies, 2012). Mainland PNG is composed of four tectonic provinces, including the Fly Platform, the Papuan Fold Belt, the New Guinea Highlands/Papuan Peninsula, and a northern series of sutured volcanic arcs (Abbot, 1995) (Figure 3.2). The Fly Platform is underlain by Australian continental crust and is covered with Quaternary sediments derived from multiple rivers feeding the GoP. The Papuan Fold Belt, an active fold and thrust belt lying to the northeast of the Fly Platform, consists primarily of deformed, uplifted Mesozoic and Neogene rocks (Abbott, 1995). The rocks composing the New Guinea Highlands and Papuan Peninsula are older, up to Late Paleozoic in age, and extremely deformed. A series of volcanic arcs are sutured to the mainland in the northeast during collision in the Neogene, but differentiating among them is unecessary for this paper, as sediments sourced from these rocks are unlikely to enter the GoP, due to the drainage divide of the PNG Highlands (Pigram et al., 1989; Abbott, 1995; Steinshouer et al., 1999).

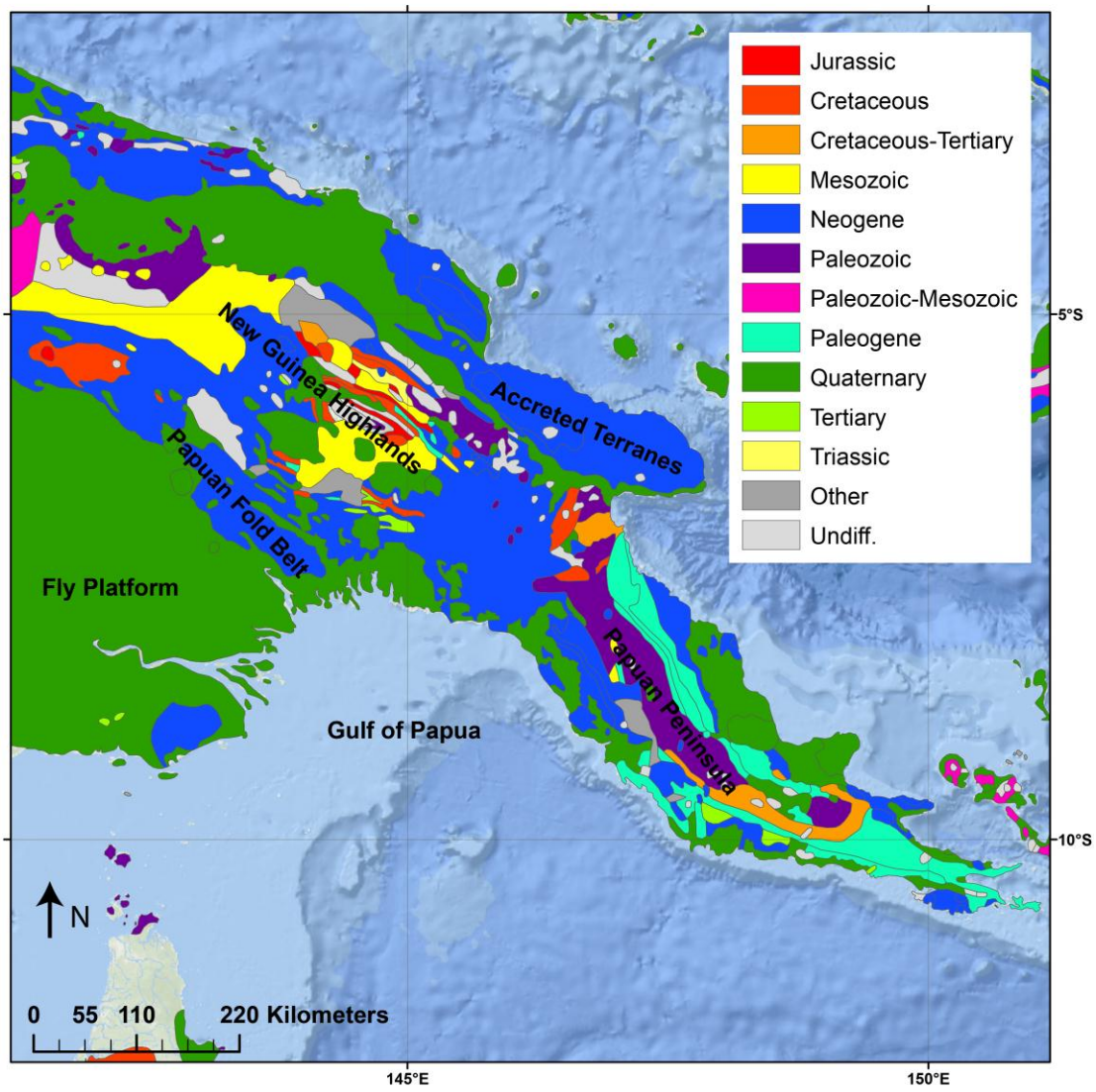

Figure 3.2. Geologic map of Papua New Guinea from Steinshouer et al. (1999).

Sedimentology in the Gulf of Papua

Many authors have studied the modern sedimentation regime in the GoP (e.g., Harris et al., 1993; Harris, 1994; Milliman, 1995; Wolanski and Alongi, 1995; Dalrymple et al., 2003; Walsh et al., 2004; Keen et al., 2006; Francis et al., 2008; Martin et al., 2008; Muhammad et al., 2008; Ogston et al., 2008; Slingerland et al., 2008a; 2008b). They established that the multiple factors discussed above play a role in determining the

variability of sedimentary processes there, including topography and climate, tidal variations, seasonal wind patterns, and the El Niño Southern Oscillation (ENSO).

The GoP is classified as a mixed siliciclastic-carbonate depositional system (Francis et al., 2008; Tcherepanov et al., 2008a), which means that both carbonate and siliciclastic sediments are delivered to the basin. A large Quaternary clinoform composed primarily of siliclastic sediments sourced from multiple rivers characterizes the inner shelf (which is greater than 100 km wide) of the western GoP (Figure 3.1) (Harris et al., 1993; Walsh et al., 2004; Slingerland et al., 2008a). Between the clinoform and the shelf break, few sediments accumulate at present, because the clinoform has not yet prograded over the marine transgressive surface created during the latest sea level rise (Harris et al., 1996; Crockett et al., 2008; Francis et al., 2008). The northern and eastern gulf has a much narrower shelf (less than 10 km) where siliciclastic deposits are delivered directly to the slope (Brunskill et al., 1995; Muhammad et al., 2008; Howell et al., 2014). Past the shelf break, most siliclastic accumulation consists of hemipelagic muds (Muhammad et al., 2008) or submarine fans in Ashmore, Pandora, and Moresby Troughs (Figure 3.1). The only area where carbonate accumulation outpaces siliciclastic sediment supply is in the southwestern gulf near the Great Barrier Reef (Francis et al., 2008; Tcherepanov et al. 2008b), although greater carbonate delivery occurred in the early Holocene (Jorry et al., 2008).

Sediment delivery to the western inner shelf: Clinoform deposits

Harris et al. (1993) estimate that up to 40% of the sediment load delivered to the GoP is contained within the clinoform (0.85×10^8 tons per annum). Walsh et al. (2004) performed an extensive study of the GoP clinoform, which consists of three major

regions, topset, foreset, and bottomset beds (Figure 3.1). Topset beds are characterized by interbedded sands and muds up to 20 meters below sea level. Sediment accumulation rates (SARs) for topset beds are approximately 0.7 cm/yr. Foreset beds are more steeply dipping muddy beds between 20 to 60 mbsl. SARs for foreset beds are much higher, between 1.5 to 4.0 cm/yr. Bottomset beds are also muddy with a carbonate-sand component and are deeper than 60 mbsl. SARs are less than 0.4 cm/yr for bottomset beds (Wolanski and Alongi, 1995; Walsh et al., 2004; Slingerland et al., 2008a; 2008b). SAR rates on the clinoform are generally higher during calmer NW-monsoon conditions, and event beds accumulate on the foreset (5-10 cm thick) during the SE-trade wind season on nearly annual timescales (Walsh et al., 2004). Sediments of the clinoform are sourced from the Fly Platform (covered with Quaternary floodplain deposits) and the Papuan Fold Belt (Mesozoic and Neogene rocks). Sediments sourced from the PNG Highlands are rare (Davies, 2012). Eagle and Higgins (1990) have noted that mining for gold and copper at the Ok Tedi Mine (near the head of the Ok Tedi River) has increased sediment discharge from the Fly River to the GoP by 40% (although this has not changed clinoform morphology).

Sediment delivery to the continental slope

Several minibasins, including Ashmore, Pandora, Bligh, and Moresby Trough, are the final accumulation sites for sediments in the GoP (Figure 3.1) (Febo, 2007). During periods of high sea level, like at present, few sediments accumulate in these troughs, because sedimentation rates are lower (less than 0.2 cm/yr) (Muhammad et al., 2008). When sea level is low, as during the Last Glacial Maximum, rivers can flush out sediment stored on the continental shelf in clinoforms, and these sediments are delivered

directly to the troughs (Harris et al., 1996; Febo, 2007; Carson et al., 2008; Crockett et al., 2008; Muhammad et al., 2008). Two major canyons in the GoP, Moresby and Bligh Canyons, act as conduits that can transport large sediment volumes. The composition of siliclastic material entering the troughs reflects sourcing from the Papuan Highlands (Vailala and Lakekamu watersheds) with higher concentrations of igneous and metamorphic minerals compared to clinoform sediments (Davies, 2012). The Eastern Plateau, in the far southeast of the GoP, accumulates only hemipelagic and pelagic sediments (Francis et al., 2008).

Modern vegetation distribution

The Quaternary vegetation history of PNG reveals changes in climate and human occupation. We can understand changes in vegetation distribution by examining the pollen and spore record. This history has been investigated by numerous authors using a combination of palynological, botanical, archaeological, and ecological approaches (Flenley, 1969; 1972; 1979; Walker and Flenley, 1979; Conn, 1995; Henty, 1995; Womersley, 1995; Haberle et al., 2001; Haberle and Ledru, 2001; McAlpine and Freyne, 2001; Denham et al., 2003; Haberle, 2003; Fairbairn et al., 2006; Haberle, 2007; Denham et al., 2009; Haberle et al., 2012; Torrence, 2012; Rowe et al., 2013).

Paijmans (1975) provides an excellent synthesis of the modern vegetation distribution on PNG (Figure 3.3 is a simplified version). The major groups include: mangroves, lowland tropical rainforest, swamps, lower montane forest, upper montane forest, scrub/savanna/grassland, and garden (grouped with scrub/savanna/grassland for palynological analyses). The highly variable topography of Papua New Guinea leads to a

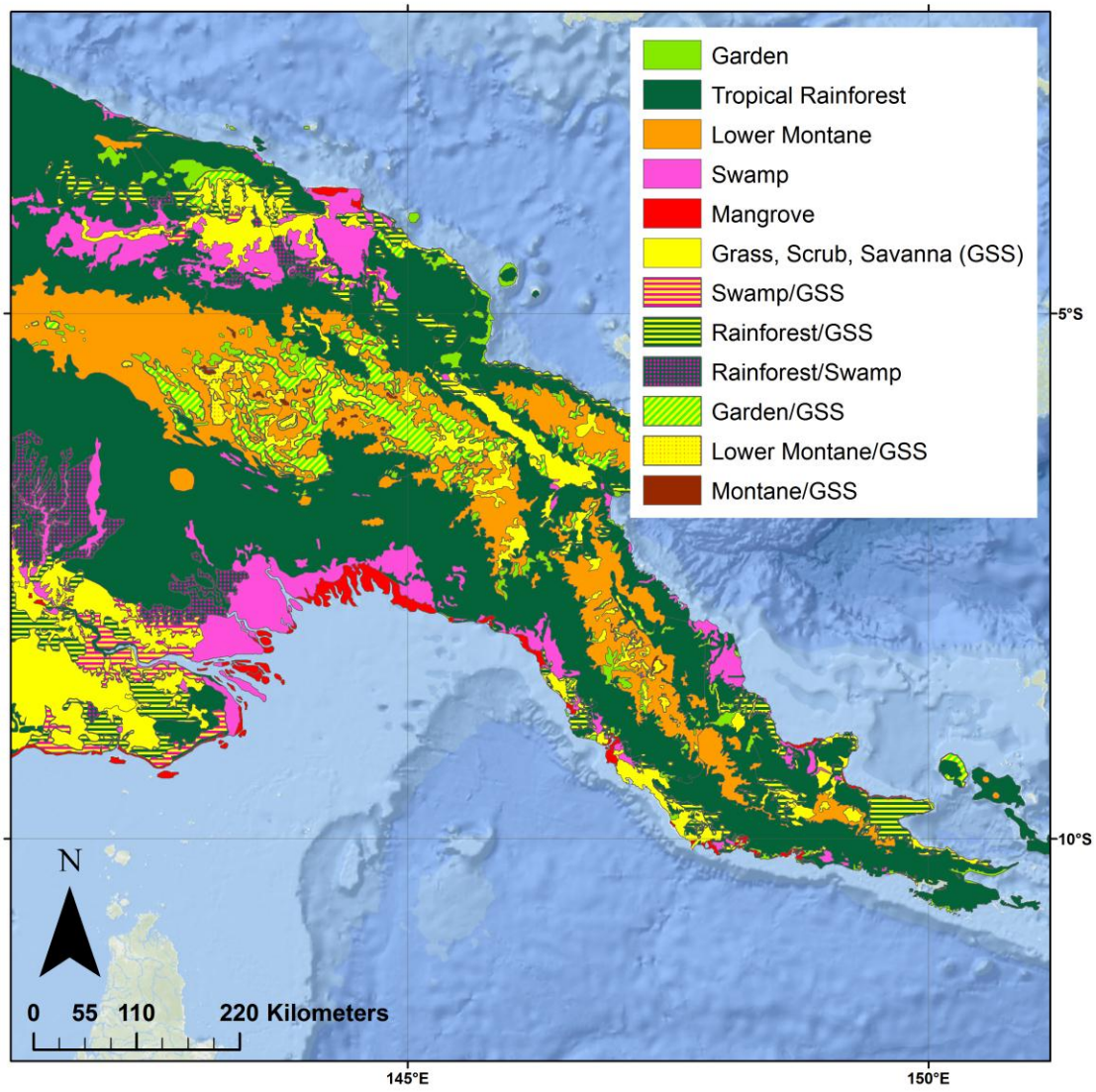

Figure 3.3. Vegetation map of Papua New Guinea, modified from Paijmans (1975). Basemap from ESRI (2015).

strong altitudinal distribution of vegetation (Figure 3.4) (van Steenis, 1934-36; Brass, 1941, 1964; Paijmans, 1975; Flenley, 1979; Walker and Flenley, 1979). In particular, montane forest taxa occupies elevations above approximately 1500 meters, while rainforest taxa live between 0 to 1500 meters above sea level. Scrub and grassland taxa can be found at all altitudes.

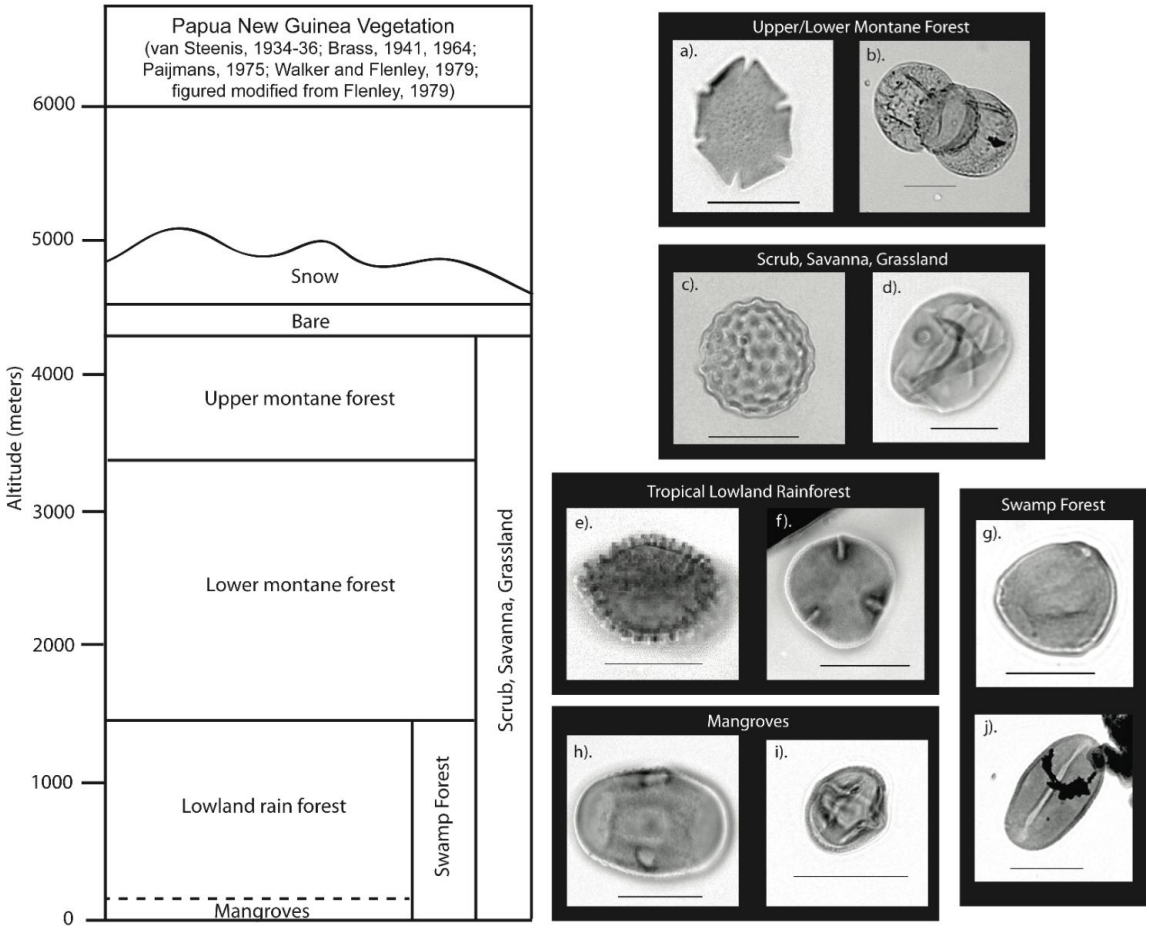

Figure 3.4. Generalized altitudinal distribution of Papua New Guinea vegetation, modified from Flenley (1979), data synthesized from van Steenis (1934-1936), Brass (1941, 1964), Paijmans (1975), Flenley (1979), and Walker and Flenley (1979). Characteristic pollen from each of the major vegetation groups and corresponding site in the GoP where they were found, a) *Nothofagus* spp., A8.5; b) Podocarpaceae, 49JPC; c) Chenopodiaceae, 02BC; d) Gramineae, A8.5; e) Rubiaceae, A8.5; f) Tiliaceae, A8.5; g) *Carya* spp., EE5; h) *Sonneratia* spp., A8.5; i) Rhizophoraceae, T13-20C; j) Arecaceae, C2-A11.

How sedimentation impacts palynomorph distribution

Many factors govern the transport and deposition of pollen and spores, including their size; density; the number of grains produced by the parent plant; the velocity and viscosity of the water transporting the palynomorphs; turbidity; and regional current

directions (Traverse, 2007). The production of marine palynomorphs, especially dinoflagellate cysts and acritarchs, is governed by many other factors in addition to the ones listed above, including temperature, salinity, and primary productivity (Batten, 1996). Pollen and spores are transported as part of the silt to very fine sand portion (4 to 125 microns) of the sediment and range in size from approximately 5 microns to greater than 100 microns. The settling rate of pollen and spores can be calculated using Stoke's law (Blatt et al., 1972), and researchers have shown that pollen and spores sink slightly more slowly than sediment grains (Muller, 1959; Stanley, 1965). Measured rates from Muller (1959) indicate palynomorphs sink on the order of 4-17 cm/hr.

Wind transport has been shown to have less impact on pollen and spore assemblages than transport by water, except for very small or bisaccate grains, because they usually reach the ground within close vicinity to the parent plant (Muller, 1959; Tauber, 1965; Peck, 1973; Mandrioli et al., 1982; Tsukada, 1982; Knapp et al., 2001; Lange et al., 2002). Hoffmeister (1954) demonstrated that the processes governing the distribution of pollen and spores are approximately the same as those governing sediments. More recent works (e.g., Muller, 1959; Heusser and Balsam, 1977; Heusser, 1983; Moss et al., 2005) have indicated transport of palynomorphs is slightly more complex than for sediments for several reasons. Palynomorphs are often found in the highest concentrations in quiet water areas with little turbulence, because they fall out of suspension as transport energy decreases. Certain palynomorph morphologies, especially bisaccate pollen, may be transported longer distances, because they have sacs containing trapped air, which increases their buoyancy (Muller, 1959; Traverse and Ginsburg, 1966; Traverse, 2007).

Certain plant groups produce vast abundances of pollen, while others produce very little pollen (Pohl, 1937a; 1937b; Wijmstra, 1978; Birks and Birks, 1980; Traverse, 2007). This, to a large degree, is determined by whether the parent vegetation is wind-pollinated (anemophilous) or animal-pollinated (zoophilous). Anemophilous vegetation, like most gymnosperms that produce bisaccate pollen, many tree species, as well as spore plants, produce huge numbers of pollen per cone, flower, or frond (close to 1.5 million pollen grains from a single cone; Pohl, 1937a; 1937b). Pollen from anemophilous vegetation generally dominates the pollen record. Zoophilous vegetation, like the Orchidaceae and most members of the Malvaceae, produce much lower numbers of pollen grains and thus have less representation in the pollen record (Traverse, 2007).

Materials and Methods

Sampling

Samples were collected on the R/V *Melville* (MV) and R/V *Western Venturer* (WV) ships during seven cruises (MV0104, MV0404, MV0803, MV24-0403, MV25-0403, MV26-0403, and WV0103) in the GoP from 2003 through 2005 (Figure 3.1). Several coring methodologies were utilized, including box cores (BC), jumbo piston cores (JPC), multi cores (MC), grab cores (GC), and kasten cores (KC). Some coring techniques, such as box coring and grab coring, can impact the top few centimeters of sediment recovered, but because the samples are averages from the top four centimeters of sedimentary cover, we believe the impact of different coring methodologies was minimal. Muhammad et al. (2008) indicate that in offshore sites with the lowest sedimentation rates (0.05 cm/yr), all sediments from the top five centimeters have been deposited within the last hundred years. Nearshore samples have accumulated much more

rapidly, and sample intervals reflect a smaller time interval of the past few years of deposition (Wolanski and Alongi, 1995; Walsh et al., 2004; Slingerland et al., 2008a). For our purpose, we have selected samples averaged from the top 0 to 4 cm of sedimentary cover, because we believe this interval effectively presents the Recent (within the last hundred years) geographic distribution of palynomorphs.

There are two subsets of samples within this study: 1) nearshore samples that have accumulated on the clinoform, and 2) offshore samples from the continental slope, rise, and abyssal plain (Figure 3.1, Table 3.1). Offshore samples are archived in the Department of Geology and Geophysics at Louisiana State University in Baton Rouge, LA, U.S.A., and nearshore samples are archived in the Department of Earth and Space Sciences at the University of Washington in Seattle, Washington, U.S.A. A large gap in sampling exists on the outer shelf which is the marine transgressive surface formed during the latest sea level rise (Harris et al., 1996; Crockett et al., 2008; Francis et al., 2008).

Processing

An external consultant processed the samples according to the procedures as outlined in Traverse (2007). Samples were "spiked" before processing with one or two *Lycopodium clavatum* tablets (batch #124961 and #1031). 10% HCl and 70% HF were used to dissolve carbonates and silicates. Samples were sieved at 10 μm, with the less than 10 μm fraction retained to make sure Rhizophoraceae pollen was not lost (e.g., Scourse et al., 2005). Organic material was separated from the remaining inorganic material with heavy liquid separation using $ZnBr_2$. Controlled oxidation with Schulze's reagent (a mixture of potassium chlorate and nitric acid) was performed for 30 seconds

Table 3.1. Information for 67 Gulf of Papua samples. Latitude and longitude are in decimal degrees. Dried sample weight is in grams (g). Core types include BC (box cores), JPC (jumbo piston cores), MC (multi cores), GC (grab cores), KC (kasten cores). Sampled intervals are in centimeters (cm). The following parameters were included in statistical analysis: water depth (meters, m) measured when the samples were taken; distance from shore (kilometers, km) measured as the nearest straight line distance; distance from slope break (kilometers, km; negative values are on the continental shelf) measured as the nearest straight line distance; and sedimentation rate (centimeters per year). Offshore sample sedimentation rates are from Muhammad et al. (2008), and nearshore sample sedimentation rates are estimated from Walsh et al. (2004).

Sample	Latitude	Longitude	Weigh t (g)	Core Type	Interval (cm)	Depth (m)	Dist. From Shore (km)	Dist. From Slope Break (km)	Sed. Rate (cm/yr)
02BC	-10.3092	144.1632	32.4	BC	0-4	-661	164	21.5	---
07TC	-10.4400	144.2050	20.1	JPC	0-4	-779	175	26.5	---
10MC	-9.8742	144.4812	28.9	MC	0-4	-584	148	10	0.05
12MC	-9.8120	144.4620	35.4	MC	0-4	-372	142	2.4	0.09
14MC	-9.9073	144.6608	34.6	MC	0-4	-760	166	18.5	0.23
16MC	-9.7443	144.7443	39.9	MC	0-4	-686	164	2.4	0.05
18MC	-8.5109	145.5134	13.9	MC	0-4	-262	61	2.9	0.26
20MC	-9.2948	145.0185	34.3	MC	0-4	-661	162.5	5.6	0.12
21MC	-9.3648	145.0570	26.3	MC	0-4	-1009	165	15	0.05
22TC	-9.7731	146.4712	3.6	JPC	0-2	-2063	73	55	---
24MC	-9.7890	146.2478	16.6	MC	0-4	-2102	92	75	0.14
26MC	-10.0090	146.3785	17.7	MC	0-4	-2232	97	80	0.07
30MC	-9.6667	146.1667	17.9	MC	0-4	-2023	87	69	0.10
32MC	-9.5520	145.3532	27.6	MC	0-4	-1620	150	52	0.05
38MC	-9.0083	145.3450	22.2	MC	0-4	-977	120	17	0.10
39MC	-8.6053	145.6060	12.2	MC	0-4	-690	68	13.5	0.13
42MC	-8.3698	145.8367	12.8	MC	0-4	-91	35.5	-3.2	0.35
43MC	-8.9120	146.4023	21.7	MC	0-4	-62	15.5	-1.9	0.34
44MC	-8.6072	146.1918	10.8	MC	0-4	-99	17.5	-2.5	0.28

(Table 3.1 continued)

Sample	Latitude	Longitude	Weigh t (g)	Core Type	Interval (cm)	Depth (m)	Dist. From Shore (km)	Dist. From Slope Break (km)	Sed. Rate (cm/yr)
47MC	-8.4347	145.8337	5.8	MC	0-4	-399	40	9	0.28
49JPC	-8.5845	145.8333	3.7	JPC	0-2	-859	51	23.5	---
50MC	-8.5933	146.0457	11.9	MC	0-4	-795	30	10	0.13
53MC	-8.7288	145.9358	15	MC	0-4	-1111	48	25	0.21
56MC	-8.9392	145.2343	22.6	MC	0-4	-450	112	2.5	0.08
59MC	-9.3882	144.9162	11.7	MC	0-4	-577	160	3.5	---
60MC	-9.2423	145.8103	21.7	MC	0-4	-1674	88	70	0.07
61JPC	-8.9998	145.9667	10	JPC	0-2	-1616	64	42	---
67MC	-9.5822	144.9048	17.8	MC	0-4	-1638	195	22.5	0.05
69MC	-9.9845	144.8745	17.6	MC	0-4	-1758	39.5	-47	0.12
72MC	-10.2543	144.6890	31.5	MC	0-4	-1320	195	57	0.07
76MC	-10.4432	144.8629	21.4	MC	0-4	-1551	225	72	0.07
A8.5	-8.3619	143.2864	19.4	GC	0-4	-12	1.3	-195	---
C2-8	-8.5743	143.9577	20	KC	0-4	-18	15.5	-130	0.70
C2-A11	-8.6559	143.9938	19.7	GC	0-4	-25	23.5	-121	1.50
CC5	-8.1796	143.9417	19.8	KC	0-4	-7	16.5	-160	0.70
CC7	-8.2753	144.0579	19.6	KC	0-4	-5	33	-136	0.70
D2	-8.8133	143.7658	19.6	KC	0-4	-15.9	19	-126	0.70
D6	-8.7200	143.7019	19.5	KC	0-4	-26	7.6	-145	1.50
EE5	-8.1166	144.0822	19.8	KC	0-4	-4	21.5	-150	0.70
EE7	-8.1752	144.1726	20.4	KC	0-4	-8	34	-145	0.70
EE9	-8.2145	144.2385	19.7	KC	0-4	-12	42	-128	0.70
G2	-9.0685	143.4930	20.6	KC	0-4	-6	6.6	-120	0.70
G3	-9.0521	143.4851	19.6	KC	0-2	-5	5.3	-121	0.70
G5	-9.0315	143.4870	20.5	KC	0-4	-6	4.9	-123	0.70

(Table 3.1 continued)

Sample	Latitude	Longitude	Weigh t (g)	Core Type	Interval (cm)	Depth (m)	Dist. From Shore (km)	Dist. From Slope Break (km)	Sed. Rate (cm/yr)
T10-20	-8.5700	144.1650	19.1	KC	0-4	-15	22.5	-105	0.70
T10-60	-8.8100	144.4100	21.4	KC	0-4	-26.1	35	-94	1.50
T11-20	-8.5000	144.2200	20.1	BC	0-4	-20.8	37	-112	1.50
T1-20	-9.1208	143.6250	19.4	BC	0-4	-62.1	72	-75	0.40
T12-20	-8.4000	144.2333	21.2	BC	0-4	-20.7	43	-115	1.50
T1-25	-9.2000	143.7080	20.4	BC	0-4	-19.1	45	-119	0.70
T13-20C	-8.3300	144.2900	20.2	KC	0-4	-29	55	-117	1.50
T13-30C	-8.3500	144.3100	20.5	BC	0-4	-37	56	-114	2.50
T2-30	-9.1333	143.7750	19	BC	0-2	-23.9	38.5	-94	1.50
T3-20KC	-9.0000	143.7550	18	BC	4-6	-20.2	33.5	-109	1.50
T3-30	-9.0500	143.8083	21.5	BC	0-4	-28.2	39.5	-100	1.50
T4-30	-8.9900	143.8575	20	BC	0-4	-28.8	44.5	-105	1.50
T4-50	-9.0900	143.9600	19.2	BC	0-4	-47.4	56.5	-90	0.70
T5-20	-8.8950	143.8950	19.4	BC	0-4	-23.2	36	-116	1.50
T6-20	-8.8375	143.9500	19.4	KC	0-4	-19.3	36	-117	0.70
T6-30	-8.8620	143.9770	19.5	KC	0-4	-30.8	39.5	-102	2.50
T7-20	-8.7800	144.0125	19.7	KC	0-4	-21.8	34.5	-105	1.50
T7-30	-8.8050	144.0363	19.5	KC	0-4	-33.2	38	-100	2.50
T8-20B	-8.6500	143.9833	22	KC	0-4	-21.3	21.5	-118	1.50
T8-30	-8.7450	144.0800	20.5	KC	0-2	-34.9	36.5	-108	2.50
T8-50	-8.7875	144.1200	11.7	KC	4-5	-67.5	43.5	-95	0.40
T8-60	-8.8525	144.1900	19.7	KC	0-4	-80	54	-86	0.40
T9-30	-8.7000	144.1800	19.8	KC	0-4	-34.8	43.5	-95	2.50

allow for easier identification of palynomorphs. Residues of both size fractions (>10 μm and <10 μM) were mounted on glass slides with clear casting resin.

Nearshore samples, in particular, show high recovery of reworked specimens, so we believe the use of an oxidant for this sample set, although it is modern, was viable. Strong oxidants, like Schulze's reagent, however, are known to damage fragile palynomorphs, such as dinoflagellate cysts and several angiosperm pollen types, especially in modern sediments (Harland, 1981; Harland, 1983; Schrank, 1988). To ensure that dinoflagellate cysts were not affected, samples were processed without controlled oxidation in LSU's CENEX (Center for Excellence in Palynology) laboratory according to a modification of O'Keefe and Eble's (2012) technique. The authors differed from O'Keefe and Eble (2012) in that potassium hydroxide (KOH) was not used.

Microscopy

A minimum of 300 palynomorphs were counted per sample on the >10 μm slides using transmitted light on an Olympus BX43 microscope at 600x magnification (Table 3.2) (Traverse, 2007). The <10 μm fraction slides were scanned to make sure no additional species were missed (e.g., Scourse et al., 2005), but these slides were not included in the count because very few pollen and no additional species were found after a routine scan. We do not believe the use of a 10 μm sieve biased mangrove pollen recovery in this study. *Lycopodium* spore counts were also tabulated while counting to allow for concentration calculations (Table 3.3) (e.g., Stockmarr, 1971; Traverse, 2007; Lignum et al., 2008) according to the following equation:

$$palynorphs\ per\ gram\ = \frac{specimens\ counted * number\ of\ tablets * \text{Lycopodium}\ in\ 1\ tablet}{Lycopodium\ counted * weight\ of\ sample\ (g)}$$

Table 3.2. Raw counts for 67 Gulf of Papua samples.

Sample	*Lycopodium*	Reworked specimens	Pollen	Spores	Fungal Spores	Dinoflag-ellate Cysts	Acritarchs	Tintinnids	Copepod Eggs	Foraminifer Linings
02BC	187	63	27	47	16	56	72	0	0	8
07TC	131	21	15	22	30	109	149	2	0	2
10MC	168	31	20	70	9	61	106	0	1	1
12MC	249	70	22	34	25	54	110	2	0	2
14MC	6	43	21	155	6	12	34	0	0	0
16MC	426	76	51	119	5	8	31	0	0	0
18MC	5	19	70	175	4	1	6	0	0	0
20MC	35	148	11	98	6	8	15	0	0	1
21MC	5	139	12	112	4	1	13	0	0	0
22TC	32	9	25	182	4	17	49	0	0	0
24MC	10	12	16	249	5	6	7	0	0	0
26MC	16	17	11	219	6	9	18	0	0	0
30MC	7	22	15	210	4	17	16	0	0	0
32MC	6	33	21	201	8	12	17	0	0	0
38MC	1	54	20	153	4	12	16	0	0	0
39MC	2	34	18	242	1	1	2	0	0	1
42MC	164	30	45	161	5	6	13	0	0	0
43MC	206	0	60	171	0	0	17	0	0	0
44MC	579	11	44	156	7	9	30	0	0	0
47MC	320	37	27	135	4	11	43	0	0	1
49JPC	69	40	32	214	2	4	6	0	0	0
50MC	452	11	42	157	14	10	13	0	0	0
53MC	66	14	28	216	3	1	19	0	0	0
56MC	3	124	59	51	2	0	8	0	0	0

(Table 3.2 continued)

Sample	*Lycopodium*	Reworked specimens	Pollen	Spores	Fungal Spores	Dinoflag-ellate Cysts	Acritarchs	Tintinnids	Copepod Eggs	Foraminifer Linings
59MC	6	184	14	78	0	9	2	0	0	0
60MC	5	31	26	222	5	2	5	0	0	0
61JPC	30	17	34	210	7	15	9	0	0	0
67MC	4	61	16	189	5	1	5	0	0	1
69MC	2	38	19	226	3	10	2	0	1	1
72MC	4	66	31	178	2	2	3	0	3	0
76MC	7	44	36	194	2	7	5	0	0	0
A8.5	40	121	65	72	0	0	3	0	0	1
C2-8	37	161	62	107	2	0	1	0	0	0
C2-A11	37	158	54	141	2	0	0	0	0	1
CC5	34	83	43	157	2	0	6	0	0	0
CC7	47	128	49	112	0	0	4	0	0	1
D2	37	201	52	73	1	1	0	0	0	1
D6	78	171	41	73	2	0	1	0	0	0
EE5	18	155	44	90	1	0	0	0	0	0
EE7	36	196	53	62	0	2	0	0	0	0
EE9	24	281	25	34	0	0	0	0	0	0
G2	18	191	50	66	2	0	0	0	0	0
G3	36	227	23	49	0	0	0	0	0	0
G5	55	281	28	38	0	0	0	1	0	0
T10-20	26	125	104	119	0	4	1	0	0	0
T10-60	53	170	35	120	0	0	0	0	0	0
T11-20	25	181	48	79	0	2	2	0	0	0
T1-20	181	263	27	21	1	1	0	0	0	0
T12-20	77	243	23	36	0	0	1	0	0	0

(Table 3.2 continued)

Sample	*Lycopodium*	Reworked specimens	Pollen	Spores	Fungal Spores	Dinoflag-ellate Cysts	Acritarchs	Tintinnids	Copepod Eggs	Foraminifer Linings
T1-25	382	210	46	49	2	2	0	0	0	0
T13-20C	54	160	44	105	0	0	1	0	0	0
T13-30C	45	234	41	87	0	0	0	0	0	0
T2-30	100	251	15	23	0	1	6	0	0	0
T3-20KC	32	215	14	60	0	0	0	0	0	0
T3-30	53	145	50	84	2	2	4	0	0	0
T4-30	108	169	39	114	2	0	0	1	0	0
T4-50	45	156	40	63	0	0	1	0	0	0
T5-20	51	220	33	75	0	0	0	0	0	0
T6-20	26	240	17	48	0	2	1	0	1	1
T6-30	83	271	27	45	0	1	3	0	0	0
T7-20	91	262	19	29	0	0	0	0	0	0
T7-30	56	227	19	47	0	1	1	0	2	2
T8-20B	42	141	47	105	1	0	0	0	0	1
T8-30	44	164	35	76	2	0	0	0	0	0
T8-50	98	189	24	118	1	2	0	1	0	1
T8-60	27	173	26	98	3	0	0	0	0	0
T9-30	47	117	66	127	1	1	1	0	0	0

Table 3.3. Abundance calculations for 67 Gulf of Papua samples. Reworked specimens includes all reworked forms of any age older than Quaternary. Terrestrial abundance includes pollen, spores, and fungal spores. Marine indicator abundance includes dinoflagellate cysts, acritarchs, tintinnids, copepod eggs, and foraminifer linings. Abundances calculated according to Stockmarr (1971), Traverse (2007), and Lignum et al. (2008).

Sample	Reworked Abundance (specimens/g sediment)	Terrestrial Abundance (specimens/g sediment)	Marine Indicator Abundance (specimens/g sediment)
02BC	261	306	563
07TC	200	352	2496
10MC	160	465	873
12MC	199	159	478
14MC	5196	21266	5558
16MC	112	251	59
18MC	6857	88426	2526
20MC	3092	2278	501
21MC	26515	23653	2861
22TC	1960	45073	14371
24MC	1813	40044	1964
26MC	1506	20372	2569
30MC	4404	45043	6807
32MC	4999	33627	4393
38MC	61015	195474	31637
39MC	34953	267289	5140
42MC	358	2462	239
43MC	0	1296	112
44MC	44	802	156
47MC	500	2189	743
49JPC	3930	24170	983
50MC	51	928	107
53MC	355	6182	532
56MC	45876	40697	3330
59MC	65747	32874	3931
60MC	7167	57335	1618
61JPC	1421	20402	2007
67MC	21491	72222	2818
69MC	27079	174590	10689
72MC	13139	41608	1792
76MC	7368	38513	2009
A8.5	3251	3681	107
C2-8	4536	4761	28
C2-A11	4519	5577	29
CC5	2570	6194	186

(Table 3.3 continued)

Sample	Reworked Abundance (specimens/g sediment)	Terrestrial Abundance (specimens/g sediment)	Marine Indicator Abundance (specimens/g sediment)
CC7	2897	3644	113
D2	5778	3593	57
D6	2344	1563	14
EE5	9067	7838	0
EE7	5564	3265	57
EE9	12391	2602	0
G2	10739	6522	0
G3	6707	2127	0
G5	5196	1220	18
T10-20	5248	9362	504
T10-60	3125	2849	0
T11-20	7509	5269	166
T1-20	1561	285	6
T12-20	3103	754	13
T1-25	562	254	5
T13-20C	3058	2848	19
T13-30C	5288	2893	0
T2-30	2754	417	77
T3-20KC	7782	2678	0
T3-30	2653	2452	110
T4-30	1631	1477	10
T4-50	3764	2485	24
T5-20	4636	2276	0
T6-20	9920	2687	207
T6-30	3491	927	52
T7-20	3047	558	0
T7-30	4334	1260	115
T8-20B	3181	3430	23
T8-30	3791	2566	0
T8-50	3436	2582	73
T8-60	6781	4860	0
T9-30	2621	4324	45

It is possible that the *Lycopodium* spp. recovery is compromised, as the counts for offshore sites are highly variable among slides, ranging from 1 to 579, despite counting similar percentages of each slide. To avoid any possible bias, concentrations were not used in the graphics, and we have chosen to present the majority of recovery data in this paper as the raw counts or relative abundances, including in the statistical analyses.

Palynomorph identification

Many references were used to identify palynomorphs and the terrestrial vegetation to which pollen and spores correspond, including Cookson and Eisenack (1957), Couper (1960), Cookson and Hughes (1964) Paijmans (1975), Flenley (1979), Walker and Flenley (1979), Muller (1981), Playford (1982), Pocknall and Mildenhall (1984), Davey (1987), Helby et al. (1987), Rigby (1997), Rigby (2001), APSA Members (2007), Playford and Rigby (2008), and Zonneveld et al. (2013). Species-level identification of pollen and spores in a tropical rainforest setting is difficult when using only transmitted light microscopy, so species are grouped into genera or family-level designations, but this has little impact on our environmental interpretations of vegetation groups. Pollen and spore taxa for the vegetation groups analyzed in this paper are presented in Table 3.4. Recognizable pollen that were not assignable to a designated genus or family taxon were included in the tropical rainforest category (the tricolporate, tricolpate, triporate forms) as this is the dominant vegetation category on Papua New Guinea. Those not attributable to any specific morphologic designation remain as unknowns.

Data analysis

Spatial bubble plots of palynomorph distribution were created using ArcGIS 10.2 (ArcGIS Desktop, 2014) with the following categories plotted as a percent of the total absolute abundance (pollen and spores; marine indicators including dinoflagellate cysts, tintinnids, foraminifer linings, copepod eggs, and acritarchs; and reworked specimens) (Table 3.3; Figures 3.5, 3.6).

Table 3.4. Familes and genera characterizing each of the major vegetation groups of Papua New Guinea.

Lowland Tropical Rainforest	Lower Montane/Montane Forest	Mangroves
Barringtonia spp.	*Alnus* spp.	*Acrostichum aureum*
Dicolpopollis spp.	*Araucaria* spp.	*Avicennia* spp.
Haloragaceae	Bisaccate undifferentiated	*Nypa* spp.
Ilex spp.	Cupressaceae	*Oncosperma* spp.
Malphigiaceae	*Dacrydium* spp.	Podocarpaceae
Malvaceae	Myrtaceae	Rhizophoraceae
Rubiaceae	*Nothofagus* spp.	*Sonneratia* spp.
Tiliaceae	*Pinus* spp.	
All other tricolpate, tricolporate, and triporate forms	*Pitryogramma* spp.	Grassland, Scrub, Savanna
	Podocarpaceae	*Acacia* spp.
		Asteraceae
	Swamp Forest	*Banksia* spp.
	Arecaceae	Chenopodiaceae
Spores	*Carya* spp.	Ericaceae
All spores, including trilete and monolete forms	Cyperaceae	*Eucalyptus* spp.
	Meliaceae	Gramineae
	Metroxylon spp.	

Onshore to offshore, along shelf, and along slope transects were created using StrataBugs 2.0 (StrataData, 2014) to more effectively present pollen and spore distribution (Figures 3.7 and 3.8 include transect locations; Figures 3.9, 3.10, 3.11, 3.12, and 3.13 are plots of palynomorph distribution along each transect). Transects were compiled based on the shortest straight-line distance between sampling locations. Some samples were projected onto the line using the right angle intersection of a straight line with the transect line between two adjacent samples. Each of the transect plots contains the following columns: distance along the transect (km); samples; reworked versus penecontemporaneous occurrences; terrestrial versus marine occurrences; vegetation groups plotted as a percent of the total count of all vegetation groups (mangrove, tropical

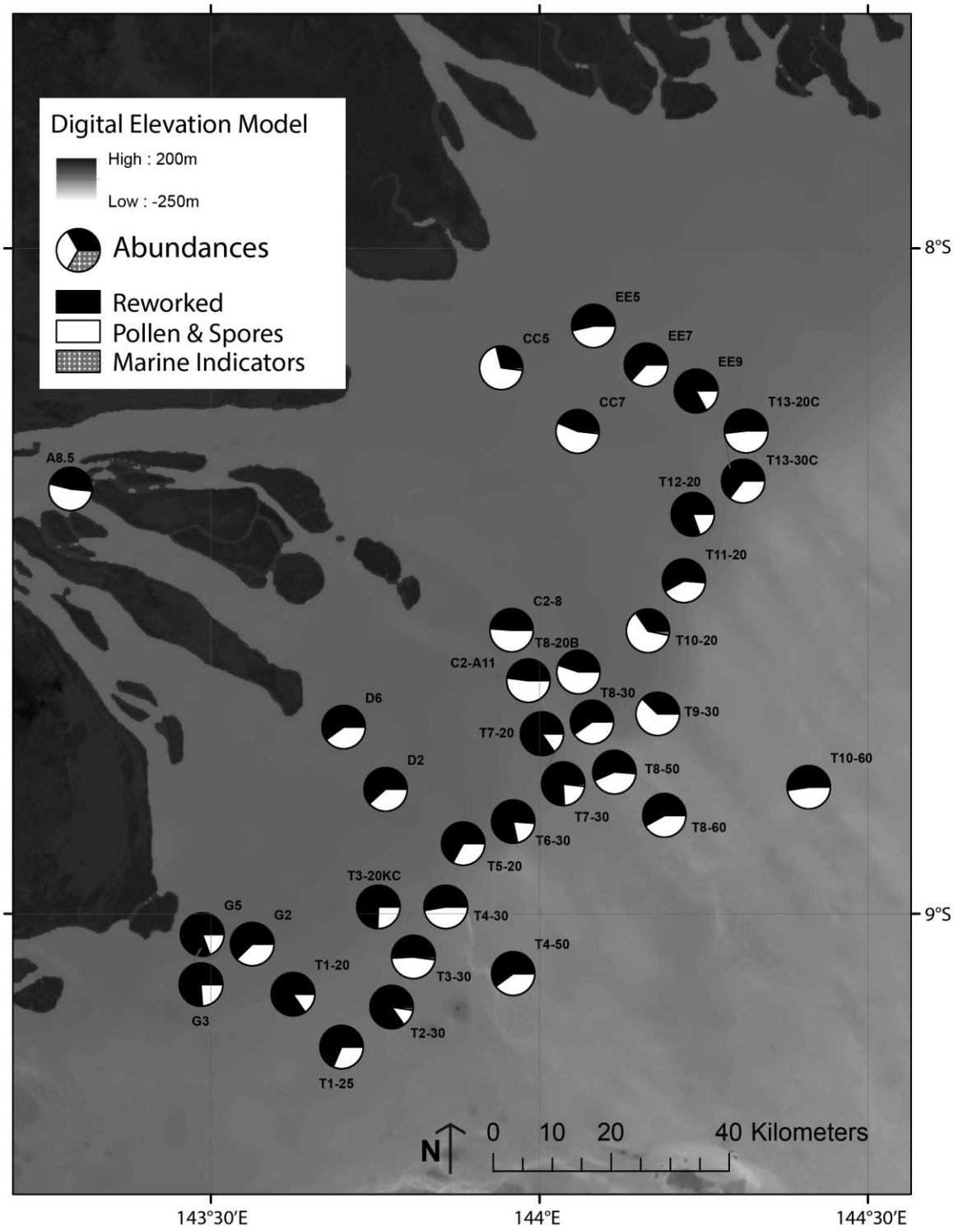

Figure 3.5. Spatial bubble plots of nearshore Gulf of Papua samples. Bathymetry (DEM, digital elevation model) from Daniell (2008).

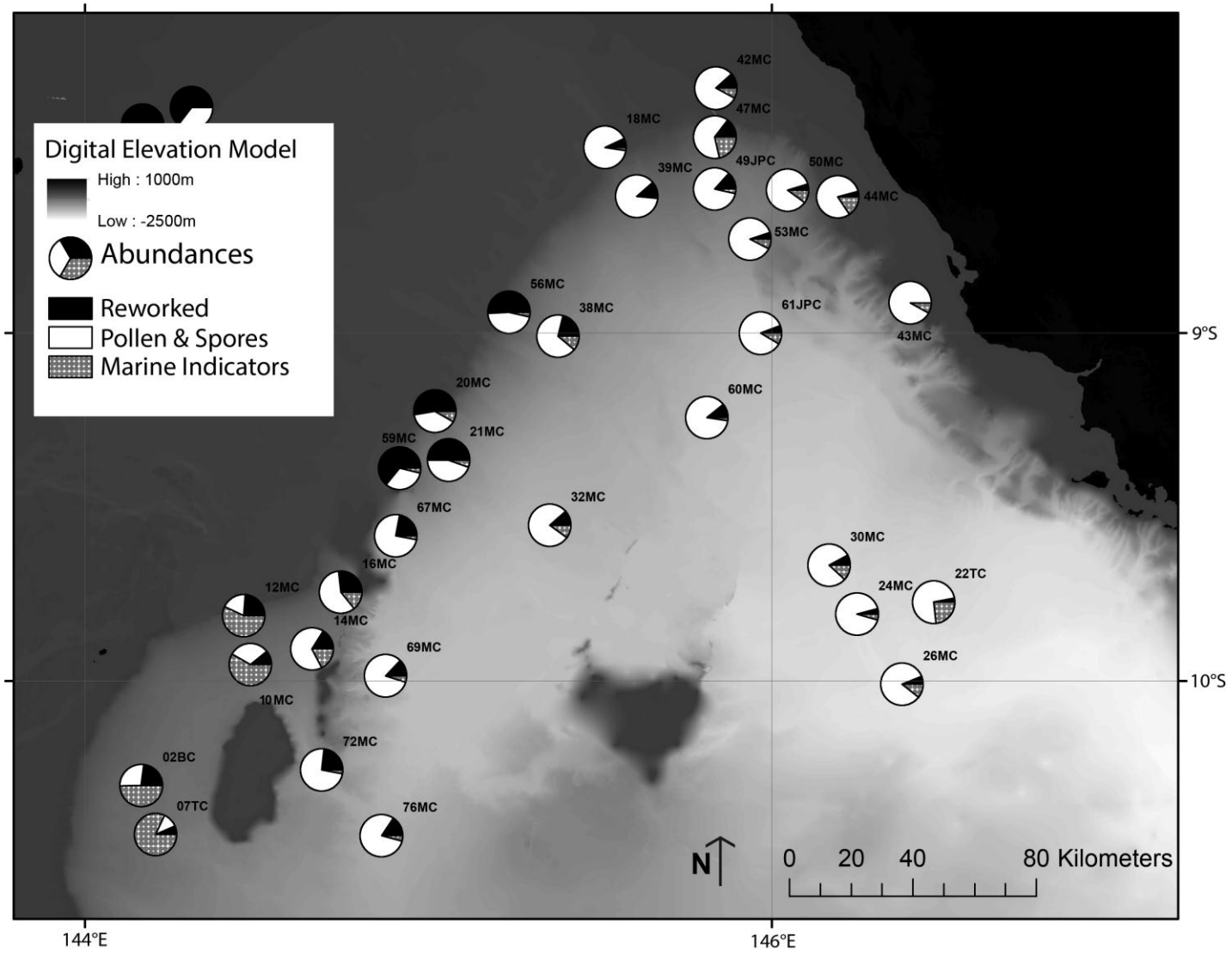

Figure 3.6. Spatial bubble plots of offshore Gulf of Papua samples. Bathymetry (DEM, digital elevation model) from Daniell (2008).

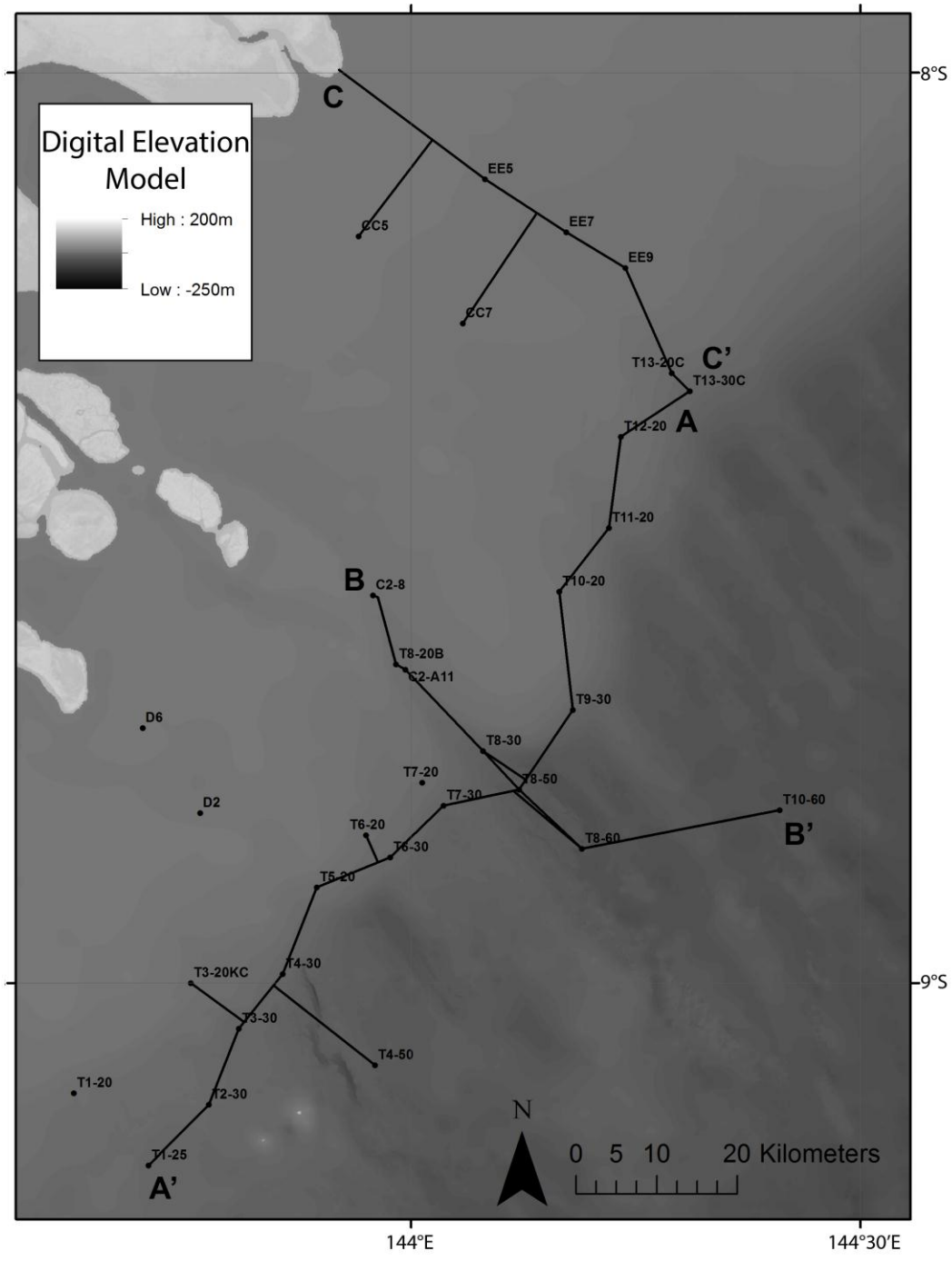

Figure 3.7. Transect locations for nearshore Gulf of Papua samples. Bathymetry (DEM, digital elevation model) from Daniell (2008).

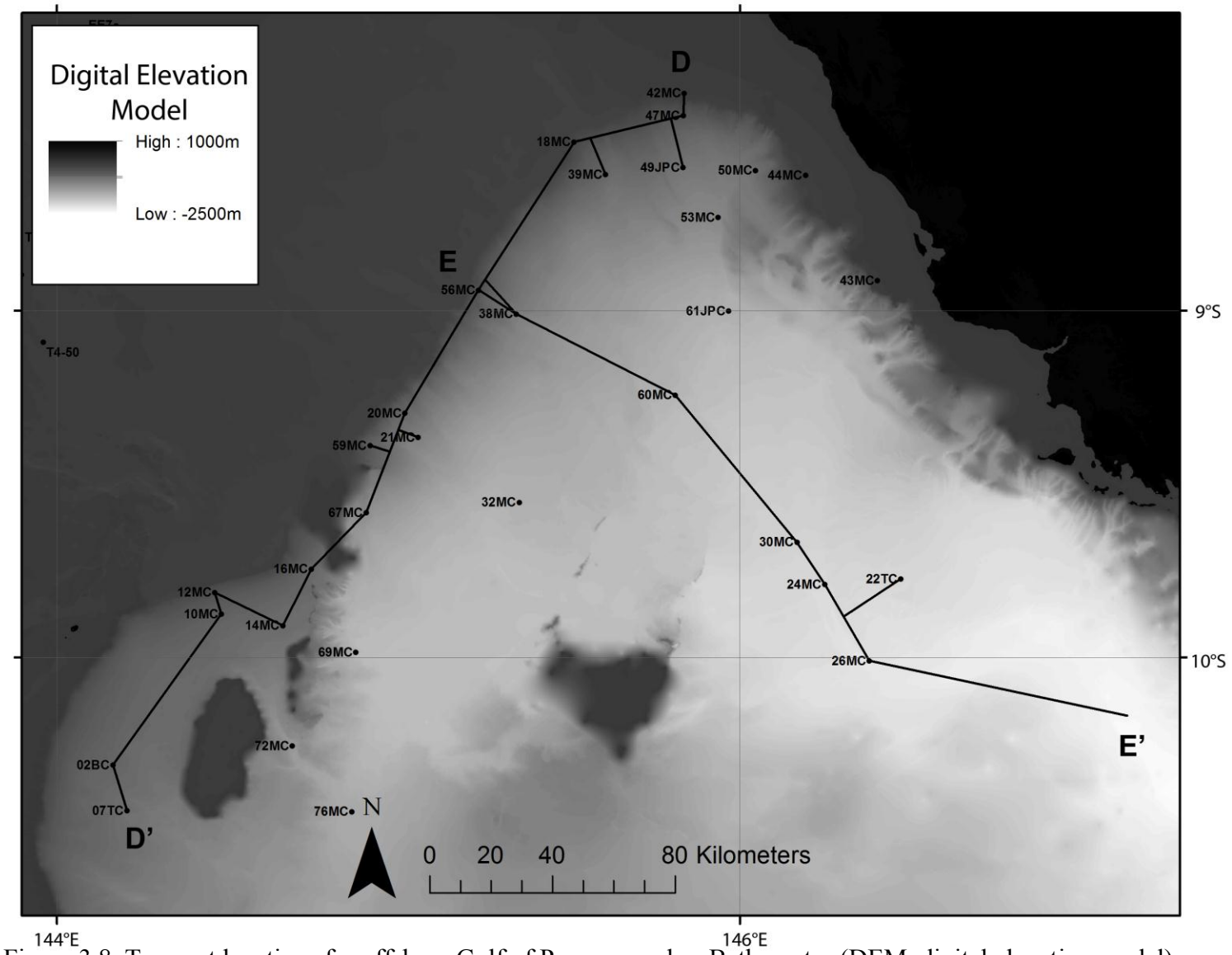

Figure 3.8. Transect locations for offshore Gulf of Papua samples. Bathymetry (DEM, digital elevation model) from Daniell (2008).

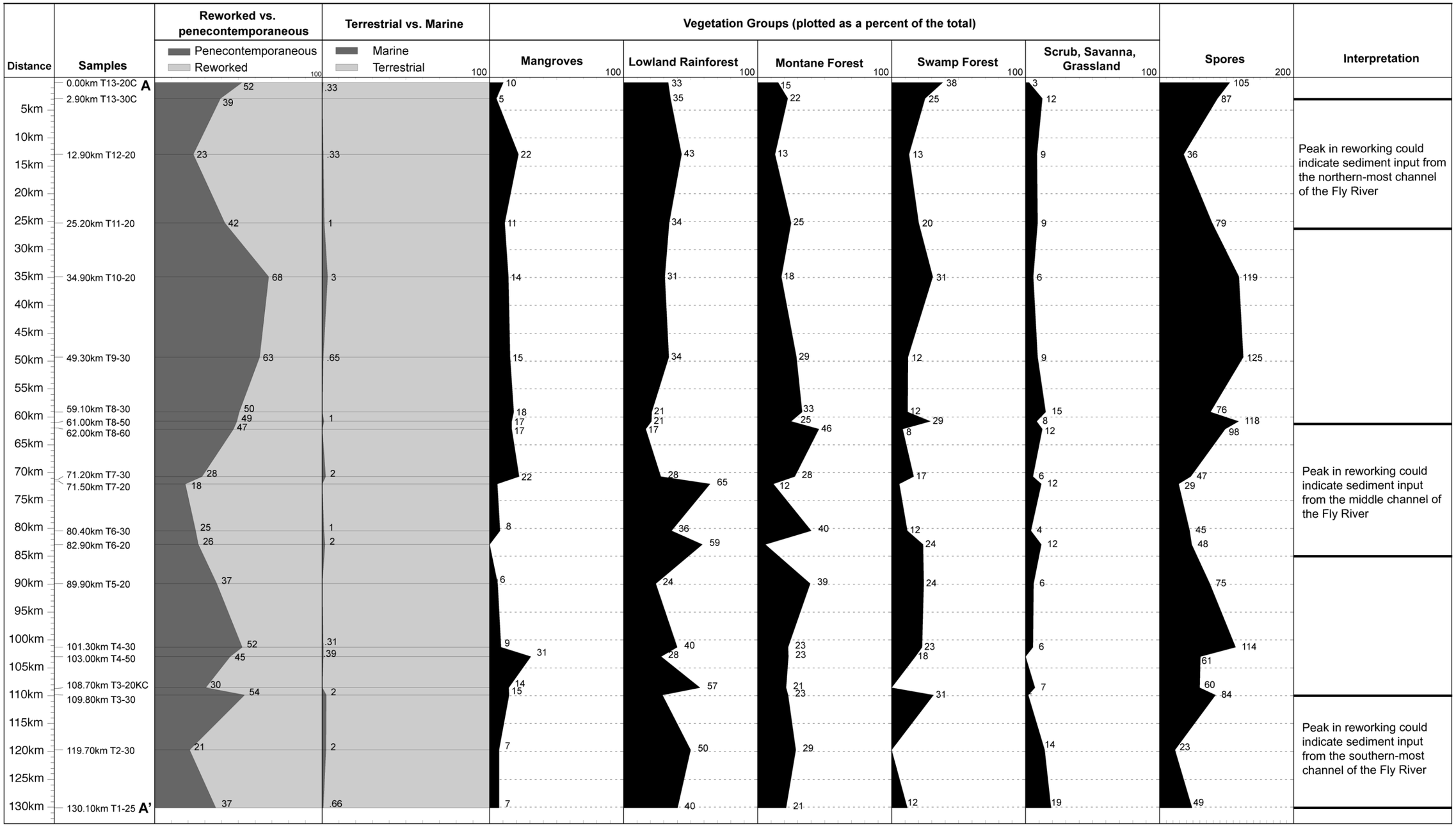

Figure 3.9. Transect A to A' alongshore from northeast to southwest, including predominantly clinoform foreset samples (location shown in Figure 3.7). Peaks in reworking could indicate input from the three major channels of the Fly River.

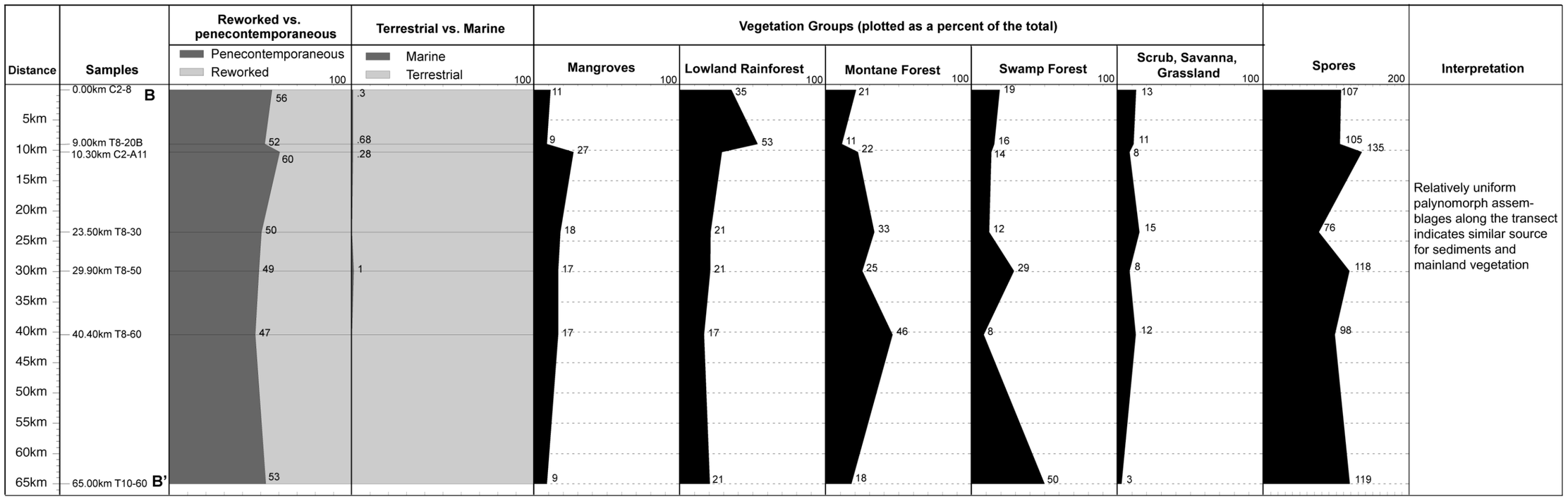

Figure 3.10. Transect B to B' from nearshore to offshore (location shown in Figure 3.7). Assemblages are uniform along the transect.

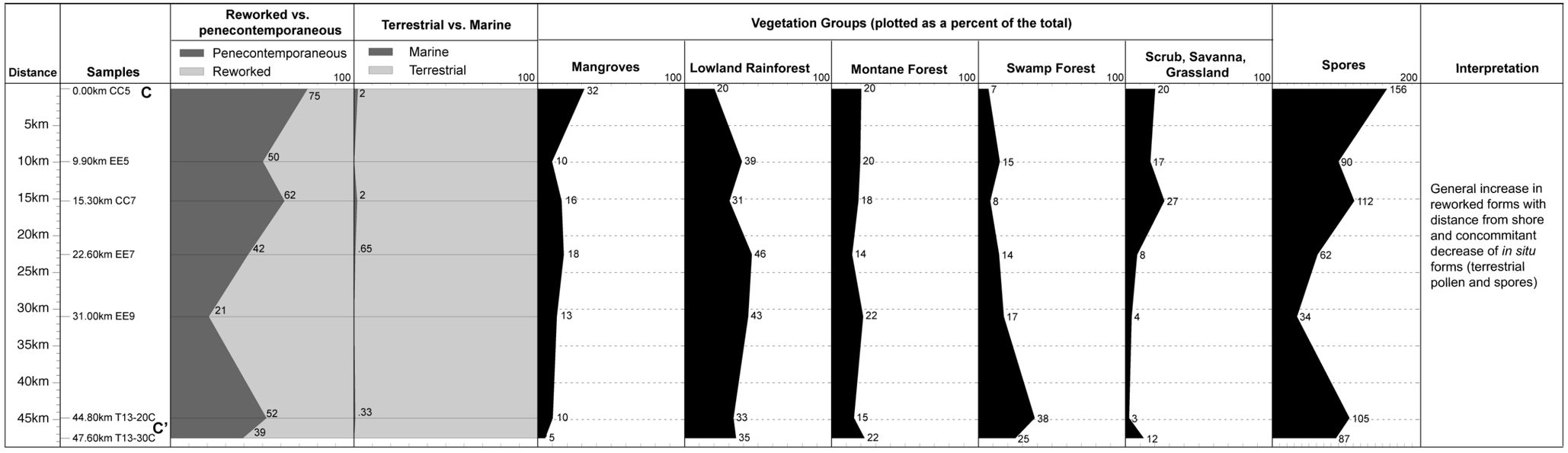

Figure 3.11. Transect C to C' from nearshore to offshore (location shown in Figure 3.7). Percentage of reworking decreases with increasing distance from shore.

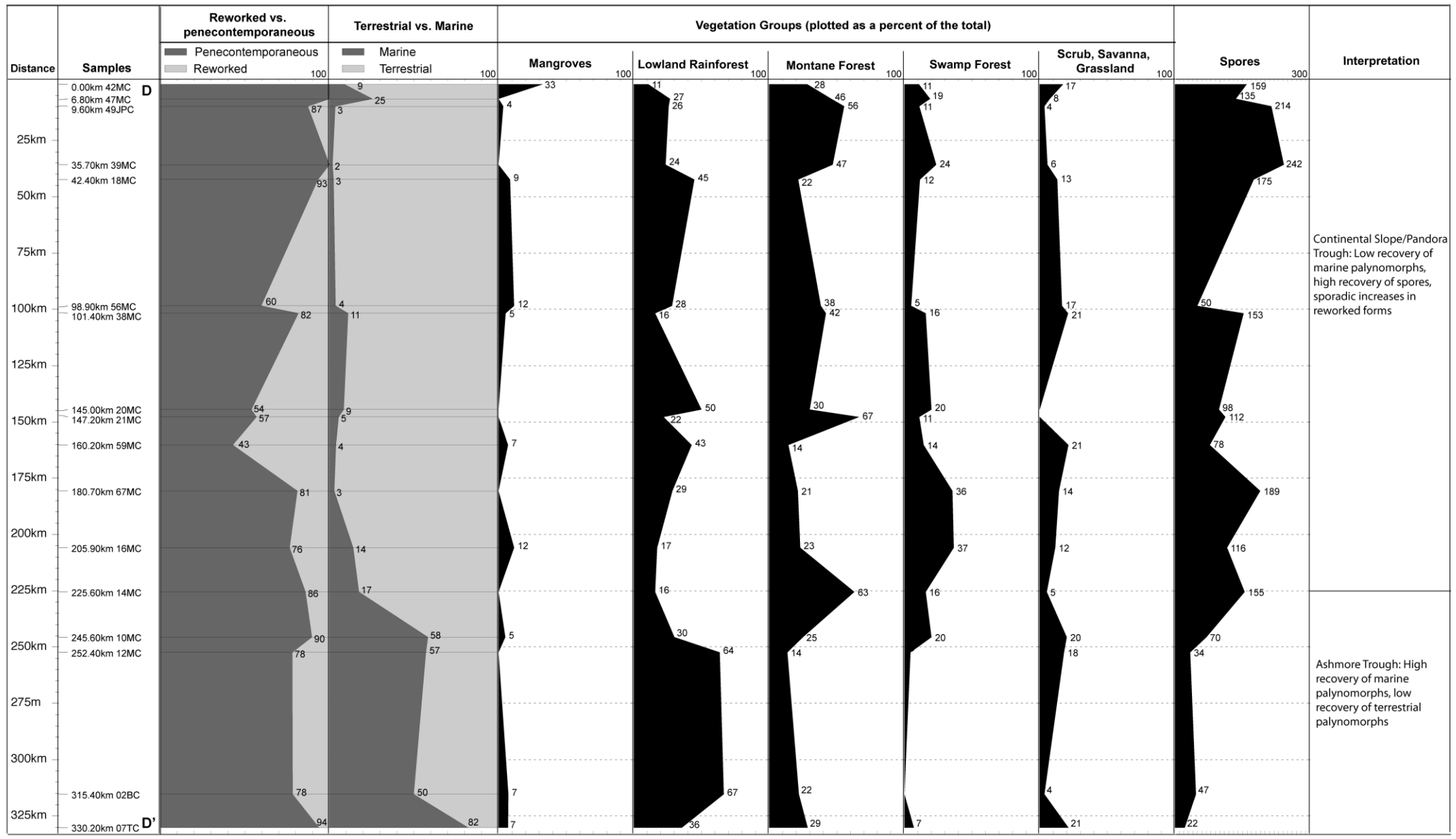

Figure 3.12. Transect D to D' from northeast to southwest along the continental shelf, Pandora Trough, and Ashmore Trough (location shown in Figure 3.8). Assemblages are significantly different between Pandora and Ashmore Troughs.

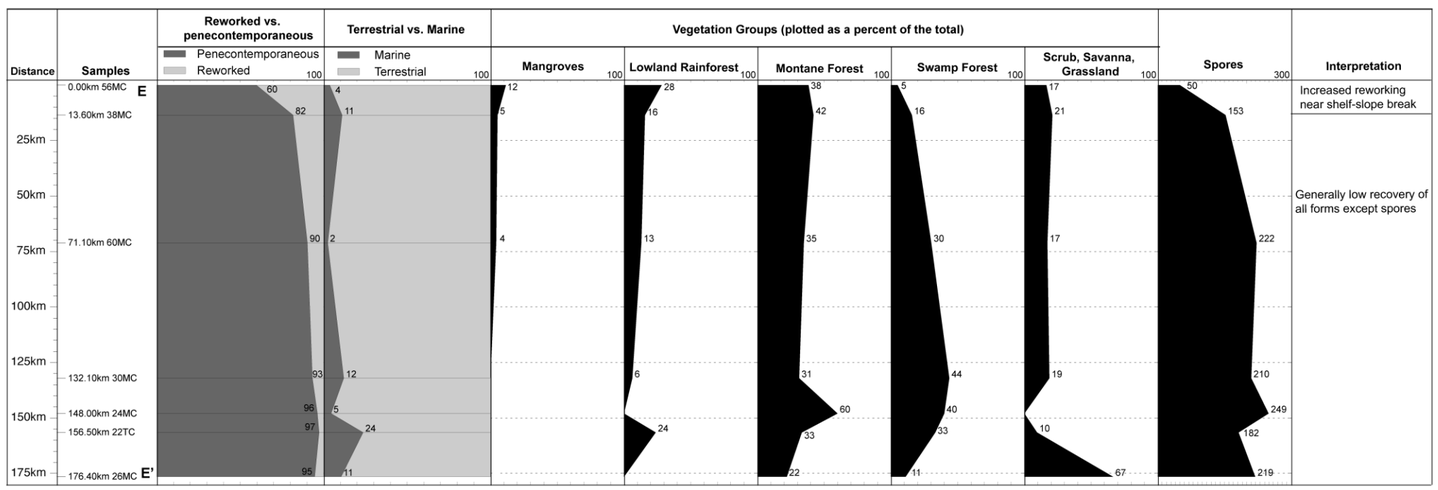

Figure 3.13. Transect E to E' from west to east across Pandora Trough (location in Figure 3.8). All palynomorphs recovered in low abundances except spores.

rainforest, montane forest, swamp forest, and scrub/savanna/grassland); and total count of spores. Spores are left out of the percent calculation for vegetation because they are abundant at most sites. Transect interpretations are included in the furthest right column.

Unconstrained Principal Component Analysis (PCA) with supplementary (environmental) variables was performed on the data using Canoco5 (Table 3.5, Figure 3.14) (Šmilauer 2012). The program calculated the first four PCA axes, and we log-transformed response data. Marine palynomorph data was left out of the statistical analysis, because recovery is very low at most sites, except for those in Ashmore Trough (Figure 3.1). Counts of the following groups were analyzed: reworked specimens, mangrove, lowland rainforest, montane forest, swamp forest, savanna/scrub/grassland, and spores. The following environmental parameters were selected: water depth (m), distance from shore (nearest straight-line distance, km), distance from slope break (km), and sedimentation rate (cm/yr). Other variables, such as sediment source, vegetation distribution on land, current direction and speed, amount of bacterial activity, reworking, time in transport, coring equipment, and human error, can also impact distribution (e.g., Traverse, 2007). Although these variables are difficult to account for statistically, we have kept them in mind for analysis of results.

Table 3.5. Principal Component Analysis (PCA) results for Gulf of Papua Samples.

Unconstrained PCA with Supplementary Variables				
Total Variation			306.81	
Environmental variables account for			46.20%	
Statistic	Axis 1	Axis 2	Axis 3	Axis 4
Eigenvalues	0.4168	0.2281	0.1453	0.0984
Explained variation (cumulative)	41.68	64.49	79.03	88.87
Pseudo-canonical correlation (suppl.)	0.9082	0.5895	0.1739	0.4463

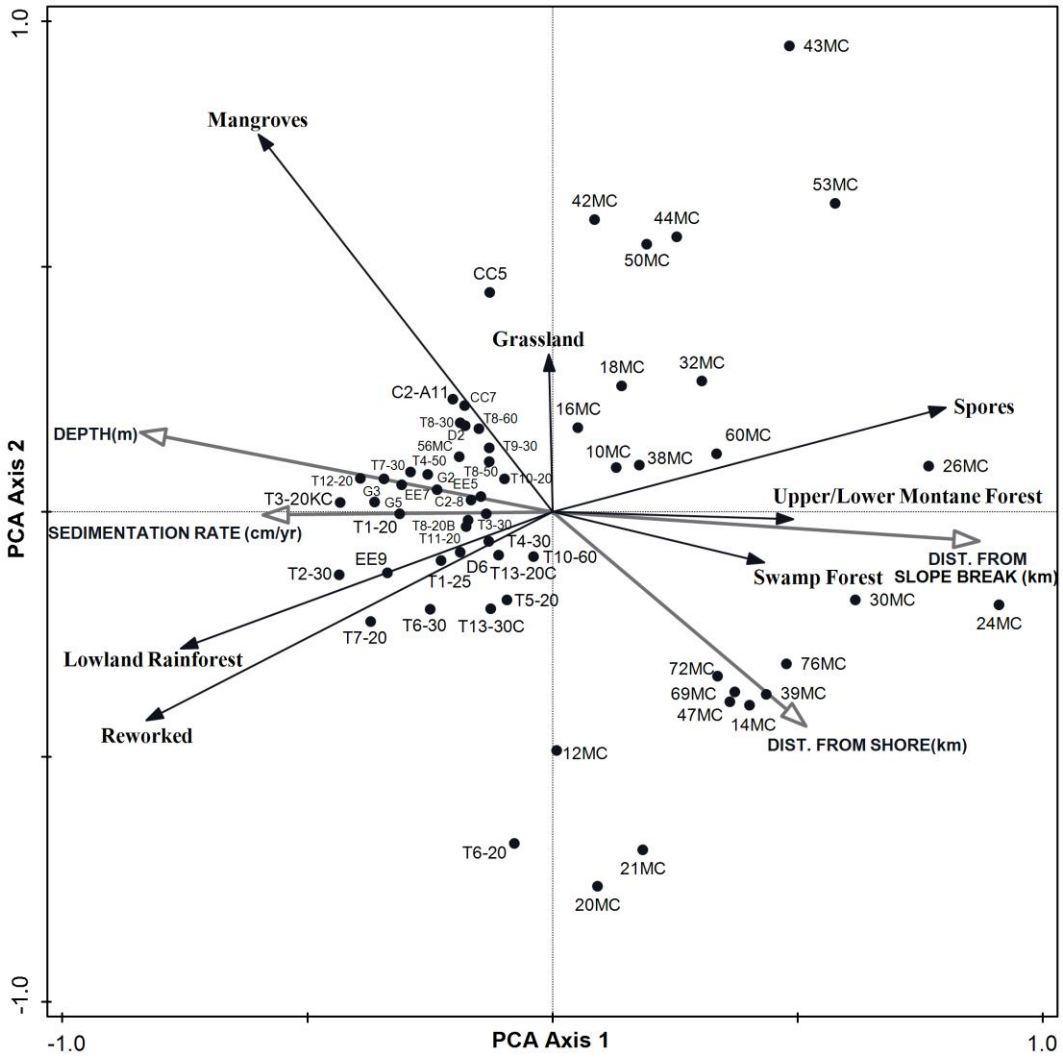

Figure 3.14. Principal Component Analysis (PCA) results. Vegetation group arrows have filled black tips, and environmental variables have empty black tips. Samples are plotted by their Euclidean distance scores (filled black circles with corresponding sample name). Water depths are negative, so increases in water depth indicate shallower water.

The PCA graph for pollen and spore data shows the first two PCA axes with samples plotted as their Euclidean distance scores (Figure 3.14). Vegetation arrows (filled black) point in the direction of their steepest increase, and longer arrows indicate better fit for that category. Environmental arrows (empty black) also point in the direction of their steepest increase. Positive correlation between categories is interpreted when

angles between arrows are acute, while negative correlation is interpreted when angles between arrows are obtuse. A summary figure has been prepared in ArcMap (ArcGIS Desktop, 2014) to show the major source of clinoform sediments (Figure 3.15).

Results

Palynomorph assemblages recovered reflect major vegetation groups on the mainland, as well as high percentages of reworked forms at some sites (mostly those in nearshore clinoform samples). All major vegetation groups (Figures 3.3, 3.4) are represented by pollen found in the GoP sedimentary record, including mangroves, tropical rainforest, montane forest, swamp forest, and scrub/savanna/grassland. Reworked forms, dominated by dinoflagellate cysts, pollen, and spores of Cretaceous to Neogene in age comprise greater than 50% of the assemblage at many nearshore sites (Figures 3.5, 3.9, 3.10, 3.11). Modern dinoflagellate cyst recovery is very low at all sites in the GoP, except for sites in Ashmore Trough (Figure 3.5, 3.6). Other marine indicators, including tintinnids, copepod eggs, foraminifer linings, and acritarchs are also rare throughout the GoP (Table 3.2).

Spatial bubble plots

Nearshore spatial bubble plots (Figure 3.5) show high abundances (greater than 50%) of reworked palynomorphs (Cretaceous and Neogene in age) at the majority of sites. Reworking generally increases offshore, with highest abundances of reworked palynomorphs in clinoform foreset deposits. Pollen and spores sourced from mainland vegetation are generally found in highest abundances nearest shore. Recovery of marine indicators is very low or absent in all nearshore sampling sites.

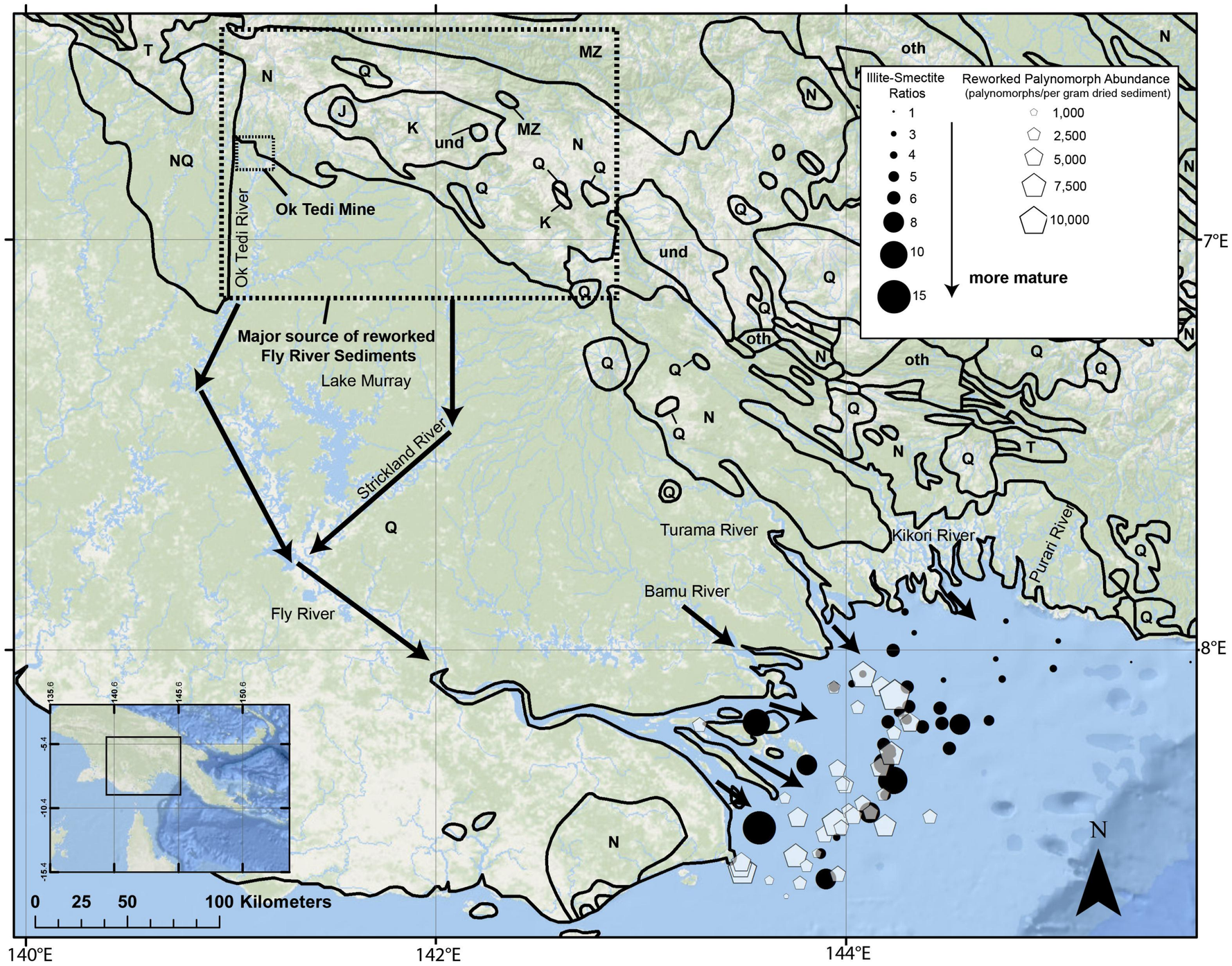

Figure 3.15. Major source of clinoform sediments. Geologic map from Steinshouer et al. (1999) with abbreviations indicating formation ages: Jurassic (J), Cretaceous (K), Cretaceous-Tertiary (KT), Mesozoic (MZ), Neogene (N) Neogene-Quaternary (NQ), other (oth), Quaternary (Q), Tertiary (T), and undifferentiated (und). Surficial illite:smectite ratios on the GoP continental shelf were provided by Xu (personal communication, 2013) and previously published by Slingerland et al. (2008a) and Howell et al. (2014). Higher ratios indicate greater sediment maturity. Reworked palynomorph abundances (Table 3.3) are calculated as palynomorphs per gram of dried sediment.

Offshore spatial bubble plots (Figure 3.6) show very different trends in palynomorph assemblages. These sites are dominated by spores sourced from the mainland, and abundances of reworked palynomorphs are very low, except in upper slope samples 20MC, 21MC, 56MC, and 59MC. Recovery of marine indicators, especially dinoflagellate cysts is much higher for offshore samples, especially those in Ashmore Trough (02BC, 07TC, 10MC, 12MC, and 14MC).

Transects

Transects of palynomorph distribution show greater detail for recovered palynomorph assemblages (Figures 3.7, 3.8). Transect A (Figure 3.9) runs along the clinoform foreset (Figure 3.1). There are three major peaks in reworked palynomorphs, which could be related to sourcing from the three channels of the Fly River, as indicated in the interpretation column. Marine indicator recovery is less than three percent for all sites along the clinoform foreset. Spores are the most dominant component of assemblages at all sites along this transect. Vegetation assemblages are dominated by lowland rainforest and montane forest species, with contributions from mangrove, swamp forest, and scrub/savanna/grassland.

Transect B (Figure 3.10) runs from nearshore to offshore from the middle channel of the Fly River, and it includes clinoform topset, foreset, and bottomset samples. The ratio of reworked to penecontemporaneous forms is remarkably consistent along the transect. Marine indicator recovery is very low and spore recovery is high, similar to Transect A. Lowland rainforest species abundance peaks in clinoform topset samples, then mangrove and montane forest species become the dominant vegetation groups farther along the transect in clinoform foreset and bottomset samples.

Transect C (Figure 3.11) also runs from nearshore to offshore north of the northernmost Fly River channel. Reworked palynomorph recovery increases offshore, as these forms can be more resistant to degradation (e.g., Needham et al., 1969; Fleming, 1994; Riding, 2005). Lowland rainforest species are the dominant component of the pollen assemblage, with lower representation from mangroves, montane forest, swamps, and grassland/scrub/savanna. A peak in mangrove pollen occurs in the sample nearest shore (CC5), which is directly offshore from mangrove forests (Figure 3.3). Counts for spores are highest near shore and decrease with increasing distance from shore.

Offshore samples (Figures 3.12, 3.13) possess very different palynomorph assemblages from nearshore samples. Transect D (Figure 3.12) crosses the continental slope from northeast to southwest. Reworked palynomorph abundances are low across the slope, except for samples 56MC, 20MC, 21MC, and 59MC. Bisaccate pollen (montane forest) and spores are the dominant representatives of terrestrial vegetation. Marine indicator recovery is very low, except for sites in Ashmore Trough.

Transect E (Figure 3.13) includes samples from the continental slope and deep GoP basin, including Pandora and Moresby Troughs. Reworking is very low for these samples, except those located on the continental slope. Marine indicator recovery is also low, except for a slight peak in sample 22TC. Spores are the dominant representative of terrestrial vegetation, with high recovery of bisaccate pollen (montane forest) and monocolpate pollen from swamp forest.

Statistical analysis

PCA compares the dissimilarity between all samples (Figure 3.14, Table 3.5). The environmental variables (water depth, distance from shore, distance from slope break,

and sedimentation rate) account for 46.20% of the variation among samples. The total variation among all 67 samples is 306.81, with the first four PCA axes (Axes 1, 2, 3, and 4) accounting for 88.87% of this variation. Nearshore samples are very similar to each other, because they plot very close together. Offshore samples are more dissimilar to each other, as well as to nearshore samples. Lowland rainforest and reworked palynomorphs are strongly correlated with increasing sedimentation rate and decreasing water depth. Spores, montane forest, and swamp forest are strongly correlated with increasing distancefrom shore and the shelf-slope break. Mangrove and grassland vegetation are weakly correlated with decreasing water depth and increasing sedimentation rate.

Discussion

As indicated by high abundances of reworked Cretaceous and Neogene palynomorphs in nearshore samples (Figures 3.5, 3.9, 3.10, 3.11), clinoform sediments are not solely sourced from the Fly Platform covered with Quaternary deposits (Figure 3.15). Although we predicted the majority of sediments to be sourced from adjacent land near the Fly River delta, it appears a large amount of sediments are sourced from the headlands of the Fly River in the Papuan Fold Belt, composed of deformed Cretaceous and Neogene rocks, and these sediments are transported over 200 kilometers. Results from Baker (1998) and Dalrymple et al. (2003) support our conclusion, as they determined most of the clinoform sediments are sourced from the Papuan Fold Belt, as well as the Fly Platform. It is very likely that mining at Ok Tedi (Figure 3.15) has contributed to the abundance of reworked palynomorphs in GoP sediments. Eagle and Higgins (1990) observed that mining near the headlands of the Ok Tedi and Strickland Rivers has increased sediment discharge to the GoP by over 40% in the last thirty years.

Because only modern sediment samples have been analyzed for this project, we can only conjecture that reworked palynomorphs have increased in abundance since mining began. Palynological analysis of Ok Tedi mine samples has not been published, so we cannot compare our reworked specimens with specimens from that site. Several authors have published on pre-Quaternary palynology at other sites in PNG (Playford, 1982; Davey, 1987; Rigby, 1997; Rigby, 2001; Playford and Rigby, 2008), and their results support predominantly Cretaceous and Neogene ages of reworked palynomorphs found in modern samples.

Comparing modern sediment mineralogy with reworked palynomorph occurrences supports our conclusion of long distance transport and sourcing from the headlands of the Fly River (Figure 3.15). Sediment maturity is indicated by the ratio of illite to smectite in sediments (e.g., Milliman, 1995; Brunskill, 2004; Howell et al., 2014). Higher ratios mean the sediments are more mature and have been in transport longer. Illite:smectite ratios of GoP clinoform sediments clearly reflect sediment source and bedrock geology. Davies (2012) notes Fly, Bamu, and Turama rivers in the western GoP are sourced by reworked and Neogene sediments which are more mature, while the more eastern Kikori and Purari rivers have less mature sediments that are dominated by volcanic components. Reworked palynomorphs are highest in abundance near sites with the highest illite:smectite ratios.

Reworked palynomorphs are much less common in offshore and northeastern shelf samples (Figures 3.6, 3.12, 3.13), although the specimens found are also Cretaceous and Neogene in age with minor Paleozoic contributions sourced from the Papuan Peninsula (Figure 3.2). Because these sites have much lower sedimentation rates and are

farther from land, long distance transport and preservation of reworked forms in offshore slope and basin samples is less likely. However, the presence of outcrops generally closer to the site of deposition for offshore samples (compared to greater than 200 km of transport for reworked palynomorphs in clinoform sediments) would lead us to predict greater abundances of reworked palynomorphs in offshore samples than are actually observed. The other major variable that could be causing the difference between nearshore and offshore samples is the lack of mining contributing to sediment source near the continental slope and GoP basin. Some offshore sites, including 56MC, 20MC, 21MC, and 59MC, do have relatively high percentages of reworked forms, and these are directly offshore from clinoform sediments. It is possible that the sediments at these sites have been transported across the GoP marine transgressive surface and preserved on the slope. Francis et al. (2008) notes it is likely the mass transport deposits found along the slope and in Pandora Trough in this region are sourced from Fly River sediments, which supports our finding of high reworked abundances at these sites. The rare occurrence of reworked forms in other offshore samples is intriguing, because the PNG highlands experience common natural landslides (e.g., Blong, 1986; Robbins et al, 2013), however, this could be explained by sediment transport pathways in the offshore GoP. Some of the terrigenous sediment delivered to the northeastern gulf is transported to the east of the study area (Keen et al., 2006).

Modern pollen and spore assemblages (Figures 3.9, 3.10, 3.11, 3.12, 3.13) for the most part reflect mainland vegetation assemblages (Figure 3.3) (Paijmans, 1975), but some major differences are noted and discussed below. As mangrove vegetation occurs at sea level and fringes the GoP, we expected to find the highest percentage of these pollen

types in our sediment samples. However, this was not the case, and mangrove pollen has much lower recovery than expected. This disparity is likely due to the fact that during high stands of sea level, like at present, most mangrove pollen is retained with the roots and sedimentary matrix of the mangrove forest in which it is produced and very little is carried into surrounding waters (e.g., Tissot and Marius, 1992).

Tropical rainforest and swamp pollen are the dominant representatives of vegetation in nearshore samples (Figures 3.9, 3.10, 3.11). As mentioned, it is difficult to differentiate pollen to species level in a tropical setting because many taxa produce similar or identical pollen grains. There are also many sub-types of rainforest and swamp forest on mainland PNG (Paijmans, 1975), so this category only provides an overview of the major families and genera representative of these vegetation types found in this study. Paijmans (1975) splits tropical rainforest vegetation into seven different categories and swamp forest into four categories, depending on such factors as canopy height, whether the canopy is open or closed, soil type, and proximity to rivers. We could not differentiate these terrestrial factors in a marine palynological study.

Grassland, scrub, and savanna are also a combination of several vegetation categories that represent dry conditions and open land. These types of vegetation also commonly represent human occupation and burning (e.g., Denham et al., 2003; Haberle, 2003; Denham and Haberle, 2008; Sniderman et al., 2009; Haberle et al., 2012). We have found these vegetation categories in low abundances throughout most of the study area, but interestingly with generally higher representation in offshore samples that are near areas with the highest human occupancy on PNG, by the capitol city, Port Moresby (Figures 3.12, 3.13).

Bisaccate pollen, which is the dominant representative of montane forest, has surprisingly sparse recovery in GoP samples. Due to presence of vast swaths of montane forest (Figure 3.3), mountainous terrain, and because bisaccate pollen can be transported long distances due to its buoyant air sacs (e.g., Muller, 1959; Traverse and Ginsburg, 1966; Traverse, 2007), we expected montane forest vegetation to dominate offshore assemblages and have better representation in nearshore assemblages. For nearshore assemblages, the vegetation (Figure 3.3) sourcing the pollen assemblages has very low presence of montane forest. For offshore assemblages, montane forests pollen is also rare in GoP samples. Keen et al. (2006) discuss potential transport pathways for terrigenous material in the GoP, which can be aid in explaining pollen distribution. Most terrigenous material on the inner shelf is retained in clinoform deposits, while sediments delivered in the northeastern gulf are potentially transported to the east out of the study area by the CSCC. Because montane forest pollen is buoyant and can be transported long distances (source), low recovery of this pollen in offshore samples likely means it has been transported out of the GoP (e.g., Muller, 1959).

Spores are, by far, the most abundant representatives of terrestrial vegetation from the mainland (Figures 3.9, 3.10, 3.11, 3.12, 3.13). The reason for their dominance is due to the fact that the parent plant produces vast quantities of spores that survive long distance transport (e.g., Pohl, 1937a, 1937b; Wijmstra, 1978; Birks and Birks, 1980; Traverse, 2007). Very few spore species are indicative of environmental conditions, as spore-producing plants, unlike pollen-producing plants, have less strict requirements governing their biogeography, except the necessity of water for reproduction. Because PNG has high annual rainfall, abundant spore recovery in our samples confirms the

humid environment throughout the study area (similar to findings by Anderson and Muller (1975) and Rull (2001), for example).

The rare occurrence of marine indicators, including dinoflagellate cysts, acritarchs, tintinnids, copepod eggs, and foraminifer linings, is likely due to sedimentological and oceanographic factors. Several authors have shown most dinoflagellate species prefer fully marine conditions and clear water with little sediment input (e.g., Marret and Zonneveld, 2003; Zonneveld et al., 2013). Because sediment discharge to the GoP is extremely high (3.84×10^8 tons/year, Milliman, 1995; Wolanski et al., 1995), it is unlikely dinoflagellate cysts would be recovered in high abundance. Low recovery of dinoflagellate cysts fits with current understanding of the GoP sedimentary regime.

As the use of controlled oxidation has been shown to degrade fragile palynomorphs, particularly dinoflagellate cysts, in modern sediments (Harland, 1981; Harland, 1983; Schrank, 1988), we reprocessed samples without controlled oxidation to determine if processing procedures affected observed assemblages. These reprocessed samples show higher, but still relatively low, recovery of dinoflagellate cysts, so the use of an oxidant in this study biased the samples only slightly. Additionally, the pollen and spore assemblages recovered in both processing procedures are quite similar, and specimens are much easier to identify on the oxidized slides. For this reason, only the data from the oxidized slides processed by the external consultant were included in this paper.

PCA (Figure 3.14) reveals how strongly palynomorph distribution is governed by the four environmental factors selected to help explain their distribution. Sedimentation rate, bathymetry, and distance from shore/slope break explain 46.20% of the variation

among palynomorph assemblages. Statistical analysis reveals the strong dissimilarity between nearshore and offshore samples. Nearshore samples are surprisingly similar to each other, with little differentiation among clinoform topset, foreset, and bottomset beds. Because assemblages are so similar to each other, this reflects our conclusion that sediments are sourced from similar areas, i.e., from the headlands of the Fly River in the Papuan Fold Belt and the Fly Platform. Lowland rainforest, mangroves, and reworked palynomorphs are the dominant components of nearshore samples, and their distribution is strongly positively correlated with shallower water depth and higher sedimentation rates. Offshore samples are much more dissimilar to each other, which means there are likely different sources contributing to the palynomorph assemblages. They are also much further apart from each other geographically than nearshore samples. These samples are dominated by spores, montane forest, and swamp forest, which are strongly positively correlated to increasing distance from shore and the slope break and strongly negatively correlated to shallower water depth and higher sedimentation rate. Grassland vegetation is the only vegetation group not strongly correlated to any of the environmental factors examined in this study. This result is likely due to the fact that grassland vegetation distribution is strongly controlled by human influence, which is difficult to account for statistically.

Conclusions

Analysis of modern palynomorph distribution in the GoP, PNG, provides better understanding of how palynomorphs are transported as part of the sediment load and what types of vegetation signals are preserved in the sediment. Nearshore clinoform palynomorph assemblages are dominated by reworked palynomorphs and pollen sourced

from mainland vegetation. Reworked Cretaceous and Neogene pollen, sourced from the headlands of the Fly River over 200 km away, reveal the major source of sediments composing the GoP clinoform, supporting the results of Baker (1998) and Dalrymple et al. (2003). Palynomorph assemblages across the three major subdivsions of GoP clinoform (topset, foreset, and bottomset) are similar (Figures 3.9, 3.10, 3.11), with slight increases in reworking with distance from shore and concomittant decreases in terrestrially sourced pollen and spores. Offshore palynomorph assemblages (Figures 3.12, 3.13) are quite different from clinoform assemblages (except for those directly offshore from the Fly River mouth, including 20MC, 21MC, 38MC, 56MC, and 59MC), most likely due to sourcing from the Papuan Peninsula as opposed to Fly Platform, and show high recovery of spores and low recoveries of reworked palynomorphs and pollen. Samples in Ashmore Trough are the only samples with high recoveries of marine palynomorphs in the GoP, especially dinoflagellate cysts, most likely due to more suitable oceanographic conditions and low sediment influx.

Recovered pollen and spores reflect the major vegetation groups on mainland PNG, including mangroves, tropical rainforest, swamp, montane forest, and grassland/scrub/savanna. Principal Component Analysis (PCA) reveals the importance of palynomorph morphology in determining its transportability; more robust forms, like spores, or the presence of air bladders, like bisaccate pollen (the dominant component of montane vegetation), allows them to be found further offshore and in deeper water. On the other hand, pollen from mangrove and tropical rainforest vegetation is deposited nearer shore where sedimentation rates are higher and in shallower water. Results provide better understanding of sediment source, transport, and deposition in the region.

References

Abbott, L.D., 1995. Neogene tectonic reconstruction of the Adelbert-Finisterre-New Britain collision, northern Papua New Guinea. Journal of Southeast Asian Earth Sciences 11, 33-51.

Anderson, J.A.R., Muller, J., 1975. Palynological study of a Holocene peat and a Miocene coal deposit from NW Borneo. Review of Palaeobotany and Palynology 19, 291-351.

APSA Members, 2007. The Australasian Pollen and Spore Atlas v. 1.0. Australian National University, Canberra. Accessed from: http://apsa.anu.edu.au/.

ArcGIS Desktop, 2014. ArcGIS Version 10.2. Esri, Redlands.

Azanza, R.V., Siringan, F.P., Diego-Mcglone, M.L.S., Yñiguez, A.T., Macalalad, N.H., Zamora, P.B., Agustin, M.B., Matsuoka, K., 2004. Horizontal dinoflagellate cyst distribution, sediment characteristics and benthic flux in Manila Bay, Philippines. Phycological Research 52, 376-386.

Baker, E.K., 1998. Sedimentation in a tidally dominated delta and the impact of upstream mining: Fly River, Papua New Guinea. Unpublished Ph.D thesis, University of Sydney, Sydney, p. 245.

Batten, D.J., 1996. Chapter 26A. Palynofacies and palaeoenvironmental interpretation, In: Jansonius, J., McGregor, D.C. (Eds.), Palynology: principles and applications. American Association of Stratigraphic Palynologists Foundation, Salt Lake City, pp. 1011-1064.

Birks, H.J.B., Birks, H.H., 1980. Quaternary Palaeoecology. Edward Arnold, London, p. 289.

Blatt, H., Middleton, G., Murray, R., 1972. Origin of Sedimentary Rocks. Prentice-Hall, Englewood Cliffs, New Jersey.

Blong, R.J., 1986. Natural hazards in the Papua New Guinea Highlands. Mountain Research and Development 6, 233-246.

Bouimetarhan, I., Marret, F., Dupont, L., Zonneveld, K., 2009. Dinoflagellate cyst distribution in marine surface sediments off West Africa (17-6°N) in relation to sea-surface conditions, freshwater input and seasonal coastal upwelling. Marine Micropaleontology 71, 113-130.

Brass, L., 1941. The 1938-39 expedition to the Snow Mountains, Netherlands New Guinea. Journal of Arnold Arbor 22, 271-342.

Brass, L., 1964. Results of the Archibold Expeditions No. 86, summary of the sixth Archibold Expedition to New Guinea (1959). Bulletin of the American Museum of Natural History 127, 145-216.

Brunskill, G.J., 2004. New Guinea and its coastal seas, a testable model of wet tropical coastal processes: an introduction to Project TROPICS. Continental Shelf Research 24, 2273-2295.

Brunskill, G.J., Woolfe, K.J., Zagorskis, I., 1995. Distribution of riverine sediment chemistry on the shelf, slope and rise of the Gulf of Papua. Geo-Marine Letters 15, 153-159.

Carson, B.E., Francis, J.M., Leckie, R.M., Droxler, A.W., Dickens, G.R., Jorry, S.J., Bentley, S.J. Sr., Peterson, L.C., Opdyke, B.N., 2008. Benthic foraminiferal response to sea level change in the mixed siliciclastic-carbonate system of southern Ashmore Trough (Gulf of Papua). Journal of Geophysical Research 113, F01S20, doi:10.1029/2006JF000629.

Conn, B.J., editor, 1995. Handbooks of the Flora of New Guinea, Volume III. Melbourne University Press, Victoria.

Cookson, I.C., Eisenack, A., 1957. Microplankton from Australian and New Guinea Upper Mesozoic sediments. Proceedings of the Royal Society of Victoria 70, 19-79.

Cookson, I.C., Hughes, N.F., 1964. Microplankton from the Cambridge Greensand (mid-Cretaceous). Palaeontology 7, 37-59.

Couper, R.A., 1960. New Zealand Mesozoic and Cainozoic Plant Microfossils. New Zealand Geological Survey Paleontological Bulletin 32, p. 66.

Crockett, J.S., Nittrouer, C.A., Ogston, A.S., Naar, D.F., Donahue, B.T., 2008. Morphology and filling of incised submarine valleys on the continental shelf near the mouth of the Fly River, Gulf of Papua. Journal of Geophysical Research 113, F01S12, doi:10/1029/2006JF000674.

Dalrymple, R.W., Baker, E.K., Harris, P.T., Hughes, M.G., 2003. Sedimentology and stratigraphy of a tide-dominated foreland-basin delta (Fly River, Papua New Guinea), Tropical Deltas of Southeast Asia – Sedimentology, Stratigraphy, and Petroleum Geology. SEPM Special Publication No. 76, pp. 147-173.

Daniell, J.J., 2008. Development of a bathymetric grid for the Gulf of Papua and adjacent areas: a note describing its development. Journal of Geophysical Research 113, F01S15, doi:10.1029/2006JF000673.

Davey, R.J., 1987. Palynological zonation of the Lower Cretaceous, Upper and upper most Middle Jurassic in the northwestern Papuan Basin of Papua New Guinea. Geological Survey of Papua New Guinea Memoir 13, 33.

Davies, H.L., 2012. The geology of New Guinea – the cordilleran margin of the Australian continent. Episodes 35, 87-102.

de Vernal, A., Eynaud, F., Henry, M., Hillaire-Marcel, C., Londeix, L., Mangin, S., Matthiessen, J., Marret, F., Radi, T., Rochon, A., Solignac, S., Turon, J.-L., 2005.

Reconstruction of sea-surface conditions at middle to high latitudes of the Northern Hemisphere during the Last Glacial Maximum (LGM) based on dinoflagellate cyst assemblages. Quaternary Science Reviews 24, 897-924.

de Vernal, A., Turon, J.-L., Guiot, J., 1993. Dinoflagellate cyst distribution in high-latitude marine environments and quantitative reconstruction of sea-surface salinity, temperature, and seasonality. Canadian Journal of Earth Science 31, 48-62.

Denham, T., Fullagar, R., Head, L., 2009. Plant exploitation on Sahul: from colonisation to the emergence of regional specialisation during the Holocene. Quaternary International 202, 29-40.

Denham, T., Haberle, S.G., 2008. Agricultural emergence and transformation in the Upper Wahgi Valley, Papua New Guinea during the Holocene: theory, method and practice. The Holocene 18, 499-514.

Denham, T.P., Haberle, S.G., Lentfer, C.J., Fullagar, R., Field, J., Therin, M., Porch, N., Winsborough, B., 2003. Origins of agriculture at Kuk Swamp in the highlands of New Guinea. Science 301, 189-193.

Eagle, A.M., Higgins, R.J., 1990. Environmental investigation on the effects of the Ok Tedi copper mine in the Fly River System, In: Lawrence, D., Cransfield-Smith, T. (Eds.), Torres Strait Baseline Study. Workshop Series 16. Great Barrier Reef Marine Park Authority, p. 535.

Esper, O., Zonneveld, K.A.F., 2007. The potential of organic-walled dinoflagellate cysts for the reconstruction of past sea-surface conditions in the Southern Ocean. Marine Micropaleontology 65, 185-212.

Ewing, J.J., Houtz, R.E., Ludwig, W.J., 1970. Sediment distribution in the Coral Sea. Journal of Geophysical Research 75, 1963-1972.

Fairbairn, A.S., Hope, G.S., Summerhayes, G.R., 2006. Pleistocene Occupation of New Guinea's Highland and Subalpine Environments. World Archaeology 38, 371-386.

Febo, L.A., 2007. Paleoceanography of the Gulf of Papua using multiple geophysical and micropaleontological proxies, Department of Geology & Geophysics. Louisiana State University, p. 163.

Fleming, R.F., 1994. Cretaceous pollen in Pliocene rocks: implications for Pliocene climate in the southwestern United States. Geology 22, 787-790.

Flenley, J.R., 1969. The Vegetation of the Wabag Region, New Guinea Highlands: a Numerical Study. Journal of Ecology 57, 465-490.

Flenley, J.R., 1972. Evidence of Quaternary Vegetational Change in New Guinea, In: Ashton, P., Ashton, M. (Eds.), The Quaternary Era in Malesia. Transactions of the

Second Aberdeen Hull Symposium on Malesian Ecology. Institute for South-East Asian Biology, University of Hull, pp. 99-109.

Flenley, J.R., 1979. The Late Quaternary vegetational history of the equatorial mountains. Progress in Physical Geography 3, 488-509.

Francis, J.M., Daniell, J.J., Droxler, A.W., Dickens, G.R., Bentley, S.J. Sr., Peterson, L.C., Opdyke, B.N., Beaufort, L., 2008. Deep water geomorphology of the mixed siliciclastic-carbonate system, Gulf of Papua. Journal of Geophysical Research 113. F01S16, doi:10.1029/2007JF000851.

Gardner, J.V., 1970. Submarine geology of the Western Coral Sea. Geological Society of America Bulletin 81, 2599-2614.

Haberle, S.G., 2003. The emergence of an agricultural landscape in the highlands of New Guinea. Archaeology in Oceania 38, 149-158.

Haberle, S.G., 2007. Prehistoric human impact on rainforest biodiversity in highland Papua New Guinea. Philosophical Transactions of the Royal Society London Series B 362, 219-228.

Haberle, S.G., Hope, G.S., van der kaars, S., 2001. Biomass burning in Indonesia and Papua New Guinea: natural and human-induced fire events in the fossil record. Palaeogeography, Palaeoclimatology, Palaeoecology 171, 259-268.

Haberle, S.G., Ledru, M.-P., 2001. Correlations among charcoal records of fires from the past 16,000 years in Indonesia, Papua New Guinea, and Central and South America. Quaternary Research 55, 97-104.

Haberle, S.G., Lentfer, C., O'Donnell, S., Denham, T., 2012. The palaeoenvironments of Kuk Swamp from the beginnings of agriculture in the highlands of Papua New Guinea. Quaternary International 249, 129-139.

Harland, R., 1981. Cysts of the colonial dinoflagellate *Polykrikos schwartzii* Biitschli 1873 (Gymnodiniales) from Recent sediments, Firth of Forth, Scotland. Palynology 5, 65-79.

Harland, R., 1983. Distribution maps of recent dinoflagellate cysts in bottom sediments from the North Atlantic Ocean and adjacent seas. Palaeontology 26, 321-387.

Harris, P.T., 1994. Incised valleys and backstepping deltaic deposits in a foreland-basin setting, Torres Strait and Gulf of Papua, Australia, In: Dalrymple, R.W., Boyd, R., Zaitlin, B.A. (Eds.), Incised Valley Systems: Origin and Sedimentary Sequences, SEPM Special Publication No. 51. Society for Sedimentary Geology, pp. 97-108.

Harris, P.T., Baker, E.K., Cole, A.R., Short, S.A., 1993. Preliminary study of sedimentation in the tidally dominated Fly River Delta, Gulf of Papua. Continental Shelf Research 13, 441-472.

Harris, P.T., Pattiaratchi, C.B., Keene, J.B., Dalrymple, R.W., Gardner, J.V., Baker, E.K., Cole, A.R., Mitchell, D., Gibbs, P., Schroeder, W.W., 1996. Late Quaternary deltaic and carbonate sedimentation in the Gulf of Papua foreland basin: response to sea level change. Journal of Sedimentary Research 66, 801-819.

Helby, R., Morgan, R., Partridge, A.D., 1987. A palynological zonation of the Australian Mesozoic. Memoirs of the Association of Australasian Paleontologists 4, 1-94.

Henty, E.E., editor, 1995. Handbooks of the Flora of New Guinea, Volume II. Melbourne University Press, Victoria, p. 286.

Heusser, L.E., 1983. Pollen distribution in bottom sediments of the western North Atlantic Ocean. Marine Micropaleontology 8, 77-88.

Heusser, L.E., Balsam, W.L., 1977. Pollen distribution in the northeast Pacific Ocean. Quaternary Research 7, 45-62.

Hodgkiss, I.J., Ho, K.C., 1997. Are changes in N:P ratios in coastal waters the key to increased red tide blooms? Hydrobiologia 352, 141-147.

Hoffmeister, W.S., 1954. Microfossil Prospecting for Petroleum. Patent version number: 2,686,108, United States Patent Office, U.S.A.

Howell, A.L., Bentley, S.J. Sr., Xu, K., Ferrell, R.E.J., Muhammad, Z., Septama, E., 2014. Fine sediment mineralogy as a tracer of latest Quaternary sediment delivery to a dynamic continental margin: Pandora Trough, Gulf of Papua, Papua New Guinea. Marine Geology 357, 108-122.

Kawahata, H., Gupta, L.P., 2004. Settling Particles Flux in Response to El Niño/Southern Oscillation (ENSO) in the Equatorial Pacific, In: Shiyomi, M., Kawahata, H., Koizumi, H., Tsuda, A., Awaya, Y. (Eds.), Global Environmental Change in the Ocean and on Land. TERRAPUB, Tokyo, pp. 95-108.

Keen, T.R., Ko, D.S., Slingerland, R.L., Riedlinger, S., Flynn, P., 2006. Potential transport pathways of terrigenous material in the Gulf of Papua. Geophysical Research Letters 33, L04608, doi:10.1029/2005GL025416.

Knapp, E.E., Goedde, M.A., Rice, K.J., 2001. Pollen-limited reproduction in blue oak: implications for wind pollination in fragmented populations. Oecologia 128, 48-55.

Lange, S., Rajewski, M., Leinemann, L., Hattemer, H., 2002. Cross-mating in the forest-love-life of yew trees. German Research 1, 28-31.

Lignum, J., Jarvis, I., Pearce, M., 2008. A critical assessment of standard processing methods for preparation of palynological samples. Review of Palaeobotany and Palynology 149, 133-149.

Limoges, A., Kielt, J.-F., Radi, T., Ruíz-Fernandez, A.C., de Vernal, A., 2010. Dinoflagellate cyst distribution in surface sediments along the south-western Mexican coast (14.76° N to 24.75°N). Marine Micropaleontology 76, 104-123.

MacFarlane, J.W., 1980. Surface and bottom sea currents in the Gulf of Papua and Western Coral Sea, Department of Primary Industries Research Bulletin No. 27, Port Moresby, p. 132.

Mandrioli, P., Negrin, M.G., Zanotti, A.L., 1982. Airborne pollen from the Yugoslavian coast to the Po Valley (Italy). Grana 21, 121-128.

Marret, F., de Vernal, A., 1997. Dinoflagellate cyst distribution in surface sediments of the southern Indian Ocean. Marine Micropaleontology, 29, 367-392.

Marret, F., Zonneveld, K.A.F., 2003. Atlas of modern organic-walled dinoflagellate cyst distribution. Review of Palaeobotany and Palynology 125, 1-200.

Martin, D.P., Nittrouer, C.A., Ogston, A.S., Crockett, J.S., 2008. Tidal and seasonal dynamics of a muddy inner shelf environment, Gulf of Papua. Journal of Geophysical Research 113, F01S07, doi:10.1029/2006JF000681.

McAlpine, J.R., Freyne, D.F., 2001. Land use change and intensification in Papua New Guinea 1975-1996. Asia Pacific Viewpoint 42, 209-218.

McAlpine, J.R., Keig, G., 1983. Climate of Papua New Guinea. Australian National University Press, Canberra, p. 200.

Melia, M.B., 1984. The distribution and relationship between palynomorphs in aerosols and deep-sea sediments off the coast of northwest Africa. Marine Geology 58, 345-371.

Milliman, J.D., 1995. Sediment discharge to the ocean from small mountainous rivers: the New Guinea example. Geo-Marine Letters 15, 127-133.

Moss, P.T., Kershaw, A.P., Grindrod, J., 2005. Pollen transport and deposition in riverine and marine environments within the humid tropics of northeastern Australia. Review of Palaeobotany and Palynology 134, 55-69.

Muhammad, Z., Bentley, S.J. Sr., Febo, L.A., Droxler, A.W., Dickens, G.R., Peterson, L.C., Opdyke, B.N., 2008. Excess ^{210}Pb inventories and fluxes along the continental slope and basins of the Gulf of Papua. Journal of Geophysical Research 113, F01S17, doi:10.1029/JF000676.

Muller, J., 1959. Palynology of Recent Orinoco Delta and shelf sediments. Micropaleontology 5, 1-32.

Muller, J., 1981. Fossil pollen records of extant angiosperms. The Botanical Review 47, 1-142.

Needham, H.D., Habib, D., Heezen, B.C., 1969. Upper Carboniferous palynomorphs as a tracer of red sediment dispersal patterns in the northwest Atlantic. Journal of Geology 77, 113-120.

NSF MARGINS Program, 2004. NSF MARGINS Program Science Plans. MARGINS Office, Columbia University, New York.

O'Keefe, J.M.K., Eble, C.F., 2012. A comparison of HF-based and non-HF-based palynology processing techniques in clay-rich lignites from the Claiborne Group, upper Mississippi Embayment. Palynology 36, 116-130.

Ogston, A.S., Sternberg, R.W., Nittrouer, C.A., Martin, D.P., Goni, M.A., Crockett, J.S., 2008. Sediment delivery from the Fly River tidally dominated delta to the nearshore marine environment and the impact of El Niño. Journal of Geophysical Research 113, F01S11, doi:10.1029/2006JF000669.

Paijmans, K., 1975. Explanatory notes to the vegetation map of Papua New Guinea. Commonwealth Scientific and Industrial Research Organization, Melbourne.

Peck, R.M., 1973. Pollen budget studies in a small Yorkshire catchment, In: Birks, H.J.B., West, R.G. (Eds.), Quaternary Plant Ecology. Blackwell Scientific, Oxford, pp. 43-60.

Pigram, C.J., Davies, H.L., 1987. Terranes and accretion history of the New Guinea orogen. Bureau of Mineral Resources Journal of Australian Geology and Geophysics 107, 331-353.

Pigram, C.J., Davies, P.J., Feary, D.A., Symonds, P.A., 1989. Tectonic controls on carbonate platform evolution in southern Papua New Guinea: passive margin to foreland basin. Geology 17, 199-202.

Playford, G., 1982. Neogene palynomorphs from the Huon Peninsula, Papua New Guinea. Palynology 6, 29-54.

Playford, G., Rigby, J.F., 2008. Permian palynoflora of the Ainim and Aiduna formations, West Papua. Revista Española de Micropaleontología 40, 1-57.

Pocknall, D.T., Mildenhall, D.C., 1984. Late Oligocene-early Miocene spore and pollen from Southland, New Zealand. New Zealand Geological Survey Paleontological Bulletin 51, p. 66.

Pohl, F., 1937a. Die pollenerzeugung der windblütler. Beiheftezum Botanischen Centralblatt 56A, 365-470.

Pohl, F., 1937b. Die pollenkorngewichte einiger windblütigen pflanzen und ihre ökologischer bedeutung. Beiheftezum Botanischen Centralblatt 57A, 112-172.

Riding, J.B., 2005. Reworked palynomorphs as a tool for determining Quaternary sediment provenance in East Anglia, UK, American Association of Stratigraphic Palynologists Program and Abstracts 38th Annual Meeting, p. 52.

Rigby, J.F., 1997. The significance of a Permian flora from Irian Jaya (west New Guinea) containing elements related to coeval floras of Gondwanaland and Cathaysialand. The Palaeobotanist 45, 295-302.

Rigby, J.F., 2001. A review of early Permian flora from Papua (west New Guinea), In: Metcalfe, I., Smith, J.M.B., Morwood, M., Davidson, I. (Eds.), Faunal and floral migrations and evolution in SE Asia-Australasia. Balkema, Lisse, pp. 85-95.

Robbins, J.C., Petterson, M.G., Mylne, K., Espi, J.O., 2013. Tumbi landslide, Papua New Guinea: Rainfall induced? Landslides 10, 673-684.

Rodbell, D.T., Seltzer, G.O., Anderson, D.M., Abbott, M.B., Enfield, D.B., Newman, J.H., 1999. An ~15,000-year record of El Niño-driven alluviation in Southwestern Ecuador. Science 283, 516-520.

Rowe, C., McNiven, I.J., David, B., Richards, T., Leavesley, M., 2013. Holocene pollen records from Caution Bay, southern mainland Papua New Guinea. The Holocene 23, 1130-1142.

Rull, V., 2001. A quantitative palynological record from the early Miocene of Western Venezuela, with emphasis on mangroves. Palynology 25, 109-126.

Schrank, E., 1988. Effects of chemical processing on the preservation of peridinioid dinoflagellates: a case study from the Late Cretaceous of NE Africa. Review of Palaeobotany and Palynology 56, 123-140.

Scourse, J., Marret, F., Versteegh, G.J.M., Jansen, J.H.F., Schefuβ, E., van der Plicht, J., 2005. High-resolution last deglaciation record from the Congo fan reveals significance of mangrove pollen and biomarkers as indicators of shelf transgression. Quaternary Research 64, 57-69.

Slingerland, R., Driscoll, N.W., Milliman, J.D., Miller, J.R., Johnstone, E.A., 2008a. Anatomy and growth of a Holocene clinothem in the Gulf of Papua. Journal of Geophysical Research 113, F01S13, doi:10.1029/2006JF000628.

Slingerland, R., Selover, R.W., Ogston, A.S., Keen, T.R., Driscoll, N.W., Milliman, J.D., 2008b. Building the Holocene clinothem in the Gulf of Papua: an ocean circulation study. Journal of Geophysical Research 113, F01S14, doi:10.1029/2006JF000680.

Šmilauer, P., 2012. Canoco5 Version 5.0. Plant Research International, Wageningen.

Sniderman, J.M.K., Finn, J., Denham, T.P., 2009. A late Holocene palaeoecological record from Ambra Crater in the highlands of Papua New Guinea and implications for agricultural history. The Holocene 19, 449-458.

Stanley, E.A., 1965. Abundance of pollen and spores off the eastern coast of the U.S. Southeastern Geology 7, 25-33.

Steinshouer, D.W., Qiang, J., McCabe, P.J., Ryder, R.T., 1999. Maps showing geology, oil and gas fields, and geologic provinces of the Asia Pacific Region U.S. Geological Survey Open File Report 97-470F. U.S.G.S., Reston.

Stockmarr, J., 1971. Tablets with spores used in absolute pollen analysis. Pollen et Spores 13, 615-621.

StrataData, Inc., 2014. Stratabugs v2.0. StrataData, Inc., Surrey.

Tauber, H., 1965. Differential pollen dispersion and the interpretation of pollen diagrams. Danmarks Geologiske Undersogelse 2, 1-69.

Tcherepanov, E.N., Droxler, A.W., Lapointe, P., Dickens, G.R., Bentley, S.J. Sr., Beaufort, L., Peterson, L.C., Daniell, J., Opdyke, B.N., 2008a. Neogene evolution of the mixed carbonate-siliciclastic system in the Gulf of Papua, Papua New Guinea. Journal of Geophysical Research 113, F01S21, doi:10.1029/2006JF000684.

Tcherepanov, E.N., Droxler, A.W., Lapointe, P., Mohn, K., 2008b. Carbonate seismic stratigraphy of the Gulf of Papua mixed depositional system: Neogene stratigraphic signature and eustatic control. Basin Research 20, 185-209.

Thom, B.G., Wright, L.D., 1983. Geomorphology of the Purari Delta, In: Petr, T. (Ed.), The Purari: Tropical Environment of a High Rainfall River Basin. Dr. W. Junk, The Hague, pp. 64-84.

Thomas, M.L., Pocknall, D.T., Warny, S., Bentley, S.J. Sr., Droxler, A.W., Nittrouer, C.A., 2015. Assessing palaeobathymetry and sedimentation rates using palynomaceral analysis: a study of modern sediments from the Gulf of Papua, offshore Papua New Guinea. Palynology, doi:10.1080/01916122.2015.1014526.

Tissot, C., Marius, C., 1992. Holocene evolution of the mangrove ecosystem in French Guiana: a palynologial study, In: Singh, K.P., Singh, J.S. (Eds.), Tropical Ecosystems: Ecology and Management. Wiley Eastern Limited, New Delhi, p. 333-347.

Torrence, R., 2012. Volcanic disasters and agricultural intensification: a case study from Willaumez Peninsula, Papua New Guinea. Quaternary International 249, 151-161.

Traverse, A., 2007. Paleopalynology. Springer, Dordrecht, p. 813.

Traverse, A., Ginsburg, R.N., 1966. Palynology of surface sediments of Great Bahama Bank as related to water movement and sedimentation. Marine Geology 4, 417-459.

Tsukada, M., 1982. *Pseudotsuga menziesii* (Mirb.) Franco: its pollen dispersal and late Quaternary history in the Pacific Northwest. Japanese Journal of Ecology 32, 159-187.

van Steenis, C.G.G.J., 1934-1936. On the origin of the Malaysian mountain flora. Bulletin du Jardin Botanique de Buitenzorg Series III 13, 14, 135-262, 289-417, 156-172.

Walker, D., Flenley, J.R., 1979. Late Quaternary Vegetational History of the Enga Province of Upland Papua New Guinea. Philosophical Transactions of the Royal Society London Series B 286, 265-344.

Walsh, J.P., Nittrouer, C.A., Palinkas, C.M., Ogston, A.S., Sternberg, R.W., Brunskill, G.J., 2004. Clinoform mechanics in the Gulf of Papua, New Guinea. Continental Shelf Research 24, 2487-2510.

Warny, S., Bart, P.J., Suc, J.-P., 2003. Timing and progression of climatic, tectonic and glacioeustatic influences on the Messinian Salinity Crisis. Palaeogeography, Palaeoclimatology, Palaeoecology 202, 59-66.

Warny, S., Wrenn, J.H., 1997. New species of dinoflagellate cysts from the Miocene-Pliocene boundary on the Atlantic coast of Morocco. Palaeobotany and Palynology 96, 281-304.

Warny, S., Wrenn, J.H., 2002. Upper Neogene dinoflagellate cyst ecostratigraphy of the Atlantic coast of Morocco. Micropaleontology 48, 257-272.

Wijmstra, T.A., 1978. Paleobotany and climatic change, In: Gribbin, J. (Ed.), Climatic Change. Cambridge University Press, Cambridge, pp. 25-45.

Winterer, E.L., 1970. Submarine valley systems around the Coral Sea basin (Australia). Marine Geology 8, 229-244.

Wolanski, E., Alongi, D.M., 1995. A hypothesis for the formation of a mud bank in the Gulf of Papua. Geo-Marine Letters 15, 166-171.

Wolanski, E., Eagle, M., 1991. Oceanography and fine sediment transport, Fly River Estuary and Gulf of Papua, In: Bell, R.G., Hume, T.M., Healy, T.R. (Eds.), Coastal Engineering, Climate for Change; Proceedings of 10th Australasian Conference on Coastal and Ocean Engineering 21. Water Quality Centre, pp. 453-457.

Wolanski, E., Norro, A., King, B., 1995. Water circulation in the Gulf of Papua. Continental Shelf Research 15, 185-212.

Wolanski, E., Pickard, G.L., Jupp, D.L.B., 1984. River plumes, coral reefs and mixing in the Gulf of Papua and the Northern Great Barrier Reef. Estuarine, Coastal, and Shelf Science 18, 291-314.

Wolanski, E., Ridd, P., Inoue, M., 1988. Currents through Torres Strait. Journal of Physical Oceanography 18, 1535-1545.

Wolanski, E., Spagnol, S., King, B., Ayukai, T., 1999. Patchiness in the Fly River plume in Torres Strait. Journal of Marine Systems 18, 369-381.

Womersley, J.S., editor, 1995. Handbooks of the Flora of New Guinea, volume I. Melbourne University Press, Victoria, p. 296.

Zonneveld, K.A.F., Marret, F., Versteegh, G.J.M., Bogus, K., Bonnet, S., Bouimetarhan, I., Crouch, E., de Vernal, A., Elshanawany, R., Edwards, L., Esper, O., Forke, S., Grøsfjeld, K., Henry, M., Holzwarth, U., Kielt, J.-F., Kim, S.-Y., Ladouceur, S., Ledu, D., Chen, L., Limoges, A., Londeix, L., Lu, S.-H., Mahmoud, M.S., Marino, G., Matsuoka, K., Matthiessen, J., Mildenhal, D.C., Mudie, P., Neil, H.L., Pospelova, V., Qi, Y., Radi, T., Richerol, T., Rochon, A., Sangiorgi, F., Solignac, S., Turon, J.-L., Verleye, T., Wang, Y., Wang, Z., Young, M., 2013. Atlas of modern dinoflagellate cyst distribution based on 2405 data points. Review of Palaeobotany and Palynology 191, 1-197.

CHAPTER 4. CLIMATIC AND OCEANOGRAPHIC CONDITIONS IN THE GULF OF PAPUA, PAPUA NEW GUINEA, DURING THE BØLLING-ALLERØD, YOUNGER DRYAS, AND MELTWATER PULSE-1B: A PALYNOLOGICAL ANALYSIS *

Introduction

Most of the world's population inhabits coastal that are highly susceptible to climatic, oceanographic, and sedimentological changes. Southeast Asia and in particular, the islands and coastal areas of Papua New Guinea are extremely vulnerable to these changes because large indigenous populations reside theree with little social and political infrastructure to support them during climatic events, such as rapid sea level rise, and intensification of the El Niño Southern Oscillation (ENSO), that induce natural hazards, such as landslides (e.g., Robbins et al. 2013). The National Science Foundation (NSF)-funded Source-to-Sink (S2S) initiative and the MD148-PECTEN (Past Equatorial Climate: Tracking El Niño) expedition conducted cruises in the Gulf of Papua (GoP), Papua New Guinea (PNG), in part to better understand how climate and oceanographic conditions have changed in this region over the latest sea level transgression and how these factors have influenced the sedimentary record (NSF MARGINS Program, 2004). Numerous studies have been published on the cores and data collected during these cruises (e.g., Dickens et al., 2006; Carson et al., 2008; Daniell, 2008; Febo et al., 2008; Francis et al., 2008; Jorry et al., 2008; Muhammad et al., 2008; Slingerland et al., 2008; Tcherepanov et al., 2008; Howell et al. 2014).

This study aims to accomplish three major objectives which are also part of the greater goals of the S2S and PECTEN initiatives: 1) reconstruct climate and

*The following chapter is in preparation for submission to Quaternary International with the following coauthors: Sophie Warny, Samuel J. Bentley, Sr., David Jarzen, André W. Droxler, Ashley L. Howell, Brandon B. Harper, Charles A. Nittrouer, and Kehui Xu. It will be submitted by August 1, 2015.

oceanographic changes over the last 14.5 kyr; 2) determine the advent of anthropogenic influence; and 3) assess changes in sediment source and transport over the study interval. Palynology, which is the study of organic-walled microfossils, can provide much information on climate and oceanographic changes. Pollen, produced by vegetation, is a very sensitive indicator of climate, because vegetation distribution shifts directly in response to climatic factors, such as insolation, precipitation and temperature (Traverse, 2007). Marine palynomorphs, including dinoflagellate cysts, foraminifer linings, copepod eggs, and tintinnids, respond to changes in oceanographic conditions, including ocean temperature, salinity, productivity, and sediment input (Zonneveld et al., 2013). Because palynological preparations contain a wide variety of both marine and terrestrial taxa, palynological analysis can be useful in reconstructing climate and oceanography over the time interval of study (e.g., Warny and Wrenn, 2002; Warny et al., 2003; Warny et al., 2009; Feakins et al., 2012). The non-palynomorph palynological component or palynomacerals (including wood particles, resin, leaf cuticle, and black fragments) extracted from modern sediments collected during the S2S and PECTEN initiatives provided critical data on paleo-water depths and distance to shore indices (Thomas et al., 2015). This study focuses on palynomorphs recovered from these cores.

Anthropogenic impacts on palynological assemblages are well documented from PNG and surrounding areas. Human occupation of PNG has been dated from at least 40 to 45 kyr BP (e.g., Torrence, 2012) with a transition to agriculture between 7 to 9 kyr BP (e.g., Haberle et al., 2012). Agricultural activities are translated in the pollen record by the appearance and increase in pollen of cultivated plants and grassland pollen (due to deforestation), as well as charcoal fragments (due to burning of fields) (Denham et al.,

2003; Haberle, 2003; Denham and Haberle, 2008; Sniderman et al., 2009; Haberle et al., 2012; Warny et al., 2012). We predict an increase in anthropogenic-related palynomorphs in the palynological record from the beginning of agriculture on PNG in the cores selected for study.

Palynological analyis can also be used to assess changes in sedimentation dynamics (e.g., Batten, 1983; Pocknall and Beggs, 1990; Courtinat et al., 2002; Schiøler et al., 2002; Skupien and Mohamed, 2008; Schiøler et al., 2010). The distribution of palynomorphs is strongly effected by the same factors that control sediment distribution, including erosion rates, current speed and direction, and particle density and morphology. Palynomorphs are transported as part of the silt to very fine sand grain size of the sediment load (e.g, Muller, 1959; Melia, 1984; Kershaw, 1994; van der Kaars, 2001; Moss et al., 2005). Reworked palynomorphs, sourced from geologic formations older than Quaternary, are useful for tracing sediment source and transport distance (e.g., Needham et al., 1969; Fleming, 1994; Riding, 2005).

Howell et al. (2014) used fine-grained sediment mineralogy to trace sediment delivery in two of the cores (MV-41 and MV-46). They determined different sediment sources for MV-41 and MV-46, despite their close proximity, likely due to complex shelf morphology and sourcing from different river catchments. Palynological assemblages, particularly the presence of different ages of reworked palynomorphs should differ significantly between the two cores, if their hypothesis is indeed correct. The third core, MD-50, is located 280 km away in Ashmore Trough, and it is dominated by carbonate sedimentation (Harper, 2014). This location has been selected to determine changes in

sea-surface conditions by analyzing marine palynomorph assemblages, particularly dinoflagellate cysts, over the last 14.5 kyr.

Area of study

The GoP (8-11°S, 143-147°E) is located southeast of PNG and north of Australia (Figure 4.1). Sediment discharge from PNG is one of the world's largest at 1.7×10^9 tons per year (Milliman, 1995). Much of this sediment discharge comes from the rivers, including the Fly, Bamu, Turama, Kikori, Purari, Vailala, and Lakekamu (listed from west to east), that enter the GoP (Milliman, 1995; Wolanski et al., 1995), a foreland basin formed during Cenozoic convergence of rifted Australian crust with the Pacific Plate (Pigram et al., 1989). Siliciclastic sediment delivered to the GoP is retained on a wide continental shelf (greater than 100 km across) in the west, while in the north and east sediments are delivered to the continental slope and a series of troughs because the shelf is very narrow (less than 10 km across) (Milliman, 1995; Francis et al., 2008). Carbonate sedimentation in the GoP is predominately located in the south near the Great Barrier Reef. Because of the large sediment discharge volumes and mixed siliciclastic-carbonate sedimentation regime, the GoP can provide important insights for studying how sediments are transported to the ocean from their source to their sink (Milliman, 1995; Thomas et al., in prep). Oceanographic and sedimentological conditions in the GoP have been extensively studied in recent years (e.g., Thom and Wright, 1983; Wolanski and Alongi, 1995; Wolanski et al., 1995; Walsh et al., 2004; Francis et al. 2008; Martin et al., 2008; Muhammad et al., 2008; Ogston et al., 2008; Slingerland et al., 2008; Howell et al., 2014) and provide important context for the present study on palynomorph distribution over the last 14.5 kyr.

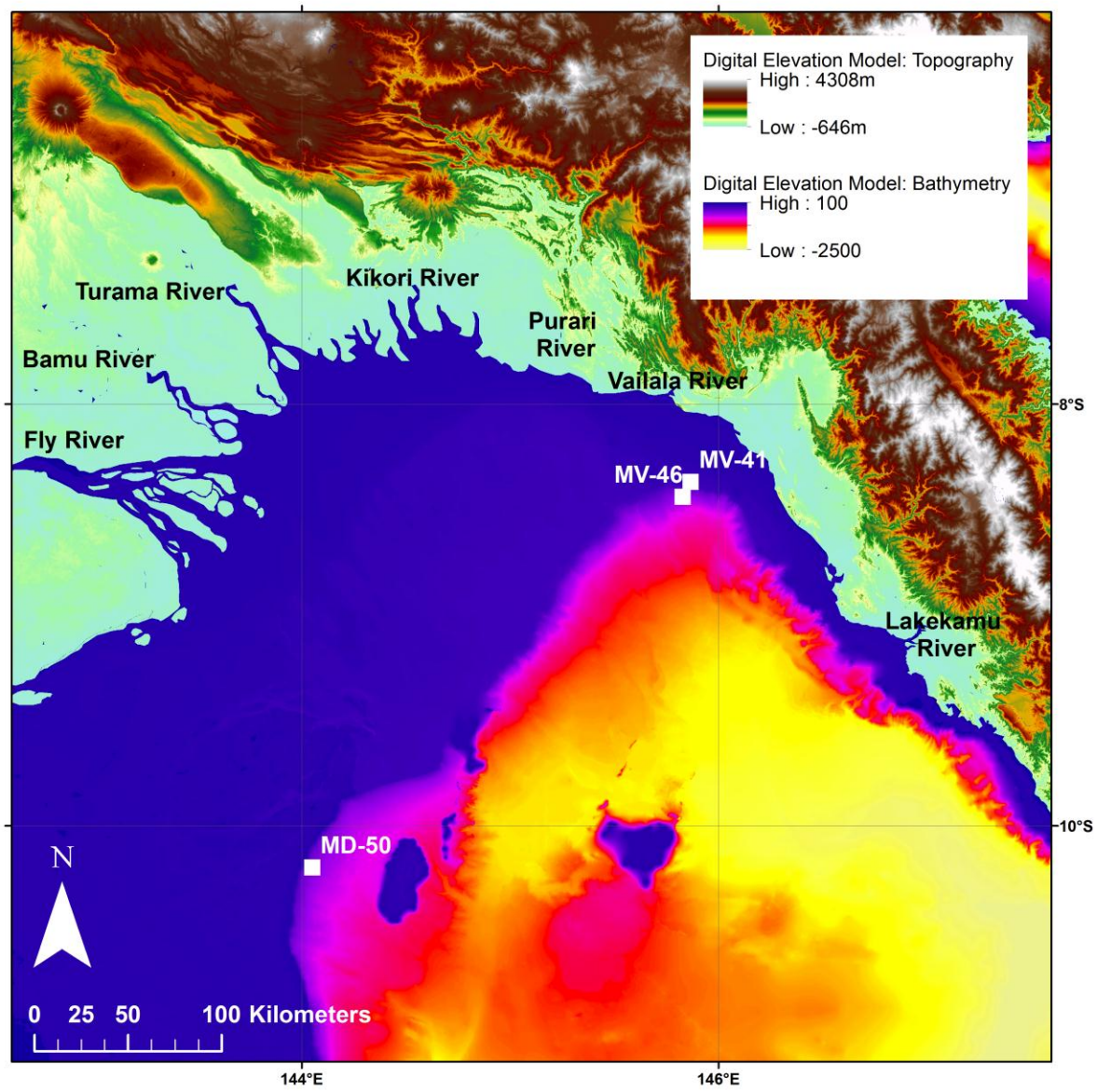

Figure 4.1. Core locations in the Gulf of Papua. Digital elevation model from Daniell (2008). MV-41 and MV-46 are located on the continental shelf and slope, and MD-50 is located in Ashmore Trough.

PNG geology

The modern geology of PNG is quite complex (Figure 4.2), due to the Cenozoic tectonic evolution of the area, which is dominated by collision of a rifted fragment of the Australian craton with the Pacific Plate that led to formation of the GoP foreland basin (Pigram and Davies, 1987; Pigram et al., 1989; Abbott, 1995). Mainland PNG is

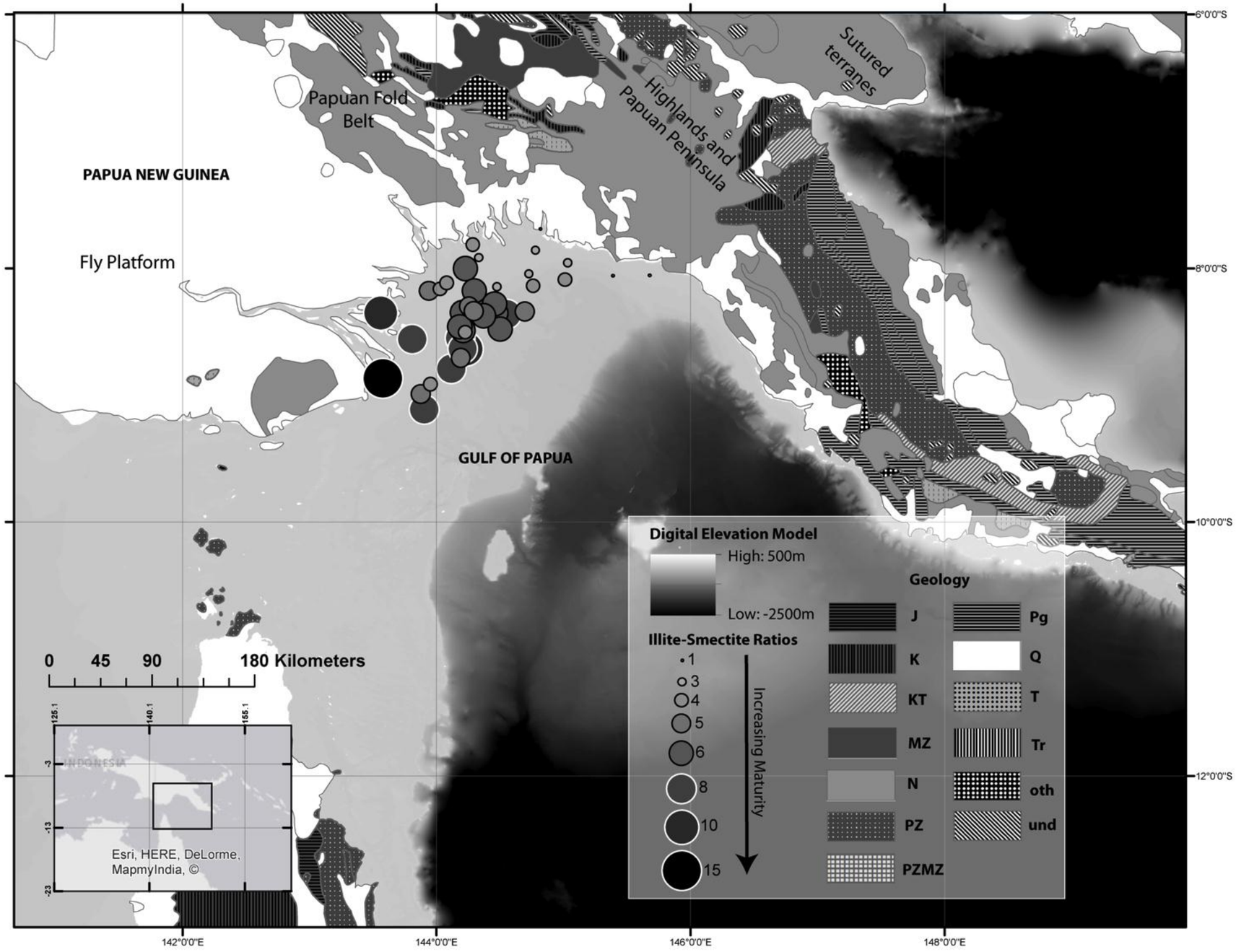

Figure 4.2. Geologic map of Papua New Guinea (Steinshouer et al., 1999). Abbreviations are formation ages: Jurassic (J), Cretaceous (K), Cretaceous-Tertiary (KT), Mesozoic (MZ), Neogene (N), Paleozoic (PZ), Paleozoic-Mesozoic (PZMZ), Paleogene (Pg), Quaternary (Q), Tertiary (T), Triassic (Tr), other (oth), and undifferentiated (und). Digital elevation model of Gulf of Papua bathymetry is from Daniell (2008). Illite:smectite ratios from modern sediment samples are from Slingerland et al. (2008), Howell et al. (2014), and Xu (2015, personal communication). Increasing ratios indicate increasing sediment maturity.

composed of four major provinces: the western Fly Platform, the Papuan Fold Belt, the New Guinea Highlands and Papuan Peninsula, and volcanic arc terranes in the north (Abbott, 1995) (Figure 4.2). The Fly Platform, composed of rifted Australian continental crust, is overlain with Quaternary sediments that source the western rivers, including the Fly, Bamu, and Turama Rivers (Davies, 2012). The Papuan Fold Belt is a currently active fold and thrust belt created by collision, and it is composed of deformed Neogene and Mesozoic rocks. The New Guinea Highlands, which make up most of the Papuan Peninsula, are extremely deformed mountain ranges composed of rocks ranging from Neogene to Paleozoic in age (Abbott, 1995). The highlands source sediments for the Kikori, Purari, Vailala, and Lakekamu river catchments (Davies, 2012). Volcanic arcs, Neogene in age, have been sutured to the mainland in the north (Abbott, 1995), but sediments sourced from these terranes are not likely to enter the GoP due to the drainage divide of the highlands (Pigram et al., 1989; Abbott, 1995; Steinshouer et al., 1999).

GoP oceanography and sedimentology

The geology of PNG governs the source and composition of sediments entering the GoP, while oceanographic conditions determine how sediments are transported and delivered to the gulf. Several factors play an important role in sediment delivery: tidal variations, seasonal wind changes, currents, and the El Niño Southern Oscillation (ENSO). River discharge is relatively constant year-round due to the tropical setting, and there is little influence from cyclonic storms (McAlpine and Keig, 1983). Tidal variations are monthly in scale, and river deltas produced interlaminated mud and sand deposits (Martin et al., 2008). Seasonal wind changes are biannual, with a summer monsoon from December to March when winds blow from the northwest to southeast and winter trade

winds from May to October when winds blow from southeast to northwest (Thom and Wright, 1983; McAlpine and Keig, 1983; Walsh et al., 2004). The Coral Sea Current (CSC) is the major current impacting sediment transport in the western GoP, and it moves sediments mostly northeastward (Brunskill et al., 1995; Wolanski and Alongi, 1995; Wolanski et al., 1995). In the northern and eastern GoP, transport is more complex where the CSC breaks down, and sediments are transported southward off the shelf onto the continental slope (Brunskill et al., 1995; Walsh et al., 2004; Martin et al., 2008). ENSO conditions occur every few years and reduce precipitation, which in turn reduces sediment discharge to the GoP (Rodbell et al., 1999; Kawahata and Gupta, 2004; Ogston et al., 2008). La Niña years result in increased precipitation and sediment discharge (Howell et al., 2014).

The GoP is classified as a mixed siliciclastic-carbonate depositional system (e.g., Dickens et al., 2006; Francis et al., 2008). Because the three cores evaluated in this study are from the northern GoP shelf/northern Pandora Trough and Ashmore Trough we will focus our discussion on sedimentological conditions in these areas (Figure 4.1). At the locations of cores MV-41 and MV-46 (northern shelf edge and northern Pandora Trough, respectively), river clinoforms reach the shelf edge (Wolanski and Along, 1995), and sediments are deposited on the slope (Brunskill et al., 1995; Walsh and Nittrouer, 2004; Muhammad et al., 2008). Howell et al. (2014) provides detailed data on the mineralogy and sedimentology of MV-41 and MV-46. MV-41 is cored in a shelf-edge deposit composed of immature sediments indicating a localized igneous rocks likely sourced from nearby Lakekamu and Vailala river catchment areas. MV-46 is cored in slope deposits, and sediments have clay mineralogies with higher maturity indicating a

different source. Howell et al. (2014) concludes sediment transport during the last marine transgression was not directly downslope from MV-41 to MV-46 and that dispersal pathways have been more heterogeneous and diagonal to the seabed gradient over the latest Quaternary. The heterogeneity of sediment sourcing for cores MV-41 and MV-46 should be apparent in palynological assemblages.

Core MD-50 is located in Ashmore Trough, which receives predominantly carbonate sediments (greater than 80%) sourced from several coral reef atolls (Ashmore Reef, Boot Reef, Portlock Reef, and the Great Barrier Reef) (Figure 4.1) (Carson et al., 2008; Francis et al., 2008; Harper, 2014). At present, the trough receives little siliciclastic sediment, but during times of lower sea level, siliciclastic sediment input was higher (Figure 4.3) (Carson et al., 2008; Francis et al., 2008; Tcherepanov et al., 2008; 2010; Harper, 2014). Harper (2014) provides sedimentological data on MD-50 and notes that the core has been dominated by carbonate sediments since at least 11.5 kyr BP.

Time interval of study

Climate and associated sea level changes play a major role in how sediments are delivered to the ocean (e.g., Droxler and Schlager, 1985; Glaser and Droxler, 1993; Andresen et al., 2003; Jorry et al., 2008). Four major climatic intervals are evaluated in this study (Figure 4.3), including the Bølling-Allerød Interstadial (~14.5 to 12.5 kyr BP), the Younger Dryas (~12.5 to 11.5 kyr BP), Meltwater Pulse-1B (MWP-1B, ~11.5 to 10.5 kyr BP), and the Holocene (~10.5 kyr BP to present). A regional sea level curve from dated coral terraces illustrates the magnitude of change over the last 22 kyr (Figure 4.4, after Muhammad, 2009; Howell et al., 2014). Sea levels in the GoP at the Last Glacial Maximum (LGM) were approximately 120 m lower (Fairbanks, 1989; Hanebuth et al.,

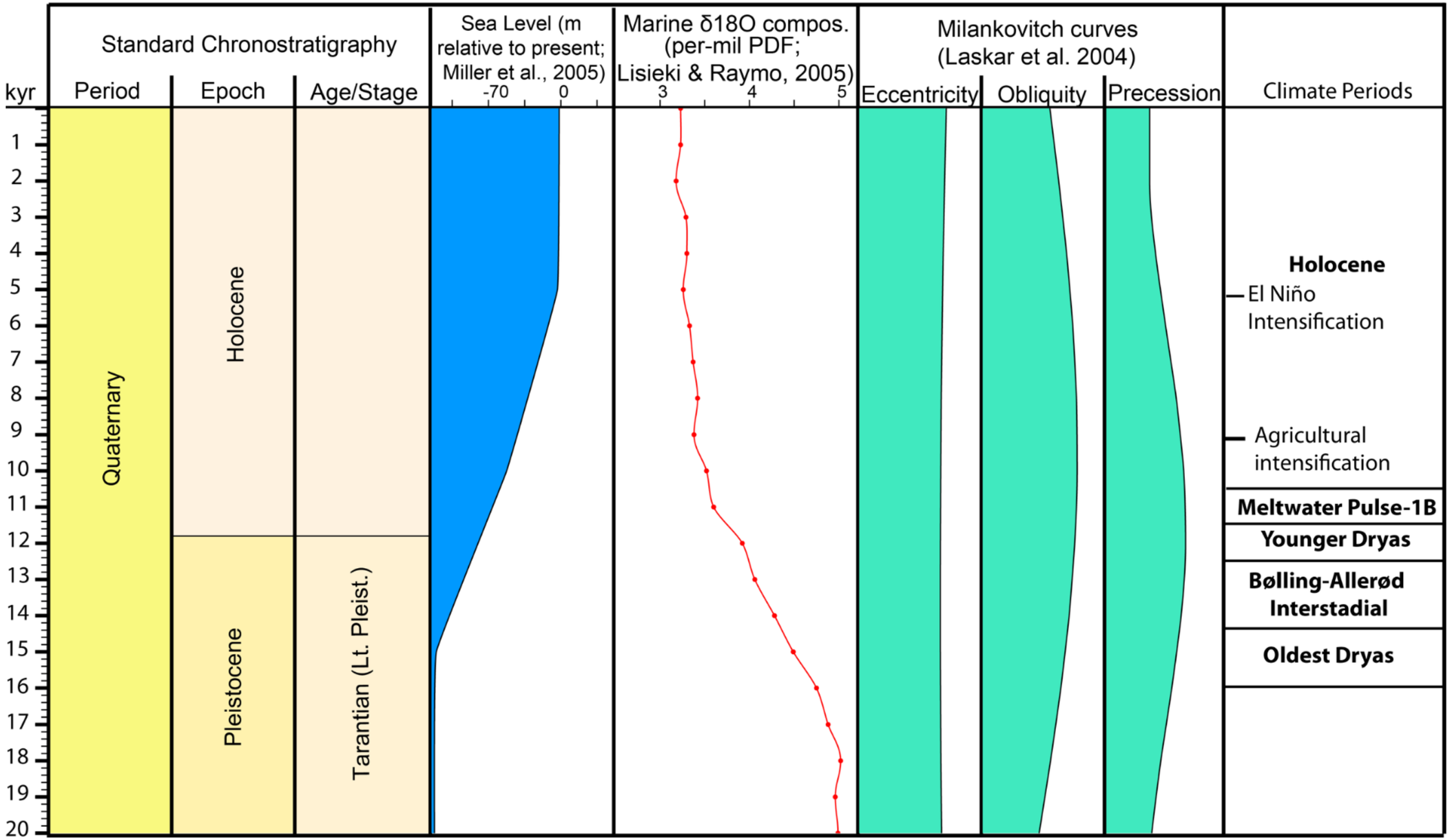

Figure 4.3. Time scale of the last 20,000 years prepared with TimeScale Creator (TSCreator, 2015, http://www.tscreator.org/). Sea level curve, in meters relative to present, is from Miller et al. (2005); oxygen-18 ($\delta^{18}O$, per mill) composite curve is from Lisiecki and Raymo (2005); Milankovitch curves are from Laskar et al. (2004); and important climate periods and events are synthesized Thom and Wright (1983), Hope et al. (1983), Denham et al. (2003), and Howell et al. (2014).

Figure 4.4. Regional relative sea level curve of the last 22,000 years synthesized from corals from the Bonaparte Sea (Yokoyama et al., 2000), Huon Peninsula (Chappell and Polach, 1991; Ota et al., 1993), and the Sunda Shelf (Hanebuth et al., 2000).

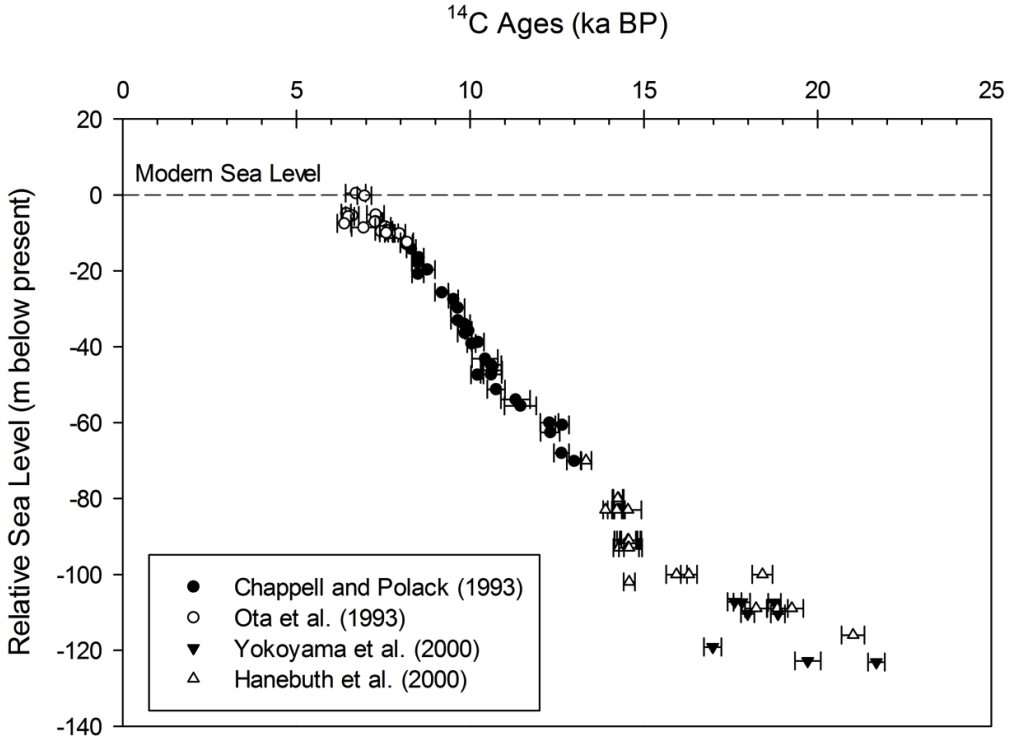

2000; Yokoyama et al., 2000), resulting in exposure of the continental shelf and delivery of siliciclastic sediments directly to the slope (Febo et al., 2008). Warming climate and melting ice at high latitudes contributed to sea level rise and transgression on the GoP shelf, beginning as early as the Oldest Dryas, approximately 15 kyr BP. During sea level rise, less siliclastic material was delivered to the slope and was instead retained on the shelf (Howell et al., 2014). Periods of rapid rise occurred during the Bølling-Allerød Interstadial (-80 to -60 m) and MWP-1B (-60 to -40 m) (Jorry et al., 2008; Howell et al., 2014). The Younger Dryas was a cool period between the Bølling-Allerød Interstadial and MWP-1B, characterized by lower temperatures, drier conditions, slowed rates of sea level rise, and higher volumes of sediment delivery to the slope (Jorry et al., 2008). After MWP-1B, sea level continued to rise, until modern sea level conditions were reached

approximately 6 to 6.5 kyr BP (Ota et al., 1993; Lambeck and Chappell, 2001; Liu et al., 2004; Kubo and Syvitski, 2006; Howell et al., 2014). At present, sediment delivery to the slope is restricted (Harris et al., 1996), and sediments that accumulate there reach it via channels as muddy turbidite flows (Ewing et al. 1970; Gardner, 1970; Winterer, 1970; Brunskill et al., 1995).

Materials and Methods

Core sampling

Cores MV-41 and MV-46 (Table 4.1, Figure 4.1) were collected using a jumbo piston corer (JPC) onboard the *R/V Melville* during 2004. MV-41, located in 92 m water depth on the continental shelf approximately 2 km from the modern shelf edge, recovered 12.84 m of sediment. MV-46, located in 399 m water depth on the upper slope approximately 8 km from MV-41, recovered 14.48 m of sediment (Howell et al., 2014).

Core MD05-2950 (MD-50) (Table 4.1, Figure 4.1) was collected with an advanced piston corer (CALYPSO II) onboard the *R/V Marion Dufresne* during the 2005 PECTEN cruise. The core site is located in Ashmore Trough near the shelf-slope break in a water depth of 476 m. 27.61 m of sediment were recovered (Beaufort, 2007; Harper, 2014).

Table 4.1. Core information, including length (meters, m), location (decimal degrees), and water depth (m) (Beaufort, 2007; Harper, 2014; Howell et al., 2014).

Core	Length (m)	Latitude	Longitude	Water Depth (m)
MV-41	12.84	-8.37°	145.87°	92
MV-46	14.48	-8.44°	145.83°	399
MD-50	27.61	-10.17°	145.09°	476

All cores were logged onboard after collection using a Geotek Multi-Sensor Core Logger (MSCL) to obtain whole-core gamma density (GD, measured in grams per cubic centimeter) and magnetic susceptibility (MS, x 10^{-6} SI) values at 10 cm intervals for MV-41 and MV-46 (Dickens et al., 2006) and at 20 cm intervals for MD-50 (Beaufort, 2007).

Dating and isotope analysis

Eighteen samples from the three cores were collected for radiocarbon (^{14}C) analysis (Table 4.2). Nine of these samples were sand-sized or larger particles of woody debris collected from MV-41 and MV-46, and age results for these two cores were presented in Muhammad (2009) and Howell et al. (2014). ^{14}C analyses for these nine samples were conducted at the Accelerator Mass Spectrometry (AMS) facility at the Woods Hole Oceanographic Institute. Four additional radiocarbon dates were obtained for MV-41 and MV-46 using planktonic foraminifer tests of *Globigerinoides ruber* and *G. sacculifer*. Approximately 100 tests per sample were analyzed at the University of Georgia in the Center for Applied Isotope Studies, and age results were presented in Howell et al. (2014). Conversion to calendar years (peak probability of ± 1σ) was performed on these ages using the Radiocarbon Calibration Program of Fairbanks et al. (2005). Six ^{14}C ages for MD-50 were obtained by analyzing approximately 300 tests of *G. ruber* and *G. sacculifer*, and results were presented in Harper (2014). MD-50 ages were converted to calendar years using the CALIB 7.0 Radiocarbon Calibration program (Stuiver et al., 2015) and Marine 09, a modelled ocean average curve from Reimer et al. (2009). For our analyses, we have placed higher weight on ages measured from planktonic foraminifers, when wood dates cause discrepancies in age determinations. It is

Table 4.2. Radiocarbon dates, including ages for planktonic foraminifer and wood samples with corresponding calibrated ages, for each core (Muhammad, 2009; Harper, 2014; Howell et al., 2014). Depths are in centimeters (cm), and ages are in years before present (yr BP).

Core and depth (cm)	Planktonic foraminifer ^{14}C age (yr BP)	Wood ^{14}C age (yr BP)	Calibrated ^{14}C age (yr BP)
MV-41: 7 - 15	690 ± 30	---	409 ± 58
MV-41: 61 - 63	---	10,150 ± 35	11,818 ± 87
MV-41: 197 - 205	6690 ± 35	---	7273 ± 33
MV-41: 552 - 553	---	10,225 ± 581	11,960 ± 108
MV-41: 881 - 883	---	10,700 ± 70	12,639 ± 63
MV-41: 1143 - 1145	---	11,800 ± 140	13,647 ± 129
MV-46: 156 - 157	---	4380 ± 40	4935 ± 71
MV-46: 309 - 311	---	6100 ± 50	6964 ± 71
MV-46: 413 - 415	---	6950 ± 100	7778 ± 102
MV-46: 592 - 599	8470 ± 30	---	9042 ± 33
MV-46: 1193 - 1195	---	9680 ± 50	11,120 ± 92
MV-46: 1331 - 1338	9590 ± 60	---	10,421 ± 98
MD-50: 140 - 142	2210 ± 45	---	2228 ± 73
MD-50: 360 - 362	4435 ± 35	---	5040 ± 96
MD-50: 870 - 872	9360 ± 70	---	10,575 ± 92
MD-50: 920 - 922	13,590 ± 45	---	15,819 ± 118
MD-50: 1051 - 1053	46,200 ± 1900	---	N/A
MD-50: 1090 -1092	43,700 ± 4200	---	N/A

possible the selected wood fragments for age determination were reworked from older material and are not representative of the time of deposition.

Harper (2014) conducted analyses on oxygen (^{18}O) and carbon (^{13}C) stable isotopes in MD-50 using the planktonic foraminifer *Globigerinoides ruber* selected from the 250-300 μm fraction. Samples were analyzed for stable isotopes of oxygen and carbon using a Delta Advantage Isotope Ratio Mass Spectrometer (IRMS) coupled to a Kiel Carbonate Device III. Analytical precision for the equipment is ± 0.6 ‰, and isotope values are reported relative to the carbonate standard, Vienna Pee Dee Belemnite (V-PDB), in delta notation, δ^{13}C and δ^{18}O (Harper, 2014).

Palynological processing

Cores were sub-sampled at approximately 50 cm intervals (Tables 4.3, 4,4, 4.5) for palynological processing, which isolates palynomorphs and organic material from inorganic sedimentary material. Samples were processed by an external consultant. All samples were spiked with exotic *Lycopodium* markers (batch number 124,961 for MD-50 and 3862 for MV-41 and MV-46) to allow for abundance calculations (Stockmarr, 1971; Traverse, 2007; Lignum et al., 2008). All samples were dried and weighed in grams before processing. Processing procedures were slightly different for MD-50 and MV-41 and MV-46.

Only approximately the top 852 cm of MD-50 was sampled, however, this time interval covers at least the last 10.5 kyr as revealed by radiocarbon dating (Table 4.2). Samples were processed in 2011 by an external consultant following a hydrochloric acid (HCl), hydrofluoric acid (HF), and controlled oxidation procedure (Traverse, 2007). This process involved the use of 10% HCl and 70% HF to dissolve carbonates and silicates, respectively. Controlled oxidation with Schulze's reagent, a mixture of potassium chlorate ($KClO_3$) and nitric acid (HNO_3) was performed for 30 seconds to help improve identification of palynomorphs. Samples were sieved at ten μm to remove the fine fraction, which can complicate identification. Heavy liquid separation with zinc bromide ($ZnBr_2$) was performed to separate organic material from remaining inorganic material not dissolved by HCl and HF. Organic residues were mounted on glass slides with clear resin.

Table 4.3. Sample intervals (centimeters) for MV-41 with dried sample weight (g), number of *Lycopodium* tablets, number of *Lycopodium* in one tablet, and raw counts of the following: *Lycopodium*, spores and pollen, reworked palynomorphs, marine indicators, and fungal spores.

Int. (cm)	Wt. (g)	No. Tablet	*Lyco.* in 1 tablet	*Lyco.* count	Spores and Pollen	RW	Marine Indi-cators	Fungal Spores
7 - 9	15.33	1	9666	11	56	166	69	15
61 - 63	2.86	1	9666	38	31	152	97	38
109 - 111	4.48	1	9666	25	51	168	63	41
157 - 159	11.89	1	9666	9	36	169	38	90
257 - 259	11.38	1	9666	13	84	124	40	81
352 - 354	9.22	1	9666	6	69	110	71	58
402 - 404	13.13	1	9666	4	60	131	45	71
462 - 464	11.34	1	9666	11	56	108	40	90
517 - 519	7.31	1	9666	12	52	132	29	105
559 - 561	7.30	1	9666	18	85	90	43	84
621 - 623	5.93	1	9666	41	65	164	105	47
673 - 675	4.19	1	9666	36	72	125	68	36
725 - 727	2.05	1	9666	45	104	113	59	56
785 - 787	7.11	1	9666	11	66	118	50	78
848 - 850	3.44	1	9666	33	92	138	35	60
903 - 905	11.17	1	9666	28	82	117	63	62
1037 - 1039	3.57	1	9666	34	89	107	50	75
1089 - 1091	12.59	1	9666	39	73	127	76	34
1143 - 1145	8.07	1	9666	24	91	133	81	27
1185 - 1187	9.72	1	9666	20	59	159	56	21
1252 - 1254	5.83	1	9666	25	63	142	69	38

Various researchers have noted the effects of oxidation on certain fragile palynomorphs in modern sediments, specifically dinoflagellate cysts (Harland, 1981; Harland, 1983; Schrank, 1988). Although dinoflagellate cyst recovery is viable in MD-50, MV-41 and MV-46 were processed without controlled oxidation in order to ensure maximum recovery of dinoflagellate cysts. Five μm sieves were used instead of ten μm sieves to maintain the smallest palynomorphs, especially Rhizophoraceae pollen (e.g.,

Table 4.4. Sample intervals (centimeters) for MV-46 with dried sample weight (g), number of *Lycopodium* tablets, number of *Lycopodium* in one tablet, and raw counts of the following: *Lycopodium*, spores and pollen, reworked palynomorphs, marine indicators, and fungal spores.

Int. (cm)	Wt. (g)	No. Tablet	*Lyco.* in 1 tablet	*Lyco.* count	Spores and Pollen	RW	Marine Indi-cators	Fungal Spores
7 - 9	4.91	1	9666	35	20	118	128	22
61 - 63	1.72	1	9666	75	37	40	79	152
109 - 111	1.26	1	9666	115	39	62	82	118
157 - 159	19.24	1	9666	19	64	96	62	126
205 - 207	4.22	1	9666	35	47	86	94	89
257 - 259	3.29	1	9666	21	56	49	56	154
309 - 311	3.4	1	9666	34	45	74	48	190
361 - 363	2.47	1	9666	32	33	56	76	134
438 - 440	4.68	1	9666	23	42	55	86	140
465 - 467	7.88	1	9666	16	61	48	72	133
537 - 539	8.31	1	9666	21	61	54	56	157
673 - 675	1.08	1	9666	100	35	44	35	219
725 - 727	5.7	1	9666	20	54	40	25	185
777 - 779	1.51	1	9666	40	53	51	25	170
842 - 844	6.38	1	9666	10	49	77	48	135
897 - 899	5.48	1	9666	27	73	63	60	137
957 - 959	6.58	1	9666	20	83	91	69	105
1037 - 1039	5.3	1	9666	21	35	101	45	139
1089 - 1091	7.37	1	9666	19	63	76	42	126
1141 - 1143	5.04	1	9666	11	50	94	47	105
1193 - 1195	4.92	1	9666	20	54	58	24	171
1245 - 1247	5.76	1	9666	17	57	77	54	138
1297 - 1299	2.82	1	9666	52	43	110	35	101
1325 - 1327	4.13	1	9666	22	64	49	19	191
1379 - 1381	4.12	1	9666	27	63	125	29	144
1439 - 1441	8.51	1	9666	26	70	115	34	70

Scourse et al., 2005). All other steps in the processing procedure remained the same in order to introduce as little bias as possible when comparing palynomorph assemblages among cores.

Table 4.5. Sample intervals (centimeters) for MD-50 with dried sample weight (g), number of *Lycopodium* tablets, number of *Lycopodium* in one tablet, and raw counts of the following: *Lycopodium*, spores and pollen, reworked palynomorphs, marine indicators, and fungal spores. Sampling covers approximately the top third of the core.

Int. (cm)	Wt. (g)	No. Tablet	*Lyco.* in 1 tablet	*Lyco.* count	Spores and Pollen	RW	Marine Indi-cators	Fungal Spores
1 - 3	17.9	2	12542	205	16	18	294	5
100 - 102	16.9	2	12542	716	43	31	250	14
150 - 152	17.4	2	12542	337	14	24	272	13
200 - 202	16.9	2	12542	1049	39	40	208	23
250 - 252	17.8	2	12542	449	35	8	225	21
301 - 303	18.2	2	12542	337	35	53	216	9
350 - 352	19.6	2	12542	1350	64	55	144	36
400 - 402	18.6	2	12542	894	71	18	159	18
452 - 454	13.2	2	12542	1639	68	80	105	36
500 - 502	17.0	2	12542	1075	54	74	137	35
550 - 552	17.0	2	12542	877	73	95	97	41
601 - 603	16.3	2	12542	916	46	117	79	40
650 - 652	12.5	2	12542	1163	70	98	70	42
700 - 702	16.5	2	12542	939	81	53	98	40
751 - 753	17.3	2	12542	716	98	59	83	55
800 - 802	18.7	2	12542	390	100	68	64	49
850 - 852	21.3	2	12542	261	81	77	79	44

Microscopy and palynomorph identification

At least 300 palynomorphs per slide were counted on an Olympus BX43 microscope at Louisiana State University's Cenex (Center for Excellence in Palynology) laboratory. Slides were counted using transmitted light at 600x magnification. All results and recovery data are presented as absolute abundance values calculated with the following formula (e.g., Stockmarr, 1971; Traverse, 2007; Lignum et al., 2008):

$$specimens\ per\ g\ sediment = \frac{counted\ specimens \times tablets\ added \times \text{Lycopodium}\ in\ 1\ tablet}{counted\ \text{Lycopodium} \times sample\ weight\ (g)}$$

Tropical rainforest settings, like PNG, have high pollen and spore diversity, and many references were utilized to identify them and the vegetation that produced them, including Paijmans (1975), Flenley (1979), Walker and Flenley (1979), Playford (1982), Davey (1987), Rigby (1997), Rigby (2001), APSA Members (2007), and Playford and Rigby (2008). As species-level identification of vegetation using pollen and spores can be difficult, species were often grouped into genera or family-level designations attributable to modern vegetation. If attribution to a specific genera or family was impossible, pollen and spores were grouped according to morphological designations, e.g. tricolporate, tricolpate, and monocolpate. Specimens unattributable to any morphological designation were kept as unknown. Dinoflagellate cysts were identified using Zonneveld et al. (2013). Additional marine indicators were also indentified, including foraminifer linings, copepod eggs, tintinnids, and acritarchs (Traverse, 2007). The dominant representatives of all groups are presented in Figure 4.5.

Analysis and correlation

StrataBugs 2.0 (StrataData, 2014) was used to create detailed plots of down-core palynomorph distribution in comparison with previously published sedimentological data (Figures 4.6, 4.7, 4.8). Each plot contains the following: depth (cm); generalized sediment lithology; magnetic susceptibility ($x10^6$ SI); sample intervals (cm); marine indicator abundance (including dinoflagellate cysts, acritarchs, tintinnids, foraminifer linings, and copepod eggs); mangrove abundance (including Rhizophoraceae, *Sonneratia* spp, *Avicennia* spp, *Nypa* spp, and *Acrostichum aureum*); total pollen and spore abundance; reworked palynomorph abundance; calibrated radiocarbon ages; and climate events. $\delta^{13}C$ and $\delta^{18}O$ values are included in the plot for MD-50 (Harper, 2014).

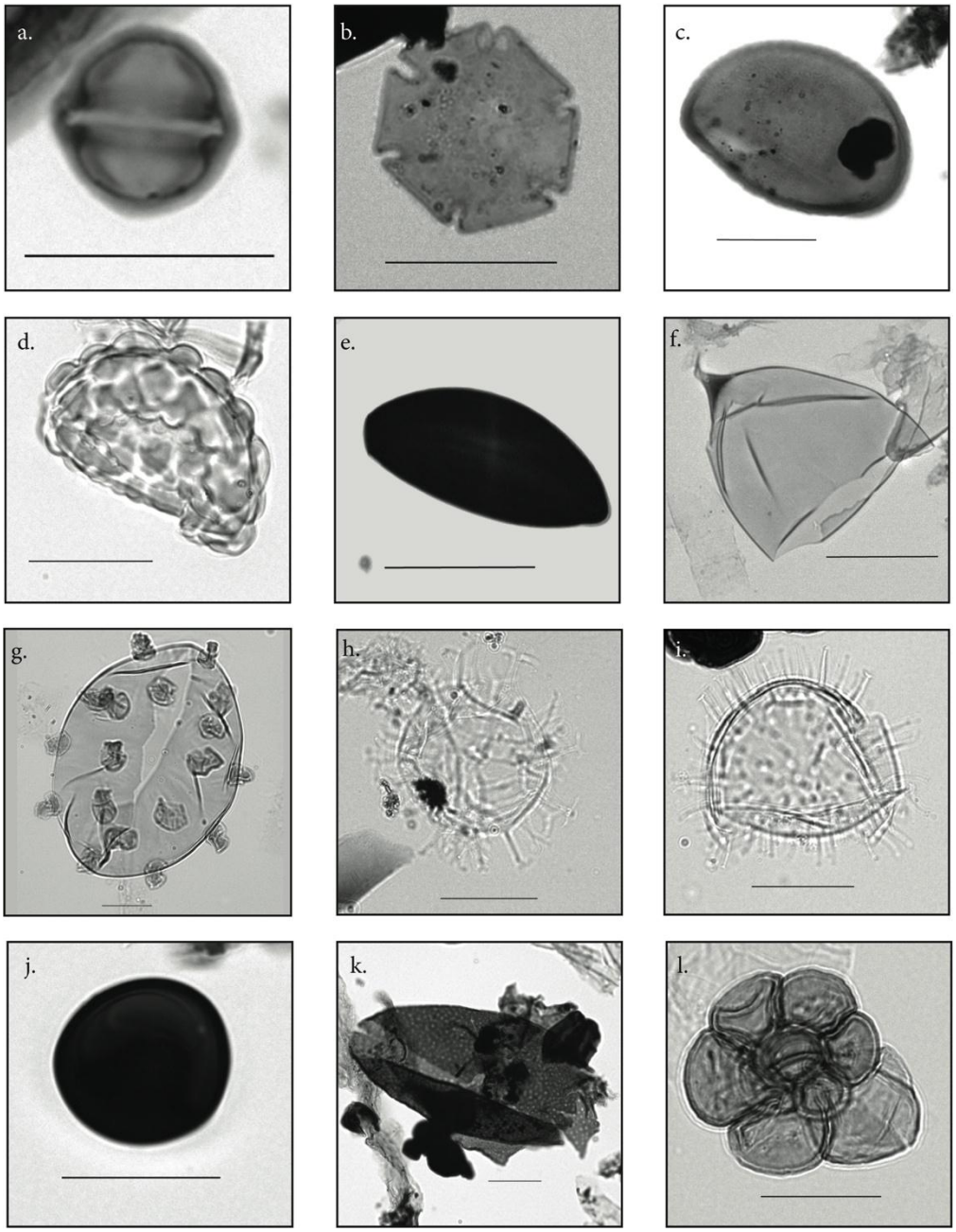

Figure 4.5. All photographs are at 600x magnification. a). *Rhizophora* sp. (mangrove pollen), MV-41, 621-623cm; b). *Nothofagus brassii* (southern beech pollen), MV-46, 537-539 cm; c). Arecaceae (palm pollen), MV-41, 7-9 cm; c). *Polypodiidites usmensis* (monolete spore), MD-50, 850-852cm; e). Fungal spore, MV-46, 1439-1441cm; f). Tintinnid, MD-50, 1-3cm; g). *Tuberculodinium vancampoae* (dinoflagellate cyst), MD-50, 400-402 cm; h). *Spiniferites ramosus* (dinoflagellate cyst), MD-50, 400-402cm; i). *Operculodinium centrocarpum* (dinoflagellate cyst), MD-50, 1-3cm; j). *Brigantedinium* spp. (dinoflagellate cyst), MD-50, 850-852cm; k). Copepod egg, MV-46, 1439-1441cm; l). Foraminifer lining, MD-50, 1-3cm.

Cores MD-50, MV-41, and MV-46 were then correlated using palynomorph assemblage data, magnetic susceptibility, and radiocarbon ages (Figure 4.9). An additional cool/warm climate curve, calculated from the ratio of cool to warm species abundance in each sample, was included for each core for better understanding of climatic changes. Correlation lines 1 through 4 are equivalent to the climate periods identified in the cores (Figures 4.6, 4.7, 4.8) and are labeled. Each correlation line is based on a combination of magnetic susceptibility shifts or peaks, changes in palynomorph assemblages, and radiocarbon ages.

Depth versus age plots were also created in Stratabugs and are presented for each core (Figure 4.10). Sediment accumulation rates are in centimeters per kiloyear. Radiocarbon dates excluded from the curve (one point in MV-41 and one in MV-46) are from reworked wood particles, and the ages determined from them are likely not representative of the age of deposition.

Results

Assemblages at MV-41, MV-46, and MD-50 are dominated by the following groups: marine indicators (including dinoflagellate cysts, foraminifer linings, tintinnids, acritarchs, and copepod eggs), mangrove pollen (mostly of Family Rhizophoraceae), spores and pollen, fungal spores, and reworked palynomorphs, which are generally not age diagnostic (Figures 4.6, 4.7, 4.8). Greater abundances of palynomorphs are found in silt and clay dominated lithologies. Peaks or shifts in magnetic susceptibility do not appear to correspond to consistent changes in palynomorph assemblages. Using radiocarbon dates and palynomorph assemblage changes, global climate periods corresponding to Figure 4.3 have been interpreted in each core.

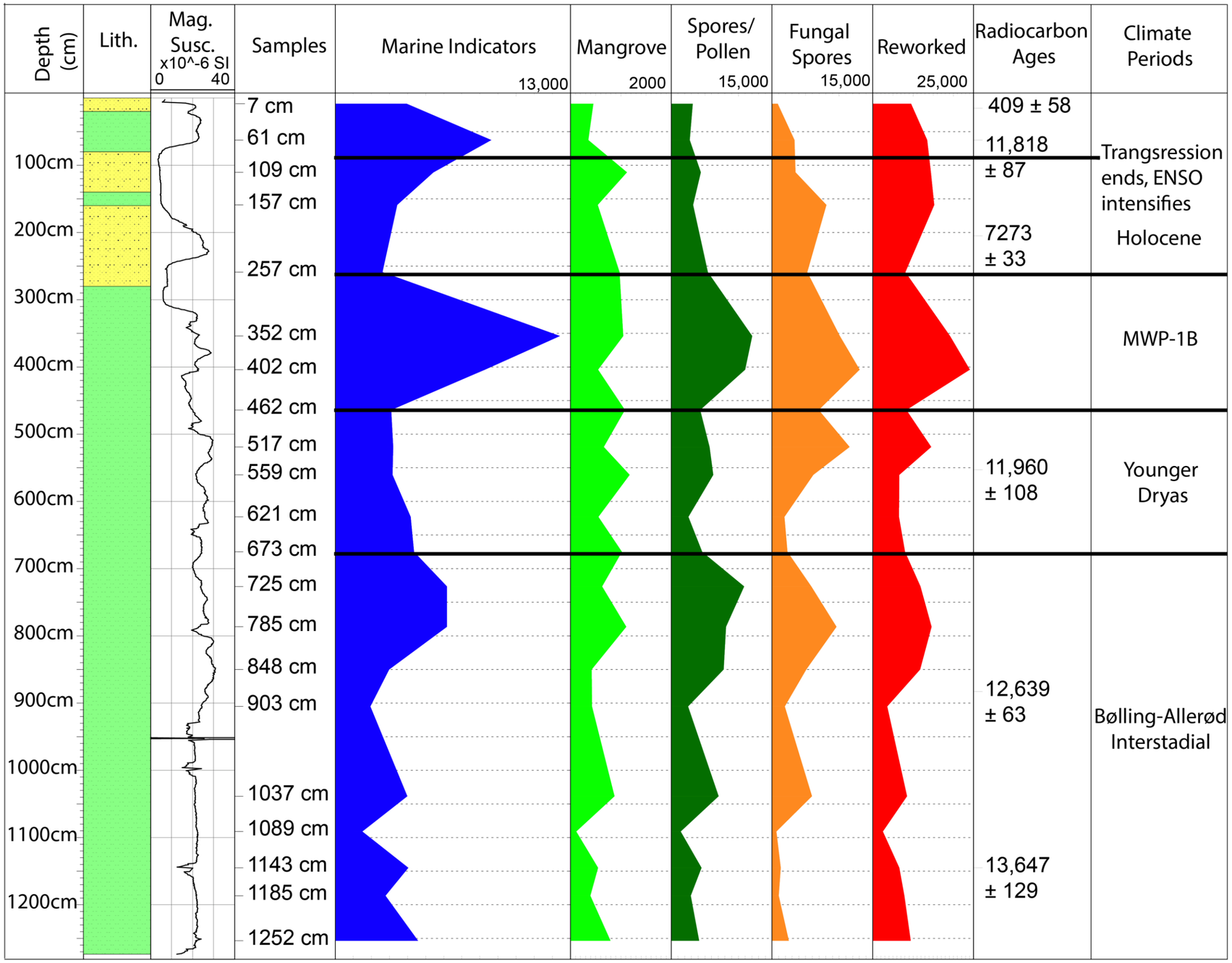

Figure 4.6. Palynomorph assemblages of MV-41. All abundances are in units of palynomorphs per gram of dried sediment. Marine indicators are more abundant in younger samples, and pollen and spores are more abundant in older samples. Reworked palynomorphs increase toward the top of the core, and high abundances of mangrove pollen mark the beginning and end of transgression. ENSO = El Niño Southern Oscillation, MWP-1B = Meltwater Pulse-1B.

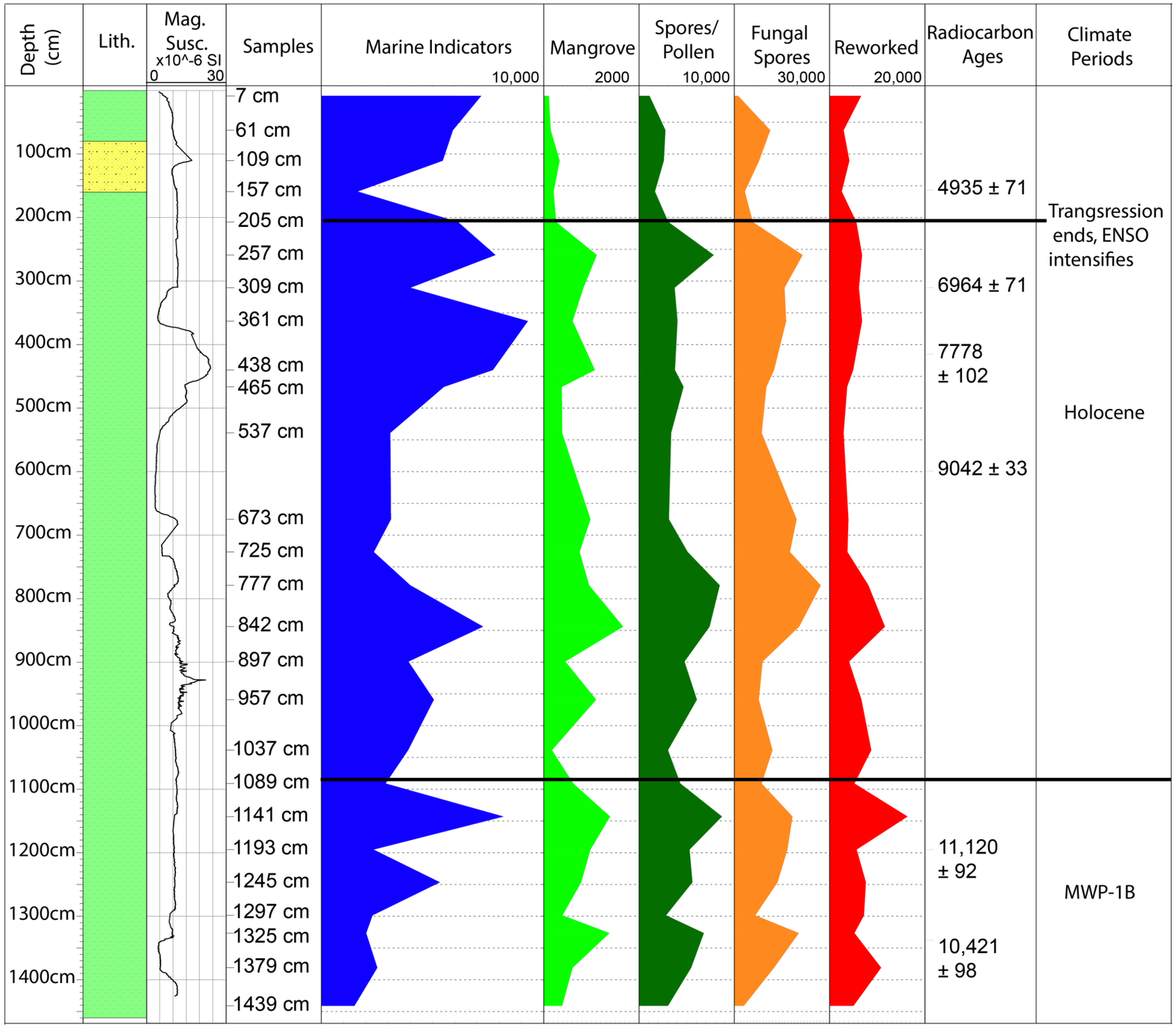

Figure 4.7. Palynomorph assemblages of MV-46. All abundances are in units of palynomorphs per gram of dried sediment. Marine indicators are generally more abundant in younger samples. Decrease in mangrove pollen abundance marks approximately the end of sea level transgression. Spores and pollen, fungal spores, and reworked palynomorphs are slightly more abundant in older samples. ENSO = El Niño Southern Oscillation, MWP-1B = Meltwater Pulse-1B.

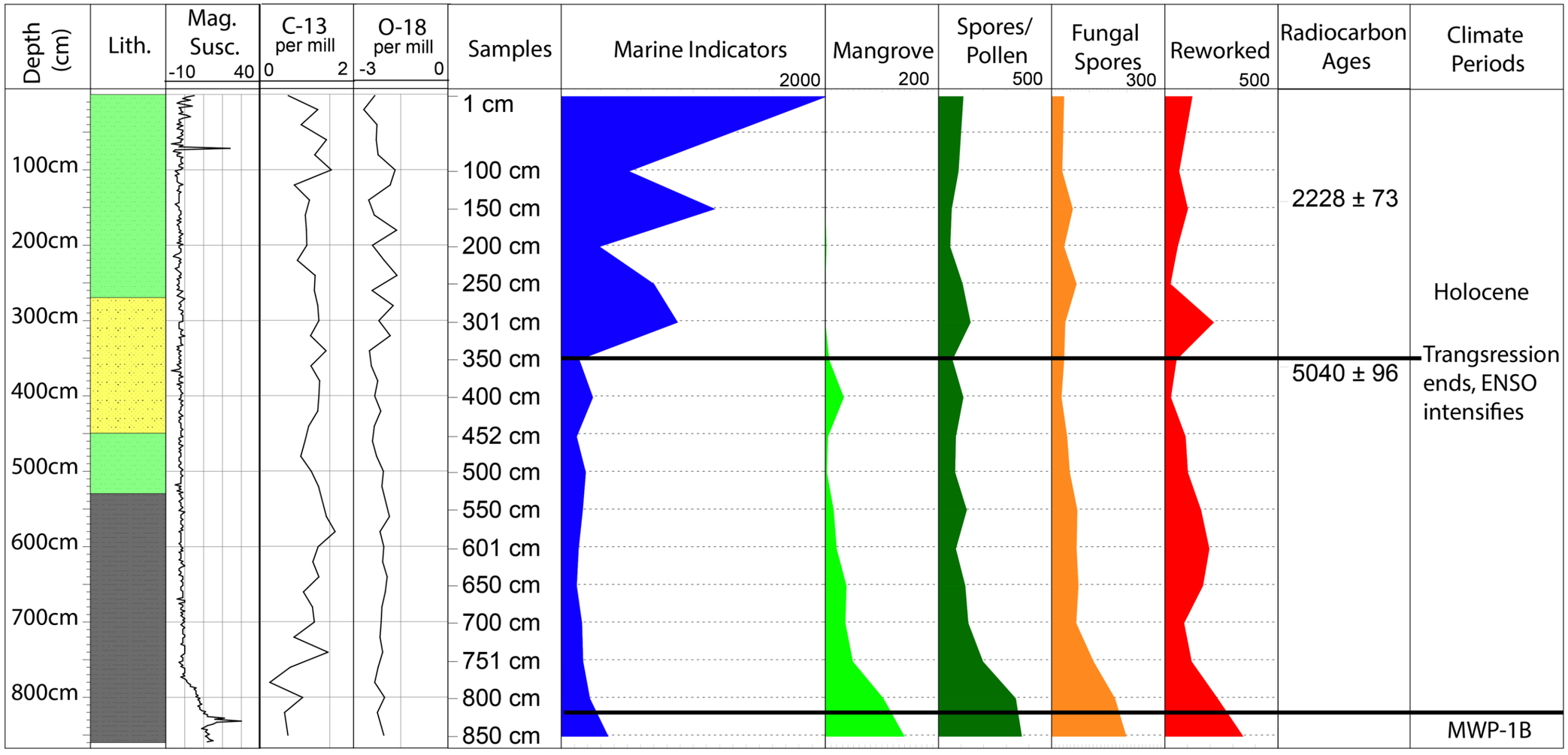

Figure 4.8. Palynomorph assemblages of MD-50. All abundances are in units of palynomorphs per gram of dried sediment. Marine indicators are much more abundant in younger samples (less than 5000 years old). Mangrove pollen is extremely reduced or absent in sea level highstand samples. Pollen and spores, fungal spores, and reworked palynomorphs are increasingly abundant in older samples. ENSO = El Niño Southern Oscillation, MWP-1B = Meltwater Pulse-1B.

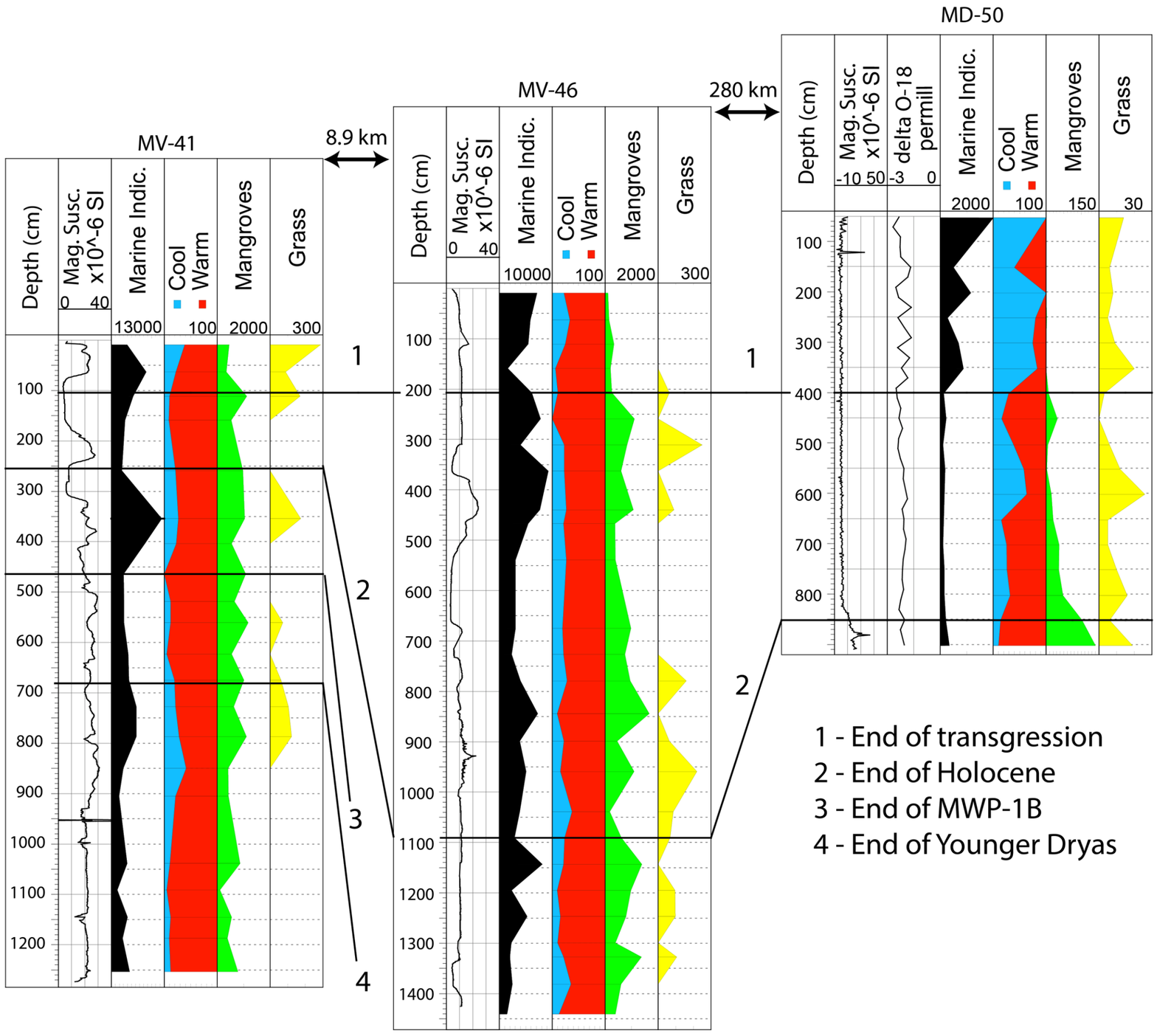

Figure 4.9. Correlation panel of MV-41, MV-46, and MD-50 based on magnetic susceptibility, palynomorph assemblages, and radiocarbon ages. Line 1 corresponds to end of marine transgression and possible El Niño Southern Oscillation (ENSO) intensification. Line 2 corresponds to beginning of Meltwater Pulse-1B (MWP-1B). Line 3 corresponds to beginning of Younger Dryas. Line 4 corresponds to beginning of Bølling-Allerød Interstadial.

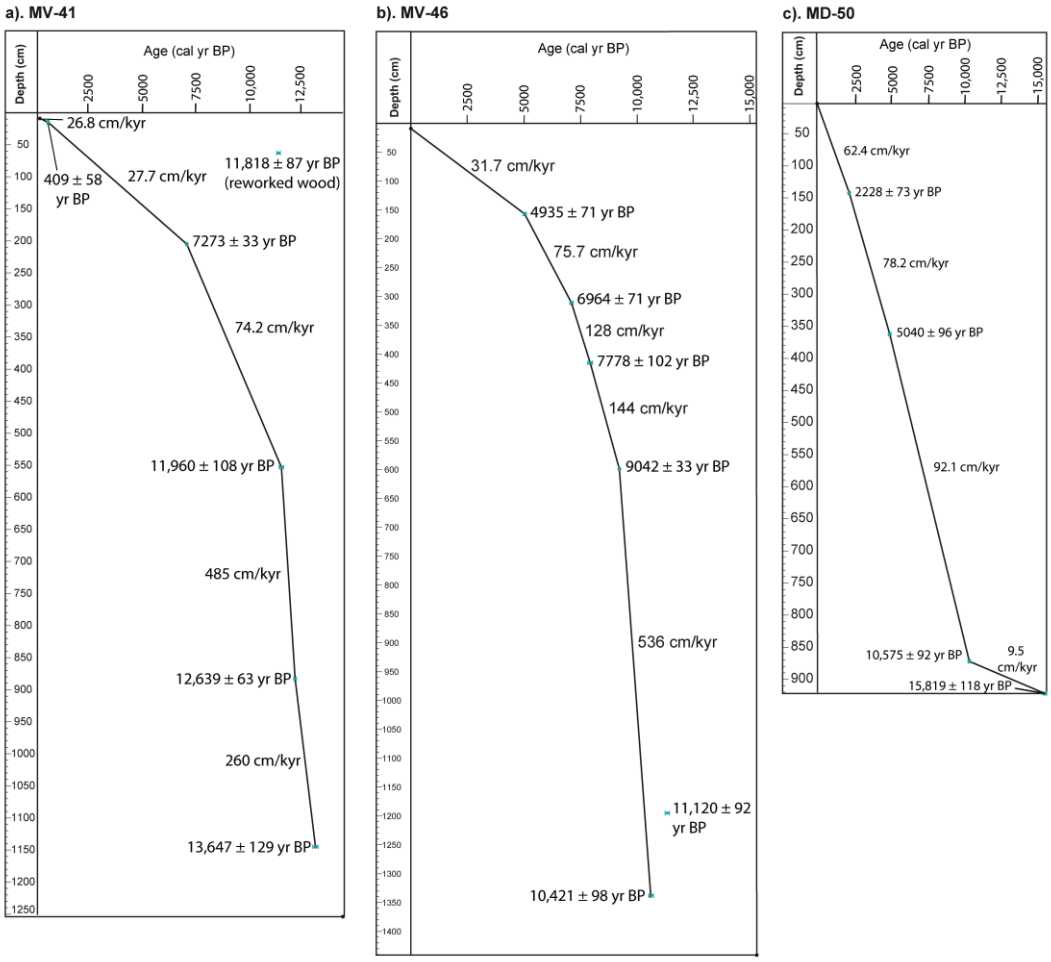

Figure 4.10. Depth versus age plots for MV-41, MV-46, and MD-50. Sediment accumulation rates are in centimeters per year, and radiocarbon ages with standard deviations are plotted in years BP.

Core MV-41 covers approximately 14 kyr (Figure 4.6). Marine indicators are dominated by dinoflagellate cysts of the genus *Brigantedinium,* a genus that is often found in coastal areas and has wide environmental tolerances (Figure 4.5, j) (Zonneveld et al., 2013). Foraminifer linings (Figure 4.5, l), copepod eggs (Figure 4.5, k), and tintinnids (Figure 4.5, f) are also abundant. Mangrove vegetation is the major vegetation representative in MV-41, with *Rhizophora* spp. being the most abundant (Figure 4.5, a). Spores (Figure 4.5, d) vastly outnumber pollen beside *Rhizophora* spp. (Figure 4.5, b, c). Fungal spores

(Figure 4.5, e) and reworked palynomorphs of undiagnostic age are abundant in MV-41 samples with abundances of greater than 18,000 and 28,000 palynomorphs per gram respectively. We have chosen to ignore the radiocarbon date of 11,818 ± 97 yr BP at a depth of 61-63 cm, as it is likely to have been determined on a fragment of reworked wood.

The sampled interval for core MV-46 covers approximately the last 10.5 kyr, with assemblages representing the end of MWP-1B and the Holocene (Figure 4.7). As for MV-41, marine indicators are dominated by *Brigantedinium* spp. dinoflagellate cysts and foraminifer linings with lower occurrences of tintinnids and copepod eggs. Spores are much more abundant than pollen besides *Rhizophora* spp. Fungal spores (abundances of close to 30,000 spores/gram) are more common in MV-46 than in MV-41, and reworked palynomorphs are less common (samples average between 10,000 to 15,000 specimens/gram).

Core MD-50 is characterized by very different palynomorph assemblages from the other two cores (Figure 4.8). Palynomorph abundance in MD-50 samples is much lower than MV-41 and MV-46 for all groups. Marine indicators in MD-50 are dominated by foraminifer linings, copepod eggs, tintinnids, and dinoflagellate cysts. The dinoflagellate cysts present include *Spiniferites* spp. (Figure 4.5, h), *Operculodinum centrocarpum* (Figure 4.5, i), *O. israelianum*, *Lingulodinium machaerophorum*, and *Tuberculodinium vancampoae* (Figure 4.5, g). Few cysts of *Brigantedinium* spp. are present in MD-50. Mangroves are dominated by Family Rhizophoraceae, and pollen abundances are low throughout the core. Spores are the major component of terrestrial

vegetation. Fungal spores and reworked palynomorphs are in much lower abundances than MV-41 and MV-46 samples.

All three cores have been correlated in transect A to A' across the GoP (Figure 4.9). Correlation lines correspond to climatic events identified in each core (Figures 4.6, 4.7, 4.8). The chart has been flattened on correlation line 1, the primary datum, which corresponds to the end of sea level transgression and possible ENSO intensification. Line 2 delineates the end of the Holocene and the beginning of MWP-1B. Lines 3 and 4 are only identified in MV-41 and correspond to the beginning of the Younger Dryas and Bølling-Allerød, respectively.

Depth vs. age plots prepared for the three cores highlight differences in the depositional environments among MV-41 and MV-46 and MD-50 (Figure 4.10). Sediment accumulation rates for MV-41 and MV-46 are comparable, while MD-50 is quite different. MV-41 and MV-46 show very high accumulation rates during sea level transgression with major decreases when sea level reached highstand conditions at approximately 5 to 6 kyr BP. MD-50, dominated by carbonate input over the Holocene, has nearly linear sediment accumulation rates during this period, with only a slight decrease in accumulation after sea level reached highstand conditions. Prior to approximately 10.5 kyr BP, sediment accumulation rates for MD-50 were much lower, with only 50 cm of sediment deposited during 5.2 kyr. No palynological samples were available from this interval in MD-50.

Discussion

The major groups of palynomorphs observed in MV-41, MV-46, and MD-50 include marine indicator taxa (foraminifer linings, dinoflagellate cysts, acritarchs,

copepod eggs, and tintinnids); terrestrial pollen and spores dominated by *Rhizophora* spp. and monolete and trilete spores; fungal spores; and reworked palynomorphs. The occurrences of these taxa in the study area are in agreement with previous work on PNG vegetation and marine taxa distribution in surrounding areas (e.g., Paijmans, 1975; Flenley, 1979; Walker and Flenley, 1979; Playford, 1982; Davey, 1987; Rigby, 1997; Rigby, 2001; Rowe, 2007a; 2007b; Playford and Rigby, 2008; Rowe et al., 2013). Dinoflagellate cyst recovery, besides *Brigantedinium* spp., is suprisingly low in MV-41 and MV-46, which leads to the conclusion that conditions at these core locations were not favorable for dinoflagellates, most of which prefer fully marine conditions and clear water (e.g., Marret and Zonneveld, 2003; Zonneveld et al., 2013). Low recovery of cysts in these cores fit well with current understanding of the GoP sedimentary regime, particularly that salinities were too low at the sites of MV-41 and MV-46 (Wolanski and Alongi, 1995; Howell et al., 2014). *Operculodinium israelianum* and *Tuberculodinium vancampoae* are known to co-occur and dominate the assemblage in warm inner neritic environments with salinites of 35 (Warny et al., 2003). The co-occurence of both *Operculodinum centrocarpum* and *O. israelianum* is also very important as it allows us to estimate the minimum sea-surface temperature throughout the core. *Operculodinium centrocarpum* is a true cosmopolitan species, tolerating sea-surface salinities ranging from 16.1-36.8 and sea-surface temperature ranging from -2.1 to 29.6ºC, but *Operculodinium israelianum* is much more restrictive and requires saline waters with sea-surface temperature higher than 11.5ºC (Marret and Zonneveld, 2003). The continuous presence of both species indicates that, even during the Younger Dryas, sea surface temperatures (SST) were above 11.5ºC.

Terrestrial pollen recovery, besides Rhizophoraceae, is low in all three cores, however it is possible most pollen has been deposited before reaching the core locations. The pollen morphologies most represented in the cores include small forms (like *Rhizophora* spp.), spores, and bisaccate forms, which can be transported longer distances (Muller, 1959; Traverse and Ginsburg, 1966; Traverse, 2007). Increases in fungal spore abundance and diversity require moist conditions. They can also indicate potentially warmer periods (e.g., Staplin, 1976; Elsik, 1980; Elsik, 1996), however in this study, increased abundance of fungal spores occurs during phases of rapid sea level rise (Figures 4.6, 4.7, 4.8). Despite comparison with works on pre-Quaternary palynomorphs on PNG (Playford, 1982; Davey, 1987; Rigby, 1997; Rigby, 2001; Playford and Rigby, 2008), we have not been able to determine ages of reworked palynomorphs in the three cores.

Changes in palynomorph assemblages in the studied cores allow identification of four global climatic intervals, although only MV-41 records the Bølling-Allerød Interstadial (673 – 1252 cm) and the Younger Dryas (462 – 673 cm). During the Bølling-Allerød Interstadial in MV-41, all groups, predominantly warm climate taxa (Figure 4.9), are recovered in low abundances, and magnetic susceptibility values are relatively low. During the Younger Dryas Period in MV-41, cool climate taxa are recovered in slightly higher abundances, and marine indicators, total spores and pollen (including mangroves), fungal spores, and reworked palynomorphs are recovered in slightly lower abundances. MWP-1B is a relatively short interval in MV-41, covering 257 to 462 cm. The highest abundances of all palynomorph groups in the sampled section, except mangrove pollen, are recovered during this climatic interval. A sharp decrease in MS values occurs at the

end of MWP-1B. The beginning of the Holocene is at 257 cm in MV-41. Generally higher occurrences of marine indicators and lower occurrences of terrestrial taxa, except reworked palynomorphs, are present during the Holocene. The end of marine transgression is interpreted at a depth of 109-111 cm from a peak in MS, increased abundance of marine indicator taxa and decreased abundance of mangrove taxa. Indeed, mangrove abundance is highest during transgression and decreases during highstand and lowstand, while dinoflagellate cyst increases can be seen during both transgression and highstand when sea-surface salinities are stable, near the global average of 35.

Samples from MV-46 cover MWP-1B and the Holocene. Samples from 1089 to 1439 cm cover MWP-1B (Figure 4.7). Marine indicator abundances are low in this climate interval, and there is a peak in warm climate taxa (Figure 4.9). Mangrove and total spore and pollen abundances are generally lower than the rest of the core. This interval is marked by low magnetic susceptibility values. Samples from 1089 cm to the top of the core represent the Holocene interval. Several peaks in marine indicator abundance are present, and cool climate taxa are of low abundance throughout the core (Figure 4.9). Mangrove pollen, total spores and pollen, fungal spores, and reworked palynomorphs are abundant until the end of transgression, interpreted at a depth of 205 cm from a peak in marine indicator abundance and radiocarbon ages. Abudance values and dinoflagellate cyst species comprising this peak are similar to a peak that occurred in the earlier Holocene (361 cm).

The sampled interval in MD-50 covers approximately the last 10.5 kyr (Figure 4.8). Samples from 800 to 850 cm cover the end of MWP-1B. During this period, we recovered higher relative abundances of mangrove pollen, total pollen and spores, fungal

spores, and reworked palynomorphs. Warm climate taxa are also more abundant (Figure 4.9). Samples from 800 cm to the top of the core cover the Holocene interval. The end of marine transgression and intensification in ENSO conditions has been interpreted from 301 to 350 cm. A sharp peak in marine indicator abundance occurs at this depth with a decrease in mangrove pollen, which is not present in the top 300 cm of the core. Potential ENSO intensification could be recorded by the greater variability of the $\delta^{18}O$ curve from 325 cm to 0 cm. The abundance of cool climate taxa increases toward the top of MD-50 (Figure 4.9), however this is likely a side effect of the core's distance from shore and decrease in total abundance of terrestrial palynomorphs. Bisaccate pollen, such as Podocarpaceae spp. which can be transported much farther due to the presence of air bladders (e.g., Muller, 1959) dominate the vegetation signal in the upper section of the core. High abundances of these types are either indicative of cooler climate or of a transgressive phase (greater "distance to shore") as discussed in Warney et al. (2003). In this case, increased bisaccate abundance is most likely linked to the Holocene highstand.

Changes in palynomorph assemblages in the studied cores allow the identification of four global climatic intervals (Figure 4.3), although only MV-41 records the Bølling-Allerød Interstadial and the Younger Dryas. The Bølling-Allerød Interstadial is a warm interval between 14.5 to 12.5 kyr BP characterized by rapid sea level rise (Howell et al., 2014), and palynomorph assemblages in this interval are dominated by warm climate taxa and low abundances of all groups. Lower abundances are likely due to high rates of sediment accumulation which can dilute the palynomorph signal (Figure 4.10).

The Younger Dryas period is a cool climate interval between 12.5 to 11.5 kyr BP with little change in sea level (Howell et al., 2014). We have interpreted the Younger

Dryas interval in MV-41 samples from an increase in cool climate taxa during this time. A decrease in fungal spore abundance could also reflect cooler conditions (e.g., Staplin et al., 1976; Elsik, 1980; Elsik, 1996). The presence of warm-loving dinoflagellate cysts indicate that SSTs were not lower than 11.5°C in the GoP during this period.

MWP-1B, a warm climate interval between 11.5 to 10.5 kyr BP that is characterized by high rates of sea level rise (Howell et al., 2014), is represented by samples in all three cores (Figures 4.6, 4.7, 4.8, 4.9). Samples covering this time period are characterized by high abundances of dinoflagellate cysts (including a 300% increase in *Brigantedinium* spp. in MV-41 and MV-46), terrestrial pollen and spores, fungal spores, and reworked palynomorphs, which support the interpretation of warmer climatic conditions during this interval. Increased abundances of all groups could be caused by increased rainfall, erosion, and thus sediment discharge from the mainland.

The Holocene period, dated from 10.5 kyr BP to present, is well recorded by palynomorph assemblages in all three cores (Figures 4.6, 4.7, 4.8, 4.9). A sharp decrease in mangove pollen and increase in marine indicator taxa in MD-50 at approximately 5 kyr BP (Figure 4.6) allows us to interpret the end of marine transgression and possible ENSO intensification. While dated coral terraces indicate marine transgression ends at approximately 6 kyr BP (Figure 4.4), the discrepancy in age dates can be resolved by the response time taken for palynomorph assemblages to change or an intensification of ENSO conditions at approximately 5 kyr BP. Palynomorph assemblages could have changed in response to the greater climatic variability caused by an intensified ENSO (Tudhope et al., 2001). An intensification of ENSO conditions caused by climatic variation is supported by greater variability in the $\delta^{18}O$ curve of MD-50 (Figure 4.8).

Although researchers have dated the advent of agriculture on PNG between 7 to 9 kyr BP (e.g., Haberle et al., 2012), evidence for agricultural intensification is not apparent in the cores selected for this study. An increase in human cultivar and grassland pollen was not observed, but previous researchers have demonstrated an increase in these palynomorphs due to human activity on mainland PNG and its surrounding islands (e.g., Denham et al., 2003; Haberle, 2003; Denham and Haberle, 2008; Sniderman et al., 2009; Haberle et al., 2012). Future work will include analysis of palynomaceral fragments on these three cores (e.g., Thomas et al., 2015), because charcoal fragments have been associated with an increase in burning and agriculture (Denham et al., 2003; Haberle et al., 2012). Documenting changes in these fragments for MV-41 and MV-46, in particular, could allow better definition of the beginnings of agriculture on PNG.

Although we could not use the ages of reworked palynomorphs to track sedimentary provenance over the study interval, Howell et al. (2014) and Francis (2007) have provided well-defined sediment transport pathways in the GoP (Figure 4.11). These transport pathways have persisted over the last 14.5 kyr despite sea level changes, and they can provide clues to the source of palynomorph assemblages. MV-41 is sourced by low maturity sediments delivered from the Vailala and Lakekamu river catchments. MV-46 is sourced by sediments of moderate maturity from the Fly, Bamu, Turama, Kikori, and Purari River catchments (Howell et al., 2014). MD-50 has little siliclastic sediment input, and the majority of its sediments are sourced from carbonaceous sediments derived from sloughing of the Great Barrier Reef, which was partially exposed during the LGM and early sea level transgression (Francis, 2007; Francis et al., 2008). Francis et al. (2008) notes a relict shelf edge delta that delivered sediments to Ashmore Trough. Mangrove

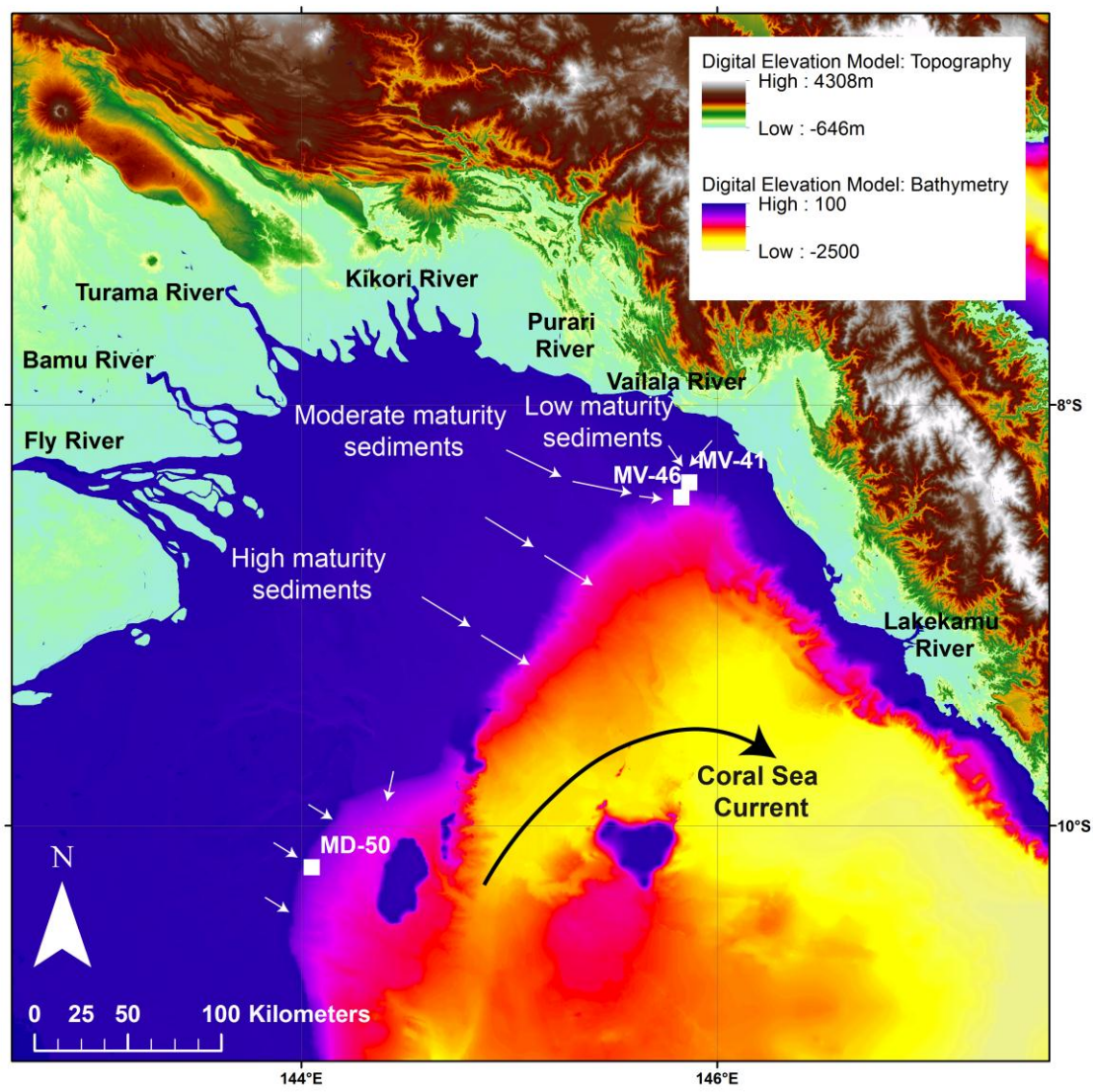

Figure 11. Sediment transport pathways in the Gulf of Papua over the last 14.5 kyr (after Francis, 2007; Howell et al., 2014). Sediment maturities are from Slingerland et al. (2008), Howell et al. (2014), and Xu (2015, personal communication). Bathymetry and topography is from Daniell (2008).

trees could have inhabited the upper parts of this delta, which is why mangrove pollen is observed in deeper samples of MD-50.

Conclusions

Four global climatic intervals have been identified: the Bølling-Allerød Interstadial (14.5 to 12.5 kyr BP), the Younger Dryas (12.5 to 11.5 kyr BP), MWP-1B (11.5 to 10.5 kyr BP), and the Holocene (10.5 kyr to present) (Howell et

al., 2014). Palynomorph assemblage changes mark the boundaries between these periods (Figure 4.9). In general, higher abundances of warm climate taxa and terrestrial palynomorphs mark warmer climatic periods, while lower abundances of warm climate taxa and terrestrial palynomorphs represent cooler climate periods. The co-occurrence of both *Operculodinium centrocarpum* and *O. israelianum* indicate that SST remained higher than 11.5°C even during the Younger Dryas.

Palynomorphs record the end of marine transgression on the GoP shelf at approximately 5 kyr BP by sharp decreases in mangrove pollen abundance in all three cores and concomitant increases in recovery of dinoflagellate cysts and other marine indicators. Increased $\delta^{18}O$ variability at approximately 5000 yr BP, as well as changes in palynological assemblages at the same sample interval in support an increase in ENSO activity at the same time in the GoP (Figure 4.9).

Human impacts on vegetation distribution were not discernible in the palynological record, because human cultivar pollen was not present in any samples and grassland pollen was recovered in very low abundances. Future work on palynomaceral fragments, particularly charcoal, could help to define the advent of agriculture on PNG, as done by previous researchers, such as Denham et al. (2003) and Haberle et al. (2012).

Identification of sedimentary provenance from palynomorph assemblages was not possible in this study, although previous researchers have extensively discussed sedimentary transport pathways in the GoP (e.g., Keen et al., 2006; Francis, 2007; Howell et al., 2014). Reworked palynomorphs in MV-41, MV-46, and MD-50 are not age diagnostic and thus cannot be traced to mainland PNG geologic formations, but may indicate changes in sediment flux (Figure 4.2). Howell et al. (2014) concludes MV-41 is

sourced from the Vailala and Lakekamu river catchments, while MV-46 is sourced from the Fly, Bamu, Turama, Kikori, and Purari river catchments. Francis (2007) notes Ashmore Trough, where MD-50 is located, is sourced predominantly by carbonate sediments sloughed from the Great Barrier Reef and smaller reefs to the north and east, including Ashmore Reef, Boot Reef, and Portlock Reef (Figure 4.11). The differences in sedimentary sourcing are likely the primary reason for assemblage differences in MV-41/MV-46 and MD-50.

References

Abbott, L.D., 1995. Neogene tectonic reconstruction of the Adelbert-Finisterre-New Britain collision, northern Papua New Guinea. Journal of Southeast Asian Earth Sciences 11, 33-51.

Andresen, N., Reijmer, J.J.G., Droxler, A.W., 2003. Timing and distribution of calciturbidites around a deeply submerged carbonate platform in a seismically active setting (Pedro Bank, Northern Nicaragua Rise Caribbean Sea). International Journal of Earth Science 92, 573-592.

APSA Members, 2007. The Australasian Pollen and Spore Atlas v. 1.0. Australian National University, Canberra. Accessed from: http://apsa.anu.edu.au/.

Batten, D.J., 1983. Identification of amorphous sedimentary organic matter by transmitted light microscopy. Geological Society of London Special Publications 12, 275-287.

Beaufort, L., 2007. Physical properties of sediment core MD05-2950, In: International Marine Global Change Study (Ed.). PANGAEA. doi:10.1594/PANGAEA.634167.

Brunskill, G.J., Woolfe, K.J., Zagorskis, I., 1995. Distribution of riverine sediment chemistry on the shelf, slope and rise of the Gulf of Papua. Geo-Marine Letters 15, 153-159.

Carson, B.E., Francis, J.M., Leckie, R.M., Droxler, A.W., Dickens, G.R., Jorry, S.J., Bentley, S.J. Sr., Peterson, L.C., Opdyke, B.N., 2008. Benthic foraminiferal response to sea level change in the mixed siliciclastic-carbonate system of southern Ashmore Trough (Gulf of Papua). Journal of Geophysical Research 113, F01S20, doi:10.1029/2006JF000629.

Chappell, J., Polach, H., 1991. Post-glacial sea-level rise from a coral record at Huon Peninsula, Papua New Guinea. Nature 349, 147-149.

Courtinat, B., Rio, M., Malartre, F., 2002. Palynofacies of marginal marine deposits: the Rhaetian of the east margin of the Massif Central (France). Revue de Micropaléontologie 45, 47-55.

Daniell, J.J., 2008. Development of a bathymetric grid for the Gulf of Papua and adjacent areas: a note describing its development. Journal of Geophysical Research 113, F01S15, doi:10.1029/2006JF000673.

Davey, R.J., 1987. Palynological zonation of the Lower Cretaceous, Upper and upper most Middle Jurassic in the northwestern Papuan Basin of Papua New Guinea. Geological Survey of Papua New Guinea Memoir 13, 77 p.

Davies, H.L., 2012. The geology of New Guinea – the cordilleran margin of the Australian continent. Episodes 35, 87-102.

Denham, T., Haberle, S.G., 2008. Agricultural emergence and transformation in the Upper Wahgi Valley, Papua New Guinea during the Holocene: theory, method and practice. The Holocene 18, 499-514.

Denham, T.P., Haberle, S.G., Lentfer, C.J., Fullagar, R., Field, J., Therin, M., Porch, N., Winsborough, B., 2003. Origins of agriculture at Kuk Swamp in the highlands of New Guinea. Science 301, 189-193.

Dickens, G.R., Droxler, A.W., Bentley, S.J. Sr., Peterson, L.C., Opdyke, B.N., Beaufort, L., Daniell, J.J., Febo, L.A., Francis, J.M., Harris, P.T., et al., 2006. Sediment accumulation on the shelf edges, adjacent slopes, and basin floors of the Gulf of Papua. NSF-MARGINS Newsletter 16, 1-4.

Droxler, A.W., Schlager, W., 1985. Glacial versus interglacial sedimentation rates and turbidite frequency in the Bahamas. Geology 13, 799-802.

Elsik, W.C., 1980. The utility of fungal spores in marginal marine strata of the Late Cenozoic, northern Gulf of Mexico. Proceedings of the Fourth International Palynological Conference, Lucknow (1976-77) 2, 436-443.

Elsik, W.C., 1996. Chapter 10. Fungi, In: Jansonius, J., McGregor, D.C. (Eds.), Palynology: Principles and Applications. American Association of Stratigraphic Palynologists, Salt Lake City, pp. 293-305.

Ewing, J.J., Houtz, R.E., Ludwig, W.J., 1970. Sediment distribution in the Coral Sea. Journal of Geophysical Research 75, 1963-1972.

Fairbanks, R.G., 1989. A 17,000 year glacio-eustatic sea level record: influence of glacial melting rates on the Younger Dryas event and deep ocean circulation. Nature 342, 637-642.

Fairbanks, R.G., Mortlock, R.A., Chiu, T.C., Cao, L., Kaplan, A., Guilderson, T.P., Fairbanks, T.W., Bloom, A.L., Grootes, P.M., Nadeau, M.J., 2005. Calibration curves spanning 0 to 50,000 years BP based on paired $^{230}Th/^{234}U/^{238}U$ and radiocarbon dates on pristine corals. Quaternary Science Reviews 24, 1781-1796.

Feakins, S.J., Warny, S., Lee, J.-E., 2012. Hydrologic cycling over Antarctica during the Middle Miocene warming. Nature Geoscience 5, 557-560.

Febo, L.A., Bentley, S.J. Sr., Wrenn, J.H., Droxler, A.W., Dickens, G.R., Peterson, L.C., Opdyke, B.N., 2008. Late Pleistocene and Holocene sedimentation, organic-carbon delivery and paleoclimatic inferences on the continental slope of the northern Pandora Trough. Journal of Geophysical Research 113, F01S18, doi:10/1029/2006JF000677.

Fleming, R.F., 1994. Cretaceous pollen in Pliocene rocks: implications for Pliocene climate in the southwestern United States. Geology 22, 787-790.

Flenley, J.R., 1979. The Late Quaternary vegetational history of the equatorial mountains. Progress in Physical Geography 3, 488-509.

Francis, J.M., 2007. Late Quaternary sediment dispersal and accumulation on the slopes of the Great Barrier Reef mixed siliciclastic-carbonate depositional system, Gulf of Papua, Papua New Guinea and North Queensland margin, Australia. Ph.D. thesis. Rice University.

Francis, J.M., Daniell, J.J., Droxler, A.W., Dickens, G.R., Bentley, S.J. Sr., Peterson, L.C., Opdyke, B.N., Beaufort, L., 2008. Deep water geomorphology of the mixed siliciclastic-carbonate system, Gulf of Papua. Journal of Geophysical Research 113, F01S16, doi:10.1029/2007JF000851.

Gardner, J.V., 1970. Submarine geology of the Western Coral Sea. Geological Society of America Bulletin 81, 2599-2614.

Glaser, K.S., Droxler, A.W., 1993. Controls and development of late Quaternary periplatform carbonate stratigraphy in Walton Basin (Northern Nicarauga Rise Caribbean Sea). Paleoceanography 8, 243-274.

Haberle, S.G., 2003. The emergence of an agricultural landscape in the highlands of New Guinea. Archaeology in Oceania 38, 149-158.

Haberle, S.G., Lentfer, C., O'Donnell, S., Denham, T., 2012. The palaeoenvironments of Kuk Swamp from the beginnings of agriculture in the highlands of Papua New Guinea. Quaternary International 249, 129-139.

Hanebuth, T., Stattegger, K., Grootes, P.M., 2000. Rapid flooding of the Sunda Shelf: a late-glacial sea-level record. Science 288, 1033-1035.

Harland, R., 1981. Cysts of the colonial dinoflagellate *Polykrikos schwartzii* Biitschli 1873 (Gymnodiniales) from Recent sediments, Firth of Forth, Scotland. Palynology 5, 65-79.

Harland, R., 1983. Distribution maps of recent dinoflagellate cysts in bottom sediments from the North Atlantic Ocean and adjacent seas. Palaeontology 26, 321-387.

Harper, B.B., 2014. Late Quaternary mixed carbonate-siliciclastic sediment slope accumulation: unexpected responses of Australia and Papua New Guinea reefs to glacio-eustatic sea level fluctuations. Ph.D. thesis. Rice University.

Harris, P.T., Pattiaratchi, C.B., Keene, J.B., Dalrymple, R.W., Gardner, J.V., Baker, E.K., Cole, A.R., Mitchell, D., Gibbs, P., Schroeder, W.W., 1996. Late Quaternary deltaic and carbonate sedimentation in the Gulf of Papua foreland basin: response to sea level change. Journal of Sedimentary Research 66, 801-819.

Hope, G.S., Golson, J., Allen, J., 1983. Palaeoecology and prehistory in New Guinea. Journal of Human Evolution 12, 37-60.

Howell, A.L., Bentley, S.J. Sr., Xu, K., Ferrell, R.E.J., Muhammad, Z., Septama, E., 2014. Fine sediment mineralogy as a tracer of latest Quaternary sediment delivery to a dynamic continental margin: Pandora Trough, Gulf of Papua, Papua New Guinea. Marine Geology 357, 108-122.

Jorry, S.J., Droxler, A.W., Mallarino, G., Dickens, G.R., Bentley, S.J. Sr., Beaufort, L., Peterson, L.C., Opdyke, B.N., 2008. Bundled turbidite deposition in the central Pandora Trough (Gulf of Papua) since Last Glacial Maximum: linking sediment nature and accumulation to sea level fluctuations at millennial timescale. Journal of Geophysical Research 113, F01S19, doi:10.1029/2006JF000649.

Kawahata, H., Gupta, L.P., 2004. Settling Particles Flux in Response to El Niño/Southern Oscillation (ENSO) in the Equatorial Pacific, In: Shiyomi, M., Kawahata, H., Koizumi, H., Tsuda, A., Awaya, Y. (Eds.), Global Environmental Change in the Ocean and on Land. TERRAPUB, Tokyo, pp. 95-108.

Keen, T.R., Ko, D.S., Slingerland, R.L., Riedlinger, S., Flynn, P., 2006. Potential transport pathways of terrigenous material in the Gulf of Papua. Geophysical Research Letters 33, L04608, doi:10.1029/2005GL025416.

Kershaw, A.P., 1994. Pleistocene vegetation of the humid tropics of northeastern Queensland, Australia. Palaeogeography, Palaeoclimatology, Palaeoecology 109, 399-412.

Kubo, Y., Syvitski, J.P.M., 2006. Inverse modeling of post Last Glacial Maximum transgressive sedimentation using 2D-SedFlux: application to the Northern Adriatic Sea. Marine Geology 234, 233-243.

Lambeck, K., Chappell, J., 2001. Sea level change thorugh the last glacial cycle. Science 292, 679-686.

Laskar, J., Robutel, P., Joutel, F., Gastineau, M., Correia, A.C.M., Levrard, B., 2004. A long-term numerical solution for the insolation quantities of the Earth. Astronomy and Astrophysics 428, 261-285.

Lignum, J., Jarvis, I., Pearce, M., 2008. A critical assessment of standard processing methods for preparation of palynological samples. Review of Palaeobotany and Palynology 149, 133-149.

Lisiecki, L.E., Raymo, M.E., 2005. A Pliocene-Pleistocene stack of 57 globally distributed benthic $\delta^{18}O$ records. Paleoceanography 20, PA1003, doi:10.1029/2004PA001071.

Liu, J.P., Milliman, J.D., Gao, S., Cheng, P., 2004. Holocene development of the Yellow River's subaqueous delta, North Yellow Sea. Marine Geology 209, 45-67.

Marret, F., Zonneveld, K.A.F., 2003. Atlas of modern organic-walled dinoflagellate cyst distribution. Review of Palaeobotany and Palynology 125, 1-200.

Martin, D.P., Nittrouer, C.A., Ogston, A.S., Crockett, J.S., 2008. Tidal and seasonal dynamics of a muddy inner shelf environment, Gulf of Papua. Journal of Geophysical Research 113, F01S07, doi:10.1029/2006JF000681.

McAlpine, J.R., Keig, G., 1983. Climate of Papua New Guinea. Australian National University Press, Canberra, p. 200.

Melia, M.B., 1984. The distribution and relationship between palynomorphs in aerosols and deep-sea sediments off the coast of northwest Africa. Marine Geology 58, 345-371.

Miller, K.G., Kominz, M.A., Browning, J.V., Wright, J.D., Mountain, G.S., Katz, M.E., Sugarman, P.J., Cramer, B.S., Christie-Blick, N., Pekar, S.F., 2005. The Phanerozoic record of global sea-level change. Science 310, 1293-1298.

Milliman, J.D., 1995. Sediment discharge to the ocean from small mountainous rivers: the New Guinea example. Geo-Marine Letters 15, 127-133.

Moss, P.T., Kershaw, A.P., Grindrod, J., 2005. Pollen transport and deposition in riverine and marine environments within the humid tropics of northeastern Australia. Review of Palaeobotany and Palynology 134, 55-69.

Muhammad, Z., 2009. Late Quaternary marine sediment record from the Gulf of Papua continental margin. Ph.D. thesis. Louisiana State University, pp. 71-109.

Muhammad, Z., Bentley, S.J. Sr., Febo, L.A., Droxler, A.W., Dickens, G.R., Peterson, L.C., Opdyke, B.N., 2008. Excess ^{210}Pb inventories and fluxes along the continental slope and basins of the Gulf of Papua. Journal of Geophysical Research 113, F01S17, doi:10.1029/JF000676.

Muller, J., 1959. Palynology of Recent Orinoco Delta and shelf sediments. Micropaleontology 5, 1-32.

Needham, H.D., Habib, D., Heezen, B.C., 1969. Upper Carboniferous palynomorphs as a tracer of red sediment dispersal patterns in the northwest Atlantic. Journal of Geology 77, 113-120.

NSF Margins Program, 2004. NSF MARGINS Program Science Plans. MARGINS Office, Columbia University, New York, p. 170.

Ogston, A.S., Sternberg, R.W., Nittrouer, C.A., Martin, D.P., Goni, M.A., Crockett, J.S., 2008. Sediment delivery from the Fly River tidally dominated delta to the nearshore marine environment and the impact of El Niño. Journal of Geophysical Research 113, F01S11, doi:10.1029/2006JF000669.

Ota, Y., Chappell, J., Kelley, R., Yonekura, N., Matsumoto, E., Nishimura, T., Head, J., 1993. Holocene coral reef terraces and coseismic uplift of Huon Peninsula, Papua New Guinea. Quaternary Research 40, 177-188.

Paijmans, K., 1975. Explanatory notes to the vegetation map of Papua New Guinea. Commonwealth Scientific and Industrial Research Organization, Melbourne.

Pigram, C.J., Davies, H.L., 1987. Terranes and accretion history of the New Guinea orogen. Bureau of Mineral Resources Journal of Australian Geology and Geophysics 107, 331-353.

Pigram, C.J., Davies, P.J., Feary, D.A., Symonds, P.A., 1989. Tectonic controls on carbonate platform evolution in southern Papua New Guinea: passive margin to foreland basin. Geology 17, 199-202.

Playford, G., 1982. Neogene palynomorphs from the Huon Peninsula, Papua New Guinea. Palynology 6, 29-54.

Playford, G., Rigby, J.F., 2008. Permian palynoflora of the Ainim and Aiduna formations, West Papua. Revista Española de Micropaleontología 40, 1-57.

Pocknall, D.T., Beggs, J.M., 1990. Palynofacies as a tool for the interpretation of depositional environments in the Waikato and Taranaki Basins, New Zealand, 1989 New Zealand Oil Exploration Conference. Petroleum and Geothermal Unit, Ministry of Commerce, Wellington.

Reimer, P.J., Baillie, M.G.L., Bard, E., Bayliss, A., Beck, J.W., Blackwell, P.G., Bronk Ramsey, C., Buck, C.E., Burr, G.S., Edwards, R.L., Friedrich, M., Grootes, P.M., Guilderson, T.P., Hajdas, I., Heaton, T.J., Hogg, A.G., Hughen, K.A., Kaiser, K.F., Kromer, B., McCormac, F.G., Manning, S.W., Reimer, R.W., Richards, D.A., Southon, J.R., Talamo, S., Turney, C.S.M., van der Plicht, J., Weyhenmeyer, C.E., 2009. IntCal09 and Marine09 radiocarbon age calibration curves, 0-50,000 years cal BP. Radiocarbon 51, 1111-1150.

Riding, J.B., 2005. Reworked palynomorphs as a tool for determining Quaternary sediment provenance in East Anglia, UK, American Association of Stratigraphic Palynologists Program and Abstracts 38th Annual Meeting, p. 52.

Rigby, J.F., 1997. The significance of a Permian flora from Irian Jaya (west New Guinea) containing elements related to coeval floras of Gondwanaland and Cathaysialand. The Palaeobotanist 45, 295-302.

Rigby, J.F., 2001. A review of early Permian flora from Papua (west New Guinea), In: Metcalfe, I., Smith, J.M.B., Morwood, M., Davidson, I. (Eds.), Faunal and floral migrations and evolution in SE Asia-Australasia. Balkema, Lisse, pp. 85-95.

Robbins, J.C., Petterson, M.G., Mylne, K., Espi, J.O., 2013. Tumbi landslide, Papua New Guinea: Rainfall induced? Landslides 10, 673-684.

Rodbell, D.T., Seltzer, G.O., Anderson, D.M., Abbott, M.B., Enfield, D.B., Newman, J.H., 1999. An ~15,000-year record of El Niño-driven alluviation in Southwestern Ecuador. Science 283, 516-520.

Rowe, C., 2007a. A palynological investigation of Holocene vegetation change in Torres Strait, seasonal tropics of northern Australia. Palaeogeography, Palaeoclimatology, Palaeoecology 251, 83-103.

Rowe, C., 2007b. Vegetation change following mid-Holocene marine transgression of the Torres Strait shelf: a record from the island of Mua, northern Australia. The Holocene 17, 927-937.

Rowe, C., McNiven, I.J., David, B., Richards, T., Leavesley, M., 2013. Holocene pollen records from Caution Bay, southern mainland Papua New Guinea. The Holocene 23, 1130-1142.

Schiøler, P., Crampton, J.S., Laird, M.G., 2002. Palynofacies and sea-level changes in the Middle Coniacian-Late Campanian (Late Cretaceous) of the East Coast Basin, New Zealand. Palaeogeography, Palaeoclimatology, Palaeoecology 188, 101-125.

Schiøler, P., Rogers, K., Sykes, R., Hollis, C.J., Ilg, B., Meadows, D., Roncaglia, L., Uruski, C., 2010. Palynofacies, organic geochemistry and depositional environments of the Tartan Formation (Late Paleocene), a potential source rock in the Great South Basin, New Zealand. Marine and Petroleum Geology 27, 351-369.

Schrank, E., 1988. Effects of chemical processing on the preservation of peridinioid dinoflagellates: a case study from the Late Cretaceous of NE Africa. Review of Palaeobotany and Palynology 56, 123-140.

Scourse, J., Marret, F., Versteegh, G.J.M., Jansen, J.H.F., Schefuβ, E., van der Plicht, J., 2005. High-resolution last deglaciation record from the Congo fan reveals significance of mangrove pollen and biomarkers as indicators of shelf transgression. Quaternary Research 64, 57-69.

Skupien, P., Mohamed, O., 2008. Campanian to Maastrichtian palynofacies and dinoflagellate cysts of the Silesian unit, outer western Carpathians. Czech Republic Bulletin of Geoscience 83, 207-224.

Slingerland, R., Driscoll, N.W., Milliman, J.D., Miller, J.R., Johnstone, E.A., 2008. Anatomy and growth of a Holocene clinothem in the Gulf of Papua. Journal of Geophysical Research 113, F01S13, doi:10.1029/2006JF000628.

Sniderman, J.M.K., Finn, J., Denham, T.P., 2009. A late Holocene palaeoecological record from Ambra Crater in the highlands of Papua New Guinea and implications for agricultural history. The Holocene 19, 449-458.

Staplin, F.L., editor, 1976. Tertiary biostratigraphy, Mackenzie Delta region, Canada. Bulletin of Canadian Petroleum Geology 24, 117-136.

Steinshouer, D.W., Qiang, J., McCabe, P.J., Ryder, R.T., 1999. Maps showing geology, oil and gas fields, and geologic provinces of the Asia Pacific Region U.S. Geological Survey Open File Report 97-470F. U.S.G.S., Reston.

Stockmarr, J., 1971. Tablets with spores used in absolute pollen analysis. Pollen et Spores 13, 615-621.

StrataData, Inc., 2014. Stratabugs v2.0. StrataData, Inc., Surrey.

Stuiver, M., Reimer, P.J., Reimer, R., 2015. CALIB Radiocarbon Calibration, 7.1 ed. Marine Reservoir Correction Database.

Tcherepanov, E.N., Droxler, A.W., Lapointe, P., Dickens, G.R., Bentley, S.J. Sr., Beaufort, L., Peterson, L.C., Daniell, J., Opdyke, B.N., 2008. Neogene evolution of the mixed carbonate-siliciclastic system in the Gulf of Papua, Papua New Guinea. Journal of Geophysical Research 113, F01S21, doi:10.1029/2006JF000684.

Tcherepanov, E.N., Droxler, A.W., Lapointe, P., Mohn, K., Larsen, O.A., 2010. Siliciclastic influx and burial of the Cenozoic carbonate system in the Gulf of Papua. Marine and Petroleum Geology 27, 533-554.

Thom, B.G., Wright, L.D., 1983. Geomorphology of the Purari Delta, In: Petr, T. (Ed.), The Purari: Tropical Environment of a High Rainfall River Basin. Dr. W. Junk, The Hague, pp. 64-84.

Thomas, M.L., Pocknall, D.T., Warny, S., Bentley, S.J. Sr., Droxler, A.W., Nittrouer, C.A., 2015. Assessing palaeobathymetry and sedimentation rates using palynomaceral analysis: a study of modern sediments from the Gulf of Papua, offshore Papua New Guinea. Palynology, doi:10.1080/01916122.2015.1014526.

Thomas, M.L., Warny, S., Jarzen, D.M., Bentley, S.J. Sr., Xu, K., Droxler, A.W., Nittrouer, C.A. In preparation. Distribution of modern palynomorphs in the Gulf of Papua, Papua New Guinea, and their relationship to sediment source, transport, and deposition.

Torrence, R., 2012. Volcanic disasters and agricultural intensification: a case study from Willaumez Peninsula, Papua New Guinea. Quaternary International 249, 151-161.

Traverse, A., 2007. Paleopalynology. Springer, Dordrecht, p. 813.

Traverse, A., Ginsburg, R.N., 1966. Palynology of surface sediments of Great Bahama Bank as related to water movement and sedimentation. Marine Geology 4, 417-459.

TSCreator, 2015. TimeScale Creator version 6.4, In: Gradstein, F.M., Ogg, J.G., Schmitz, M.D., Ogg, G.M. (Eds.). Geologic TimeScale Foundation.

Tudhope, A.W., Chilcott, C.P., McCulloch, M.T., Cook, E.R., Chappell, J., Ellam, R.M., Lea, D.W., Lough, J.M., Shimmield, G.B., 2001. Variability in El Nino-Southern Oscillation through a glacial-interglacial cycle. Science 291, 1511-1517.

van der kaars, S., 2001. Pollen distribution in marine sediments from the south-eastern Indonesian waters. Palaeogeography, Palaeoclimatology, Palaeoecology 171, 341-361.

Walker, D., Flenley, J.R., 1979. Late Quaternary Vegetational History of the Enga Province of Upland Papua New Guinea. Philosophical Transactions of the Royal Society London Series B 286, 265-344.

Walsh, J.P., Nittrouer, C.A., 2004. Mangrove-bank sedimentation in a mesotidal environment with large sediment supply, Gulf of Papua. Marine Geology 208, 225-248.

Walsh, J.P., Nittrouer, C.A., Palinkas, C.M., Ogston, A.S., Sternberg, R.W., Brunskill, G.J., 2004. Clinoform mechanics in the Gulf of Papua, New Guinea. Continental Shelf Research 24, 2487-2510.

Warny, S., Askin, R.A., Hannah, M.J., Mohr, B.A.R., Raine, J.I., Harwood, D.M., Florindo, F., SMS Science Team, 2009. Palynomorphs from a sediment core reveal a sudden remarkably warm Antarctica during the middle Miocene. Geology 37, 955-958.

Warny, S., Bart, P.J., Suc, J.-P., 2003. Timing and progression of climatic, tectonic and glacioeustatic influences on the Messinian Salinity Crisis. Palaeogeography, Palaeoclimatology, Palaeoecology 202, 59-66.

Warny, S., Jarzen, D.M., Evans, A., Hesp, P., and Bart, P.J., 2012. Environmental significance of abundant and diverse hornwort spores in a potential submerged Paleoindian site in the Gulf of Mexico. Palynology 36(2): 234-253.

Warny, S., Wrenn, J.H., 2002. Upper Neogene dinoflagellate cyst ecostratigraphy of the Atlantic coast of Morocco. Micropaleontology 48, 257-272.

Winterer, E.L., 1970. Submarine valley systems around the Coral Sea basin (Australia). Marine Geology 8, 229-244.

Wolanski, E., Alongi, D.M., 1995. A hypothesis for the formation of a mud bank in the Gulf of Papua. Geo-Marine Letters 15, 166-171.

Wolanski, E., Norro, A., King, B., 1995. Water circulation in the Gulf of Papua. Continental Shelf Research 15, 185-212.

Xu, K., 2015. Personal communication.

Yokoyama, Y., Lambeck, K., De Deckker, P., Johnston, P., Fifield, K., 2000. Timing of the Last Glacial Maximum from observed sea-level minima. Nature 406, 713-716.

Zonneveld, K.A.F., Marret, F., Versteegh, G.J.M., Bogus, K., Bonnet, S., Bouimetarhan, I., Crouch, E., de Vernal, A., Elshanawany, R., Edwards, L., Esper, O., Forke, S., Grøsfjeld, K., Henry, M., Holzwarth, U., Kielt, J.-F., Kim, S.-Y., Ladouceur, S., Ledu, D., Chen, L., Limoges, A., Londeix, L., Lu, S.-H., Mahmoud, M.S., Marino, G., Matsuoka, K., Matthiessen, J., Mildenhal, D.C., Mudie, P., Neil, H.L., Pospelova, V., Qi, Y., Radi, T., Richerol, T., Rochon, A., Sangiorgi, F., Solignac, S., Turon, J.-L., Verleye, T., Wang, Y., Wang, Z., Young, M., 2013. Atlas of modern dinoflagellate cyst distribution based on 2405 data points. Review of Palaeobotany and Palynology 191, 1-197.

CHAPTER 5. CONCLUSIONS

The 2003-2005 NSF (National Science Foundation)-funded MARGINS Source-to-Sink cruises in the Gulf of Papua (GoP), Papua New Guinea (PNG) aimed to better understanding of sedimentary processes on continental margins. Palynology can be used as a tool to assess sediment source, depositional environment, and climatic/oceanographic changes that affect sedimentary dynamics, so this dissertation aids in accomplishing the larger goals of the Source-to-Sink initiative. The projects discussed in the proceeding chapters accomplish four major objectives: 1) understanding climatic and oceanographic changes in the GoP over the last 14.5 kyr; 2) improving understanding of sedimentation dynamics using palynology; 3) assessing modern vegetation biodiversity and distribution with palynomorph recovery; and 4) determining if human impacts on vegetation distribution can be observed in marine palynomorph assemblages. Chapters 2 and 3 fulfill goals 2 and 3; and Chapter 4 fulfills goals 1 and 4.

Results from Chapters 2 and 3 increase understanding of modern sedimentary processes in the GoP and provide an indirect method of assessing vegetation distribution and biodiversity on mainland PNG. Principal component analysis performed on the modern palynomaceral and palynomorph assemblages reveals a clear correlation between their distribution and bathymetry, sedimentation rate, and distance from shore. Certain depositional environments, including the clinoform topset, foreset, and bottomset, as well as the continental slope/ocean basin, appear to be characterized by a distinct assemblage of palynomorph and palynomaceral fragments. Chapter 3 demonstrates reworked palynomorphs can provide clues to sediment source, although this is complicated by the presence of reworked palynomorphs of many ages. Exact species determination for

reworked groups is difficult, which complicates age assignments. Modern pollen and spores clearly reflect vegetation diversity and distribution on mainland PNG, with representation from the following groups: mangroves; tropical rainforest; lower montane/upper montane; swamps; and grass/scrub/savanna.

Results from Chapter 4 show distinct changes in climatic and oceanographic conditions over the last 14.5 kyr B.P., but human impact on the vegetation record is unclear. Four globally known climatic changes can be recognized in palynomorph assemblages: the Bølling-Allerød Interstadial (14.5 to 12.5 kyr BP), the Younger Dryas (12.5 to 11.5 kyr BP), Meltwater Pulse-1B (11.5 to 10.5 kyr BP), and the Holocene (10.5 kyr BP to present). From the palynological record, the end of transgression on the GoP shelf is clearly recorded by reduced abundance of mangrove pollen at approximately 5 to 7 kyr BP. An increase in El Niño Southern Oscillation (ENSO) activity is observed at approximately 5 kyr BP from increased variability in the oxygen-18 record (MD-50) and pollen and spore recovery.

The results from the projects completed during this dissertation provide a significant contribution to the previously published literature associated with the MARGINS Source-to-Sink initiative (Dickens et al., 2006; Keen et al., 2006; Aalto et al., 2008; Alin et al., 2008; Aller et al., 2008a; 2008b; Carson et al., 2008; Crockett et al., 2008; Daniell, 2008; Day et al., 2008; Febo et al., 2008; Francis et al., 2008; Goni et al., 2008; Jorry et al., 2008; Lauer et al., 2008; Muhammad et al., 2008; Ogston et al., 2008; Slingerland et al., 2008a; 2008b; Swanson et al., 2008; Tcherepanov et al., 2008a; 2008b; Tcherepanov et al., 2010; Howell et al., 2014). Palynology increases our understanding of sediment source, transport, and deposition. Modern palynology in the GoP has never

been performed, except in mangrove forests along the shoreline (Rowe et al. 2013). This study also contributes knowledge to the Quaternary palynological community, because it documents the distribution of palynomorph assemblages in the GoP. Palynological analysis of cores covering the last 14.5 kyr has allowed us to determine changes in climatic and oceanographic conditions in the area that fit well with previously published literature for the surrounding region and the world (e.g., Fairbanks, 1989; Yokoyama et al., 2000; Lambeck and Chappell, 2001; Clark et al., 2004; Liu et al. 2004; Kubo and Syvitski, 2006; Carson et al., 2008; Febo et al., 2008; Jorry et al., 2008; Tcherepanov et al., 2008a; 2008b; 2010; Howell et al., 2014). Several areas for future study include a higher resolution analysis of the last 5 kyr to better understand the impact of intensified ENSO on palynomorph assemblages; further documentation of the distribution of dinoflagellate cysts (which have only been observed in significant abundance in Ashmore Trough and along the northeast slope); palynological analysis of sediment samples older than 14.5 kyr from long cores; and palynomaceral work on paleoenvironmental cores in hopes of better defining the advent of agriculture on PNG.

References

Aalto, R., Lauer, J.W., Dietrich, W.E., 2008. Spatial and temporal dynamics of sediment accumulation and exchange along Strickfland River floodplains (Papua New Guinea) over decadal-to-centennial timescales. Journal of Geophysical Research 113, F01S04, doi:10.1029/2006JF000627.

Alin, S.R., Aalto, R., Goni, M.A., Richey, J.E., Dietrich, W.E., 2008. Biogeochemical characterization of carbon sources in the Strickland and Fly rivers, Papua New Guinea. Journal of Geophysical Research 113, F01S05, doi:10.1029/2006JF000625.

Aller, J.Y., Alongi, D.M., Aller, R.C., 2008a. Biological indicators of sedimentary dynamics in the central Gulf of Papua: seasonal and decadal perspectives. Journal of Geophysical Research 113, F01S08, doi:10.1029/2007JF000823.

Aller, R.C., Blair, N.E., Brunskill, G.J., 2008b. Early diagenetic cycling, incineration, and burial of sedimentary organic carbon in the central Gulf of Papua (Papua New Guinea). Journal of Geophysical Research 113, F01S09, doi:10.1029/2006JF000689.

Carson, B.E., Francis, J.M., Leckie, R.M., Droxler, A.W., Dickens, G.R., Jorry, S.J., Bentley, S.J. Sr., Peterson, L.C., Opdyke, B.N., 2008. Benthic foraminiferal response to sea level change in the mixed siliciclastic-carbonate system of southern Ashmore Trough (Gulf of Papua). Journal of Geophysical Research 113, F01S20, doi:10.1029/2006JF000629.

Clark, P.U., Marshall, A., McCabe, A., Mix, A.C., Weaver, A.J., 2004. Rapid rise of sea level 19000 years ago and its global implications. Science 304, 1141-1144.

Crockett, J.S., Nittrouer, C.A., Ogston, A.S., Naar, D.F., Donahue, B.T., 2008. Morphology and filling of incised submarine valleys on the continental shelf near the mouth of the Fly River, Gulf of Papua. Journal of Geophysical Research 113, F01S12, doi:10/1029/2006JF000674.

Daniell, J.J., 2008. Development of a bathymetric grid for the Gulf of Papua and adjacent areas: a note describing its development. Journal of Geophysical Research 113, F01S15, doi:10.1029/2006JF000673.

Day, G., Dietrich, W.E., Rowland, J.C., Marshall, A., 2008. The depositional web on the floodplain of the Fly River, Papua New Guinea. Journal of Geophysical Research 113, F01S02, doi:10.1029/2006JF000622.

Dickens, G.R., Droxler, A.W., Bentley, S.J. Sr., Peterson, L.C., Opdyke, B.N., Beaufort, L., Daniell, J.J., Febo, L.A., Francis, J.M., Harris, P.T., Jorry, S., Mallarino, G., McFadden, M., Muhammad, Z., Carson, B., Patterson, L., Tcherepanov, E., Zarikian, C.A., 2006. Sediment accumulation on the shelf edges, adjacent slopes, and basin floors of the Gulf of Papua. NSF-MARGINS Newsletter 16, 1-4.

Fairbanks, R.G., 1989. A 17,000 year glacio-eustatic sea level record; influence of glacial melting rates on the Younger Dryas event and deep ocean circulation. Nature 342, 637-642.

Febo, L.A., Bentley, S.J. Sr. Wrenn, J.H., Droxler, A.W., Dickens, G.R., Peterson, L.C., Opdyke, B.N., 2008. Late Pleistocene and Holocene sedimentation, organic-carbon delivery and paleoclimatic inferences on the continental slope of the northern Pandora Trough. Journal of Geophysical Research 113, F01S18, doi:10/1029/2006JF000677.

Francis, J.M., Daniell, J.J., Droxler, A.W., Dickens, G.R., Bentley, S.J. Sr., Peterson, L.C., Opdyke, B.N., Beaufort, L., 2008. Deep water geomorphology of the mixed siliciclastic-carbonate system, Gulf of Papua. Journal of Geophysical Research 113. F01S16, doi:10.1029/2007JF000851.

Goni, M.A., Monacci, N., Gisewhite, R., Crockett, J., Nittrouer, C., Ogston, A., Alin, S.R., Aalto, R., 2008. Terrigenous organic matter in sediments from the Fly River delta-clinoform system (Papua New Guinea). Journal of Geophysical Research 113, F01S10, doi:10.1029/2006JF000653.

Howell, A.L., Bentley, S.J. Sr., Xu, K., Ferrell, R.E.J., Muhammad, Z., Septama, E., 2014. Fine sediment mineralogy as a tracer of latest Quaternary sediment delivery to a dynamic continental margin: Pandora Trough, Gulf of Papua, Papua New Guinea. Marine Geology 357, 108-122.

Jorry, S.J., Droxler, A.W., Mallarino, G., Dickens, G.R., Bentley, S.J. Sr., Beaufort, L., Peterson, L.C., Opdyke, B.N., 2008. Bundled turbidite deposition in the central Pandora Trough (Gulf of Papua) since Last Glacial Maximum: linking sediment nature and accumulation to sea level fluctuations at millennial timescale. Journal of Geophysical Research 113, F01S19, doi:10.1029/2006JF000649.

Keen, T.R., Ko, D.S., Slingerland, R.L., Riedlinger, S., Flynn, P., 2006. Potential transport pathways of terrigenous material in the Gulf of Papua. Geophysical Research Letters 33, L04608, doi:10.1029/2005GL025416.

Kubo, Y., Syvitski, J.P.M., 2006. Inverse modeling of post Last Glacial Maximum transgressive sedimentation using 2D-SedFlux: application to the Northern Adriatic Sea. Marine Geology 234, 233-243.

Lambeck, K., Chappell, J., 2001. Sea level change through the last glacial cycle. Science 292, 679-686.

Lauer, J.W., Parker, G., Dietrich, W.E., 2008. Response of the Strickland and Fly River confluence to postglacial sea level rise. Journal of Geophysical Research 113, F01S06, doi:10.1029/2006JF000626.

Liu, J.P., Milliman, J.D., Gao, S., Cheng, P., 2004. Holocene development of the Yellow River's subaqueous delta, North Yellow Sea. Marine Geology 209, 45-67.

Muhammad, Z., Bentley, S.J. Sr., Febo, L.A., Droxler, A.W., Dickens, G.R., Peterson, L.C., Opdyke, B.N., 2008. Excess ^{210}Pb inventories and fluxes along the continental slope and basins of the Gulf of Papua. Journal of Geophysical Research 113, F01S17, doi:10.1029/JF000676.

Ogston, A.S., Sternberg, R.W., Nittrouer, C.A., Martin, D.P., Goni, M.A., Crockett, J.S., 2008. Sediment delivery from the Fly River tidally dominated delta to the nearshore marine environment and the impact of El Niño. Journal of Geophysical Research 113, F01S11, doi:10.1029/2006JF000669.

Rowe, C., McNiven, I.J., David, B., Richards, T., Leavesley, M., 2013. Holocene pollen records from Caution Bay, southern mainland Papua New Guinea. The Holocene 23, 1130-1142.

Slingerland, R., Driscoll, N.W., Milliman, J.D., Miller, J.R., Johnstone, E.A., 2008a. Anatomy and growth of a Holocene clinothem in the Gulf of Papua. Journal of Geophysical Research 113, F01S13, doi:10.1029/2006JF000628.

Slingerland, R., Selover, R.W., Ogston, A.S., Keen, T.R., Driscoll, N.W., Milliman, J.D., 2008b. Building the Holocene clinothem in the Gulf of Papua: an ocean circulation study. Journal of Geophysical Research 113, F01S14, doi:10.1029/2006JF000680.

Swanson, K.M., Watson, E., Aalto, R., Lauer, J.W., Bera, M.T., Marshall, A., Taylor, M.P., Apte, S.C., Dietrich, W.E., 2008. Sediment load and floodplain deposition rates: comparison of the Fly and Strickland rivers, Papua New Guinea. Journal of Geophysical Research 113, F01S03, doi:10.1029/2006JF000623.

Tcherepanov, E.N., Droxler, A.W., Lapointe, P., Dickens, G.R., Bentley, S.J. Sr., Beaufort, L., Peterson, L.C., Daniell, J., Opdyke, B.N., 2008a. Neogene evolution of the mixed carbonate-siliciclastic system in the Gulf of Papua, Papua New Guinea. Journal of Geophysical Research 113, F01S21, doi:10.1029/2006JF000684.

Tcherepanov, E.N., Droxler, A.W., Lapointe, P., Mohn, K., 2008b. Carbonate seismic stratigraphy of the Gulf of Papua mixed depositional system: Neogene stratigraphic signature and eustatic control. Basin Research 20, 185-209.

Tcherepanov, E.N., Droxler, A.W., Lapointe, P., Mohn, K., Larsen, O.A., 2010. Siliciclastic influx and burial of the Cenozoic carbonate system in the Gulf of Papua. Marine and Petroleum Geology 27, 533-554.

Yokoyama, Y., Lambeck, K., De Deckker, P., Johnston, P., Fifield, K., 2000. Timing of the Last Glacial Maximum from observed sea-level minima. Nature 406, 713-71.

APPENDIX I. GRANTING PERMISSION FOR REPRINTING CHAPTER 2

Subject: RE: Permission to include article in dissertation (ID# TPAL 1014526)

From: Taylor, Zoe (Zoe.Taylor@tandf.co.uk)

To: mlthomas716@yahoo.com;

Date: Friday, April 17, 2015 7:40 AM

Dear Marie,

I hope you are well?

I'm happy to say that you may proceed and use your TPAL article in your dissertation. Please use the following statement as an acknowledgment:

Acknowledgement: This <chapter *or* book> is derived in part from an article published in <JOURNAL TITLE> <date of publication> <copyright the Society>, available online: http://www.tandfonline.com/ <Article DOI>

Best wishes,

Zoë Taylor
Production Editor, Journals

Taylor & Francis

Taylor & Francis Group
an informa business

zoe.taylor@tandf.co.uk

www.tandfonline.com

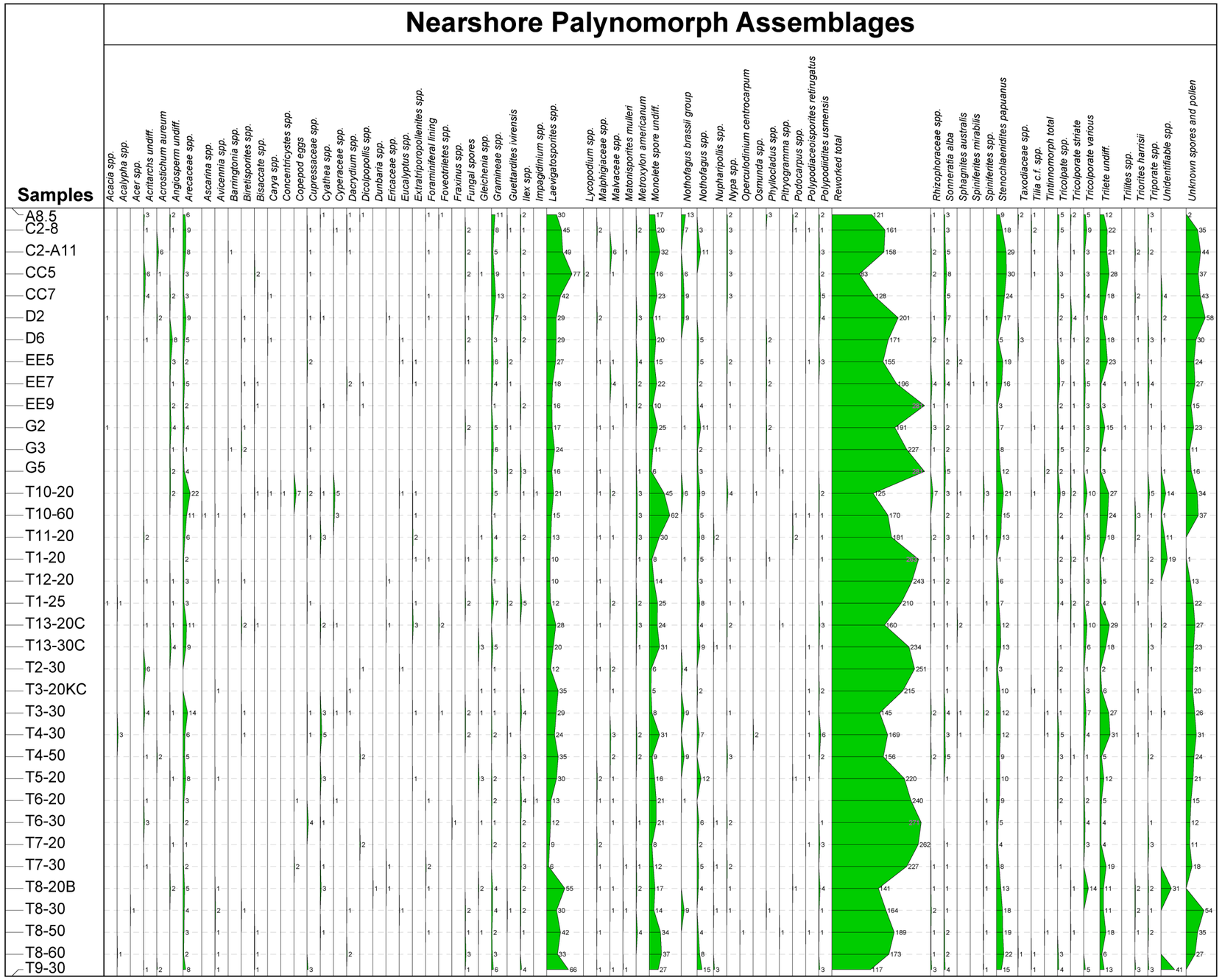
Nearshore Palynomorph Assemblages
Samples
A8.5
C2-8
C2-A11
CC5
CC7
D2
D6
EE5
EE7
EE9
G2
G3
G5
T10-20
T10-60
T11-20
T1-20
T12-20
T1-25
T13-20C
T13-30C
T2-30
T3-20KC
T3-30
T4-30
T4-50
T5-20
T6-20
T6-30
T7-20
T7-30
T8-20B
T8-30
T8-50
T8-60
T9-30
Acacia spp.
Acalypha spp.
Acer spp.
Acritarchs undiff.
Acrostichum aureum
Angiosperm undiff.
Arecaceae spp.
Ascarina spp.
Avicennia spp.
Barringtonia spp.
Biretisporites spp.
Bisaccate spp.
Carya spp.
Concentricystes spp.
Copepod eggs
Cupressaceae spp.
Cyathea spp.
Cyperaceae spp.
Dacrydium spp.
Dicolpopollis spp.
Dunbaria spp.
Ericaceae spp.
Eucalyptus spp.
Extratriporopollenites spp.
Foraminiferal lining
Foveotriletes spp.
Fraxinus spp.
Fungal spores
Gleichenia spp.
Gramineae spp.
Guettardites ivirensis
Ilex spp.
Impagidinium spp.
Laevigatosporites spp.
Lycopodium spp.
Malphigiaceae spp.
Malvaceae spp.
Matonisporites mulleri
Metroxylon americanum
Monolete spore undiff.
Nothofagus brassii group
Nothofagus spp.
Nuphariopollis spp.
Nypa spp.
Operculodinium centrocarpum
Osmunda spp.
Phyllocladus spp.
Pityrogramma spp.
Podocarpus spp.
Polypodiaceoisporites retirugatus
Polypodiidites usmensis
Reworked total
Rhizophoraceae spp.
Sonneratia alba
Sphagnites australis
Spiniferites mirabilis
Spiniferites spp.
Stenochlaenidites papuanus
Taxodiaceae spp.
Tilia c.f. spp.
Tintinnomorph total
Tricolpate spp.
Tricolporate striate
Tricolporate various
Trilete undiff.
Trilites spp.
Triorites harrisii
Triporate spp.
Unidentifiable spp.
Unknown spores and pollen

Offshore Palynomorph Assemblages

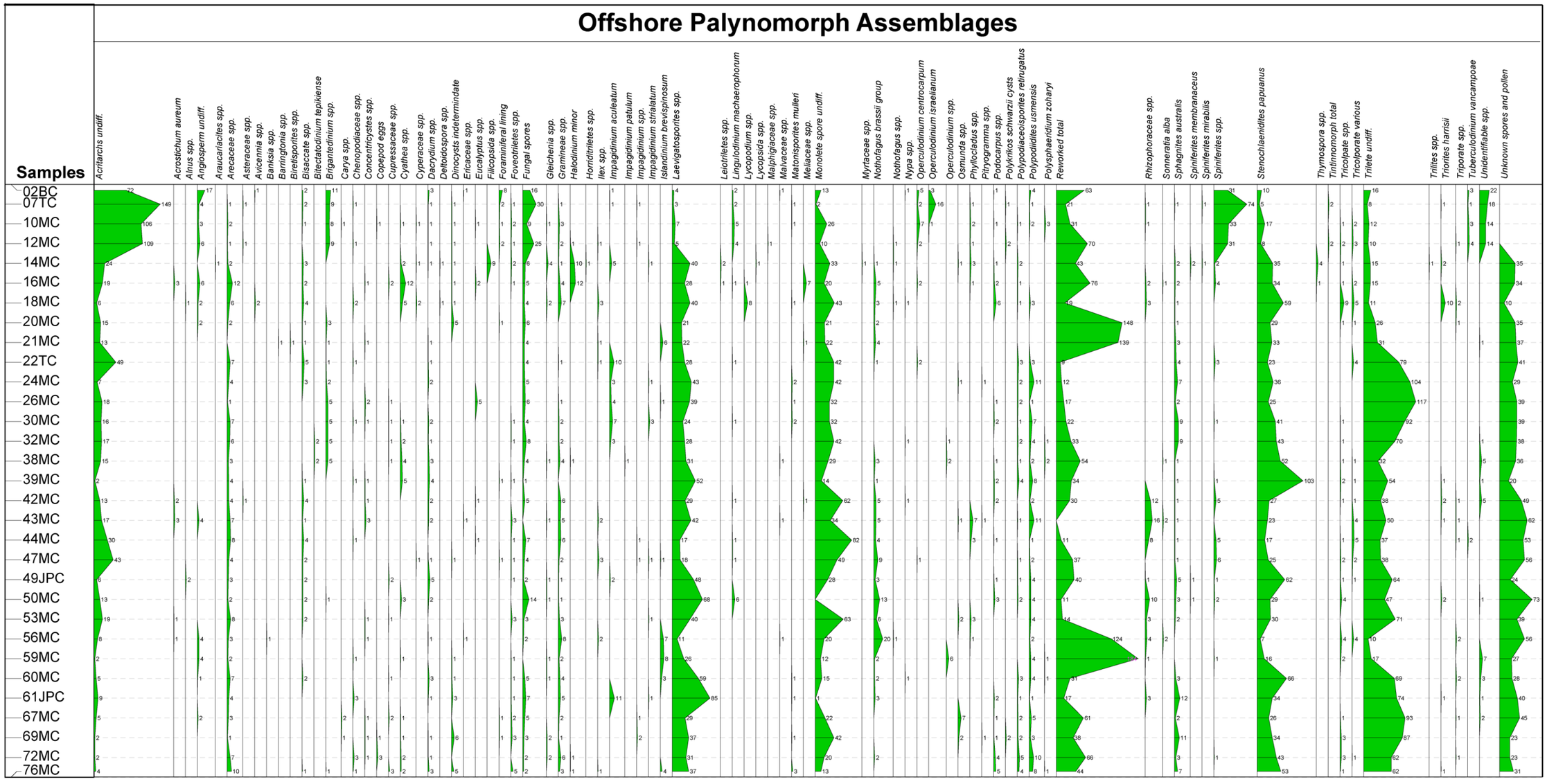

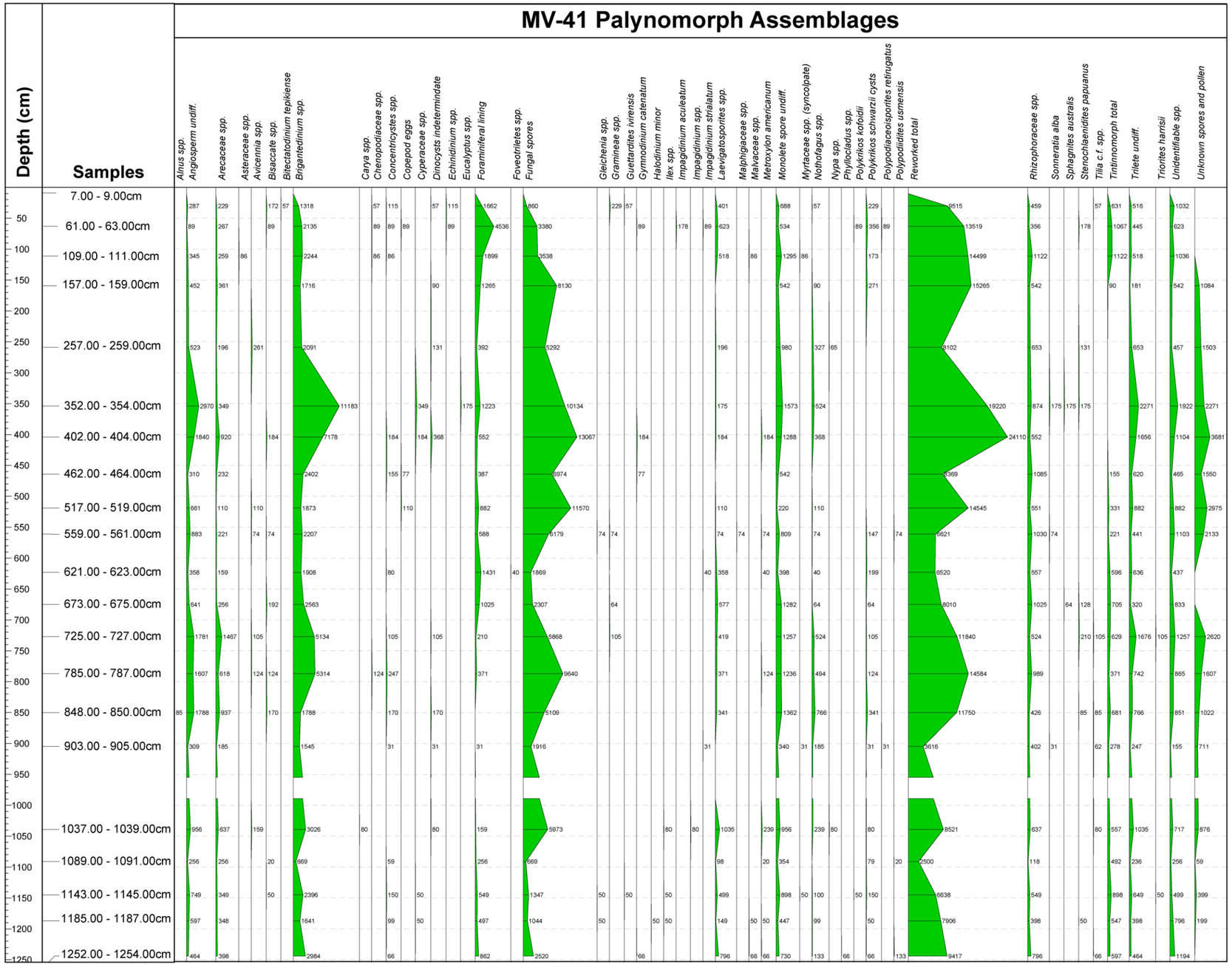
MV-41 Palynomorph Assemblages
Depth (cm)
Samples
Alnus spp.
Angiosperm undiff.
Arecaceae spp.
Asteraceae spp.
Avicennia spp.
Bisaccate spp.
Bitectatodinium tepikiense
Brigantedinium spp.
Carya spp.
Chenopodiaceae spp.
Concentricystes spp.
Copepod eggs
Cyperaceae spp.
Dinocysts indeterminate
Echinidinium spp.
Eucalyptus spp.
Foraminiferal lining
Foveotriletes spp.
Fungal spores
Gleichenia spp.
Gramineae spp.
Guettarcites ivirensis
Gymnodinium catenatum
Halodinium minor
Ilex spp.
Impagidinium aculeatum
Impagidinium spp.
Impagidinium striatum
Laevigatosporites spp.
Malphigiaceae spp.
Malvaceae spp.
Metroxylon americanum
Monolete spore undiff.
Myrtaceae spp. (syncolpate)
Nothofagus spp.
Nypa spp.
Phyllocladus spp.
Polykrikos kofoidii
Polykrikos schwarzii cysts
Polypodiaceoisporites retirugatus
Polypodiidites usmensis
Reworked total
Rhizophoraceae spp.
Sonneratia alba
Sphagnites australis
Stenochlaenidites papuanus
Tilia c.f. spp.
Tintinnomorph total
Trilete undiff.
Triorites harrisii
Unidentifiable spp.
Unknown spores and pollen
7.00 - 9.00cm
61.00 - 63.00cm
109.00 - 111.00cm
157.00 - 159.00cm
257.00 - 259.00cm
352.00 - 354.00cm
402.00 - 404.00cm
462.00 - 464.00cm
517.00 - 519.00cm
559.00 - 561.00cm
621.00 - 623.00cm
673.00 - 675.00cm
725.00 - 727.00cm
785.00 - 787.00cm
848.00 - 850.00cm
903.00 - 905.00cm
1037.00 - 1039.00cm
1089.00 - 1091.00cm
1143.00 - 1145.00cm
1185.00 - 1187.00cm
1252.00 - 1254.00cm

MV-46 Palynomorph Assemblages

Depth (cm)	Samples	*Acalypha spp.*	*Acritarchs undiff.*	*Angiosperm undiff.*	*Arecaceae spp.*	*Asteraceae spp.*	*Avicennia spp.*	*Bireispsorites spp.*	*Bisaccate spp.*	*Brigantedinium spp.*	*Concentricystes spp.*	*Copepod eggs*	*Cupressaceae spp.*	*Cyperaceae spp.*	*Dinocysts indeterminate*	*Ericaceae spp.*	*Eucalyptus spp.*	*Foraminiferal lining*	*Foveotriletes spp.*	*Fungal spores*	*Gleichenia spp.*	*Gramineae spp.*	*Guettardites iviriensis*	*Gymnodinium catenatum*	*Halodinium minor*	*Ilex spp.*	*Impagidinium spp.*	*Impagidinium striatum*	*Laevigatosporites spp.*	*Linguludinium machaerophorum*	*Malphigiaceae spp.*	*Malvaceae spp.*	*Metroxylon americanum*	*Monolete spore undiff.*	*Nothofagus spp.*	*Operculodinium centrocarpum*	*Operculodinium israelianum*	*Phyllocladus spp.*	*Polykrikos kofoidii*	*Polykrikos schwarzii cysts*	*Polypodiidites usmensis*	*Reworked total*	*Rhizophoraceae spp.*	*Sphagnites australis*	*Spiniferites mirabilis*	*Spiniferites spp.*	*Stenochlaenidites papuanus*	*Tintinnomorph total*	*Tricolpate spp.*	*Tricolporate various*	*Trilete undiff.*	*Triorites harrisii*	*Triporate spp.*	*Unidentifiable spp.*	*Unknown spores and pollen*
0	7.00 - 9.00cm			112	169				112	1462	112	337						3994		1237			56					169						169					56	169	6637					1181			112	56	1462		1462
50	61.00 - 63.00cm	525			150				75	599		525			899			2847		11389							150		75				674	150		75			75	2997					225	75	300			450		1049
100	109.00 - 111.00cm	267			67				67	800		467			467			3402	67	7872													467	67					4136				133	67		467			200		934
150	157.00 - 159.00cm	291	79	106		26			26	555	26	53			26			635		3332								53					212		26				2538				26		26	317	26	26			608
200	205.00 - 207.00cm		65	196			65			524		654	65	458				3861	65	5824		65						327					262		65			65	5628					393		393			524		1309
250	257.00 - 259.00cm	700	839	420	140					1259	280	1399	140			140		3358		21545					140			280				1959						6855	979			420	560		700	140	140	420		2099
300	309.00 - 311.00cm	251	334	251	84					669		167			585	167	1923			15887		84				84	334	84	84			251	167					6188	753		167	84	84		84	167		167		920
350	361.00 - 363.00cm		489	367						611	245	611	122		856			5870		16387						122	367					245	367				122	6848	611	122			1101	122	245			611		978
400																																																			
450	438.00 - 440.00cm	180	359	180	90			90	898		2245			629	90	3053		12572						90		180	90				269		90			4939	988		359		180		90	269	180	359	898	
465	465.00 - 467.00cm	77	307	383					843		843			767		2837		10197													920	230				77	3680	383	77			153		690					1533
500																																																			
550	537.00 - 539.00cm	166	332	166					775		55	720		277		997		8696										277				222	222					2991	388			55	166		55	388		55		1274
600																																																		
650																																																		
700	673.00 - 675.00cm	179	179	90					537		716					1701		19601													358	358					3938	985						358	448		358		358	358
750	725.00 - 727.00cm		190	853					569	95	284					1327	95	17536										284		95	853	474					3792	758				190			474		95		1043
800	777.00 - 779.00cm		1600	480					1440		640	160	160	160		1440		27200										480			1440	320					8162	960	160			320		160	1280		800		1280
850	842.00 - 844.00cm		455	758	152				1212		606			455		4394		20453										303		303	606	303				152	11666	1515			152	455			909				1818
900	897.00 - 899.00cm		457	131					588		784			261		1568		8950			196	65	65	65		65		261		65	327	196				131	4116	457			65	457		65	849	131	131		1307
950	957.00 - 959.00cm	147	441	734					1028		1028			294	73	2057		7712				147	73		73	73		367			514	147				367	6684	1102				220			881		73		1396
1000																																																		
1050	1037.00 - 1039.00cm		434	174					695		434			955	87	1129		12072			87				87			434			521	174	87			174	8771	174				347		521		347		434
1100	1089.00 - 1091.00cm		276	138	69				1312	69			69	207		897		8698			138	69							69		690	207				138	6246	552			69	345		552		207		1450
1150	1141.00 - 1143.00cm		1046	523					2267	349	697					4533	349	18307										349			523	523				523	349	16389	1395	174			174		697			2964		2790
1200	1193.00 - 1195.00cm	295	982	393					884	196				98		982		16798				98	98					786	98		491	98					5697	982			98	98	295	295			295		589
1250	1245.00 - 1247.00cm		592	296					888	99	99		99	790		2369		13622			99	99			197			691			987			296	197		7601	790				494		494			395		1481
1300	1297.00 - 1299.00cm		132	198					923	66	66					1055		9858							66						593	66				132	7251	395				132		395			659		989
1350	1325.00 - 1327.00cm	213	1383	532	106				638	106	106			106		957		20319										426			1170	426					5213	1383							319				1064
1400	1379.00 - 1381.00cm		87	174					608							1477		12513										131			348	434				87	10862	608				348		695			348		3128
	1439.00 - 1441.00cm		262	87					1005	44	131			44		175		3058				44						131			437	87				44	5024	393			44	87		437	44	131			1092

MD-50 Palynomorph Assemblages

| Depth (cm) | Samples | *Acacia spp.* | *Acritarchs undiff.* | *Acrostichum aureum* | *Angiosperm undiff.* | *Arecaceae spp.* | *Asteraceae spp.* | *Avicennia spp.* | *Barringtonia spp.* | *Bisaccate spp.* | *Bitectatodinium tepikiense* | *Brigantedinium spp.* | *Carya spp.* | *Chenopodiaceae spp.* | *Concentricystes spp.* | *Copepod eggs* | *Cyathea spp.* | *Cyperaceae spp.* | *Dacrydium spp.* | *Dinocysts indeterminate* | *Eucalyptus spp.* | *Foraminiferal lining* | *Foveotriletes spp.* | *Fungal spores* | *Gleichenia spp.* | *Gramineae spp.* | *Guettardites ivirensis* | *Gymnodinium catenatum* | *Halodinium minor* | *Ilex spp.* | *Impagidinium aculeatum* | *Impagidinium spp.* | *Impagidinium striatatum* | *Laevigatosporites spp.* | *Lingulodinium machaerophorum* | *Malvaceae spp.* | *Metroxylon americanum* | *Monolete spore undiff.* | *Nothofagus brassii group* | *Nothofagus spp.* | *Nypa spp.* | *Operculodinium centrocarpum* | *Operculodinium israelianum* | *Operculodinium spp.* | *Phyllocladus spp.* | *Podocarpus spp.* | *Pollen clump* | *Polykrikos schwarzii cysts* | *Polypodiaceoisporites retirugatus* | *Polypodiidites usmensis* | *Polysphaeridium zoharyi* | *Reworked total* | *Rhizophoraceae spp.* | *Sonneratia alba* | *Sphagnites australis* | *Spiniferites membranaceus* | *Spiniferites mirabilis* | *Spiniferites spp.* | *Stenochlaenidites papuanus* | *Tilia c.f. spp.* | *Tintinnomorph total* | *Trilete undiff.* | *Triorites harrisii* | *Tuberculodinium vancampoae* | *Unidentifiable spp.* |
|---|---|---

VITA

Marie graduated summa cum laude from Millsaps College in 2011 with a double major in Geology and Biology. At Millsaps, she studied the distribution of a modern salamander species, *Plethodon websteri*, and completed an Honors Thesis. Marie enjoyed hunting salamanders, but decided she wanted to do something more practical in graduate school. She decided to attend Lousiaiana State University for geology after obtaining her B.Sc. and pursue her Ph.D. upon the advice of numerous Millsaps faculty. Although she knew she didn't want to study salamanders forever, Marie was unsure of her future career goals, until she interned at Hess Corporation during the summer of 2013. Marie ultimately completed two internships with Hess and has accepted an offer to work with them as a geologist upon completion of her dissertation.

At LSU, Marie has continued to be successful academically, maintaining a 4.0 GPA, presenting at conferences, and working on publishing her research on Quaternary palynology in the Gulf of Papua. She has been very active in the graduate student chapter of AAPG, completed a three-year fellowship as a Marathon GeoDE Research Assistant, and one year as a teaching assistant for the department. Marie has also spent time tutoring student athletes. She received several scholarships: the AASP Student Scholarship, an Encana scholarship, and funding from the Mary Jo Klosterman Professorship. Marie is the graduate student representative to GCSSEPM (Gulf Coast Section of the Society of Economic Palaeontologists and Mineralogists). She is a member of several organizations: AASP – The Palynology Society, Geological Society of America, and the American Association of Petroleum Geologists.